

INFORMATION TO USERS

This material was produced from a microfilm copy of the original document. While the most advanced technological means to photograph and reproduce this document have been used, the quality is heavily dependent upon the quality of the original submitted.

The following explanation of techniques is provided to help you understand markings or patterns which may appear on this reproduction.

1. The sign or "target" for pages apparently lacking from the document photographed is "Missing Page(s)". If it was possible to obtain the missing page(s) or section, they are spliced into the film along with adjacent pages. This may have necessitated cutting thru an image and duplicating adjacent pages to insure you complete continuity.
2. When an image on the film is obliterated with a large round black mark, it is an indication that the photographer suspected that the copy may have moved during exposure and thus cause a blurred image. You will find a good image of the page in the adjacent frame.
3. When a map, drawing or chart, etc., was part of the material being photographed the photographer followed a definite method in "sectioning" the material. It is customary to begin photoing at the upper left hand corner of a large sheet and to continue photoing from left to right in equal sections with a small overlap. If necessary, sectioning is continued again — beginning below the first row and continuing on until complete.
4. The majority of users indicate that the textual content is of greatest value, however, a somewhat higher quality reproduction could be made from "photographs" if essential to the understanding of the dissertation. Silver prints of "photographs" may be ordered at additional charge by writing the Order Department, giving the catalog number, title, author and specific pages you wish reproduced.
5. PLEASE NOTE: Some pages may have indistinct print. Filmed as received.

University Microfilms International

300 North Zeeb Road
Ann Arbor, Michigan 48106 USA
St. John's Road, Tyler's Green
High Wycombe, Bucks, England HP10 8HR

7824598

HATHI, VIDYUTKUMAR VAMANRAY
THERMAL AND KINETIC ANALYSIS OF THE PYROLYSIS
OF COALS.

THE UNIVERSITY OF OKLAHOMA, PH.D., 1978

University
Microfilms
International

300 N. ZEEB ROAD, ANN ARBOR, MI 48106

THE UNIVERSITY OF OKLAHOMA

GRADUATE COLLEGE

THERMAL AND KINETIC ANALYSIS OF THE PYROLYSIS OF COALS

A DISSERTATION

SUBMITTED TO THE GRADUATE FACULTY

in partial fulfillment of the requirements for the

degree of

DOCTOR OF PHILOSOPHY

BY

VIDYUTKUMAR V. HATHI

Norman, Oklahoma

1978

THERMAL AND KINETIC ANALYSIS OF THE PYROLYSIS OF COALS

APPROVED BY

C. M. Sleepovich

J. M. Downey

Carl E. Foch

Red Walker

E. E. Brown

DISSERTATION COMMITTEE

ABSTRACT

The thermal decomposition (pyrolysis) of nine bituminous coals of the United States was investigated in a nitrogen atmosphere.

Weight loss and rate of weight loss were measured at heating rates of 160, 80, 40, 20 and 10°C/min. The qualitative behavior of these data confirmed observations reported by others on similar coals in that the major devolatilization occurred between 300-700°C with the peaks shifting to higher temperatures at faster heating rates. Kinetic parameters for each heating rate were derived from these measurements by means of a model which has been used successfully to describe the pyrolysis of woods and wildland fuels.

Energetic effects during pyrolysis were measured directly up to 727°C on a Perkin-Elmer differential scanning calorimeter (DSC-2) at heating rates of 320, 160 and 40°C/min. The decomposition of bituminous coals is endothermic up to 500°C and exothermic thereafter; the energy of pyrolysis is more exothermic with decreasing heating rates. However, quantitative repeatability of these energetic measurements was less than desired because of baseline shifts arising from condensation of decomposition products on the surfaces of the sample holder.

ACKNOWLEDGEMENT

Without assistance, encouragement and unselfish support of Professor Cedomir M. Sliepcevich, George Lynn Cross Research Professor of Engineering, this thesis would not have been possible. Therefore, I express my sincere gratitude and hearty thanks to him.

I also acknowledge the following:

the Bureau of Mines of U. S. Department of Interior and Pennsylvania State University for providing the coal samples;

Dr. S. P. Muhlenkamp for his suggestions and valuable assistance during the experimental work;

Drs. J. R. Welker and L. E. Brown for suggestions and advice and for services on the graduate committee;

Drs. F. M. Townsend and C. E. Locke for their services on the graduate committee;

Dr. J. A. Havens for suggestions during the experimental work;

Mrs. Janet K. Cummings for typing this manuscript; and

Electric Power Research Institute, Palo Alto, CA for financial support.

V. V. Hathi

TABLE OF CONTENTS

	Page
LIST OF TABLES	vii
LIST OF ILLUSTRATIONS.	viii
Chapter	
I. INTRODUCTION	1
Background	2
Resume of Previous Work.	3
II. METHODS OF DIFFERENTIAL THERMAL ANALYSIS	13
Classical Differential Thermal Analysis.	14
Dynamic Difference Calorimeter (DDC)	21
Differential Scanning Calorimeter (DSC).	24
III. EXPERIMENTAL PROCEDURE	32
TGA Calibrations	32
DSC Calibrations	43
Experiments with Coals	51
IV. RESULTS.	59
Thermogravimetric Analysis of Coal	59
Differential Scanning Calorimetry of Coal.	105
V. CONCLUSIONS AND RECOMMENDATIONS:	161
BIBLIOGRAPHY	164
APPENDICES	168
A: TGA AND DSC THERMOGRAMS FOR COAL SAMPLE A.	169
B: TGA AND DSC THERMOGRAMS FOR COAL SAMPLE B.	178
C: TGA AND DSC THERMOGRAMS FOR COAL SAMPLE C.	187

TABLE OF CONTENTS--Continued

APPENDICES	Page
D: TGA AND DSC THERMOGRAMS FOR COAL SAMPLE D.	196
E: TGA AND DSC THERMOGRAMS FOR COAL SAMPLE E.	205
F: TGA AND DSC THERMOGRAMS FOR COAL SAMPLE F.	214
G: TGA AND DSC THERMOGRAMS FOR COAL SAMPLE G.	223
H: TGA AND DSC THERMOGRAMS FOR COAL SAMPLE H.	232
I: TGA AND DSC THERMOGRAMS FOR COAL SAMPLE I.	241
J: TABULATED DATA FROM TGA AND DSC RUNS	250

LIST OF TABLES

Table	Page
III-1. Summary of Coal Samples.	33
III-2. Analyses of Coal Samples Supplied by the Bureau of Mines, U. S. Department of Interior.	34
III-3. Analyses of Coal Samples Supplied by the Pennsylvania State University	35
III-4. Magnetic Standards for TGS-1 Furnace Calibration . . .	40
III-5. Transition Temperatures and Energies of Transitions for Standards Used on the DSC-2 Instrument	47
III-6. Values of Ordinate Calibration Constant (K_d) at Different Heating Rates for DSC.	52
IV-1. Kinetic Parameters of Coal Samples for Heating Rates Studied in This Project.	83
IV-2. Revised Kinetic Parameters for Coal Samples - A, E, and H.	95
IV-3. Heats of Pyrolysis for Coal Samples for a Heating Rate of 320°C/min as Obtained by DSC	142
IV-4. Heats of Pyrolysis for Coal Samples for a Heating Rate of 160°C/min as Obtained by DSC	142
IV-5. Heats of Pyrolysis for Coal Samples for a Heating Rate of 40°C/min as Obtained by DSC.	143
J-1. Tabulated Data from TGA of Coal Samples.	251
J-2. Tabulated Data from the Best DSC Runs.	256

LIST OF ILLUSTRATIONS

Figure	Page
II- 1. Comparison of Sample Temperature, Reference Temperature, and Differential Temperature Curves in Differential Thermal Analysis.	16
II- 2. Schematic Diagrams of "Dynamic Difference Calorimetry" Type Cells Manufactured by duPont	22
II- 3. Typical Calibration Curve of duPont Calorimetry	25
II- 4. Schematic of Differential Scanning Calorimeter Manufactured by Perkin-Elmer	27
II- 5. Block Diagram of Perkin-Elmer Calorimeter	28
III- 1. Perkin-Elmer TGS-1 Thermobalance and UU-1 Temperature Programmer.	36
III- 2. Schematic Diagram of Perkin-Elmer TGS-1 Weighing Mechanism	37
III- 3. Cahn Time Derivative Computer	39
III- 4. Calibration Curves for TGS-1 Furnace.	42
III- 5. Perkin-Elmer Differential Scanning Calorimeter DSC-2.	44
III- 6. DSC-2 Sample Holder Assembly.	45
III- 7. Effect of Temperature on Specific Heat of Sapphire.	50
IV- 1. Effect of Heating Rate on TG (Weight Loss) Thermogram for Coal Sample A	63
IV- 2. Effect of Heating Rate on Differential TG (Rate of Weight Loss) Thermogram for Coal Sample A	64
IV- 3. Effect of Heating Rate on TG (Weight Loss) Thermogram for Coal Sample B	65

LIST OF ILLUSTRATIONS--Continued

Figure	Page
IV- 4. Effect of Heating Rate on Differential TG (Rate of Weight Loss) Thermogram for Coal Sample B.	66
IV- 5. Effect of Heating Rate on TG (Weight Loss) Thermogram for Coal Sample C.	67
IV- 6. Effect of Heating Rate on Differential TG (Rate of Weight Loss) Thermogram for Coal Sample C.	68
IV- 7. Effect of Heating Rate on TG (Weight Loss) Thermogram for Coal Sample D.	69
IV- 8. Effect of Heating Rate on Differential TG (Rate of Weight Loss) Thermogram for Coal Sample D.	70
IV- 9. Effect of Heating Rate on TG (Weight Loss) Thermogram for Coal Sample E.	71
IV-10. Effect of Heating Rate on Differential TG (Rate of Weight Loss) Thermogram for Coal Sample E.	72
IV-11. Effect of Heating Rate on TG (Weight Loss) Thermogram for Coal Sample F.	73
IV-12. Effect of Heating Rate on Differential TG (Rate of Weight Loss) Thermogram for Coal Sample F.	74
IV-13. Effect of Heating Rate on TG (Weight Loss) Thermogram for Coal Sample G.	75
IV-14. Effect of Heating Rate on Differential TG (Rate of Weight Loss) Thermogram for Coal Sample G.	76
IV-15. Effect of Heating Rate on TG (Weight Loss) Thermogram for Coal Sample H.	77
IV-16. Effect of Heating Rate on Differential TG (Rate of Weight Loss) Thermogram for Coal Sample H.	78
IV-17. Effect of Heating Rate on TG (Weight Loss) Thermogram for Coal Sample I.	79
IV-18. Effect of Heating Rate on Differential TG (Rate of Weight Loss) Thermogram for Coal Sample I.	80
IV-19. Comparison Between Experimental and Calculated (By the Kinetic Parameters Listed in Table IV-1 for 160°C/min Heating Rate) TGA Thermograms for Coal Sample A at 160°C/min	85

LIST OF ILLUSTRATIONS--Continued

Figure	Page
IV-20. Comparison Between Experimental and Calculated (By the Kinetic Parameters Listed in Table IV-1 for 40°C/min Heating Rate) TGA Thermograms for Coal Sample A at 40°C/min	86
IV-21. Comparison Between Experimental and Calculated (By the Kinetic Parameters Listed in Table IV-1 for 10°C/min Heating Rate) TGA Thermograms for Coal Sample A at 10°C/min	87
IV-22. Comparison Between Experimental and Calculated (By the Kinetic Parameters Listed in Table IV-1 for 160°C/min Heating Rate) TGA Thermograms for Coal Sample E at 160°C/min	88
IV-23. Comparison Between Experimental and Calculated (By the Kinetic Parameters Listed in Table IV-1 for 40°C/min Heating Rate) TGA Thermograms for Coal Sample E at 40°C/min	89
IV-24. Comparison Between Experimental and Calculated (By the Kinetic Parameters Listed in Table IV-1 for 10°C/min Heating Rate) TGA Thermograms for Coal Sample E at 10°C/min	90
IV-25. Comparison Between Experimental and Calculated (By the Kinetic Parameters Listed in Table IV-1 for 160°C/min Heating Rate) TGA Thermograms for Coal Sample H at 160°C/min	91
IV-26. Comparison Between Experimental and Calculated (By the Kinetic Parameters Listed in Table IV-1 for 40°C/min Heating Rate) TGA Thermograms for Coal Sample H at 40°C/min	92
IV-27. Comparison Between Experimental and Calculated (By the Kinetic Parameters Listed in Table IV-1 for 10°C/min Heating Rate) TGA Thermograms for Coal Sample H at 10°C/min	93
IV-28. Comparison Between Experimental and Calculated (By the Kinetic Parameters Listed in Table IV-2 for 160°C/min Heating Rate) TGA Thermograms for Coal Sample A at 160°C/min	96
IV-29. Comparison Between Experimental and Calculated (By the Kinetic Parameters Listed in Table IV-2 for 40°C/min Heating Rate) TGA Thermograms for Coal Sample A at 40°C/min	97

LIST OF ILLUSTRATIONS--Continued

Figure	Page
IV-30. Comparison Between Experimental and Calculated (By the Kinetic Parameters Listed in Table IV-2 for 10°C/min Heating Rate) TGA Thermograms for Coal Sample A at 10°C/min	98
IV-31. Comparison Between Experimental and Calculated (By the Kinetic Parameters Listed in Table IV-2 for 160°C/min Heating Rate) TGA Thermograms for Coal Sample E at 160°C/min	99
IV-32. Comparison Between Experimental and Calculated (By the Kinetic Parameters Listed in Table IV-2 for 40°C/min Heating Rate) TGA Thermograms for Coal Sample E at 40°C/min	100
IV-33. Comparison Between Experimental and Calculated (By the Kinetic Parameters Listed in Table IV-2 for 10°C/min Heating Rate) TGA Thermograms for Coal Sample E at 10°C/min	101
IV-34. Comparison Between Experimental and Calculated (By the Kinetic Parameters Listed in Table IV-2 for 160°C/min Heating Rate) TGA Thermograms for Coal Sample H at 160°C/min	102
IV-35. Comparison Between Experimental and Calculated (By the Kinetic Parameters Listed in Table IV-2 for 40°C/min Heating Rate) TGA Thermograms for Coal Sample H at 40°C/min	103
IV-36. Comparison Between Experimental and Calculated (By the Kinetic Parameters Listed in Table IV-2 for 10°C/min Heating Rate) TGA Thermograms for Coal Sample H at 10°C/min	104
IV-37. An Uncorrected DSC Run as Obtained on the Chart Paper at 160°C/min Heating Rate for Coal Sample H.	106
IV-38. An Uncorrected DSC Run as Obtained on the Chart Paper at 160°C/min Heating Rate for Coal Sample A.	107
IV-39. Comparison of Runs Obtained on DSC at a Heating Rate of 320°C/min for Coal Sample A	112
IV-40. Comparison of Runs Obtained on DSC at a Heating Rate of 320°C/min for Coal Sample B	113

LIST OF ILLUSTRATIONS--Continued

Figure	Page
IV-41. Comparison of Runs Obtained on DSC at a Heating Rate of 320°C/min for Coal Sample C	114
IV-42. Comparison of Runs Obtained on DSC at a Heating Rate of 320°C/min for Coal Sample D	115
IV-43. Comparison of Runs Obtained on DSC at a Heating Rate of 320°C/min for Coal Sample E	116
IV-44. Comparison of Runs Obtained on DSC at a Heating Rate of 320°C/min for Coal Sample F	117
IV-45. Comparison of Runs Obtained on DSC at a Heating Rate of 320°C/min for Coal Sample G	118
IV-46. Comparison of Runs Obtained on DSC at a Heating Rate of 320°C/min for Coal Sample H	119
IV-47. Comparison of Runs Obtained on DSC at a Heating Rate of 320°C/min for Coal Sample I	120
IV-48. Comparison of Runs Obtained on DSC at a Heating Rate of 160°C/min for Coal Sample A	121
IV-49. Comparison of Runs Obtained on DSC at a Heating Rate of 160°C/min for Coal Sample B	122
IV-50. Comparison of Runs Obtained on DSC at a Heating Rate of 160°C/min for Coal Sample C	123
IV-51. Comparison of Runs Obtained on DSC at a Heating Rate of 160°C/min for Coal Sample D	124
IV-52. Comparison of Runs Obtained on DSC at a Heating Rate of 160°C/min for Coal Sample E	125
IV-53. Comparison of Runs Obtained on DSC at a Heating Rate of 160°C/min for Coal Sample F	126
IV-54. Comparison of Runs Obtained on DSC at a Heating Rate of 160°C/min for Coal Sample G	127
IV-55. Comparison of Runs Obtained on DSC at a Heating Rate of 160°C/min for Coal Sample H	128
IV-56. Comparison of Runs Obtained on DSC at a Heating Rate of 160°C/min for Coal Sample I	129

LIST OF ILLUSTRATIONS---Continued

Figure	Page
IV-57. Comparison of Runs Obtained on DSC at a Heating Rate of 40°C/min for Coal Sample A.	130
IV-58. Comparison of Runs Obtained on DSC at a Heating Rate of 40°C/min for Coal Sample B.	131
IV-59. Comparison of Runs Obtained on DSC at a Heating Rate of 40°C/min for Coal Sample C.	132
IV-60. Comparison of Runs Obtained on DSC at a Heating Rate of 40°C/min for Coal Sample D.	133
IV-61. Comparison of Runs Obtained on DSC at a Heating Rate of 40°C/min for Coal Sample E.	134
IV-62. Comparison of Runs Obtained on DSC at a Heating Rate of 40°C/min for Coal Sample F.	135
IV-63. Comparison of Runs Obtained on DSC at a Heating Rate of 40°C/min for Coal Sample G.	136
IV-64. Comparison of Runs Obtained on DSC at a Heating Rate of 40°C/min for Coal Sample H.	137
IV-65. Comparison of Runs Obtained on DSC at a Heating Rate of 40°C/min for Coal Sample I.	138
IV-66. Effect of Heating Rate on DSC Thermograms for Coal Sample A	144
IV-67. Effect of Heating Rate on DSC Thermograms for Coal Sample B	145
IV-68. Effect of Heating Rate on DSC Thermograms for Coal Sample C	146
IV-69. Effect of Heating Rate on DSC Thermograms for Coal Sample D	147
IV-70. Effect of Heating Rate on DSC Thermograms for Coal Sample E	148
IV-71. Effect of Heating Rate on DSC Thermograms for Coal Sample F	149
IV-72. Effect of Heating Rate on DSC Thermograms for Coal Sample G	150

LIST OF ILLUSTRATIONS--Continued

Figure		Page
IV-73.	Effect of Heating Rate on DSC Thermograms for Coal Sample H	151
IV-74.	Effect of Heating Rate on DSC Thermograms for Coal Sample I	152
IV-75.	Comparison Between an Oak Wood DSC Run made by Havens (1969) at 20°C/min and a DSC Run for Oak Wood made at 320°C/min in this Work.	155
A-1.	TGA Thermograms (Weight Loss and Rate of Weight Loss) for Coal Sample A at 160°C/min	170
A-2.	TGA Thermograms (Weight Loss and Rate of Weight Loss) for Coal Sample A at 80°C/min.	171
A-3.	TGA Thermograms (Weight Loss and Rate of Weight Loss) for Coal Sample A at 40°C/min.	172
A-4.	TGA Thermograms (Weight Loss and Rate of Weight Loss) for Coal Sample A at 20°C/min.	173
A-5.	TGA Thermograms (Weight Loss and Rate of Weight Loss) for Coal Sample A at 10°C/min.	174
A-6.	Corrected DSC Scan for the Coal Sample A at a Heating Rate of 320°C/min.	175
A-7.	Corrected DSC Scan for the Coal Sample A at a Heating Rate of 160°C/min.	176
A-8.	Corrected DSC Scan for the Coal Sample A at a Heating Rate of 40°C/min	177
B-1.	TGA Thermograms (Weight Loss and Rate of Weight Loss) for Coal Sample B at 160°C/min	179
B-2.	TGA Thermograms (Weight Loss and Rate of Weight Loss) for Coal Sample B at 80°C/min.	180
B-3.	TGA Thermograms (Weight Loss and Rate of Weight Loss) for Coal Sample B at 40°C/min.	181
B-4.	TGA Thermograms (Weight Loss and Rate of Weight Loss) for Coal Sample B at 20°C/min.	182
B-5.	TGA Thermograms (Weight Loss and Rate of Weight Loss) for Coal Sample B at 10°C/min.	183

LIST OF ILLUSTRATIONS--Continued

Figure		Page
B-6.	Corrected DSC Scan for the Coal Sample B at a Heating Rate of 320°C/min.	184
B-7.	Corrected DSC Scan for the Coal Sample B at a Heating Rate of 160°C/min.	185
B-8.	Corrected DSC Scan for the Coal Sample B at a Heating Rate of 40°C/min	186
C-1.	TGA Thermograms (Weight Loss and Rate of Weight Loss) for Coal Sample C at 160°C/min	188
C-2.	TGA Thermograms (Weight Loss and Rate of Weight Loss) for Coal Sample C at 80°C/min.	189
C-3.	TGA Thermograms (Weight Loss and Rate of Weight Loss) for Coal Sample C at 40°C/min.	190
C-4.	TGA Thermograms (Weight Loss and Rate of Weight Loss) for Coal Sample C at 20°C/min.	191
C-5.	TGA Thermograms (Weight Loss and Rate of Weight Loss) for Coal Sample C at 10°C/min.	192
C-6.	Corrected DSC Scan for the Coal Sample C at a Heating Rate of 320°C/min.	193
C-7.	Corrected DSC Scan for the Coal Sample C at a Heating Rate of 160°C/min.	194
C-8.	Corrected DSC Scan for the Coal Sample C at a Heating Rate of 40°C/min	195
D-1.	TGA Thermograms (Weight Loss and Rate of Weight Loss) for Coal Sample D at 160°C/min	197
D-2.	TGA Thermograms (Weight Loss and Rate of Weight Loss) for Coal Sample D at 80°C/min.	198
D-3.	TGA Thermograms (Weight Loss and Rate of Weight Loss) for Coal Sample D at 40°C/min.	199
D-4.	TGA Thermograms (Weight Loss and Rate of Weight Loss) for Coal Sample D at 20°C/min.	200
D-5.	TGA Thermograms (Weight Loss and Rate of Weight Loss) for Coal Sample D at 10°C/min.	201

LIST OF ILLUSTRATIONS--Continued

Figure		Page
D-6.	Corrected DSC Scan for the Coal Sample D at a Heating Rate of 320°C/min.	202
D-7.	Corrected DSC Scan for the Coal Sample D at a Heating Rate of 160°C/min.	203
D-8.	Corrected DSC Scan for the Coal Sample D at a Heating Rate of 40°C/min	204
E-1.	TGA Thermograms (Weight Loss and Rate of Weight Loss) for Coal Sample E at 160°C/min	206
E-2.	TGA Thermograms (Weight Loss and Rate of Weight Loss) for Coal Sample E at 80°C/min.	207
E-3.	TGA Thermograms (Weight Loss and Rate of Weight Loss) for Coal Sample E at 40°C/min.	208
E-4.	TGA Thermograms (Weight Loss and Rate of Weight Loss) for Coal Sample E at 20°C/min.	209
E-5.	TGA Thermograms (Weight Loss and Rate of Weight Loss) for Coal Sample E at 10°C/min.	210
E-6.	Corrected DSC Scan for the Coal Sample E at a Heating Rate of 320°C/min.	211
E-7.	Corrected DSC Scan for the Coal Sample E at a Heating Rate of 160°C/min.	212
E-8.	Corrected DSC Scan for the Coal Sample E at a Heating Rate of 40°C/min	213
F-1.	TGA Thermograms (Weight Loss and Rate of Weight Loss) for Coal Sample F at 160°C/min	215
F-2.	TGA Thermograms (Weight Loss and Rate of Weight Loss) for Coal Sample F at 80°C/min.	216
F-3.	TGA Thermograms (Weight Loss and Rate of Weight Loss) for Coal Sample F at 40°C/min.	217
F-4.	TGA Thermograms (Weight Loss and Rate of Weight Loss) for Coal Sample F at 20°C/min.	218
F-5.	TGA Thermograms (Weight Loss and Rate of Weight Loss) for Coal Sample F at 10°C/min.	219

LIST OF ILLUSTRATIONS--Continued

Figure		Page
F-6.	Corrected DSC Scan for the Coal Sample F at a Heating Rate of 320°C/min.	220
F-7.	Corrected DSC Scan for the Coal Sample F at a Heating Rate of 160°C/min.	221
F-8.	Corrected DSC Scan for the Coal Sample F at a Heating Rate of 40°C/min	222
G-1.	TGA Thermograms (Weight Loss and Rate of Weight Loss) for Coal Sample G at 160°C/min	224
G-2.	TGA Thermograms (Weight Loss and Rate of Weight Loss) for Coal Sample G at 80°C/min.	225
G-3.	TGA Thermograms (Weight Loss and Rate of Weight Loss) for Coal Sample G at 40°C/min.	226
G-4.	TGA Thermograms (Weight Loss and Rate of Weight Loss) for Coal Sample G at 20°C/min.	227
G-5.	TGA Thermograms (Weight Loss and Rate of Weight Loss) for Coal Sample G at 10°C/min.	228
G-6.	Corrected DSC Scan for the Coal Sample G at a Heating Rate of 320°C/min.	229
G-7.	Corrected DSC Scan for the Coal Sample G at a Heating Rate of 160°C/min.	230
G-8.	Corrected DSC Scan for the Coal Sample G at a Heating Rate of 40°C/min	231
H-1.	TGA Thermograms (Weight Loss and Rate of Weight Loss) for Coal Sample H at 160°C/min	233
H-2.	TGA Thermograms (Weight Loss and Rate of Weight Loss) for Coal Sample H at 80°C/min.	234
H-3.	TGA Thermograms (Weight Loss and Rate of Weight Loss) for Coal Sample H at 40°C/min.	235
H-4.	TGA Thermograms (Weight Loss and Rate of Weight Loss) for Coal Sample H at 20°C/min.	236
H-5.	TGA Thermograms (Weight Loss and Rate of Weight Loss) for Coal Sample H at 10°C/min.	237

LIST OF ILLUSTRATIONS-Continued

Figure		Page
H-6.	Corrected DSC Scan for the Coal Sample H at a Heating Rate of 320°C/min.	238
H-7.	Corrected DSC Scan for the Coal Sample H at a Heating Rate of 160°C/min.	239
H-8.	Corrected DSC Scan for the Coal Sample H at a Heating Rate of 40°C/min	240
I-1.	TGA Thermograms (Weight Loss and Rate of Weight Loss) for Coal Sample I at 160°C/min	242
I-2.	TGA Thermograms (Weight Loss and Rate of Weight Loss) for Coal Sample I at 80°C/min.	243
I-3.	TGA Thermograms (Weight Loss and Rate of Weight Loss) for Coal Sample I at 40°C/min.	244
I-4.	TGA Thermograms (Weight Loss and Rate of Weight Loss) for Coal Sample I at 20°C/min.	245
I-5.	TGA Thermograms (Weight Loss and Rate of Weight Loss) for Coal Sample I at 10°C/min.	246
I-6.	Corrected DSC Scan for the Coal Sample I at a Heating Rate of 320°C/min.	247
I-7.	Corrected DSC Scan for the Coal Sample I at a Heating Rate of 160°C/min.	248
I-8.	Corrected DSC Scan for the Coal Sample I at a Heating Rate of 40°C/min	249

THERMAL AND KINETIC ANALYSIS OF THE PYROLYSIS OF COALS

CHAPTER I

INTRODUCTION

Thermal analysis of materials has been practiced since LeChatelier's time. The technique of thermal analysis has primarily been used to investigate the response of materials to temperature change and, thereby, to identify constituting elements. Materials such as chemicals and catalysts, soils, mineral ores, and solid fuels have been analyzed by these techniques.

Since coal has been used as a fuel ever since the beginning of industrial development, it has been among the earliest materials to be subjected to thermal analysis. Much of this effort has been directed to the possibility of utilizing data from thermal analysis for quantitative characterization according to the rank of the coal. However, these efforts have been only marginally successful because of the complex nature of coal and inherent limitations in the techniques of thermal analysis.

The major tools of thermal analysis have been thermogravimetric analysis and classical differential thermal analysis. Whereas the

former provides quantitative results the latter is, at best, only semi-quantitative. Primarily because of this deficiency in classical differential analysis, an alternative technique, differential scanning calorimetry, has become available within the last 15 years which, without question, offers a more quantitative approach. The purpose of the investigation reported herein was to study the thermal decomposition of a variety of coals by a combination of thermogravimetric analysis and differential scanning calorimetry.

Background

In thermogravimetric analysis (TGA) weight change of the material is observed as it is heated, usually at a constant rate of temperature rise. The record of weight loss or gain with respect to time or temperature is termed a thermogravimetric (TG) thermogram. When the rate of weight loss (the derivative with respect to time) is recorded as a function of time or temperature, it is called a differential thermogravimetric (DTG) thermogram. The DTG has been used to study the kinetics of thermal decomposition reactions of a variety of solids, including coal. Much of this work is based on the assumption that the thermal decomposition is describable by an overall first order reaction and follows the Arrhenius-type equation

$$K = K_0 e^{-E/RT} \quad (\text{I-1})$$

where K = decomposition rate constant (sec^{-1})

K_0 = frequency factor (sec)

E = "pseudo" activation energy (cal/gm-mole)

T = absolute temperature ($^{\circ}\text{K}$)

R = gas law constant (cal/gm-mole $^{\circ}\text{K}$)

In differential thermal analysis (DTA) the temperature difference between the sample and a reference (inert) material is recorded while both are heated under identical conditions. On the other hand, the more recent differential scanning calorimeter (DSC) of the Perkin-Elmer type records the differences in energy inputs between a sample and inert reference material which are required to maintain both at the same temperature at a prescribed heating rate.

Resume of Previous Work

A large number of studies have been reported on thermogravimetric and differential thermal analysis in attempts to explain kinetics of thermal decomposition of coal and to obtain qualitative information on energetics of coal pyrolysis. Literature reviews on these subjects of thermal analysis are available from Howard (1963), Kirov and Stephens (1967), Lawson (1970), and Anthony and Howard (1976). Kirov and Stephens (1967) have described progress made in the development of thermobalances. Major differences in the thermobalances used for the studies of Honda (1915), Guichard (1926), Vallet (1932), Rigollet (1934), Dubois (1935), Longechambon (1936) and Jouin (1947) were mentioned by Kirov and Stephens (1967). These thermobalances recorded weight loss with respect to time or temperature. A thermobalance was introduced by Waters (1956) which enabled, for the first time, simultaneous recording of weight loss and rate of weight loss data for coal to this author's knowledge.

According to Howard (1963), who discussed literature related to pyrolytic reactions of coal, Audibert (1926) reported for the first time results of thermogravimetry of coal. However, the observations of weight loss data were not applied to study kinetics of coal decomposition

reactions, to this author's knowledge, until the study of Van Krevelen, Van Heerdan and Huntjens (1951). They studied the rates of decomposition of Dutch coals on a thermobalance that recorded weight loss data continuously over the temperature range 200-550°C at a heating rate of 2°C/min. A mathematical equation was presented to describe the rate of decomposition of coals. It was concluded that the decomposition process is first order with respect to the fraction of undecomposed coal. The studies of Shapatina, et. al. (1950) and Stone, et. al. (1954) did not use thermobalances to record weight loss of coals; instead they measured rates of evolution of volatile matter from coals. Shapatina, Kalyuzhnyi, and Chukhanov (1950) studied the rate of evolution of volatile matter by dropping the powdered Russian coal sample into a furnace held at a constant temperature. The volume of gas evolved as a function of temperature was measured for several lengths of time. These measurements were made over a temperature range 300-600°C. They observed that initial devolatilization is rapid removal of moisture and oxides of carbon, the middle devolatilization is slow and consists of removal of main volatile matter from coal, and the final devolatilization is a slow process of outgassing the residuals. The first order reaction rate constants for the middle devolatilization, according to Howard (1963), showed a low value of activation energy (5.3K cal/mole) which does not compare well with those reported in the literature for Western European Coals (40-50K cal/mole). Boyer (1953) studied the decomposition of French coals and reported that the decomposition process is first order. Stone, Batchelor and Johnston (1954) also studied isothermal devolatilization of three American Bituminous coals in a fluidized bed. The coal samples

were removed from the fluidized bed, and they were analyzed for loss in volatile matter. The experiments were performed at temperatures of 410°C, 454°C, and 510°C. The decomposition process was assumed to be represented by

$$\frac{-dV}{dt} = K(V - V_c)^n \quad (I-2)$$

where V = volatile matter content at any time (t)

V_c = ultimate volatile content after heating to the constant temperature

n = order of reaction

K = velocity constant

At a particular temperature it was observed that the order of the decomposition reaction changed with time. For example, at low temperature (410°C), the first order relation held over a longer length of time; but after the end of first order period, fractional order was observed.

Van Krevelen, Huntjens and Dormans (1956) made thermogravimetric runs over a 350-600°C temperature range at slow heating rates (0.6 to 6°C/min) and also made several isothermal runs. It was observed from the results of isothermal coal devolatilization that after a typical high initial rate of weight loss, the rate abruptly tapers off to essentially zero. Brown (1957) studied Australian coals on a thermobalance developed by Waters (1956). The coal samples were heated at 3°C/min. He observed a maximum in the rate of weight loss curve for coking coal at approximately 440°C and below 440°C for lower rank coals. Isothermal decomposition of coal samples confirmed the results of Van Krevelen et. al. (1956). Smutkina and Kasatochkin (1957) studied

the kinetics of decomposition of Russian coals up to temperatures of 850°C. The analysis of the kinetics of coal pyrolysis showed that the velocity constant for the first order reaction changed so much that they concluded that the thermal decomposition of coal cannot be described by a single first order reaction. They also observed that the activation energy for the decomposition reaction increased with an increase in the degree of decomposition.

According to Anthony and Howard (1976) who reviewed the literature related to devolatilization and hydrogasification of coals, it was realized in the early 1960's from the results of several studies (Badzioch, 1961; Jones, 1964; Peters and Bertling, 1965) that the rapid heating of coal generated more volatiles than slow heating. Since this development, most studies on devolatilization have been done at extremely high heating rates, on the order of 1000°C per second (Jountgen and Van Heek, 1968; Mentser, 1970; Anthony, et al, 1976). The complexities in correlating the kinetics are illustrated by the recent work of Reidelbach and Summerfield (1975); they proposed a coal pyrolysis model with fifteen kinetic rate parameters.

The above discussion is intended to provide only an introduction to the literature of coal devolatilization and decomposition. Subsequently, direct comparisons between the results of this study and those reported in literature will be made wherever possible.

Differential thermal analysis of coal began, according to Lawson (1970), when Hollings and Cobb (1914, 1915, and 1923) performed DTA experiments on coal in nitrogen up to a temperature of 1100°C at heating rates of 2 to 12°C/min. Coke, produced from the pyrolysis of a coal

corresponding to the coal being tested, was used as a reference material. The thermograms resulting from the DTA of coals indicated that the decomposition of coal is endothermic up to a temperature of 410°C, and again in the temperature range, 470 to 610°C. Two exothermic regions were observed in the temperature ranges 410-470°C and 610-750°C. The thermograms for coals differing in ranks were also distinguished. Since the studies of Hollings and Cobb (1914, 1915, 1923), little work on DTA pyrolysis of coals was done until the period of Whitehead and his co-workers (Whitehead and King, 1951; Berger and Whitehead, 1951).

Whitehead and King (1951) made DTA experiments on various petrographic constituents of coal at heating rates of 20°C/min. They found that most of the constituents of coal are exothermic in nature in the temperature range of carbonization (330-500°C). Breger and Whitehead (1951) studied the role of lignin in the development of coal through various ranks on a vacuum differential thermal analyzer up to 1000°C. They found that the presence of lignin is indicated by a large exothermic peak between 400°C and 500°C. This exothermic peak associated with lignin became less pronounced with an increase in the rank of the coals; thus, for anthracite coal no peak was observed.

Yagishita and Araki (1951) observed three endothermic and two exothermic peaks in the DTA thermograms of coal up to 1000°C. These peaks on the DTA curves, according to Lawson (1970) corresponded to those observed in the studies of Hollings and Cobb (1914, 1915, 1923).

Glass (1954) studied the relation between the ranks of coal and their DTA characteristics when he heated coal samples from room temperature to 1000°C at 10°C/min in the atmosphere of gaseous products

evolved during the decomposition. He classified five different types of curves, mostly, endothermic, according to the rank of coal.

King and his colleagues (King and Whitehead, 1955; King and Kelley, 1955) performed differential thermal analysis of coals in a vacuum. King and Whitehead (1955) examined vitrains from bituminous coals in an attempt to correlate the rank of coal with the temperature of the exothermic peak that had been previously observed by Breger and Whitehead (1951). King and Whitehead concluded that DTA is useful for detection of cellulose in lignites. King and Kelley (1955) tested coking coals on vacuum DTA at a heating rate of 10°C/min over the temperature range from room temperature to 600°C. They observed an exothermic peak commencing in the range 340°-440°C and reaching a maximum approximately between 440-520°C.

Clegg (1955), in an attempt to explain the discrepancies in the DTA curves observed in previous studies by others, analyzed the experimental factors that could influence the DTA curves. He concluded that a large number of factors, such as manner of packing, covering of the sample, geometry of the holders, etc., affect DTA thermograms. Therefore, DTA curves can be reproduced only if experimental factors are precisely controlled. Clegg (1955), in emphasizing the reliability of the results of Glass (1954) which were obtained in the same laboratory, confirmed that DTA thermograms for coal do reflect that the decomposition reactions for coal are indeed endothermic.

Differential thermal analyses on Canadian coals (ranging in carbon contents from 73% to 90%) were made by Berkowitz (1957) at a heating rate of 6°C/min up to a temperature of 550°C. He observed,

besides an endothermic peak at approximately 120°C, three or four exothermic peaks on the thermograms. His work is in general agreement with Breger and Whitehead (1951). Berkowitz also recognized the experimental difficulties emphasized by Clegg (1955).

Kroger and Pohl (1957) tested macerals, exinite, vitrinite and micrinite separated from German coals on DTA over a temperature range of 100-750°C at a heating rate of 8°C/min. They observed that due to changes in the thermal properties (specific heat and thermal conductivity) of the coal and reference materials, the baseline (zero level line) is depressed until 500°C, then it is raised until it reached the zero value at approximately 800°C. When the DTA curves were corrected for this change in levels of the baseline, four regions, three endothermic and, the last, exothermic, were observed. The uncorrected DTA thermograms, according to Lawson (1970), always lie on the endothermic side of the baseline.

A baseline correction was also applied to the thermograms obtained by Kessler and Romovackova (1961) who studied the behavior of eastern European coal on DTA up to a temperature of 1000°C at a heating rate of 10°C/min. They concluded that a baseline correction was necessary since the baseline obtained with reference material (alumina) in both holders was not a straight zero line but made an angle from 30° to 45° with the zero line. This correction, however, is not the same as reported by Kroger and Pohl who corrected their thermograms for changes in the thermal properties of coal and coke with temperature.

The corrected thermograms of the study of Kessler and Romovackova (1961) were similar in form to those obtained by Glass (1954), predominantly endothermic.

Luther, et. al. (1966), examined the effect of factors such as heating rate, degree of packing of the sample, pressure and nature of gas phase, on the DTA thermograms of coals of different ranks. According to Lawson (1970), an expression was developed to give the value of ΔT (ΔT is the differential temperature between the two holders) in terms of packing density and thermal properties of the sample and the reference material for a given value of the heating rate. It was shown that changes in thermal properties with temperature can produce an endothermic effect at about 575-600°C. The DTA thermograms from the study of Luther, et. al. (1966) were similar to those of Glass (1954).

Yoshimura and Mitsui (1966), according to Lawson, show that the temperature of an endothermic peak at 400-500°C increases with rank but decreases when the pressure above the sample is reduced. Luther (1966) also found that in changing from a nitrogen atmosphere to a vacuum for pyrolysis, the size and temperature of the endothermic peak at 350-450°C were reduced. Luther, et. al. (1966), explained that this behavior is due to changes in the thermal properties of the materials.

Basden (1960) introduced a fluidized bed DTA system which essentially is the same as the classical DTA instruments except both the sample and reference holder beds are fluidized. According to Lawson (1970), this process offers considerable advantages since it provides uniform heat transfer within the bed and intimate contact between the particles and the fluidizing medium. As a result, uniform baselines and rapid response to thermal changes are possible. Disadvantages of the fluidized bed DTA are that large samples (on the order of 20-25 mg) are required and that the coals which tend to agglomerate (above about

400°C) cannot be fluidized. Stephens (1963) used the fluidized bed DTA to pyrolyze four Australian coals at a heating rate of 3°C/min and up to the temperature at which agglomeration prevented fluidization. Both endothermic and exothermic effects were reported for coals.

It is clear from these DTA studies that very little reliable information on quantitative energetics of coal pyrolysis is available. Kirov and Stephens (1967) presented results of studies by others (Terres, 1928; Pieper, 1956; Sanyal, 1960) in which the heats of carbonization and coking of coals were measured by techniques other than DTA. Briefly, Kirov and Stephens (1967) concluded that quantitative data on the energetics of coal pyrolysis is meagre.

In summary, the results to date on the kinetics of coal pyrolysis based on thermogravimetric analyses are inconsistent. Whereas, most studies (such as Van Krevelen, 1951; Boyer, 1953) observed first order kinetics, others (Kirov and Stephens, 1967; Smutkina and Kasatochkin, 1957) concluded that the kinetics of decomposition cannot be described as a single first order reaction. For natural fuels like wood and coal the thermal decompositions are much more complex due to the simultaneous progress of many reactions. This premise is supported, for example, by the extensive studies on the pyrolysis of woods at the Flame Dynamics Laboratory of the University of Oklahoma (Havens, 1969; Brown, 1972; Sardesai, 1973; Duvvuri, 1974; Muhlenkamp, 1975; Puskoor, 1976). It is further abetted by the present work which is dedicated to the kinetics of decomposition of U. S. coals.

In summary, most of the DTA work on coal was done during the 1950's; in general, the results reported by various investigators are

conflicting. For example, Whitehead and his co-workers (1951), King and his colleagues (1955), and Berkowitz reported primarily exothermic peaks. Conversely, Glass (1954), Kroger and Pohl (1957), and Luther, et. al. (1966) observed predominantly endothermic behavior for coal decomposition. Stephens (1963) observed both endothermic and exothermic behavior during fluidized-bed DTA of Australian coals.

To date, the application of the DSC technique to studies on coal pyrolysis has been limited. Mahajan, Tomita, and Walker (1976) reported coal pyrolysis experiments in a duPont "DSC cell." The present study has obtained quantitative measurements of the energetics of coal pyrolysis reactions on a Perkin-Elmer DSC-2 instrument.

Before preceeding with the substance of this study, it is essential to call attention to the basic differences, not only between the DTA and DSC techniques, but also between the two, so-called DSC instruments currently available. Failure to recognize these differences -- even the more subtle aspects -- is the source of confusion regarding the capabilities and limitations of these instruments. For this reason, the next chapter will attempt to clarify these points.

CHAPTER II

METHODS OF DIFFERENTIAL THERMAL ANALYSIS

Qualitative and quantitative thermal analyses have been practiced extensively. A text on differential thermal analysis by Smother and Chiang (1966) lists nearly 4000 publications between 1900 and 1966. These publications describe studies performed on many types of equipment which range from in-house fabrications to commercial instruments. Since neither equipment design nor experimental procedure has been standardized, most of these previous studies require detailed examination before the results can be properly evaluated. As if to aggravate this undesirable predicament, with the introduction of more sophisticated instruments for thermal analysis came new terminology such as differential scanning calorimetry (DSC) and dynamic differential calorimetry (DDC) to distinguish from classical differential thermal analysis (DTA). The purpose of the following discussion is to focus on the distinctive features of these various techniques and thereby establish a rational basis for selecting the most appropriate instrument commensurate with the task.

In his doctoral dissertation, Havens (1969) presented a comprehensive comparison of the various methods for thermal analysis. A substantial part of the discussion which follows represents a condensation from this reference.

Classical Differential Thermal Analysis

This technique, commonly known as DTA, being the oldest has been used most widely. It is based on measurement of the difference in temperature between an inert reference material and the sample material under investigation when both are heated in the same thermal environment as follows:

1. The reference material is so chosen that its physical and thermal properties such as density, heat capacity, and thermal conductivity are, as closely as possible, identical to the material under study.
2. The materials are then placed in two separate, but identically-built, chambers in a metal heating block. The sample and reference materials are located symmetrically with respect to a heating element.
3. A temperature measurement device, such as a thermocouple, is placed in each chamber.
4. As the materials are heated at a constant rate, the differences in sample and reference temperatures of the sample and reference materials are monitored with a differential thermocouple and are recorded as a function of time or temperature.

Consider two materials, one a sample and the other a reference, having identical properties in all respects except that the sample material experiences physical or chemical transitions with increasing

temperatures whereas the reference material remains inert and its properties do not change with temperature. Another questionable assumption is that the thermal properties of the sample material remain the same before and after transition.

Referring to Figure II-1, if the sample and reference materials are heated simultaneously and identically at a constant rate, the temperature of the reference material will increase linearly throughout the test, as shown by line A, since it does, as shown by Curve A, not undergo any transitions. On the other hand, the temperature of the sample material will increase identically with the temperature of the reference material until a temperature, T_1 , is reached. At this temperature, the sample temperature begins to lag the reference temperature due to an endothermic transition as shown by Curve B in Figure II-1. When the transition is completed, the sample gradually returns to the temperature of the reference material. If the difference between the sample temperature (T_s) and reference temperature (T_r) is recorded with respect to the temperature of the reference material (or the time, t), this difference, $\Delta T = T_s - T_r$, is zero until the sample transition temperature T_1 is reached. At temperature T_1 , the difference increases until a maximum is reached and then decreases until the sample and reference temperatures again become equal. Thus a pronounced 'peak' is obtained on a plot of ΔT vs T (or t); such a graph is called a thermogram.

In a typical DTA run of sample material, the number, shape, and temperature position of the various transitional peaks (endothermic or exothermic) are used as a means for the qualitative identification of the material under study. Since the magnitudes of the areas

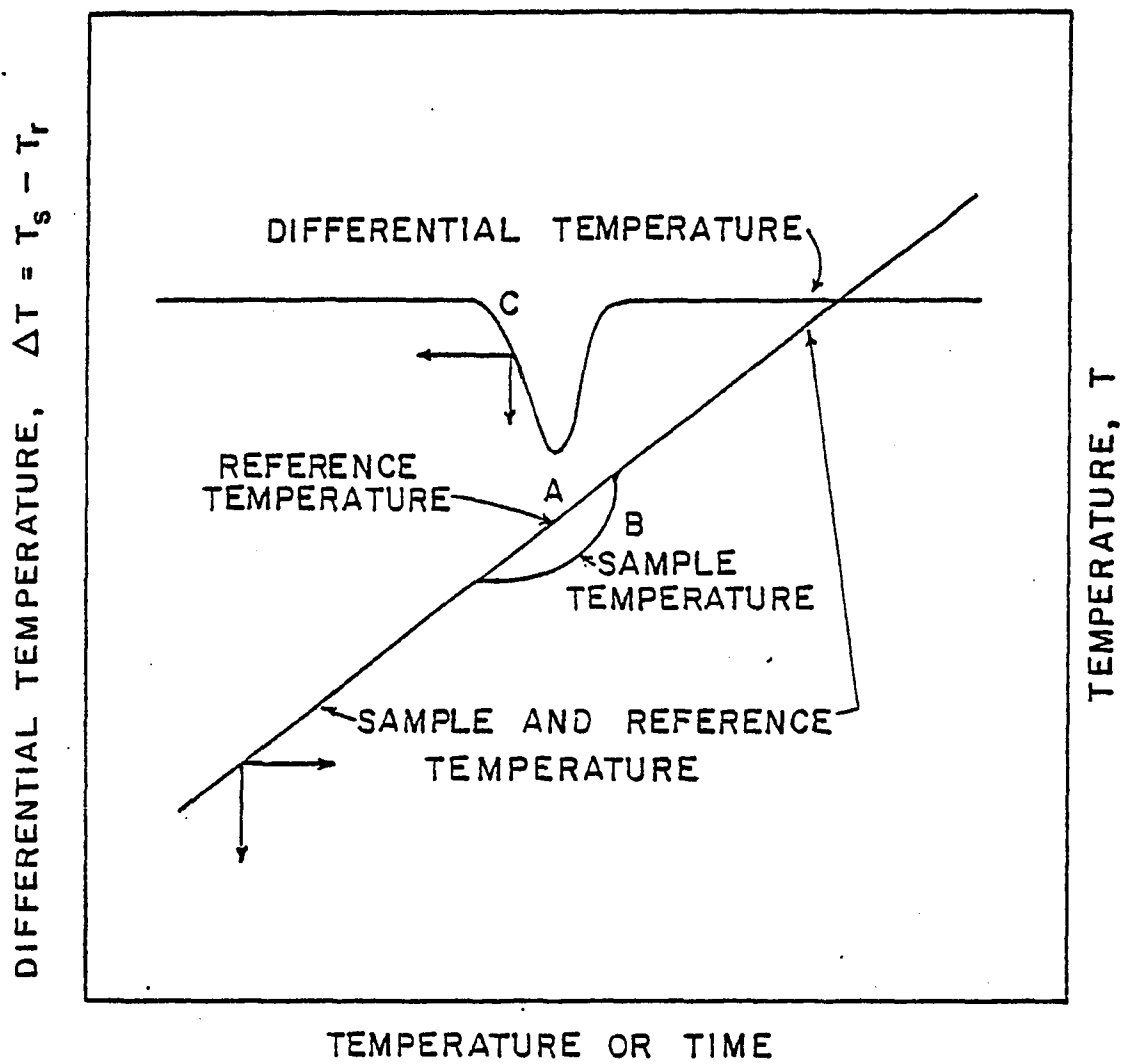


Figure II-1. Comparison of Sample Temperature, Reference Temperature, and Differential Temperature Curves in Differential Thermal Analysis.

circumscribed by the differential temperature curves are dependent on magnitudes of the heats of transitions, this graphical representation could be used, "theoretically," to compute quantitative heats of transitions for the sample. Unfortunately, it has been observed experimentally that the shape and extent of the DTA curves depend on factors related to the instrument and to the properties of the sample (Smothers and Chaing, 1966). The instrumental factors are as follows:

1. Furnace atmosphere
2. Furnace size and shape
3. Sample holder material
4. Sample holder geometry
5. Wire and junction size of thermocouples
6. Furnace heating rate
7. Response of recording instrument
8. Thermocouple location in sample.

The sample characteristics are as follows:

1. Practical size
2. Thermal conductivity
3. Heat capacity
4. Packing density
5. Swelling or shrinkage of sample
6. Amount of sample
7. Effect of diluent
8. Degree of crystallinity.

Consequently, it is not surprising that it is difficult to achieve consistent reproduction of DTA curves for a given sample even in the

same instrument. Although the temperatures at which the transitions occur are adequately reproducible, it is questionable whether the correct magnitudes for the heats of transitions are derivable from DTA.

Considerable discussion has been presented and several theories have been advanced for quantitative measurements on DTA. One of the most widely-held theories is due to Spiel (1945). He proposed to calculate the amount of energy involved during a transition of the sample as observed in DTA by

$$\Delta E_s = \frac{gh_s}{M_s} \int_a^c \Delta T dt \quad (\text{II-1})$$

where ΔE_s = change in heat content due to transition by the sample
over the time limits, cal/gm

g = geometrical shape constant, cm^2

h_s = heat transfer coefficient between the heating-block wall
and sample material, assumed constant, ($\text{cal}/\text{cm}^2 \text{ sec } ^\circ\text{C}$)

M_s = mass of the sample, gm

ΔT = difference in sample and reference temperature,

$$T_s - T_r, \text{ } ^\circ\text{C}$$

Equation II-1 requires the following assumptions:

1. The physical and thermal properties of the sample and reference material are assumed to be the same.
2. The geometrical constant (g) is assumed to be the same for the sample and reference.
3. It is assumed that no temperature gradient exists within the mass of the sample and within the reference materials.

4. The effect of differences in heat losses from the sample and reference holders are neglected.
5. The heat transfer coefficients (h_s and h_r) between the heating block wall and the two materials are assumed equal and constant.
6. The mass of the sample (M_s) is assumed to remain constant.

Assumptions 1, 2, and 3 are related primarily to the sample and reference materials. Selection of the reference material is made carefully to insure that its properties are nearly the same as the material under investigation. These properties may also be controlled by mixing diluent into the sample material and, thereby, making the properties of the mixture more similar to the reference material. Sizes of the sample and reference materials are kept to a minimum in order to minimize the possibility of a temperature gradient within the mass of the materials. (Most commercially available instruments use a sample smaller than 20 mg). Furthermore, instruments are carefully designed so that the sample and reference materials are located symmetrically with respect to the heating element.

Assumption 4 is the bane of all differential thermal analyses, whether it be in classical DTA or, as will be discussed later, in the more sophisticated DSC. With increasing temperatures the differences in heat losses from the sample and the reference become more pronounced due to disparate changes in their respective radiation characteristics. In addition, Boersma (1955) reports that heat loss from the materials by conduction through the thermocouple wires should be considered.

Assumption 5 can be accommodated, by means of an overall calibration constant which is obtained experimentally on the DTA instrument. This constant presumably takes care of any changes in the heat transfer coefficients.

Assumption 6 requires that the DTA be used for only "pure" transition wherein no mass is lost, such as by volatilization during the transition. In cases where a weight loss occurs during transition, its magnitude (as a function of time or temperature) must be determined experimentally by an independent measurement, such as TGA.

The coefficient of the integral gh_s/m_s , in Equation II-1 is determined experimentally by making a DTA run for a material of known weight and known heat of transition. Materials like calcium carbonate, benzoic acid and silver nitrate have been used as calibration materials for DTA studies.

According to Havens (1969) for "pure" (constant mass of solid) phase transitions, the results obtained with Speil's model, Equation II-2, show acceptable variation. However, where transitions are accompanied by changes in the thermal properties of the sample, the classical DTA technique which relies on direct contact of a thermocouple with the sample to sense temperature differences becomes questionable. Boersma (1955) and Schwiete and Ziegler (1958) observed that the heat effects indicated by a thermocouple embedded in a powdered sample are usually limited to the region immediately surrounding the thermocouple bead. During a transition, such as thermal decomposition in which particle rearrangement and/or chemical changes occur, the thermal resistance between the thermocouple junction and powdered sample changes sufficiently to invalidate the temperature differentials sensed by the instrument.

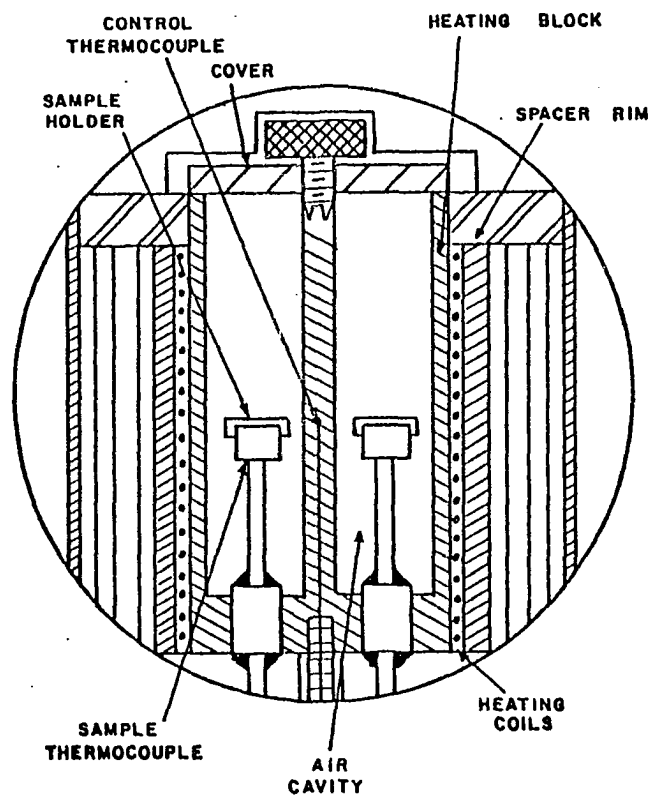
Dynamic Difference Calorimeter (DDC)

To circumvent the problem of sensing temperature in a sample whose thermal properties change during transitions, Boersma (1955) and Schwiete and Ziegler (1958) modified the classical DTA by transferring the thermocouples embedded inside the sample and reference materials to the external bottoms of the two holders for containing the sample and reference materials. Thus, the temperature difference between the two crucibles and their contents, rather than the contents alone, became the quantity to be measured. By further maintaining a thin layer of material in the crucible, it is claimed that much of the variability in the results from the classical DTA can be eliminated.

Based on the modification suggested by Boersma, the duPont Company produced a calorimetric cell which is shown in Figure II-2a. The holders for the sample and reference materials are located in separate air cavities in a heating block. A resistance heating element is wound around the block. Chromel-alumel thermocouples are welded to the bottoms of the sample and reference holders. The isolation of the sample and reference holders by the air cavity provides high resistance to heat transfer so that when the sample undergoes transition or reaction, the heat effect is retained by the holder. The energy change, ΔE_s , is claimed to be independent of sample size, specific heat, and packing density.

This calorimetry cell was latter replaced by a new design shown in Figure II-2b. Although it is marketed under the trade name, Differential Scanning Calorimetry Cell, it will be referred to herein as the duPont Cell to avoid confusion with a fundamentally different type (to be discussed subsequently) by Perkin-Elmer who apparently originated the

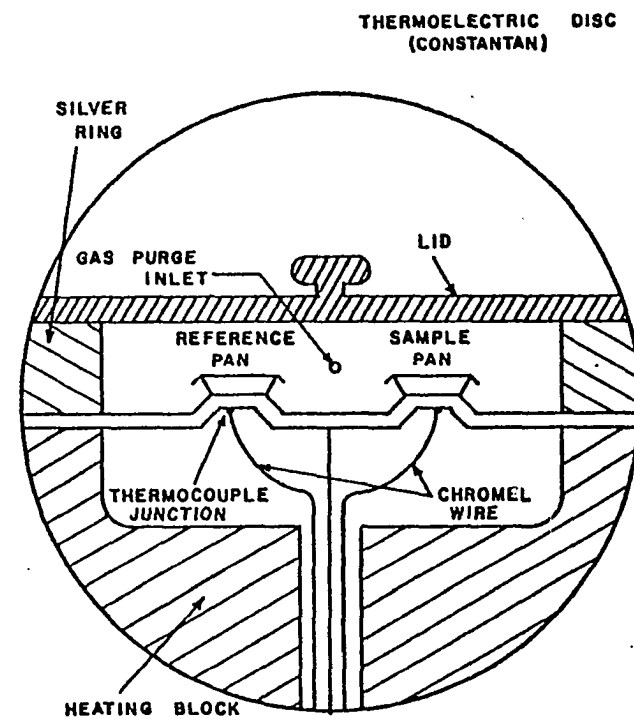
DU PONT BOERSMA-TYPE
DIFFERENTIAL CALORIMETRY CELL



CELL CROSS-SECTION

(a)

DU PONT DIFFERENTIAL
SCANNING CALORIMETRY CELL



CELL CROSS-SECTION

(b)

Figure II-2. Schematic Diagrams of "Dynamic Difference Calorimetry"
Type Cells Manufactured by duPont.

trade name. The duPont design includes a thermoelectric disc consisting of a constantan plate with raised platforms for placement of sample and reference in shallow 6.6 mm diameter aluminum pans. The constantan disc serves two functions: 1) it provides a heat transfer path from the block to the sample and reference and 2) it is an integral part of the temperature measuring thermocouples. A chromel wire is welded at the center of each platform providing a thermocouple junction in direct contact with the bottom of each pan for measurement of temperature difference. An alumel wire is welded at the center of the sample platform providing a chromel-alumel thermocouple junction for determining the temperature of the sample pan.

A calorimetric constant has to be calculated for either of the duPont cells. The following relation is used:

$$\Delta E_s \text{ (mcal/mg)} = E \frac{A \Delta T_s T_s}{Ma} \quad (\text{II-2})$$

where E = calibration coefficient (mcal/°C-min)

A = peak area (cm²)

ΔT_s = sensitivity of the y-axis of the recorder (°C/cm)

T_s = sensitivity of the x-axis of the recorder (°C/cm)

M = mass of sample (mg)

a = heating rate (°C/min)

The relation is of the same form as the model reported by Speil (1945), Equation II-1, in this thesis. The calibration coefficient, E , is determined with a material of known weight and transition energy, as previously discussed for classical DTA. Unfortunately, the coefficient, E , is sensitive to changes in the conductive and radiative heat transfer contributions to the differential temperature measurement. Therefore,

it is quite temperature dependent as shown by the calibration curve in Figure II-3 which was obtained from several metals with accurately known heats of fusion. This variability in the coefficient represents a major drawback in this instrument even though it offers a distinct improvement over classical DTA.

Differential Scanning Calorimeter (DSC)

Perkin-Elmer developed an entirely new instrument. To call attention to the fact that it represented a fundamentally different approach to differential thermal analysis, they introduced the terminology, differential scanning calorimeter (DSC). Whereas the classical DTA, the Boersma modification and the duPont versions previously described rely on a measurement of the temperature difference between the sample and the reference materials while both are being heated at identical rates, the Perkin-Elmer design is based on a "null-balance" principle which maintains the sample and reference materials at the same temperature by adding or abstracting heat to or from the sample and reference materials to compensate for the energy absorbed or evolved by the sample during a transition. Therefore, since the Perkin-Elmer instrument measures directly the differential energy transfers to the sample and reference materials, individual electrical heating elements have to be provided for the sample and reference holders so that the electrical power which must be dissipated at each holder to maintain a zero temperature difference can be controlled separately. Thus, power can be increased to the sample holder while reducing power at the reference holder, or vice versa. In actual practice, however, the differential power is split equally between the two holders to improve the thermal response

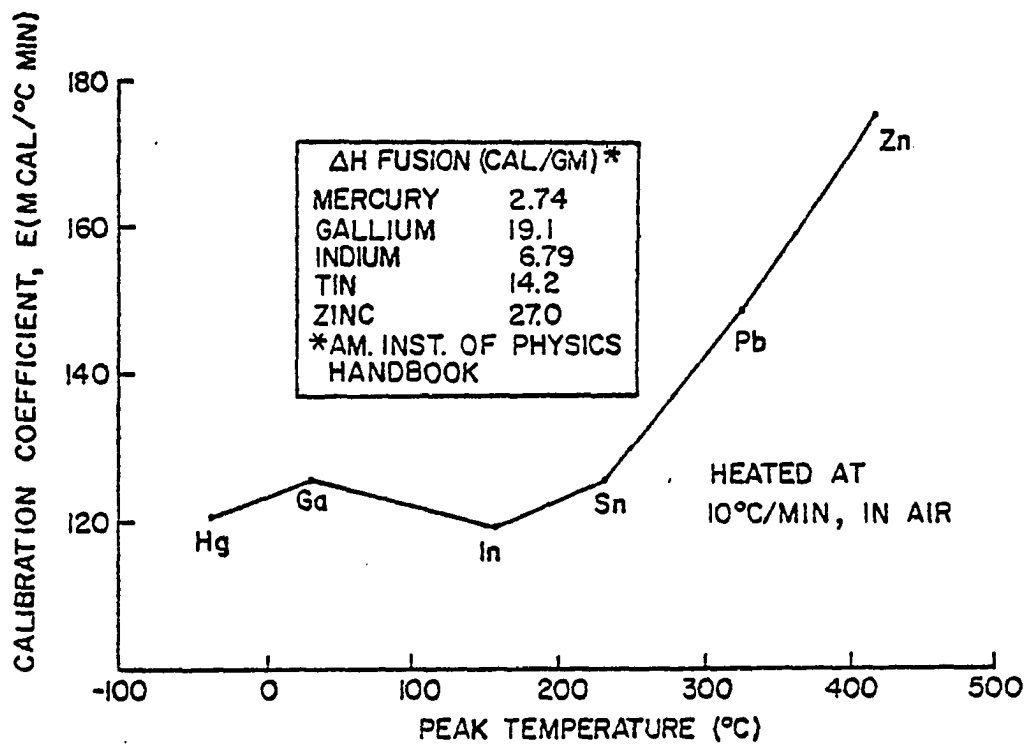


Figure II-3. Typical Calibration Curve of duPont Calorimeter (Havens, 1969).

characteristics. Another distinctive feature of the Perkin-Elmer instrument is that the temperature sensors are platinum resistance elements rather than the thermocouples which are used in other differential thermal analyzers. A simplified cross-section of the Perkin-Elmer calorimeter is shown in Figure II-4.

A block diagram of the instrument is presented in Figure II-5. The maintenance of equality of temperature in the sample and reference holders is obtained by a differential temperature control loop. Temperature signals measured by the platinum resistance thermometers in the sample and reference holders are sent to the differential temperature amplifier via a comparator circuit. The comparator circuit determines which of the two temperatures is greater. The output of the amplifier is used via a feedback circuit to adjust the differential power increment into the reference and sample holders in the direction and magnitude necessary to correct any temperature difference between them. A signal proportional to this differential power is transmitted to a potentiometric recorder producing a recording from which the differential power versus time (or temperature) can be obtained. The area under a sample transition peak is claimed to be directly proportional to the heat energy absorbed or liberated by the sample.

In a separate control loop, a programmer provides a linearly increasing electrical signal that is proportional to the desired rate of rise in the sample temperature. This programmer signal is compared with a signal received from the platinum resistance thermometers imbedded in the sample and reference holders via an average temperature computer. The error signal is used, via feedback, to effect a linearly increasing temperature in both the sample and reference holders.

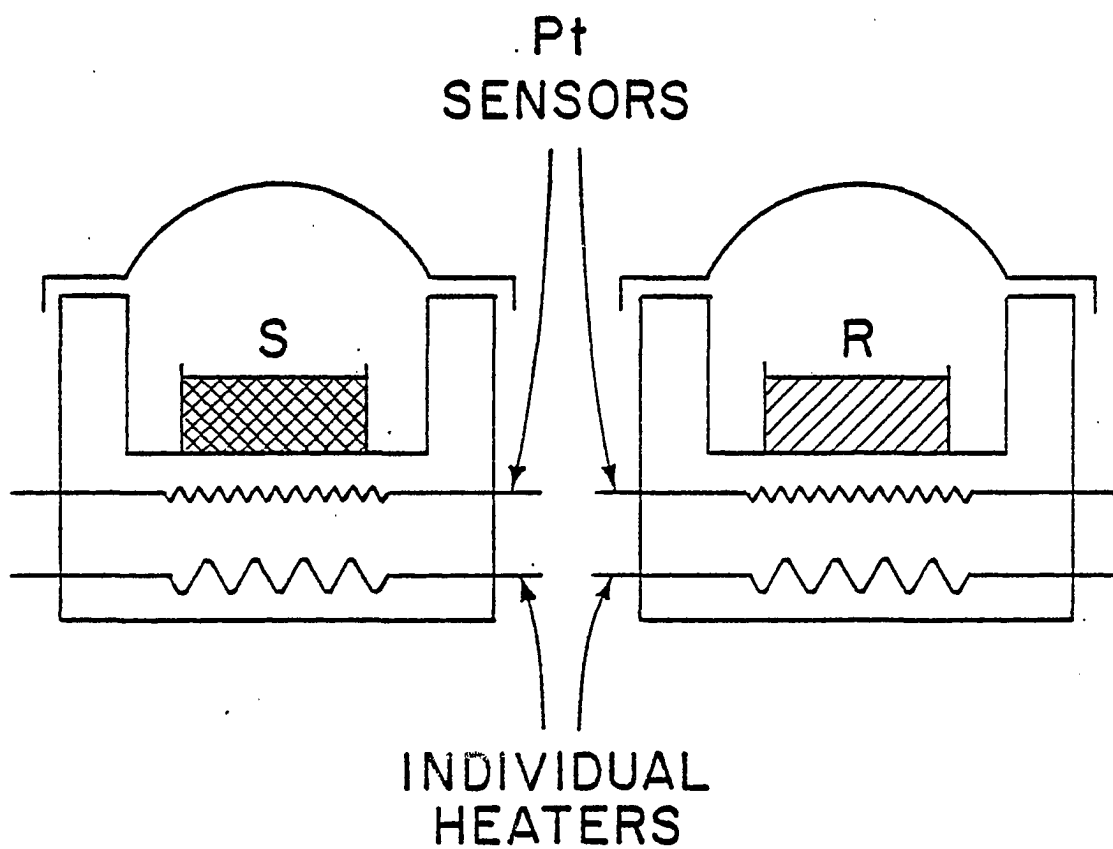


Figure II-4. Schematic of Differential Scanning Calorimeter
Manufactured by Perkin-Elmer.

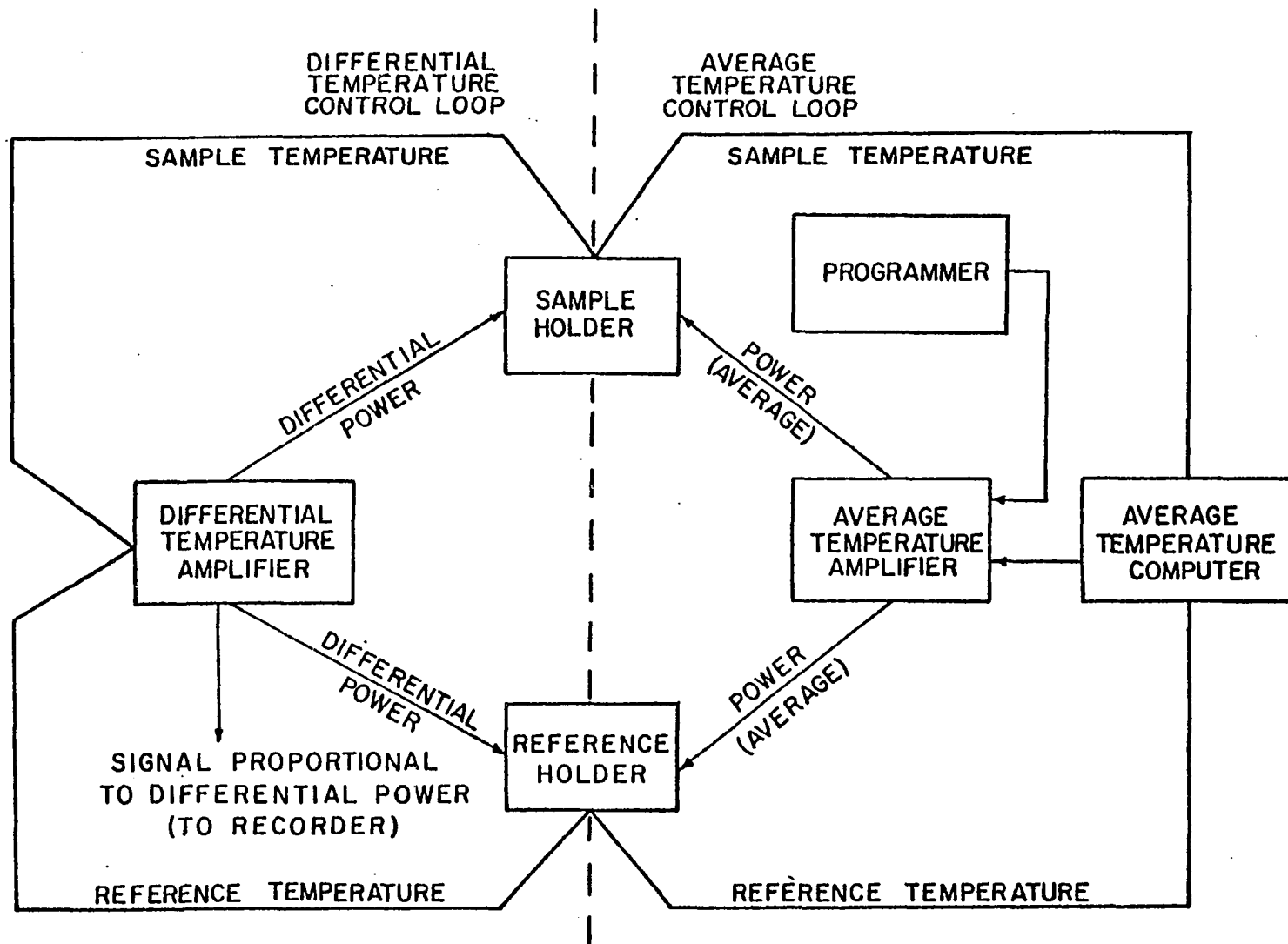


Figure II-5. Block Diagram of Perkin-Elmer Calorimeter.

To describe how feedback temperature control is applied in the Perkin-Elmer DSC-2 system, the simplified presentation by Muhlenkamp (1975) should suffice. First, consider a DTA or DDC system in which a feedback temperature controller is not used. In this case, then, sample transitions are identified solely by the difference in temperature between the sample and reference pans. This "open-loop" temperature difference (ΔT) can be expressed as the product of the energy of sample transition (Q_s) and the thermal resistance (R) between the sample and surroundings,

$$\Delta T = Q_s R \quad (\text{II-3})$$

However, if the loop is closed by introducing negative feedback so that the energy flow to the sample pan is proportional to the difference in temperature between the sample and reference holders, the closed loop temperature difference ($\Delta T'$) is related to the amount of energy input (Q) and the amplifier gain, G by

$$Q = -G\Delta T' \quad (\text{II-4})$$

For this closed loop system, the temperature difference is given by a relation similar to Equation II-3,

$$\Delta T' = (Q_s + Q)R \quad (\text{II-5})$$

Eliminating $\Delta T'$ from the two previous equations,

$$Q = -Q_s \frac{1}{1 + 1/GR} \quad (\text{II-6})$$

If the product, GR , is made very large by design, the power from the feedback temperature control (Q) is equal but opposite in sense to the energy effect due to a sample transition (Q_s). In other words the amount of energy supplied by the feedback control exactly

counteracts the energy of sample transition. Furthermore referring to Equation II-4, as the amplifier gain becomes very large, $\Delta T' \rightarrow 0$ to achieve a "null" balance. Thus, negative feedback temperature control can be used in this manner to monitor the energy changes within the sample holder.

In the Perkin-Elmer system, it is advantageous to split the differential power requirement between the sample and reference holder. Thus, when the sample absorbs power (endothermic) from the holder at a rate ΔQ_s , $\Delta Q/2$ additional power is delivered to the sample holder and $\Delta Q/2$ less power is provided to the reference holder.

To summarize, by conducting a comprehensive analysis of electrical circuit analogs and the transient response characteristics of the sample temperature to a sudden heat flow rate Havens (1969) concluded that isothermal calorimetry was superior to any approach available for obtaining quantitative energy content information from samples undergoing transitions. In isothermal calorimetry, an intensive parameter, temperature, is the independent, reproducible variable while the energy content, an extensive parameter is the dependent, measured variable. This technique has high resolution capabilities as a consequence of being able to achieve small time constants. By utilizing proportional feedback temperature control, the Perkin-Elmer instrument approaches the performance of a true, isothermal scanning calorimeter.

In adiabatic calorimetry, the roles of the variables are just the opposite from isothermal operation; namely, the intensive parameter is the dependent variable while the extensive parameter is the independent, measured variable. Although many suggested designs and applications

have been reported in the literature, its low resolution capabilities (large time constants) make them inapplicable for the purposes intended herein despite the fact that it has advantages of simplicity over the isothermal method.

The classical DTA and its descendents of the DDC type do not represent a good approach to either isothermal or adiabatic calorimetry since they inherently lack reproducibility of quantitative measurement of heat affects for materials undergoing transitions with evolutions of gases and changes in the thermal properties of the sample.

Although the Perkin-Elmer instrument was judged to be superior to any instrument available for thermal decomposition studies of the type reported herein, it too appears to have serious deficiencies. As will be shown in Chapter IV, this instrument failed to give reproducible (neither qualitative nor quantitative) information above 500°C even though its capability is purported to extend to 750°C.

CHAPTER III

EXPERIMENTAL PROCEDURE

The coal samples used in this project were supplied by the 1) Bureau of Mines, United States Department of Interior (six samples) and 2) Pennsylvania State University (three samples).

The place of origin, mine and seam designation of the nine coal samples are listed in Table III-1 along with identification letters to facilitate future reference in this report. Tables III-2 and III-3 summarize analyses provided by the suppliers for their coal samples.

The coal samples, as received, covered a broad range of particle sizes, up to minus 20-mesh. Since the amount of coal required for each test was on the order of 5 mgs or less, all samples were ground in a mortar and pestle to less than minus 200-mesh to assure a more representative or homogeneous sample for TGA and DSC measurements on the Perkin-Elmer instruments.

TGA Calibrations

Thermogravimetric analyses of nine samples were made from ambient to 1000°C at heating rates of 160, 80, 40, 20, and 10°C/min on a TGS-1 thermobalance with UU-1 temperature programmer. These instruments are shown in Figure III-1.

TABLE III-1

SUMMARY OF COAL SAMPLES

Laboratory Identification Letter	Coal Type
From U. S. Department of Interior	
A	Illinois Coal #6, Orient Mine
B	Indiana Coal #6, Chrisney #1 Mine, Spencer County
C	Kentucky Coal (Blend), Seams #9, 11, 12 Ohio Co., Western Kentucky
D	Pennsylvania Coal, Clearfield Lower Kittanning Bed, Manor #44, Mine, Clearfield, PA
E	West Virginia Coal, Pittsburgh Seam, Ireland Mine, WV
F	Wyoming Coal, Rock Springs, Wyoming
From Penn State University	
G	Saline Co., Illinois, Channel Sample (Penn. State No. PSOC-26)
H	Kentucky #14 Seam, Run of Mine Sample (PSOC-216)
I	Kentucky Coal, Muhlenburg Co., Channel Sample (PSOC-272)

The TGS-1 thermobalance consists of a microelectronic weighing mechanism, shown in Figure III-2, which monitors weight changes of the samples as it is heated by a furnace. As shown in the Figure III-2 the sample is suspended on a nichrome wire which is long enough to protect the weighing system from the hot corrosive decomposition gases. A baffle plate assembly is situated slightly above the sample pan which also protects the weighing system from the decomposition products. The

TABLE III-2

ANALYSIS OF COAL SAMPLES SUPPLIED BY THE BUREAU OF MINES, U. S. DEPARTMENT OF INTERIOR

IDENTIFI- CATION LETTER	ORIGIN	RANK OF COAL	PROXIMATE ANALYSIS						ULTIMATE ANALYSIS** (as received basis) percentage				
			As Received Percentage				d.a.f.* Percentage		C	H	N	S	O
			Moisture	Ash	Volatile Matter	Fixed Carbon	Volatile Matter	Fixed Carbon					
A	Illinois	NA [†]	2.5	14.1	33.7	49.8	40.4	59.6	65.9	4.7	1.4	1.8	12.1
B	Indiana	hvbb ¹	6.4	14.0	38.7	40.9	48.61	51.38	61.7	5.1	1.2	5.8	12.2
C	Kentucky	hvab ²	4.2	16.5	36.2	43.1	45.65	54.35	60.7	4.8	1.2	5.5	11.3
D	Penn- sylvania	mvb ³	0.8	14.6	23.0	61.6	27.18	72.81	73.7	4.3	1.4	4.1	1.9
E	West Virginia	hvab ²	1.6	8.1	41.6	48.6	46.12	53.88	73.8	5.3	1.4	3.8	7.6
F	Wyoming	hvb ⁴	1.5	2.0	NA	NA	NA	NA	75.0	5.4	1.7	0.8	13.6

* Dry, Ash-free basis

** The balance of the ultimate analysis is ash and moisture in the amounts reported for the proximate analysis

† Not available

- (1) High volatile B bituminous, moist Btu per pound greater than 13000 but less than 14000
- (2) High volatile A bituminous, dry fixed carbon less than 69 percent on mineral-matter free basis, dry volatile matter greater than 31 percent, moist Btu per pound 14000 or greater
- (3) Medium volatile bituminous, dry fixed carbon between 69 and 78 percent on mineral-matter free basis, dry volatile matter between 22 and 31 percent
- (4) High volatile bituminous

TABLE III-3
ANALYSIS OF COAL SAMPLES SUPPLIED BY THE PENNSYLVANIA STATE UNIVERSITY

IDENTIFI- CATION LETTER	ORIGIN	RANK OF COAL	PROXIMATE ANALYSIS						ULTIMATE ANALYSIS** (as received basis) percentage					
			As Received Percentage				d.a.f.* Percentage		C	H	N	Cl	S	O
			Moisture	Ash	Volatile Matter	Fixed Carbon	Volatile Matter	Fixed Carbon						
G	Illinois	hvc ¹	12.10	9.53	35.78	42.59	45.66	54.44	60.58	4.40	0.89	0.00	5.85	6.65
H	Kentucky	hvb ²	5.54	7.74	38.34	48.38	44.21	55.79	68.8	5.0	1.52	0.03	4.3	7.48
I	Kentucky	hvb ²	6.11	8.36	37.25	48.28	43.55	56.44	67.99	4.75	2.07	0.01	3.89	6.84

* Dry, Ash-free basis

** The moisture and ash contents are the same as reported for the proximate analysis

(1) High volatile C bituminous, moist Btu per pound between 11000 and 13000; either agglomerating or non-weathering

(2) High volatile bituminous

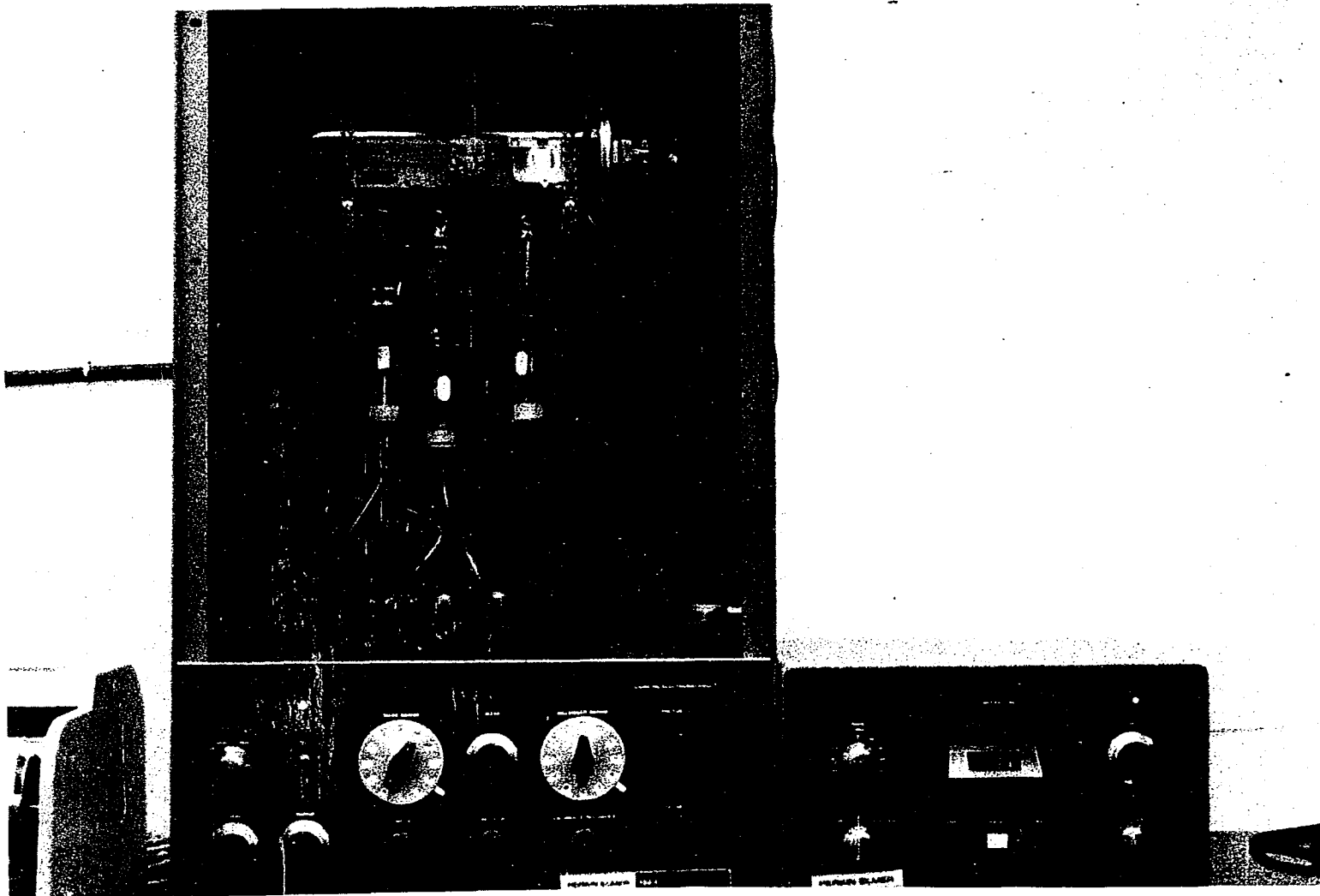


Figure III-1. Perkin-Elmer TGS-1 Thermobalance and UU-1 Temperature Programmer.

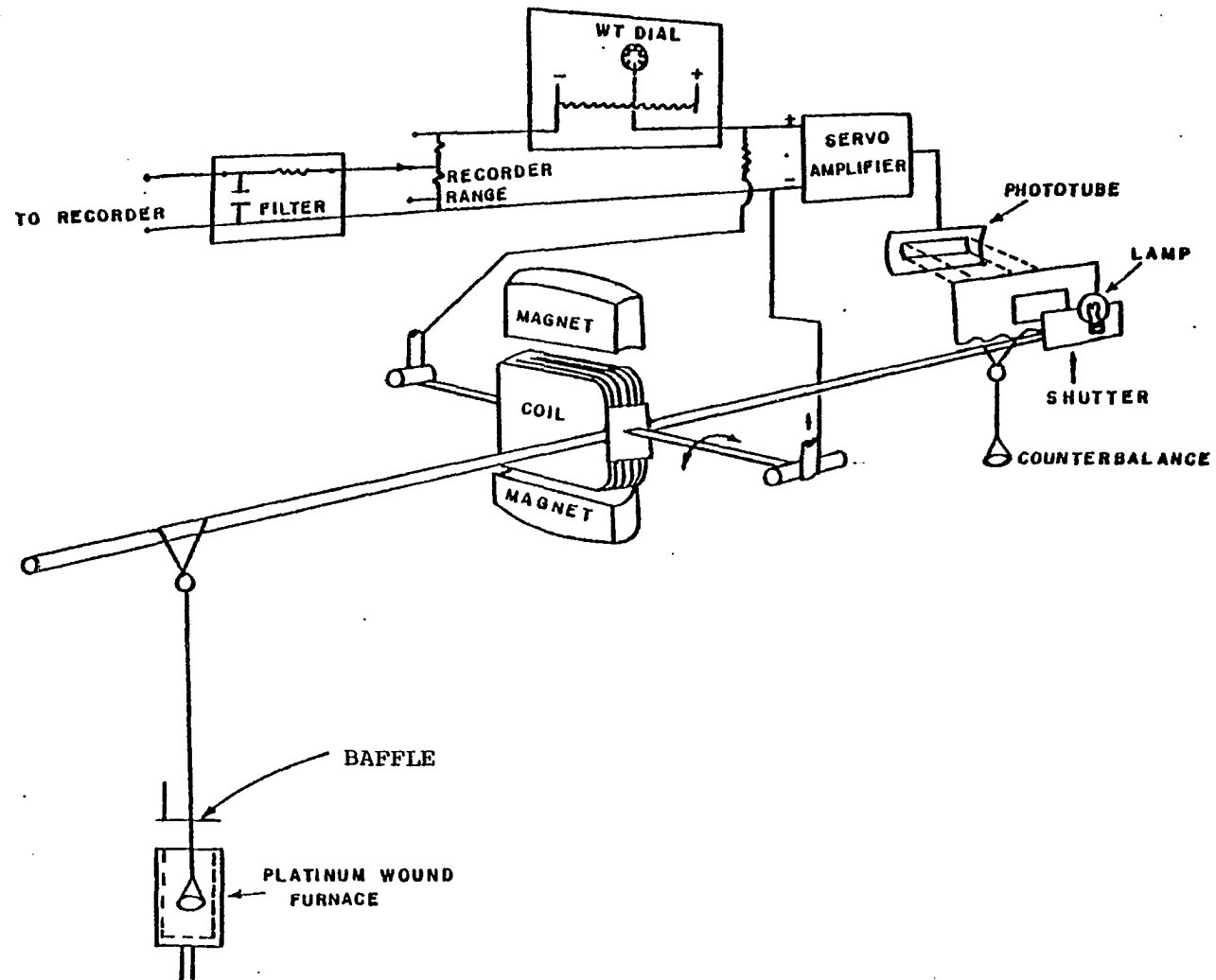


Figure III-2. Schematic Diagram of Perkin-Elmer TGS-1 Weighing Mechanism.

entire weighing mechanism is enclosed in a glass chamber within which a nitrogen atmosphere is maintained.

The furnace assembly for the TGS-1 instrument consists of a platinum wire wound on a ceramic cylinder. The heating element was protected from decomposition products by a ceramic collar and quartz wool plug (Brown, 1973). The furnace acts both as a heater and a sensor; it is controlled by a signal from the UU-1 temperature programmer.

The TGS-1 thermobalance is designed to be operated in only one mode; either weight loss or rate of weight loss may be recorded with respect to time or temperature. A Cahn time derivative computer, which is shown in Figure III-3, was used to obtain a rate of weight loss signal. The weight loss signal from the TGS-1 and rate of weight loss signal from the computer were recorded on a two-channel Leeds and Northrup recorder.

The TGS-1 furnace should be calibrated in a manner that its temperature corresponds to the temperature displayed on the UU-1 programmer dial.

The temperature calibration for the TGS-1 furnace, as displayed on the UU-1 programmer dial, is obtained by observing the magnetic transition temperatures for several ferromagnetic standards listed in Table III-4. The temperatures at which these standards lose their magnetic characteristics are well defined. This transition appears as a sharp loss in weight on the recorder chart. The temperature at which this behavior occurs is compared with the temperature indicated on the programmer dial.

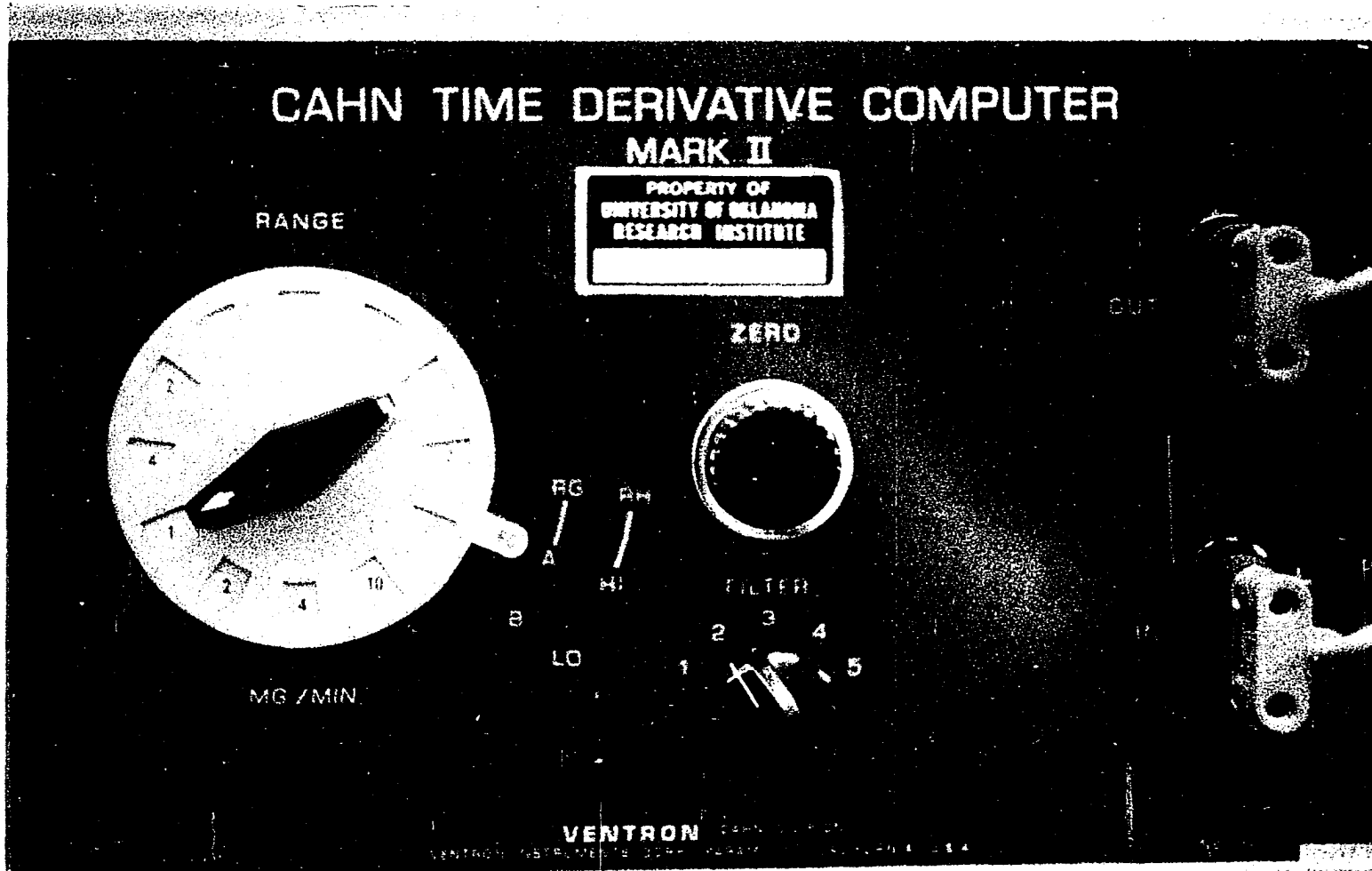


Figure III-3. Cahn Time Derivative Computer.

TABLE III-4

MAGNETIC STANDARDS FOR TGS-1 FURNACE CALIBRATION

Metal	Magnetic Transition Temperature (°C)
Monel	65
Alumel	163
Nickel	354
Mumetal	395
Nicoseal	438
Perkalloy	596
Iron	780
Hi-Sat 50	1000

The furnace calibration procedure can be summarized as follows:

1. A slow flow of nitrogen is maintained through the glass chamber.
2. A small amount of ferromagnetic alloy is placed on a platinum sample pan. A small amount of alumina is also added to improve heat transfer.
3. The sample pan is then suspended on the nichrome wire.
4. The furnace is carefully placed around the sample pan.
5. A magnet is placed around the outside of the glass chamber in such a manner that the sample pan does not touch the furnace wall. A slight contact is easily recognized by the presence of "spiky" noise on the recorder chart.
6. The sample is heated at a rate of heating for which the furnace is to be calibrated.
7. A sharp peak on the derivative weight loss curve is recorded at the

transition temperature of the standard. Transition temperatures for all standards are observed.

8. These indicated temperatures are compared with the actual temperatures for all standards listed in Table III-4. The difference between the actual and the indicated temperature is minimized by adjusting the dials provided for calibration on the TGS-1 thermobalance and the UU-1 programmer.
9. The procedure is repeated with re-adjusted dial settings until the deviation from the actual temperature is minimized as much as possible.

After dial settings were optimized for minimum difference between the indicated and actual temperatures, a temperature correction was applied to these indicated temperatures to obtain actual temperature. Figure III-4 shows the results of temperature calibration for thermogravimetric experiments made at five heating rates of 160, 80, 40, 20, and 10°C/min. For each heating rate, the temperature calibration was made before the TG runs on coals were made.

For TG experimentation at all heating rates, except 10°C/min, at least two runs were made for each coal sample to check repeatability. Since longer exposures to pyrolysis products caused failures in the furnace, only one TG run for each coal was made at the 10°C/min heating rate.

The experimental procedure corresponds to the calibration standards listed on the Table III-4 except that the use of a magnet is not required. The weight loss and rate of weight loss for coals are recorded as the temperature is increased at a constant rate of heating.

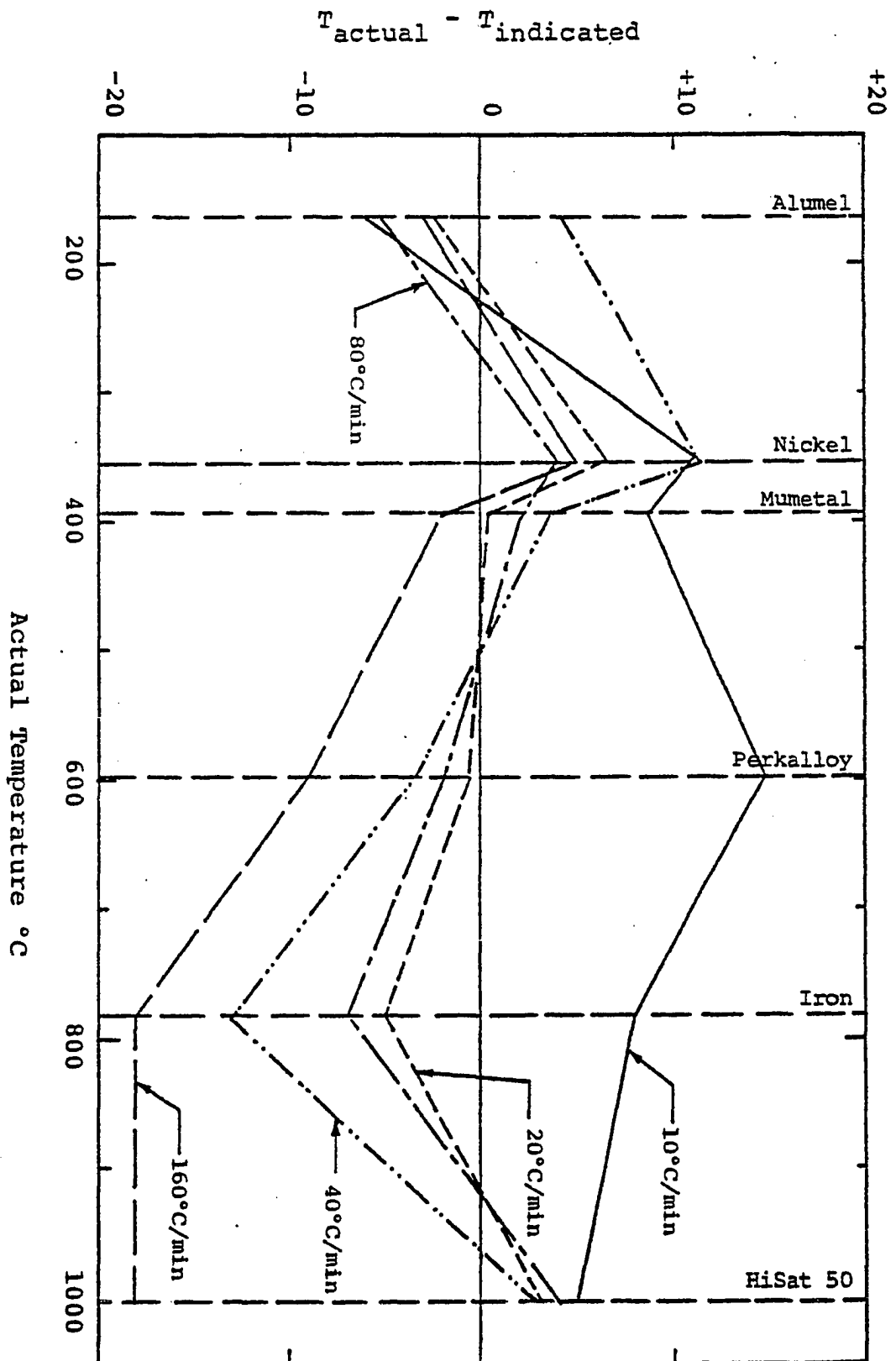


Figure III-4. Calibration Curves for TGS-1 Furnace.

DSC Calibrations

Energy changes occurring during pyrolysis of coals were measured at three heating rates of 320, 160, and 40°C/min on a Perkin-Elmer, DSC-2 differential scanning calorimeter. This instrument is shown in Figure III-5. A discussion on the principle of operation of Perkin-Elmer DSC system has been described in the previous chapter. Following are the important features of the DSC-2 instrument:

1. Each sample holder (reference and sample) has an individual heater and a temperature sensor. As discussed earlier this provision is the most important feature of direct calorimetric measuring systems. The holders, which are shown in Figure III-6, are made of platinum-iridium alloy and are mounted on an aluminum block.
2. A sophisticated temperature programmer allows individual control of heating and cooling rates (in multiples of two from 0.31°C/min to 320°C/min) within 100 to 1000°K. The programmer has controls for either automatic operation or manual operation. Water is used as cooling medium for experiments above ambient conditions. For sub-ambient temperatures, liquid nitrogen or dry ice may be used as a coolant.
3. Control dials are located on the instrument that permit baseline optimization and temperature and energy calibrations.
4. The differential power required to maintain the 'balance' between the sample holder and the reference holder is supplied by a feedback temperature control; this output is recorded in millicalories per second on the recorder chart. This differential power is equivalent to energy absorption or evolution by the sample.

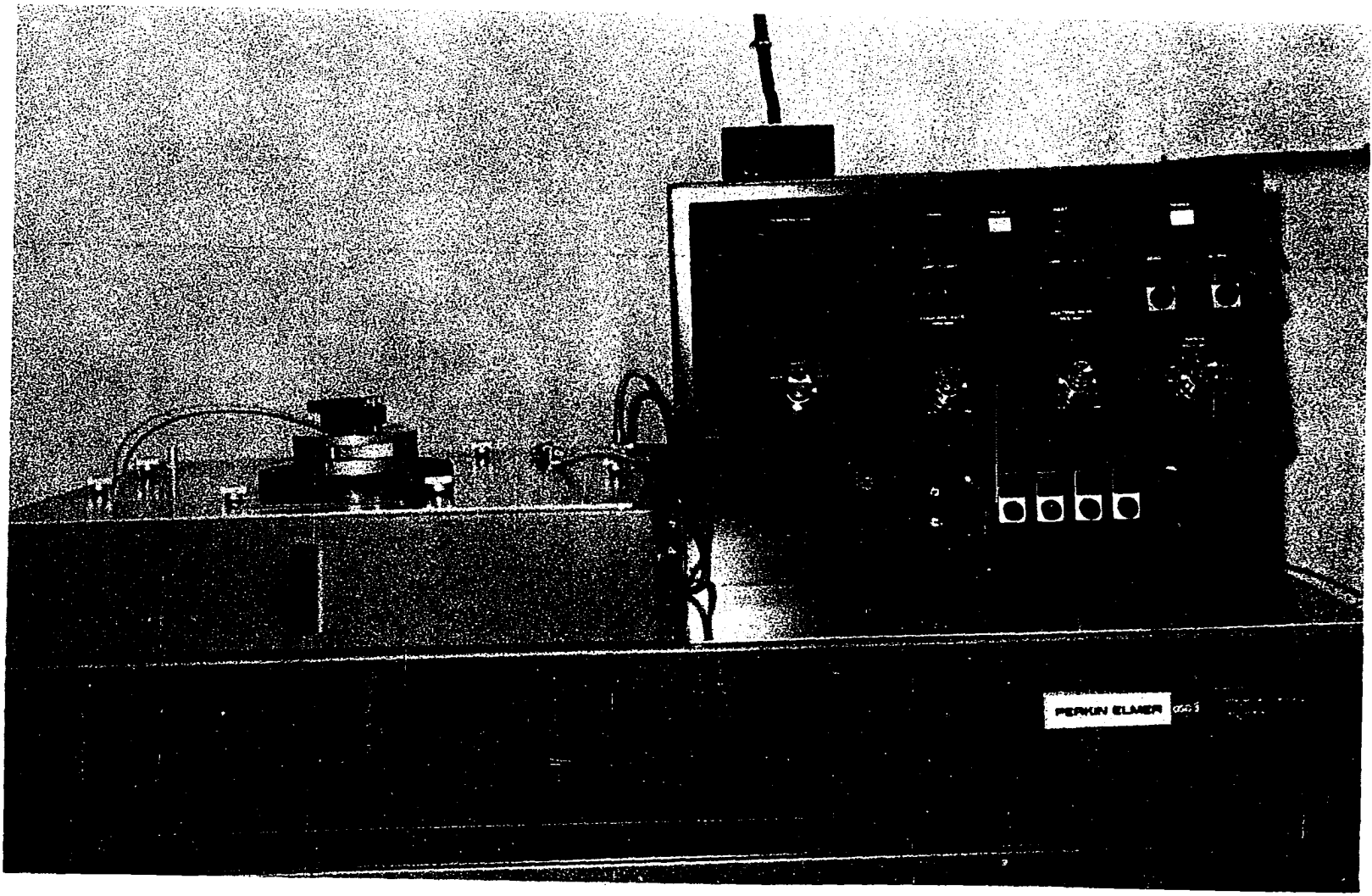


Figure III-5. Perkin-Elmer Differential Scanning Calorimeter DSC-2.

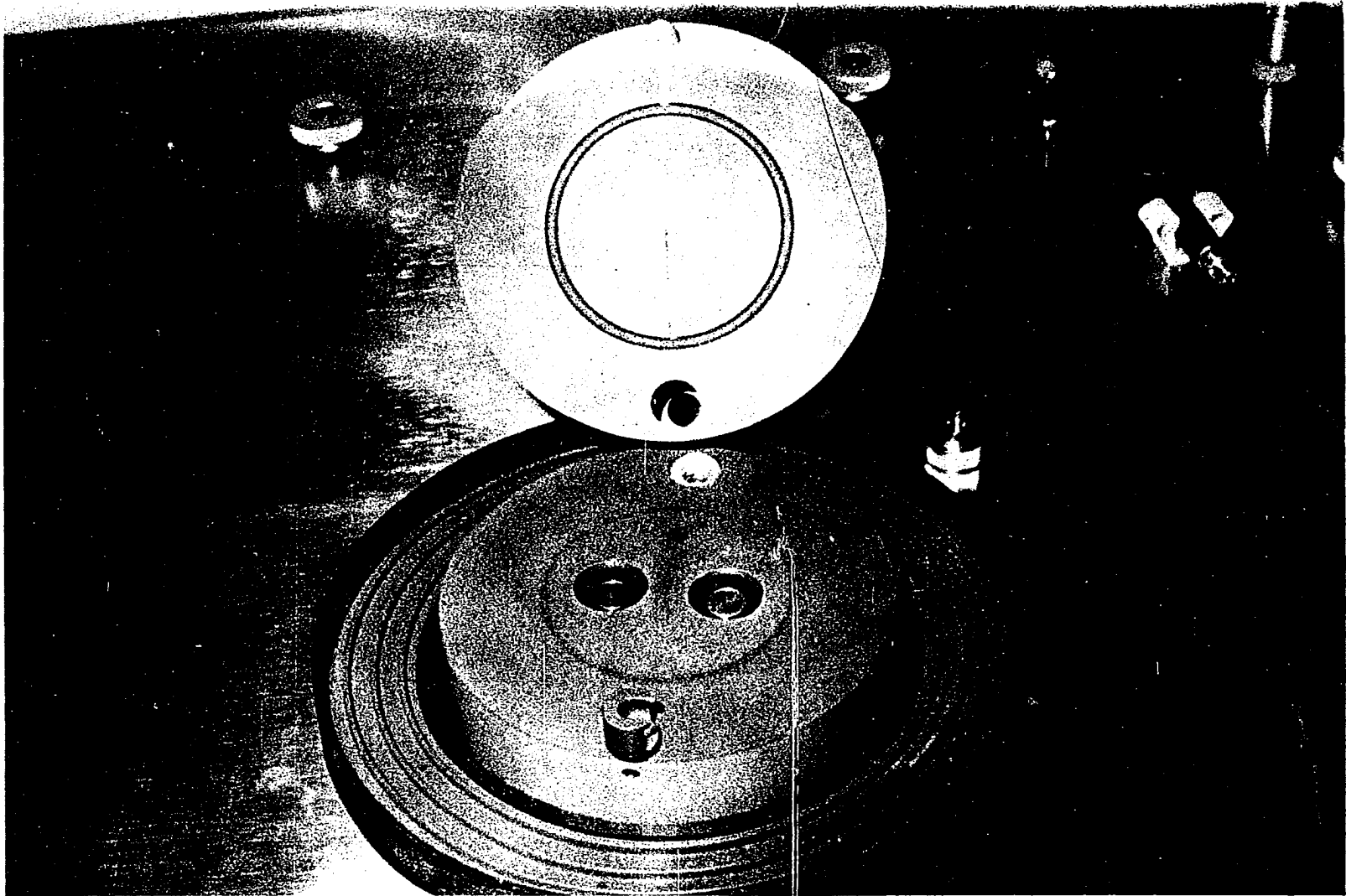


Figure III-6. DSC-2 Sample Holder Assembly.

A Brooks flow controller was installed in the nitrogen flow line of the DSC-2 instrument to alleviate difficulties in obtaining a baseline of zero-slope within the temperature range 50-727°C (Muhlenkamp, 1975). Calibrations for temperature and energy are required for the DSC-2 instrument.

Temperature Calibration

The temperature calibration of the DSC consists of heating standard materials which have known transition temperatures, such as indium and potassium chromate. Since the temperature programmer for the DSC-2 is linear, the use of only two of the calibration standards listed in Table III-5 is necessary. A transition temperature of a standard is observed which is then compared with the known exact transition temperature. The controls are provided on the instrument for minimizing the deviation from the exact transition temperatures of the standards. The method for calculating the changes required in the control dials is included in the manufacturer's operating manual; it has also been discussed in the doctoral dissertation of Duvvuri (1974).

It was observed that transition temperatures of indium, potassium sulfate, and potassium chromate were within 4°C from the actual temperatures of the standards listed in Table III-5. Therefore, no calibration adjustments were made to the factory-adjusted controls.

Energy Calibration

This calibration consists of measurements of the peak areas corresponding to the transition energies and the ordinate displacement in the determination of specific heat.

TABLE III-5

TRANSITION TEMPERATURES AND ENERGIES OF TRANSITIONS
FOR STANDARDS USED ON THE DSC-2 INSTRUMENT

Material	Transition Temperature (°C)	Transition Energy (cal/gm)
Indium	156.6	6.8
Tin	231.88	14.45
Lead	327.47	5.5
Zinc	419.47	25.9
K ₂ SO ₄	585.0 ± 0.5	7.95
K ₂ CrO ₄	670.0 ± 0.5	8.50

Peak Area Measurements. A "Range" sensitivity switch located on the front panel of the equipment, adjusts the sensitivity of the output signal in millicalories per second on a 10 mv recorder span. This sensitivity is accurate to within 5 percent and must remain independent from effects of change in mode of operation, sample size, and geometry. The exact value of sensitivity is obtained by observing the area under the transition peak for the Standards listed in Table III-5.

The area under the transition peak of a weighted indium standard is measured with a planimeter. The instrument constant, K, which is a proportionally constant in the relationship between the actual and indicated range, is calculated as follows:

$$K = \frac{(\Delta H_f) (W_{in}) (S)}{(R) (A_{in})} \quad \text{(III-1)}$$

where ΔH_f = heat of transition of standard (mcal/mg)

W_{in} = weight of indium standard (mg)

R = setting of range control (mcal/sec) on the instrument
divided by chart span in inches

A_{in} = area under the transition curve of the standard (in²)

S = chart speed (in/sec)

Ideally, the value of the instrument constant should be unity, but this value is not critical since the actual range is obtained by the product of the instrument constant K and the range indicated on the instrument. However, the 'w calib' control located on the instrument may be adjusted to make the value of $K = 1$.

After the value of the instrument constant is obtained, the transition energy of the sample can be calculated by the relation

$$\Delta H_t = \frac{(K) (R) (A_{\text{samp}})}{(W_{\text{samp}}) (S_{\text{samp}})} \quad (\text{III-2})$$

where ΔH_t = heat of transition for sample (mcal/mg)

W_{samp} = weight of sample (mg)

S_{samp} = recorder chart speed (in/sec)

K = instrument constant

R = indicated range setting divided by chart span in inches

A_{samp} = area under sample transition curve (in²)

The sensitivity calibration can be made simultaneously with the temperature calibration since the standards required for both are the same. This energy calibration must be made when studying samples which go through sharp transitions like melting, fusion, crystallization, etc., on the DSC-2.

Ordinate Displacement. A standard (Al_2O_3) of known specific heat is required to calibrate the ordinate displacement recorded on the chart paper. The method is as follows:

1. The baseline (no sample) must be optimized before the sapphire scan. This no-sample baseline is a reference line with which the sample displacement is compared at all temperatures.
2. A weighed sample of sapphire (Al_2O_3) is placed in a gold sample pan (the pan must be the same as the one used for the baseline).
3. The sample pan is placed in the sample holder in the same orientation as it was originally placed before the baseline scan. The platinum holder cover is also placed on the holder.
4. Controls set for the baseline scan must remain the same.
5. After a few minutes at the lower limit, the temperature scan is initiated at the heating rate at which the calibration is desired.

The ordinate displacement constant K_d can be calculated from

$$K_d = \frac{(W_{\text{sap}})(Cp_{\text{sap}})}{D_{\text{sap}}} \quad (\text{III-3})$$

where W_{sap} = weight of sapphire (mg)

Cp_{sap} = specific heat of sapphire (mcal/mg-°C)

D_{sap} = displacement for sapphire scan from the baseline scan
(mm)

Specific heat is obtained from Figure III-7 in which the dependence of specific heat on temperature is reported.

The constant K_d does not change with temperature and is proportional to the heating rate and sensitivity setting on the DSC. The ordinate calibration constant changes approximately by the same factor

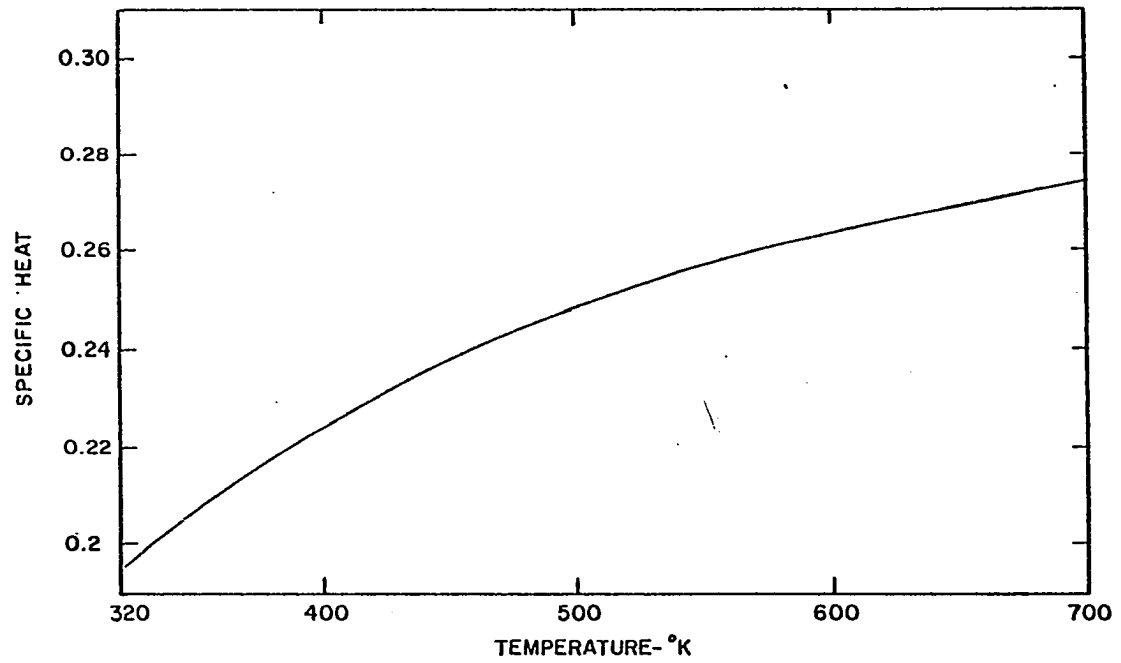


Figure III-7. Effect of Temperature on Specific Heat of Sapphire.

as the heating rate changes. For the same sensitivity setting on the instrument, as the heating rate is doubled, the value of this constant is approximately halved. The values of ordinate calibrations for the three heating rates are reported in Table III-6.

After the constant K_d is known, the procedure is repeated using the sample instead of sapphire. The dependence of sample specific heat with respect to temperature is known by making displacement measurements at various temperatures and using the following relationship:

$$C_{p_{\text{samp}}} = \frac{K_d D_{\text{samp}}}{W_{\text{samp}}} \quad (\text{III-4})$$

where D_{samp} = displacement of sample scan from baseline scan (mm) at the temperature for which the specific heat of the sample is required

W_{samp} = weight of sample (mg)

$C_{p_{\text{samp}}}$ = specific heat of sample (mcal/mg - °C)

The temperature and energy calibrations were checked three times during the course of the DSC experimentation on coal pyrolysis.

Experiments With Coal

The weight loss and rate of weight loss curves for coal obtained on the TGS-1 thermobalance were reproducible for runs made at the same heating rate up to 1000°C. However, measurement of the energetics of coal pyrolysis on the DSC-2 instrument presented a number of problems:

1. Large sample and baseline deflections were observed due to experimentation over a wide temperature range.
2. Baseline drift during the sample scan.

Table III-6
 VALUES OF ORDINATE CALIBRATION CONSTANT (K_d) AT DIFFERENT HEATING RATES FOR DSC

HEATING RATE °C/min	WEIGHT OF SAPPHIRE SAMPLE, mg	TEMPERATURE °K	DIFFERENCE BETWEEN THE SAPPHIRE SCAN AND THE BASELINE SCAN AT TEMPERATURE* (in Number of Chart Divisions)	SPECIFIC HEAT AT TEMPERATURE cal/gm-°C	ORDINATE CALIBRATION CONSTANT K_d^{**}
320	19.58	450	58.9	.23835	.0792
320	19.58	900	71.3	.28791	.0790
160	19.56	900	36.1	.28791	.1560
40	19.58	900	8.5	.28791	.6630

* A Leeds and Northrup Chart No. 990173 (100 divisions in 25 cm span) was used for all the DSC runs. However, the sensitivity setting on the instrument was 20 mcal/sec and the recorder full scale was 20 mv for all DSC runs.

** The constant (K_d) has units of calories per chart division per °C. Therefore, the instrument sensitivity must be mentioned with the value of the constant, as done here by the above footnote.

3. Determination of the scan up to 727°C (the maximum operating temperature of the DSC-2) at which temperature the pyrolysis of the coal samples should be essentially complete.

The following discussion describes the attempts to solve the problems listed above.

DSC operation over a wide temperature range (323-1000°K) resulted in a large deflection during the baseline and sample scans. A DSC setting of 20 mcal/sec and recorder chart range of 20 mv full scale were used for all experimental runs. It was observed that a large deflection occurs between the baseline isothermal level and the scan level, when the heating mode is initiated. This deflection is increased with an increase in heating rate; it is also affected by a change in the weight balance of the sample and reference holders. The amount of this deflection decreases when the thermal mass on the reference holder is decreased. The reference holder usually contains an empty, clean, gold sample pan and a gold lid in balance with the sample holder during DSC experimentation. Since no reference sample material (as in DTA) is required for DSC work, the thermal mass of the reference holder could be varied to advantage. Therefore, only a sample pan lid was used in the reference holder for 320°C/min DSC experiments, and an empty clean sample pan without a lid was used for 160°C/min and 40°C/min DSC experimental runs to reduce the amount of deflection when the scan is initiated. Since all measurements are made relative to a baseline obtained under the same conditions as the sample run, this arrangement does not affect the results. It only shifts the scan on the chart paper. This shifting of the scan by 10 percent of the chart width was found to be very useful because the

millivolt output range of the DSC-2 equipment was limited to approximately 67 divisions from recorder zero in either direction with the recorder setting of 20 mv full-scale and DSC sensitivity setting on 20 mcal/sec. These problems emphasize the importance of sample size selection (usually 1.80 to 2.0 mg) for experimental work since the magnitude of chart deflection observed during the DSC sample scan is related to the sample size. In fact, for a scan of some samples (for example sample E, G and I) a smaller sample size than the usual (1.80 ± 0.005 mg) was used to avoid exceeding the output range during DSC experimentation at the 320°C/min heating rate.

The problem of baseline shift in DSC experimental work has been discussed by Havens (1969). The baseline is a reference line against which the behavior of the sample deflection is compared. The baseline establishes levels of heat losses from the system that would occur without the sample. If any change in the heat losses established by the baseline occurs, the baseline changes. In order to keep this level of heat losses the same, the conditions for the baseline must be exactly repeated for the sample scan and should remain the same during the sample scan. Unfortunately, most organic solids (including coal) liberate heavy products during decomposition. These products condense on the cooler areas of the sample holder system during the sample scan, such as the sample cover. Condensation changes the heat loss levels observed during the baseline scan as well as the baseline level during the sample scan. The variations in the heat losses are due to changes in the surface emissivity of the sample holder cover. (Havens, 1969, estimated that a change in emissivity of only 10 percent would result in a

discrepancy in the differential heat measurement of an order of magnitude greater than the transition heat being monitored). If the pyrolysis products are removed as quickly as they are given off by the sample, they cannot condense on the cover. For this reason, a high rate of nitrogen flow of 110°cc/min was maintained during the DSC experimental work in this project. With a nitrogen flow rate higher than 110°cc/min, the DSC thermogram became excessively "noisy."

Another approach to avoid baseline shift is to start the experimental work with a sample holder cover whose emissivity equals the surface emissivity of the holder cover at the end of the sample scan so that the heat transfer characteristics of the cover do not change. Several heat-resistant paints were applied on the sample holder cover in the present study but were found to deteriorate because of the high temperatures in the coal experiments. In this work, the problem was alleviated somewhat by darkening the cover with "Oildag," a suspension of graphite in petroleum oil (Acheson Colloids Company). This coating should have an emittance comparable to the coal decomposition products. The surface of the sample holder cover was first coated with paint and then oxidized to provide a surface on which the "Oildag" would adhere. The "Oildag" coating was then applied to the inside of the cover. It was first heated in an oven for a minimum period of one hour and then baked in the DSC at the maximum operating temperature of the instrument (1000°K) until no further vaporization could be observed from the coating. This coating adhered well to the cover of the holder and was also found to be quite resistant to high temperatures. Because of progressive degradation of the coating during a run and cleaning of the covers between

sample runs, a new coating was applied every 3 to 4 runs. Only one cover (sample holder) was coated on the inside during preliminary experimentation. Subsequently, it was observed in experimentation that both covers had to be fully coated (inside and outside). All calibration and sample runs except nine runs (one for each sample) at 160°C/min heating rate were made with fully-coated covers. The first nine runs were made with the coating only on the inside of the sample holder cover.

In order to determine the extent of coal pyrolysis at the end of the scan and to develop a consistent procedure for DSC experimentation on coal, it was decided to perform experiments initially on one coal sample. The coal sample H was selected since several runs, not necessarily of the same sample size, had been made at the time of decision. Also, since the magnitude of the DSC output signal is dependent on the coal sample size, the sample size was restricted to 1.90 ± 0.05 mg during these experiments. Experimental runs were made at 160°C/min heating rate with a partially coated (inside only) sample holder cover.

Several runs were made with coal samples over the temperature range 50-727°C. Some isothermal runs at 727°C were also made. The procedure for scans was similar to that described for the ordinate calibration run of sapphire. The baseline for both the scan and isothermal section were obtained; the procedure was repeated for coal sample H. The following observations were made from these experiments.

1. Over the temperature range, 50-450°C, the difference between the baseline and the sample level remained approximately the same for all runs. This difference indicates that over this temperature range, the emissivity of the sample holder cover does not

change, and therefore, the baseline does not change.

2. Figure H-1 in Appendix H shows a rate of weight loss curve with respect to temperature for coal sample H obtained on the TGS-1 at a heating rate of 160°C/min. It is indicated by the figure that the maximum devolatilization of the coal sample occurs at 525°C and continues up to about 650°C. Within the temperature range 450-650°C, the maximum sample weight loss occurs as the products are liberated, they condense on the cover, changing its emissivity and causing the baseline to drift upward.
3. After the scan, the sample was held isothermally at 727°C. At this temperature, further degradation of the sample is very slow, as was observed by weighing the sample at the end of the isothermal runs held for different lengths of time.
4. After a period of 2 to 4 hours at 727°C, the final energy level of the sample scan gradually returns close to the final isothermal baseline level. This behavior is due to degradation of products condensed on the sample holder cover during the scan and, simultaneously, a very slow degradation of the charred coal sample. To verify these observations, the weight changes of the sample holder cover were monitored for several runs. The cover, which was coated on the inside with "Oildag," gained some weight during the sample scan and lost weight during the isothermal section of the run. These weight changes indicated that volatiles condense on the cover during the scan and degrade during the isothermal part of the run. Thus, isothermal runs at 727°C cannot yield a reliable result since the DSC thermogram obtained during the isothermal period also relates to

degradation of the condensed coal-devolatilization products. Degradation of the charred coal sample contributes very little to this effect since the weight loss of the coal sample during the isothermal portion of the run was very small. This negligible weight loss indicates that pyrolysis of the sample is completed during the scan.

5. When the sample and reference holder covers are coated with "Oildag" on both the inside and outside, the final energy level (at this end of the sample scan) was closer to the baseline level than the final energy level attained with a single, partially-coated cover. This closer approach to the baseline level is due to a decrease in the emissivity change during the sample scan.

The observations from DSC experiments on coal sample H should be applicable to all of the other coal samples investigated in this study because most of the coal samples are of the same, high-volatile bituminous, type. Thus, it appears that the coal devolatilization is completed during the scan up to 727°C at a heating rate of 160°C/min. Since only small amounts of products are evolved during the early part of the scan (50-450°C), the baseline does not change in this region. On the other hand, the baseline does shift (even when two fully "Oildag" coated covers were used) over the temperature range 450-727°C due to condensation of the pyrolysis products on the sample holder cover. To summarize, the problem of baseline shift could not be completely solved. Therefore, the DSC scans for all coal samples were corrected for the baseline shift. The procedure for this correction will be described in the next chapter.

CHAPTER IV

RESULTS

In this chapter the pertinent results from the thermogravimetric analyses and differential scanning calorimetry for the nine coal samples will be presented and, where possible, will be compared with related studies by others. Complete thermograms and supporting data are given in the appendices.

Thermogravimetric Analysis of Coal

The experimental procedure for thermogravimetric analysis described in Chapter III was used to obtain weight loss and rate of weight loss thermograms for nine coal samples described in Tables III-1 and III-2. The TGA data during pyrolysis of coals were obtained at heating rates of 160, 80, 40, 20 and 10°C/min on a Perkin-Elmer TGS-1 thermo-balance over a 25-1000°C temperature range. To assure consistency and reproducibility, at least two runs were made for each sample at each heating rate except only one run was made at the 10°C/min heating rate.

After obtaining the raw TG curves on the recorder, these curves are converted to actual weight loss and rate of weight loss as a function of temperature. Since the recorder readings are directly proportional to the weight remaining in the sample pan, this conversion is straight

forward with knowledge of the initial and final sample weights. The conversion of the rate-of-weight-loss recorder readings to actual rate of weight loss readings is based on the area under the rate of weight loss curve. On a curve of the derivative of non-dimensional weight with respect to temperature, dW/dT vs. temperature, the area under the curve must equal unity. Using this principle, the recorder readings are converted to rate of weight loss readings by setting the area under the non-dimensional rate of weight loss curve to unity. All temperature readings are corrected to the calibration temperatures by least squares.

A typical run has been shown for each of the heating rates studied in this work in Appendices A through I. The experimental runs of the thermogravimetric analyses of coal Sample A are shown in Figures A-1 through A-5 of the Appendix A. Similarly, TGA results for other coal samples (B through I) are shown in Appendices B through I. Details of all TG runs (such as, sample, residue weights, and other pertinent information) made in this project are presented in Table J-1 of Appendix J.

From thermogravimetric runs for all coal samples, the following observations were made:

1. It was observed that most of the coal sample weight loss occurred in the approximate temperature range of 400-700°C.
2. The difference between the initial sample weight and the final residue weight indicated that about the same percentage of initial weight of a coal sample was lost at the end of TGA runs made at different heating rates.

3. Most coal samples lost about 25 to 45 percent of the original sample weight during a heating cycle (ambient to 1000°C). Among all samples, a medium volatile coal Sample D was observed to lose the lowest amount of the sample weight (25-30%). The other eight coal samples, which were ranked as high volatile (Tables III-2 and III-3) lost approximately 30 to 45% of the sample size.
4. With the exception of Sample D, all coal samples either contract or show no volumetric change upon heating at different heating rates. Pennsylvania coal Sample D expanded when heated at high rates of heating (160°C/min and 80°C/min). At other heating rates the coal Sample D showed no observable volume change. This observation is in agreement with the observation reported by Johnson and Auth (1951) for lower volatile coals.
5. When DTG curves of all samples obtained at one heating rate are compared, it is observed that the temperature at which maximum rate of weight loss occurs is higher for coal Sample D - a medium volatile Pennsylvania coal - than those for other coal samples. Van Krevelen, et. al. (1956), have reported that the temperature of maximum devolatilization increases with decrease in volatile matter content. Therefore, the observation for coal Sample D is consistent with that reported by Van Krevelen, et. al. (1956). A relationship between the temperature of maximum devolatilization and rank (or percent fixed carbon d.a.f.) of the coal could not be presented here because the coal samples selected for this investigation do not show sufficient variation in percentage fixed carbon or volatile matter content.

6. In Figures IV-1 through IV-18, the effect of heating rate on the TGA curves of all nine samples is presented. The DTG curves for all samples are shown only in the temperature range over which high weight losses occur in order to show distinguishable peaks for all heating rates. It is observed from these figures that the TGA curves are shifted to higher temperatures with increasing heating rates. Therefore, the temperature at which the maximum weight loss occurs also shifts to a high value with the increasing heating rate. Other investigations have reported similar observation for coals (Van Krevelen, et. al., 1956; Brown, 1957; Howard, 1963), for woods (Havens, 1969; Muhlenkamp, 1975; Duvvuri, 1974), and for plastics (Woodard, 1974). TGA curves for 10°C/min are not shown on Figures IV-1 to IV-18, since the 10°C/min TG and DTG curves follow the 20°C/min TGA curves very closely. The data for 10°C/min may be obtained from Figures 5 of Appendices A through I for coal Samples A through I or from Table J-1 of Appendix J.

The weight loss and rate of weight loss thermograms of all coal samples are similar to TG and DTG curves obtained by several investigators, (Havens, 1969; Brown, 1972; Muhlenkamp, 1975; Woodard, 1974) for woods, wildland fuels, and plastics. They used a thermal decomposition kinetic model, originally proposed by Goldfarb, et. al. (1968), in their studies. The same model was used to process the TGA curves of coal samples. The model is described below:

$$\frac{-dW}{dt} = Ae^{-E/RT} (W)^n \quad (\text{IV-1})$$

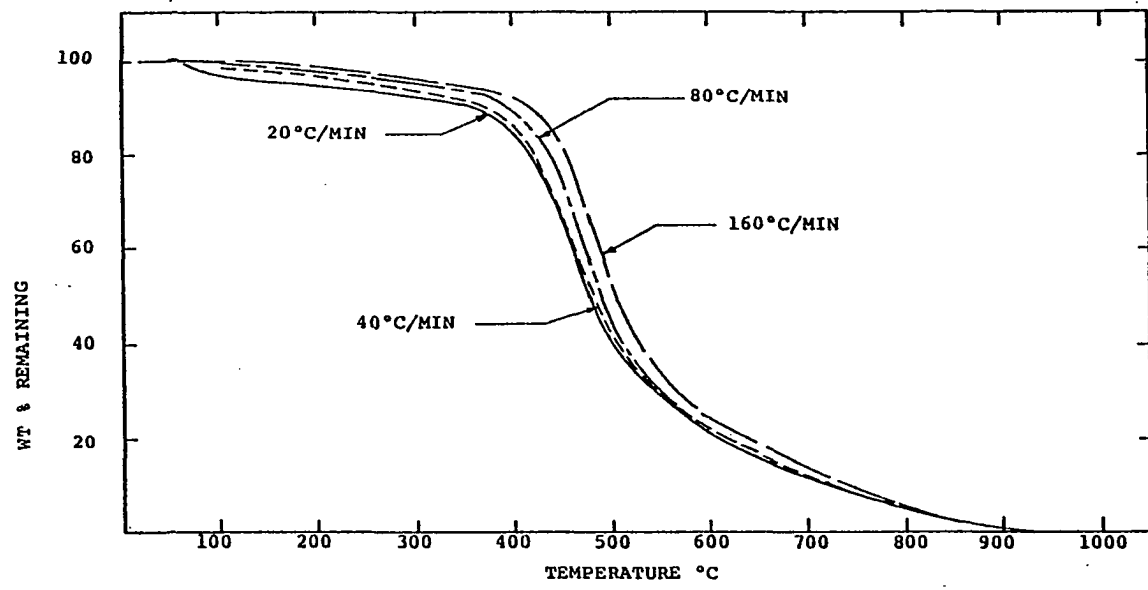


Figure IV-1. Effect of Heating Rate on TG (Weight Loss) Thermogram for Coal Sample A. (From Figures A-1, A-2, and A-4 of Appendix A).

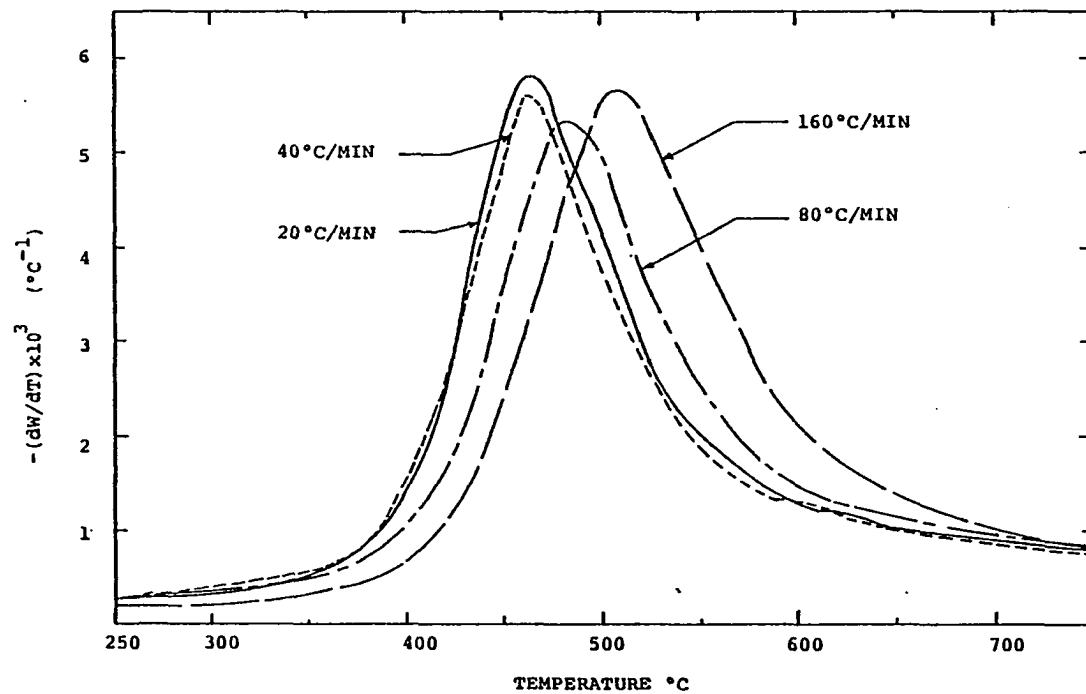


Figure IV-2. Effect of Heating Rate on Differential TG (Rate of Weight-Loss) Thermogram for Coal Sample A. (From Figures A-1, A-2, and A-4 of Appendix A).

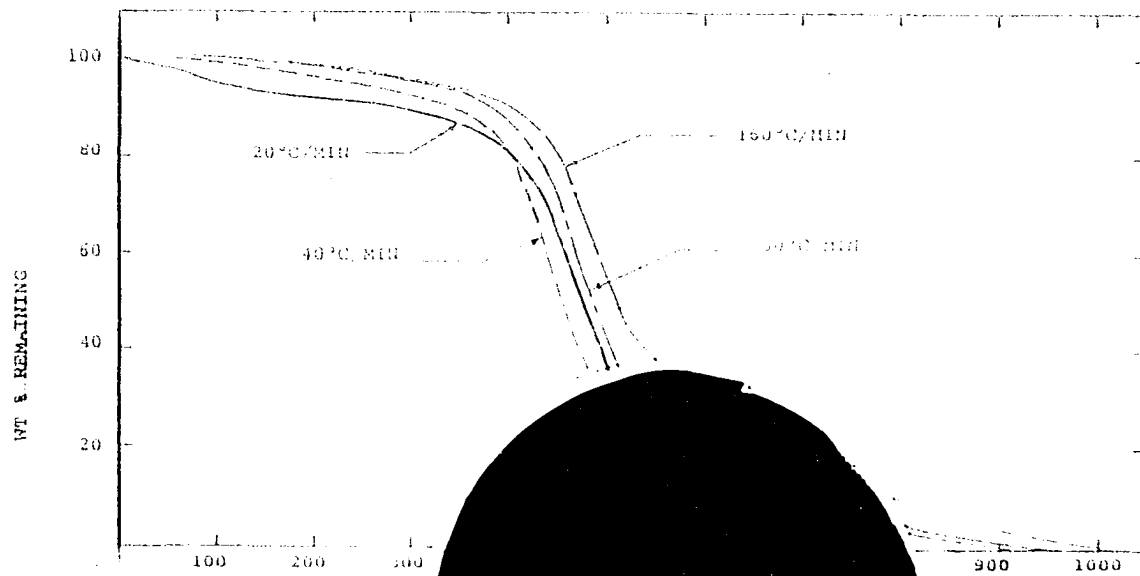


Figure 11

and

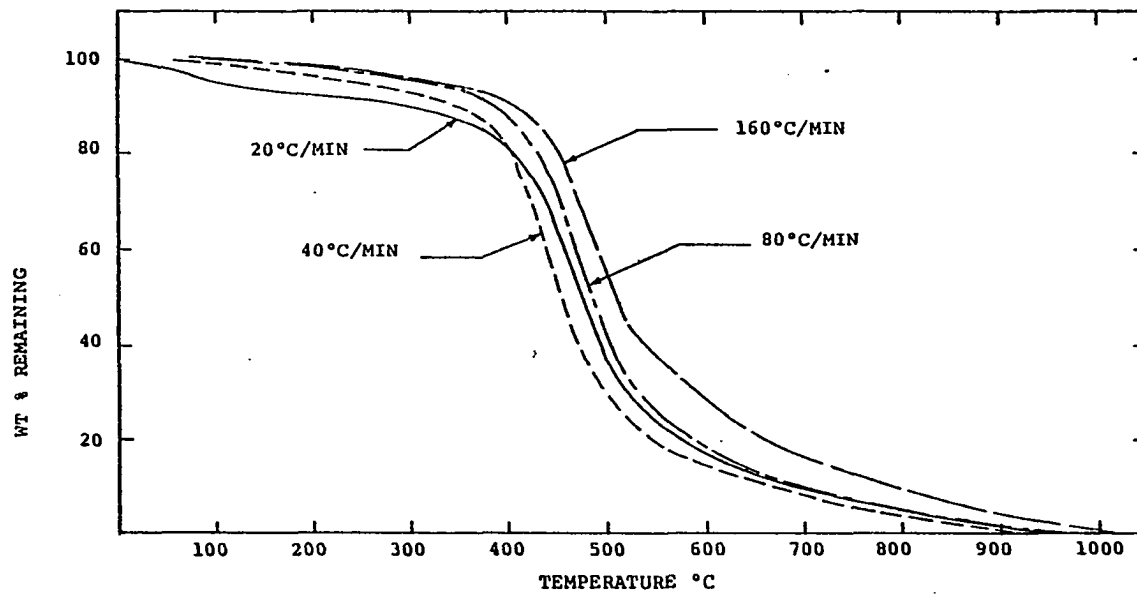


Figure IV-3. Effect of Heating Rate on TG (Weight Loss) Thermoqram for Coal Sample B. (From Figures B-1, B-2, B-3, and B-4 of Appendix B).

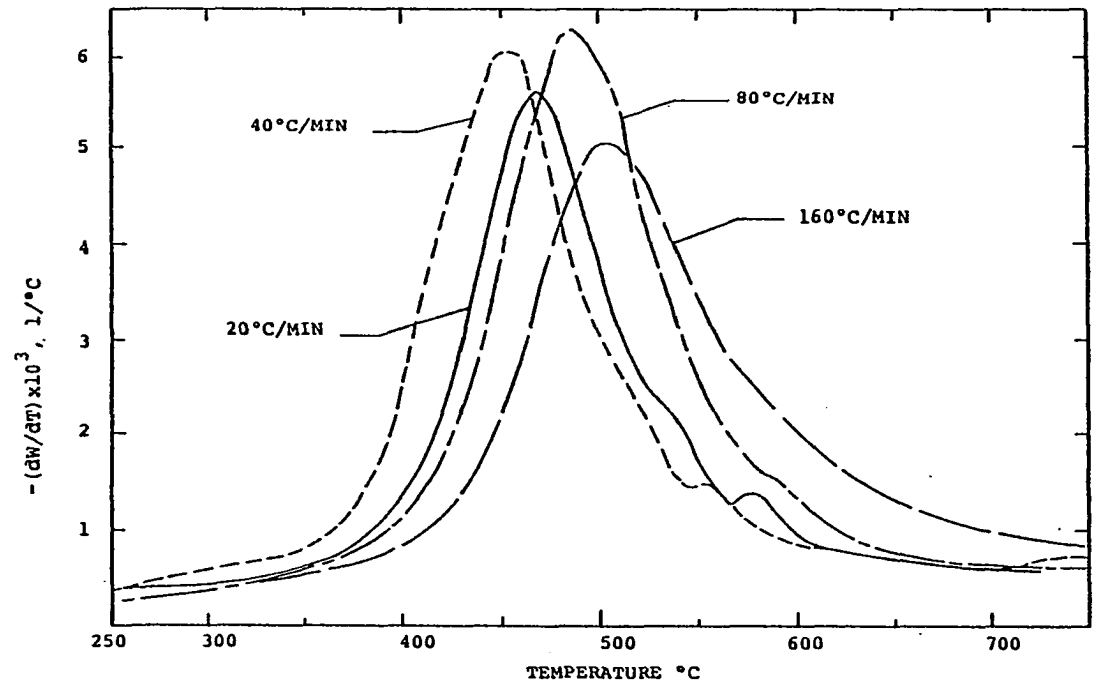


Figure IV-4. Effect of Heating Rate on Differential TG (Rate of Weight-Loss) Thermogram for Coal Sample B. (From Figures B-1, B-2, B-3, and B-4 of Appendix B).

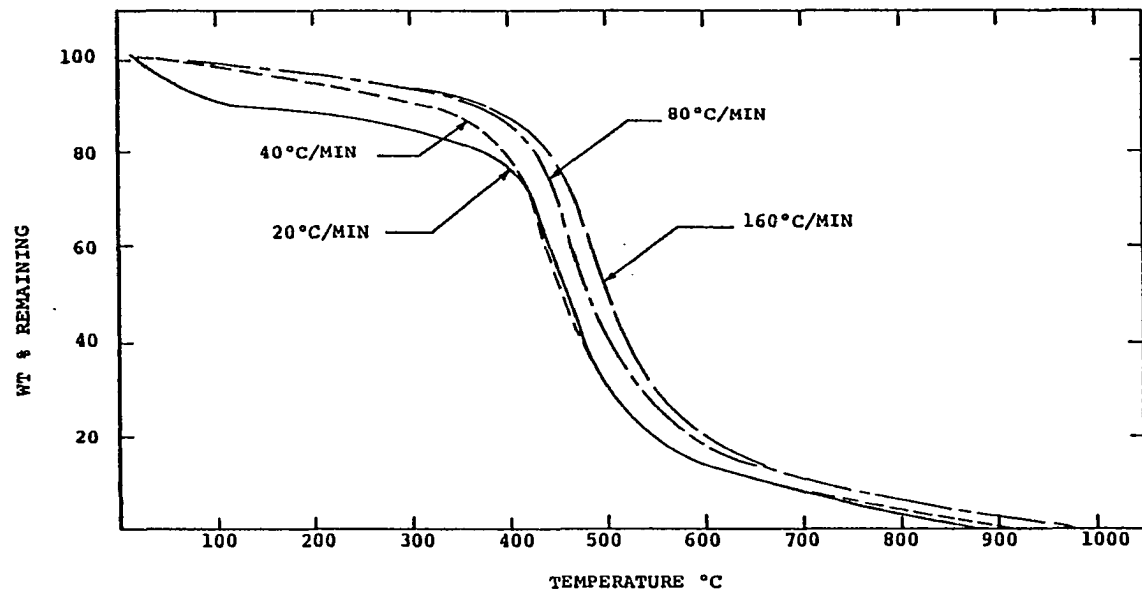


Figure IV-5. Effect of Heating Rate on TG (Weight Loss) Thermogram for Coal Sample C. (From Figures C-1, C-2, C-3 and C-4 of Appendix C).

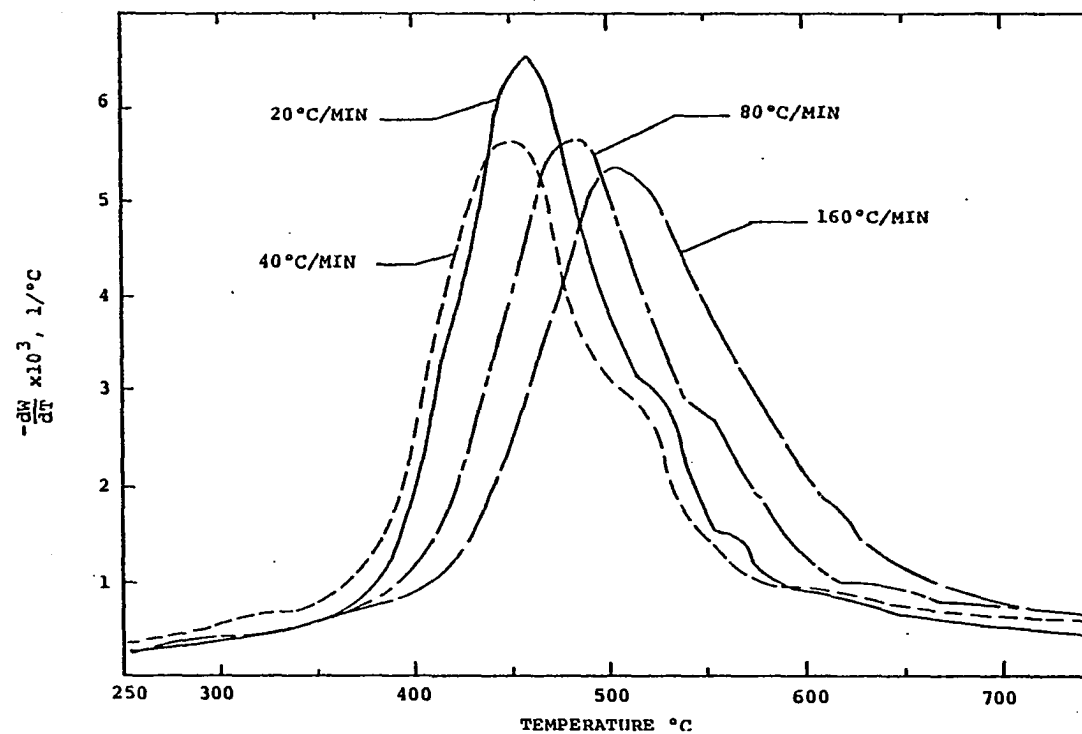


Figure IV-6. Effect of Heating Rate on Differential TG (Rate of Weight-Loss) Thermogram for Coal Sample C. (From Figures C-1, C-2, C-3, and C-4 of Appendix C).

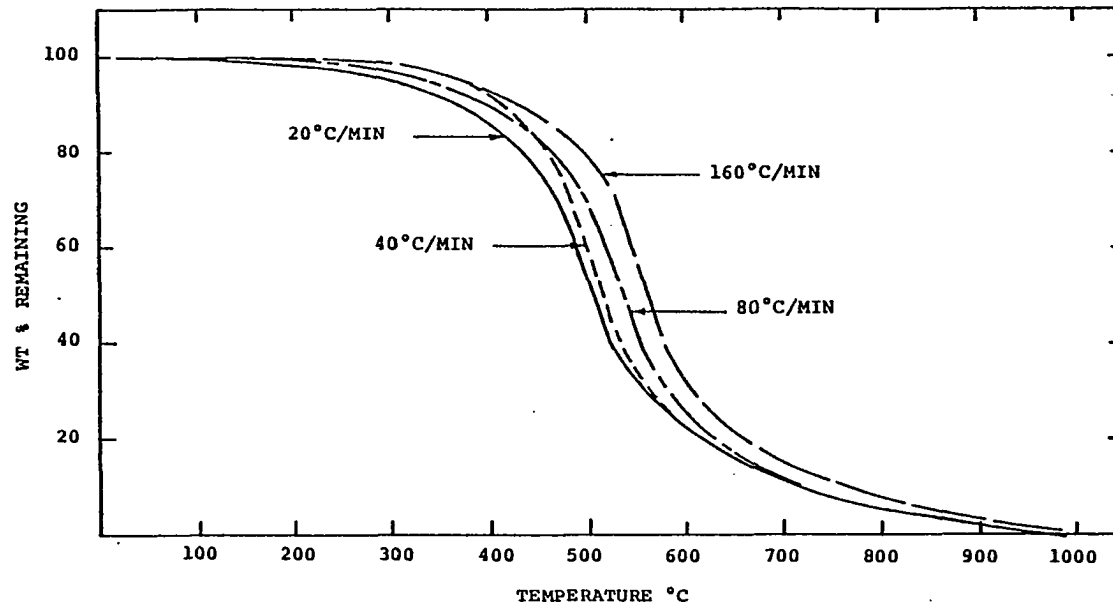


Figure IV-7. Effect of Heating Rate on TG (Weight Loss) Thermogram for Coal Sample D. (From Figures D-1, D-2, D-3 and D-4 of Appendix D).

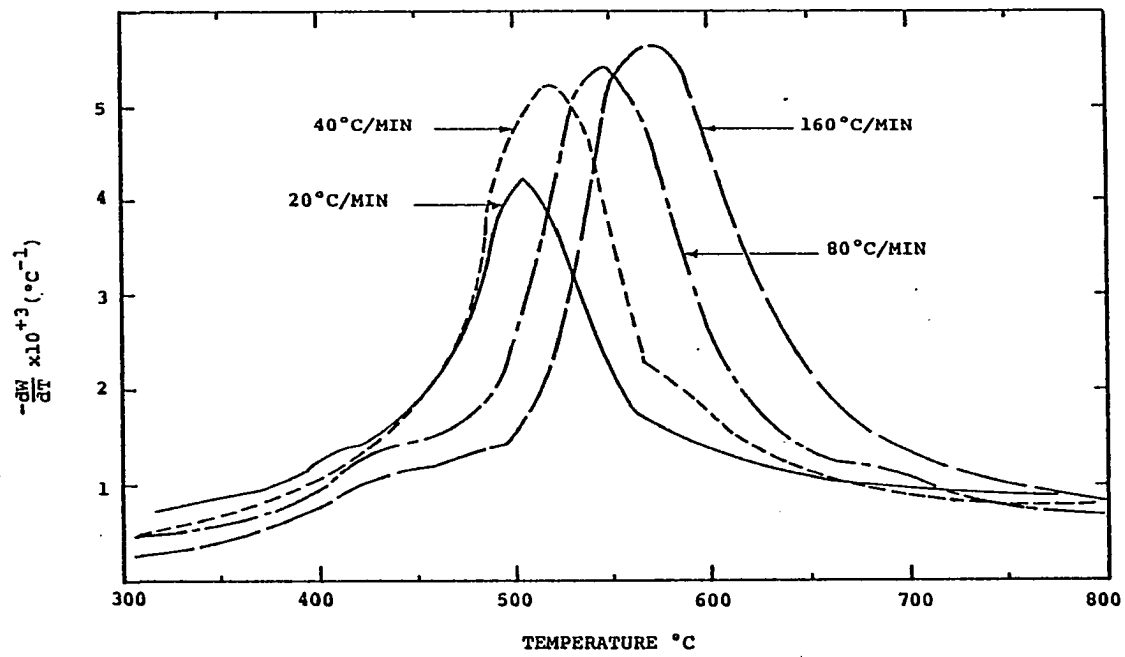


Figure IV-8. Effect of Heating Rate on Differential TG (Rate of Weight-Loss) Thermogram for Coal Sample D. (From Figures D-1, D-2, D-3, and D-4 of Appendix D).

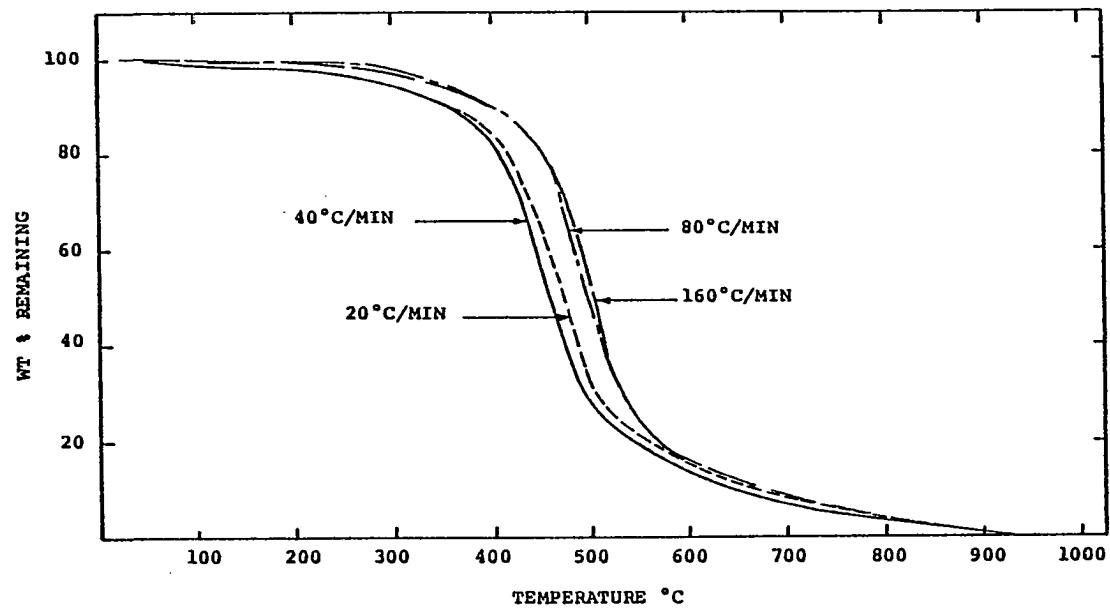


Figure IV-9. Effect of Heating Rate of TG (Weight Loss) Thermogram for Coal Sample E. (From Figures E-1, E-2, E-3, and E-4 of Appendix E).

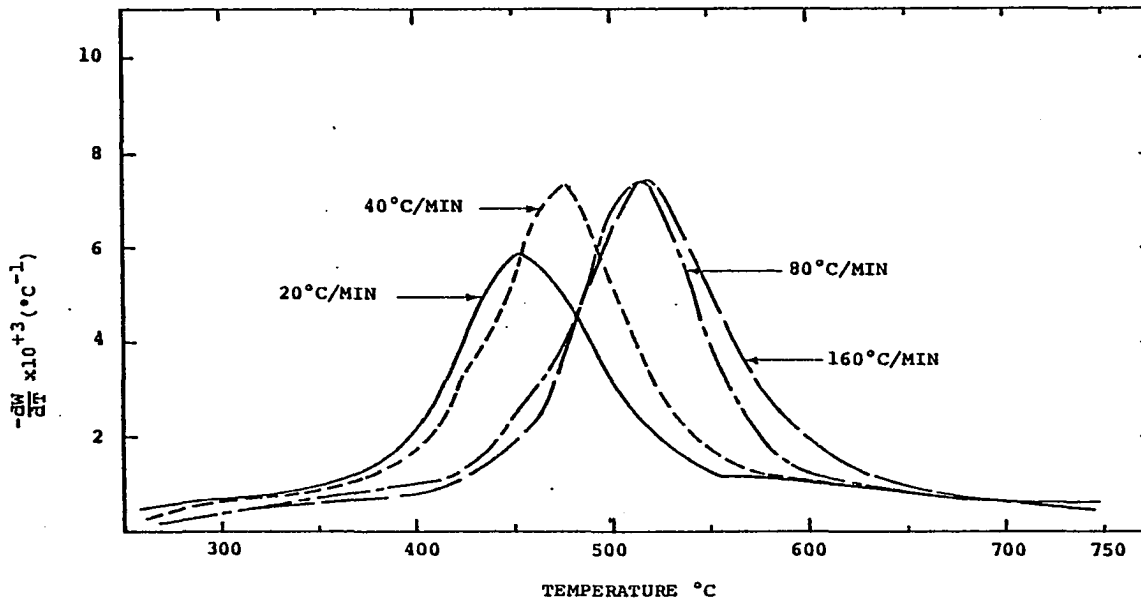


Figure IV-10. Effect of Heating Rate on Differential TG (Rate of Weight-Loss) Thermogram for Coal Sample E. (From Figures E-1, E-2, E-3, and E-4 of Appendix E).

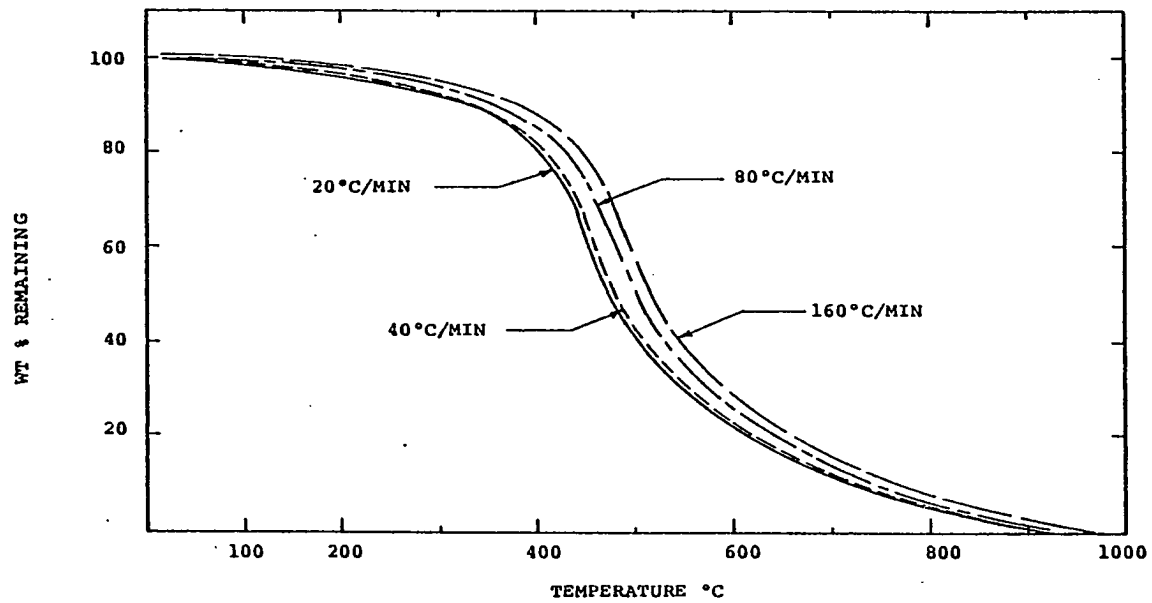


Figure IV-11. Effect of Heating Rate on TG (Weight Loss) Thermogram for Coal Sample F. (From Figures F-1, F-2, F-3, and F-4 of Appendix F).

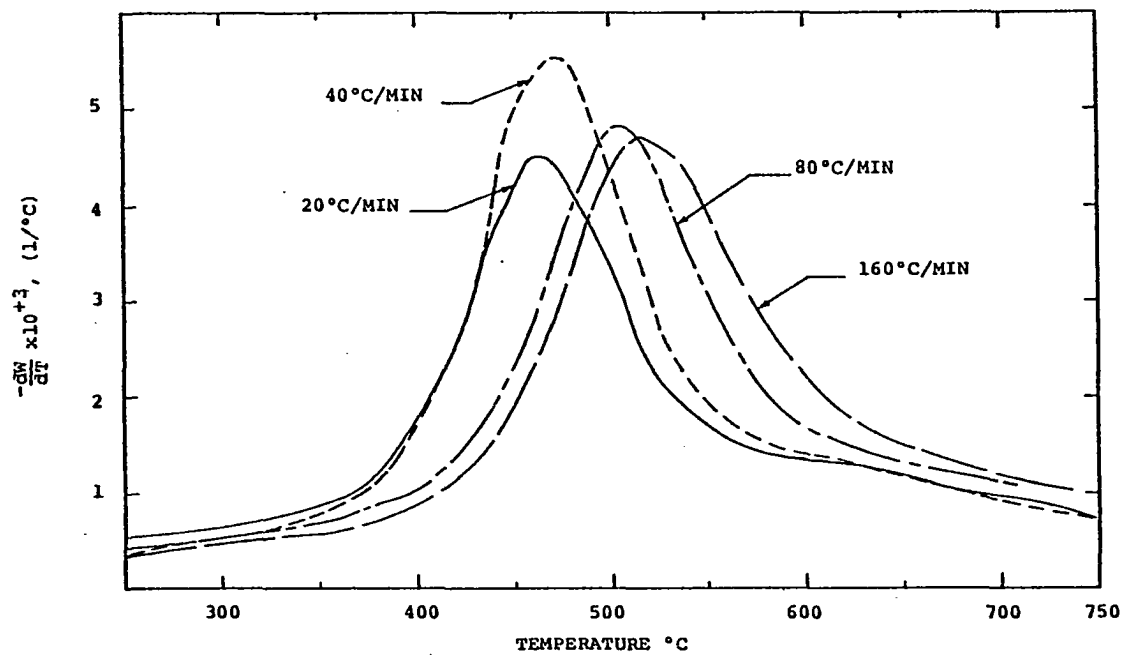


Figure IV-12. Effect of Heating Rate on Differential TG (Rate of Weight-Loss) Thermogram for Coal Sample F. (From Figures F-1, F-2, F-3, and F-4 of Appendix F).

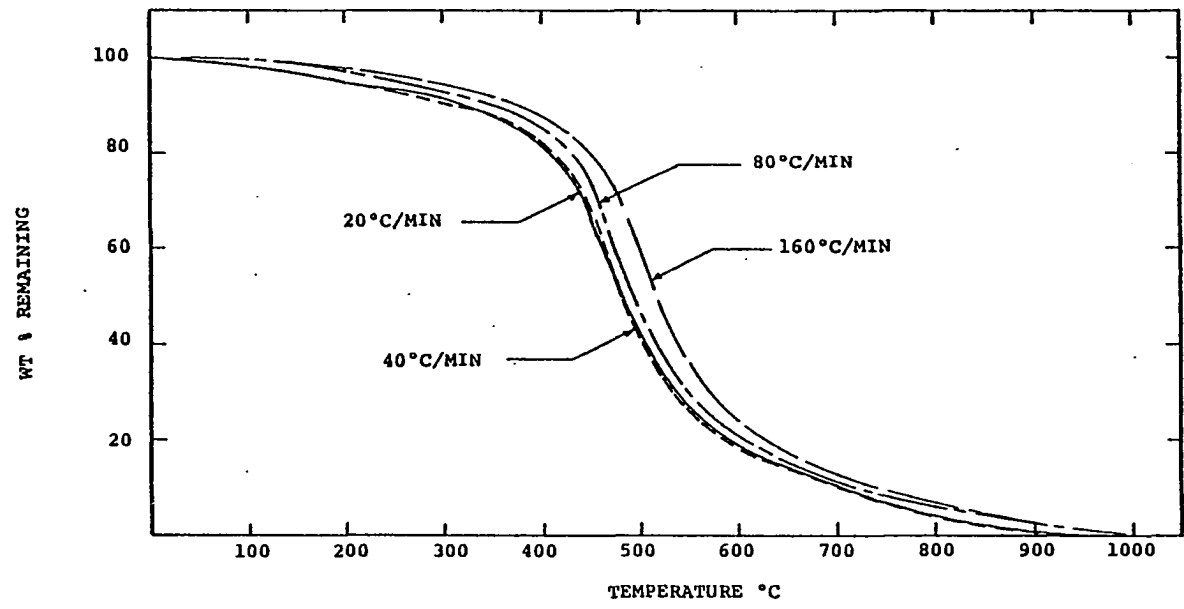


Figure IV-13. Effect of Heating Rate on TG (Weight Loss) Thermogram for Coal Sample G. (From Figures G-1, G-2, G-3, and G-4 of Appendix G).

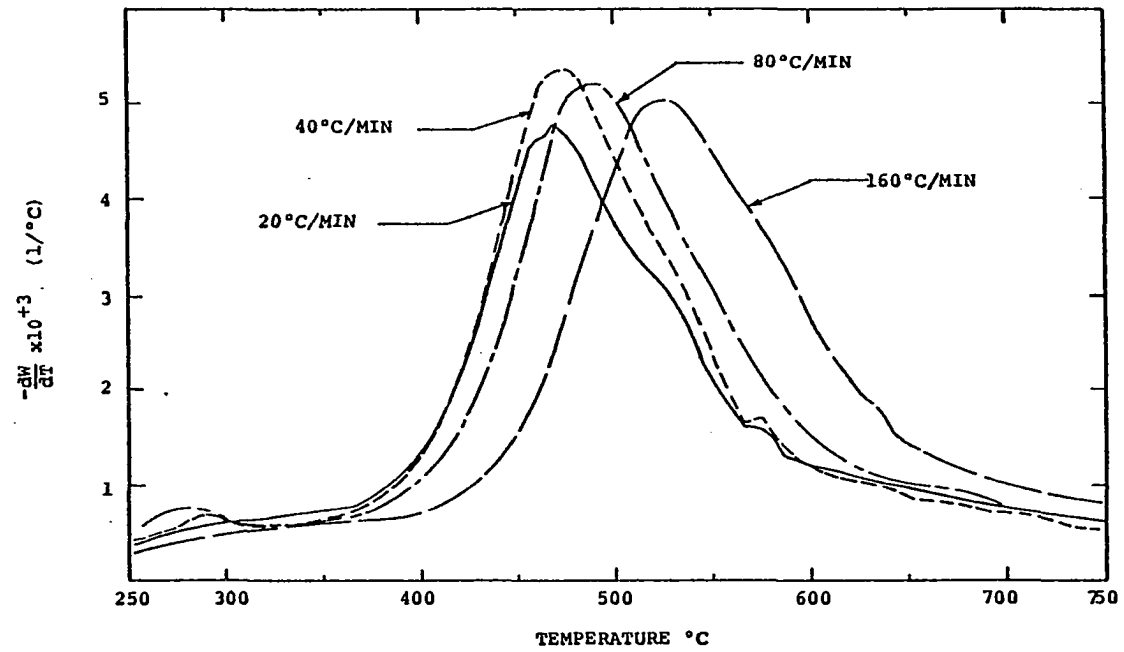


Figure IV-14. Effect of Heating Rate on Differential TG (Rate of Weight-Loss) Thermogram of Coal Sample G. (From Figures G-1, G-2, G-3, and G-4 of Appendix G).

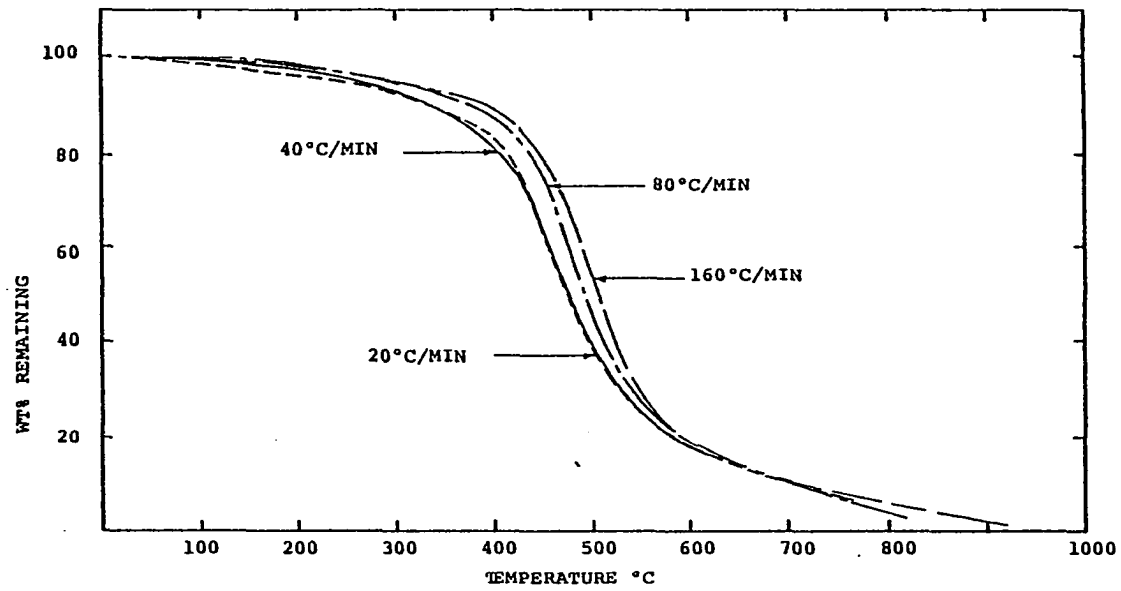


Figure IV-15. Effect of Heating Rate of TG (Weight Loss) Thermogram for Coal Sample H. (From Figures H-1, H-2, H-3, and H-4 of Appendix H).

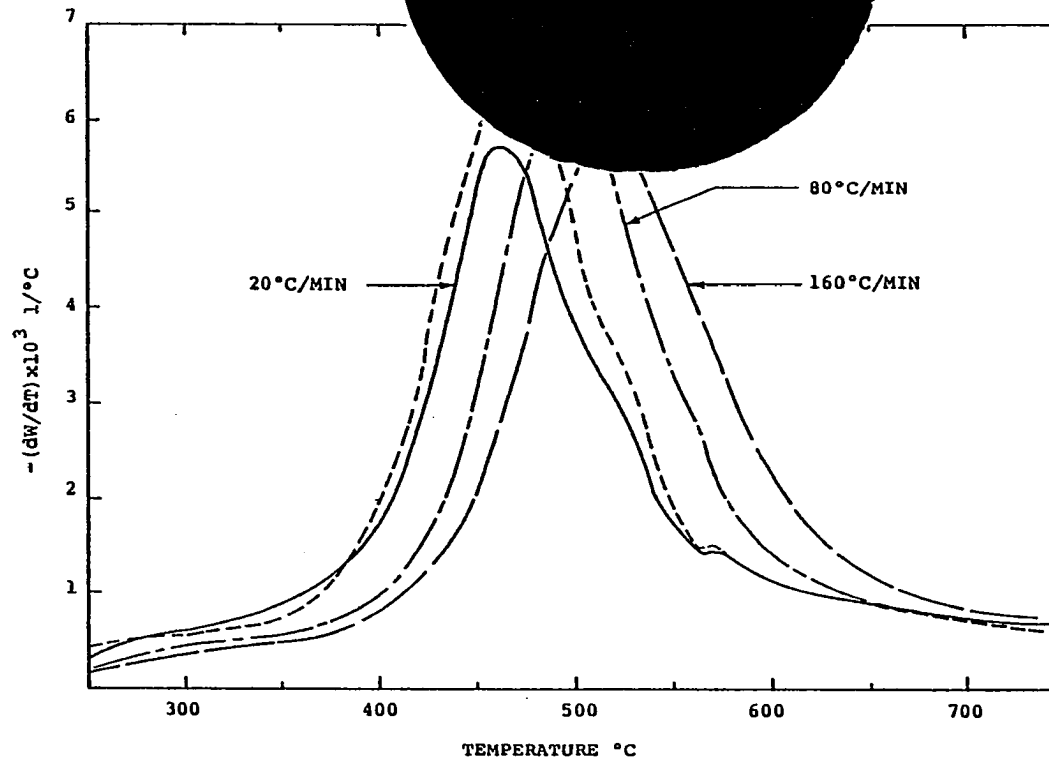


Figure IV-16. Effect of Heating Rate on Differential TG (Rate of Weight-Loss) Thermogram for Coal Sample H. (From Figures H-1, H-2, H-3, and H-4 Shown in Appendix H).

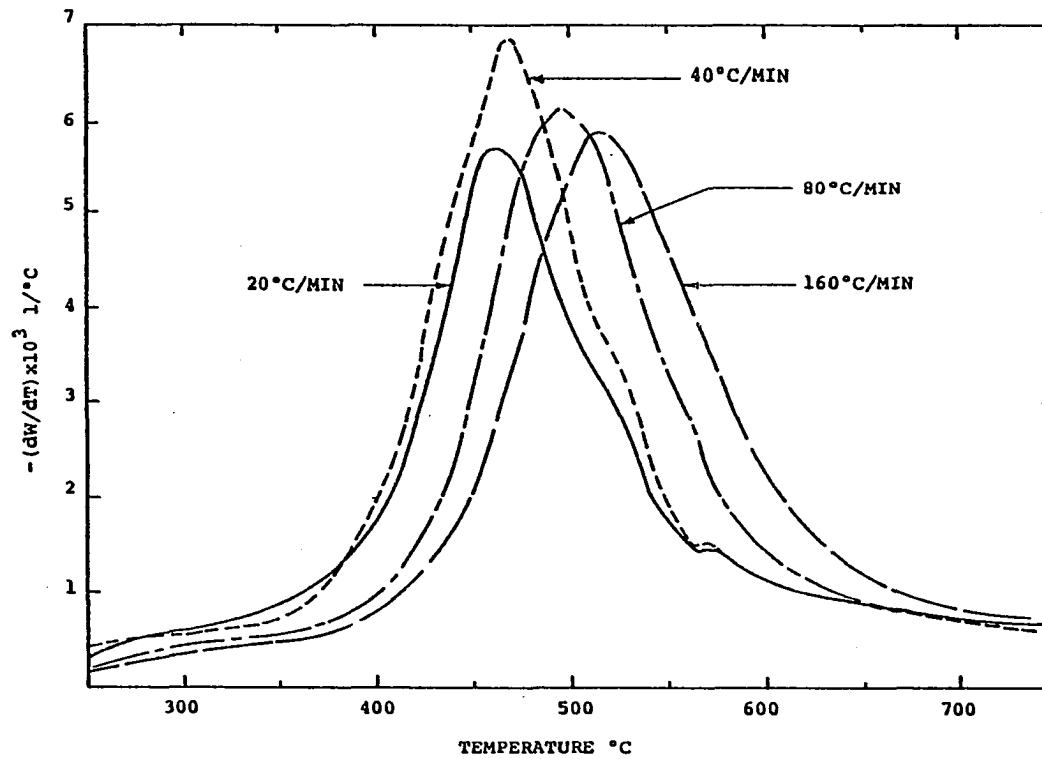


Figure IV-16. Effect of Heating Rate on Differential TG (Rate of Weight-Loss) Thermogram for Coal Sample H. (From Figures H-1, H-2, H-3, and H-4 Shown in Appendix H).

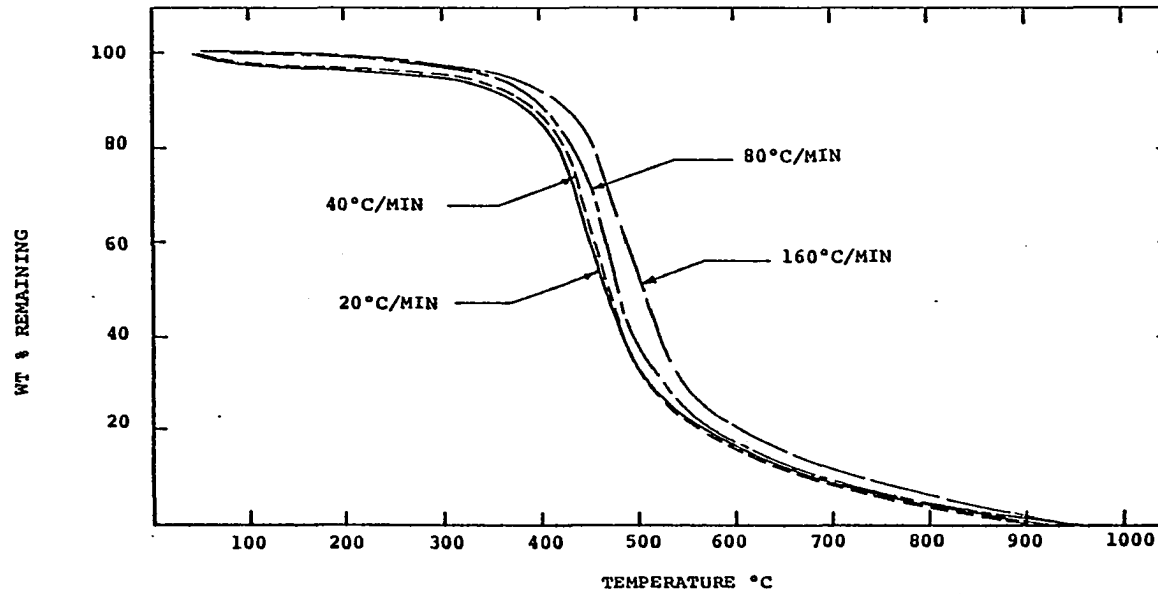


Figure IV-17. Effect of Heating Rate on TG (Weight Loss) Thermogram for Coal Sample I. (From Figures I-1, I-2, I-3, and I-4 of Appendix I).

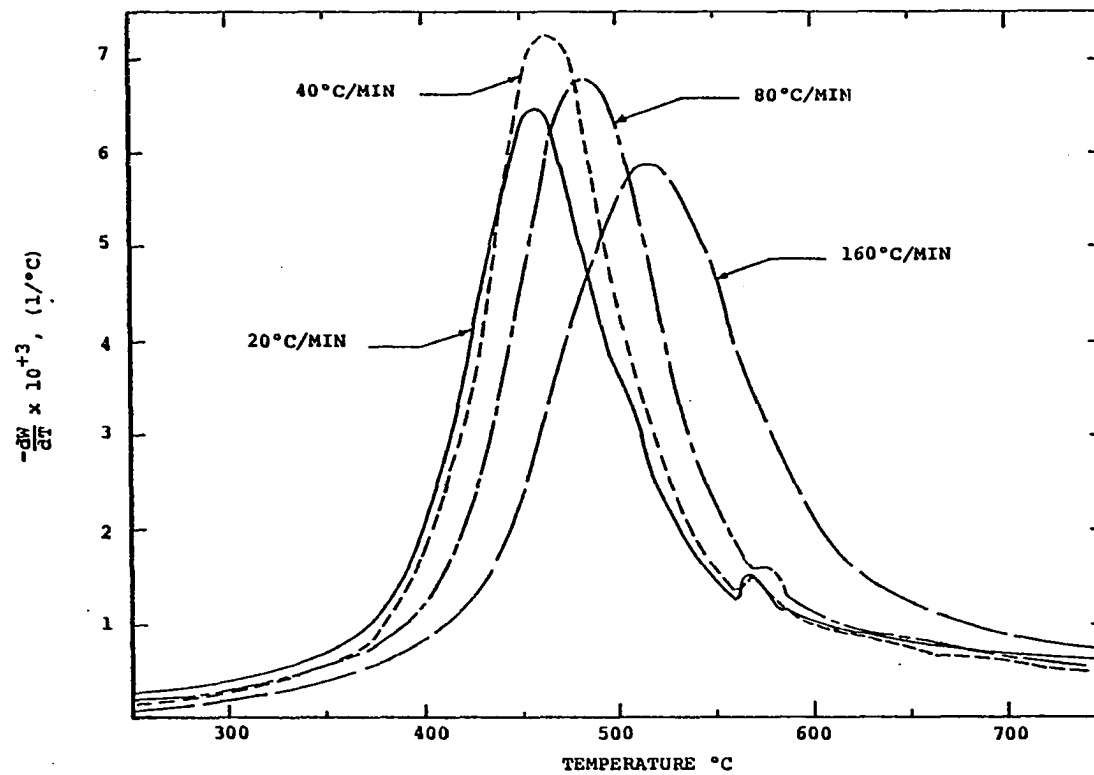


Figure IV-18. Effect of Heating Rate on Differential TG (Rate of Weight-Loss) Thermogram for Coal Sample I. (From Figures I-1, I-2, I-3, and I-4 of Appendix I).

where $W = \text{weight fraction} = \frac{w - w_f}{w_o - w_f}$ (IV-2)

$A = \text{pre-exponential factor (min}^{-1}\text{)}$

$E = \text{Activation energy (cal/gm - mole)}$

$T = \text{absolute temperature (}^\circ\text{K)}$

$R = \text{gas constant (cal/mole }^\circ\text{K)}$

$t = \text{time (min)}$

$w = \text{weight at time } t \text{ (mg)}$

$w_o = \text{initial weight of sample (mg)}$

$w_f = \text{final weight of sample (mg)}$

$n = \text{order of reaction}$

After substituting for W and taking logarithms, the model

becomes:

$$\log \left[-\frac{1}{w_o - w_f} \frac{dw}{dt} \right] = \log A - \frac{E}{2.303 RT} + n \log \left[\frac{w - w_f}{w_o - w_f} \right] \quad (\text{IV-3})$$

which is of the form: $y = B + Cx + Dz$ (IV-4)

where $y = \log \left[\frac{-1}{w_o - w_f} \frac{dw}{dt} \right]$

$$x = \frac{1}{2.303 RT}$$

$$z = \log \left[\frac{w - w_f}{w_o - w_f} \right]$$

$$B = \text{Log } A$$

$$C = -E$$

$$D = n$$

A least squares technique was applied to the experimental data.

The resulting simultaneous equations were solved with a Gauss-Jordan

numerical technique to obtain values of log A, E, and n. A set of values of parameters for a sample may be obtained either by considering data of all heating rates or by considering TGA data of runs made at one individual heating rate. Table IV-1 lists the values of kinetic parameters for 160, 80, 40, 20, and 10°C/min heating rates and values obtained when data for all runs were considered collectively. For each sample the experimental data from two runs were considered for obtaining a set of kinetic parameters. Since only one run was made at 10°C/min, data from only one run were used to obtain the values of log A, E, and n at 10°C/min.

Effect of Heating Rate on Kinetic Parameters

For thermal decompositions of punky wood and cellulose, Muhlenkamp (1975) observed that kinetic parameters and heating rate are related by the expression:

$$[KP] = C_1 (HR)^{C_2} \quad (IV-5)$$

where [KP] = value of kinetic parameter (log A, E, or n)

HR = heating rate (°C/min)

C_1 and C_2 are constants of the equation

The Equation IV-5 implies that a log-log plot of kinetic parameters vs heating rate is a straight line with a slope of C_2 and intercept equal to logarithm of C_1 . However, this relationship did not hold for the coal pyrolysis in this study.

Comparison Between the Experimental and Calculated TGA Data

The values of parameters log A, E, and n may be used in the model described by Equation IV-1 to calculate weight loss and rate of

Table IV-1

KINETIC PARAMETERS OF COAL SAMPLES FOR HEATING RATES STUDIED IN THIS PROJECT

SAMPLE	PARAMETER	HEATING RATE, °C/min					Overall (b)
		160	80	40	20 (a)	10	
A	Log A	4.11	2.20	1.62	0.6	0.72	1.96
	E	13918.63	8785.6	7427.3	5261.0	6463.6	8200.9
	n	1.79	1.34	1.42	1.10	1.33	1.38
B	Log A	3.05	3.55	1.66	0.41	0.25	1.80
	E	10429.3	12557.8	7287.8	4506.7	5050.11	7696.6
	n	1.47	1.59	1.24	1.01	1.03	1.28
C	Log A	3.32	2.15	1.11	0.073	0.81	1.40
	E	11108.0	8280.1	5742.2	3389.2	6444.0	6403.6
	n	1.52	1.33	1.07	0.9985	1.25	1.21
D	Log A	4.29	3.42	3.49	1.01	1.72	3.64
	E	15507.1	13236.4	14160.4	7170.8	10353.1	14538.5
	n	1.62	1.45	1.63	1.03	1.39	1.67
E	Log A	5.04	4.95	3.53	2.50	2.64	5.00
	E	16620.8	17120.33	12981.9	10719.9	11899.4	17462.1
	n	1.79	1.89	1.70	1.56	1.73	2.09
F	Log A	2.97	2.36	1.29	0.48	0.50	1.92
	E	10485.0	9288.3	6567.4	5218.1	5953.5	8454.1
	n	1.42	1.34	1.18	0.98	1.15	1.34
G	Log A	2.95	2.51	1.10	0.47	0.13	1.66
	E	10235.4	9513.2	5923.2	5006.8	4888.0	7619.5
	n	1.37	1.40	1.08	0.95	0.91	1.22
H	Log A	4.13	3.54	1.87	2.10	0.26	2.54
	E	13838.61	12606.0	7926.9	9822.5	5077.9	10064.4
	n	1.65	1.62	1.38	1.53	1.02	1.48
I	Log A	6.62	6.23	1.84	1.37	0.61	2.79
	E	24927.0	20709.5	7842.1	7387.3	6042.5	10721.4
	n	2.38	2.46	1.30	1.29	1.19	1.56

NOTES: (a) The data for the heating rate of 20°C/min do not follow the quite orderly trends in the kinetic parameters for the other heating rates.

(b) The overall values do not have any significance other than to indicate relative magnitudes of the kinetic parameters for the various coals. For example, in Coal Sample E the overall value for log A is obviously not an "average" value; this aberration is inherent in the regression analysis and has been encountered by others before.

weight-loss data at different temperatures. With the parameters listed in Table IV-1 for heating rates 160, 40, and 10°C/min, the weight loss and rate of weight loss were calculated for coal samples A, E, and H over the entire temperature range of 100-1000°C of TG experiments. The calculated data for three coal samples are shown in Figures IV-19 through IV-27 with the experimental data obtained at 160, 40, and 10°C/min heating rates. It is observed that weight loss and rate of rate weight loss calculated from the kinetic parameters listed in Table IV-1 do not fit well to the experimental data, especially at lower and upper temperature ranges of the DTG curve. Though the exact temperatures at which the maximum devolatilizations take place compare closely for both experimental and calculated curves, the calculated value of maximum devolatilization is lower than the experimentally observed value in all cases of Figures IV-19 through Figure IV-27. It must be noted, from the experimental TGA curves, that over the initial temperature range of the scan (25-400°C) only small percentages of the weight loss take place. Most of the weight loss occurs over a temperature range between 400-700°C. Then, the weight loss decreases considerably in the temperature range of 700-1000°C. Since data from the entire temperature scan were used to compute the kinetic parameters listed in Table IV-1, the kinetic parameters are the best fit for the entire temperature range. The net effect of computing a set of kinetic parameters with largely differing experimental weight loss data is that the kinetic parameters describe only the average behavior over the entire temperature range. This reason possibly explains the departure between the experimental and calculated curves shown in Figures IV-19 through IV-27.

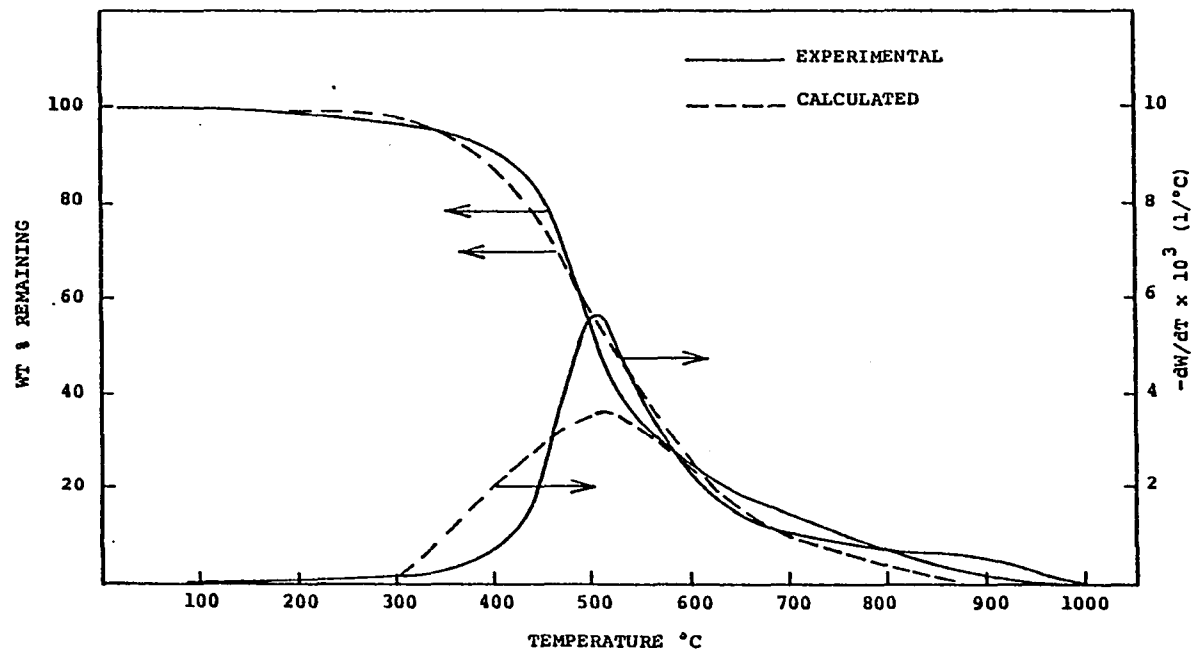


Figure IV-19. Comparison Between Experimental and Calculated (by the Kinetic Parameters Listed in Table IV-1 for 160°C/min Heating Rate) TGA Thermograms for Coal Sample A at 160°C/min. (Experimental Data from Figure A-1 of Appendix A.)

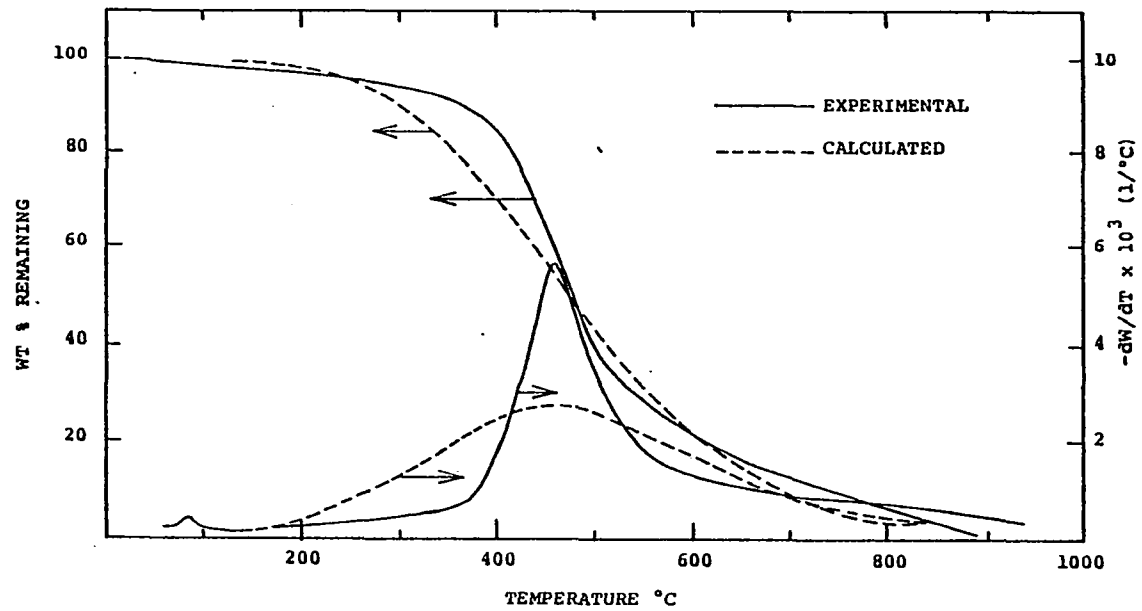


Figure IV-20. Comparison Between Experimental and Calculated (by the Kinetic Parameters Listed in Table IV-1 for 40°C/min Heating Rate) TGA Thermograms for Coal Sample A at 40°C/min. (Experimental Data From Figure A-3 of Appendix A.)

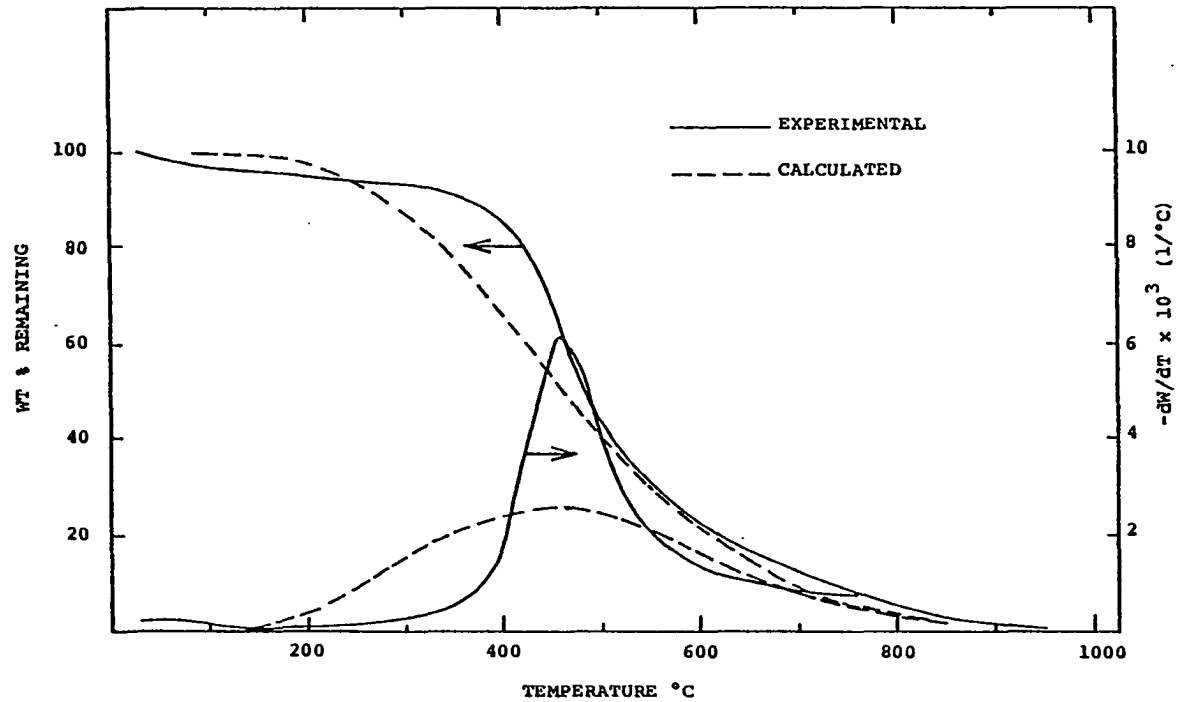


Figure IV-21. Comparison Between Experimental and Calculated (by the Kinetic Parameters Listed in Table IV-1 for 10°C/min Heating Rate) TGA Thermograms for Coal Sample A at 10°C/min. (Experimental Data from Figure A-5 of Appendix A.)

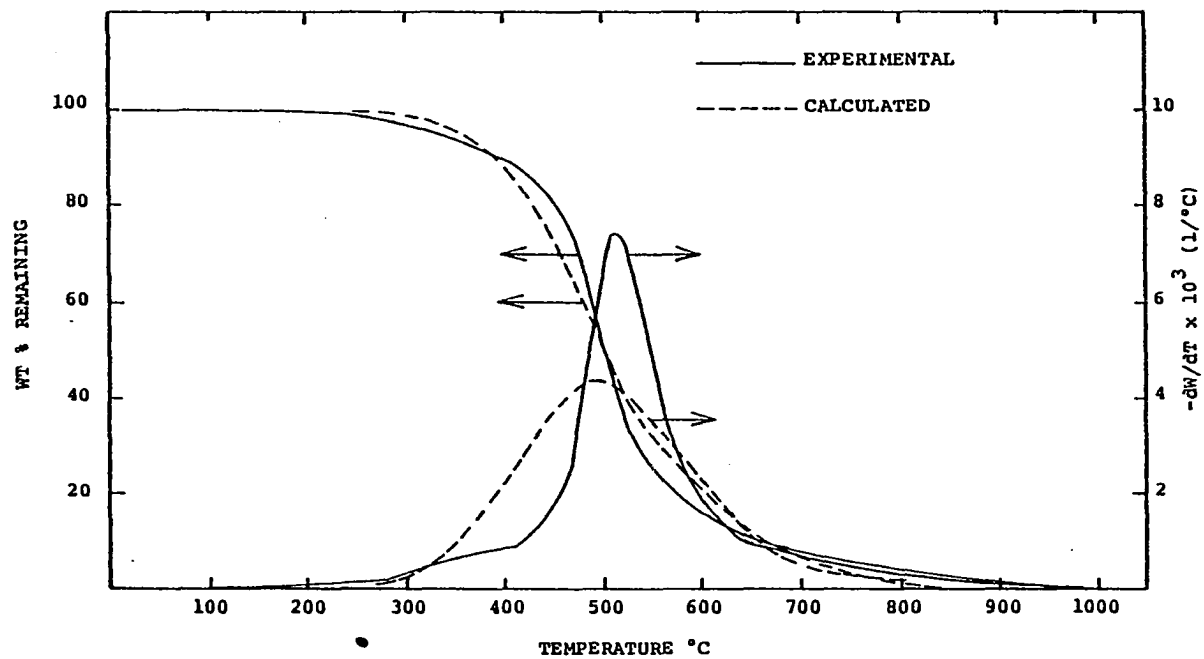


Figure IV-22. Comparison Between Experimental and Calculated (by the Kinetic Parameters Listed in Table IV-1 for 160°C/min Heating Rate) TGA Thermograms for Coal Sample E at 160°C/min. (Experimental Data from Figure E-1 of Appendix E.)

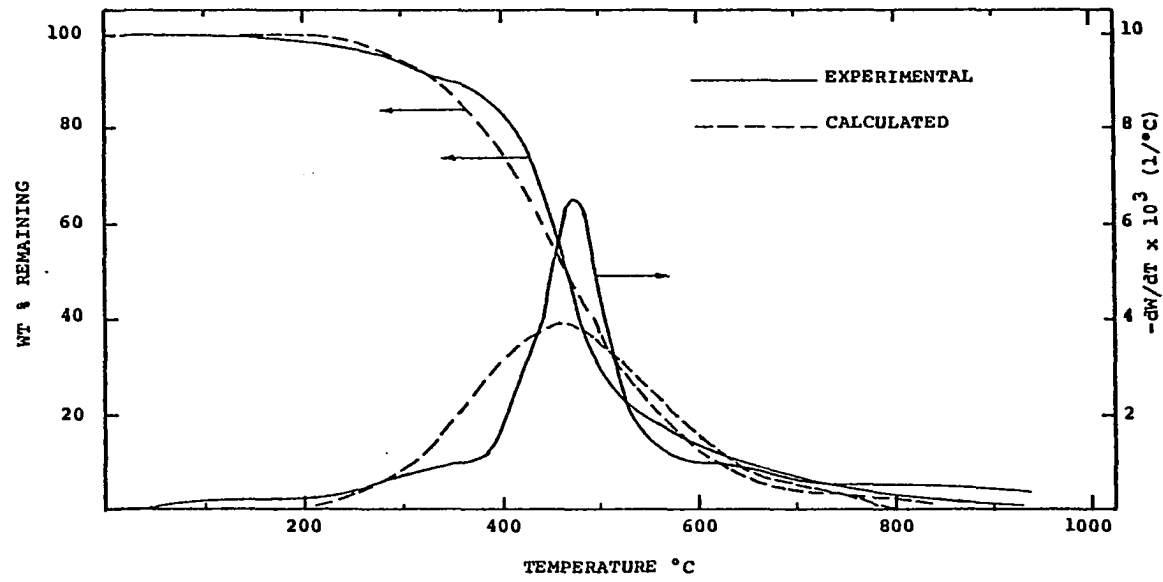


Figure IV-23. Comparison Between Experimental and Calculated (by the Kinetic Parameters Listed in Table IV-1 for 40°C/min Heating Rate) TGA Thermograms for Coal Sample E at 40°C/min. (Experimental Data from Figure E-3 of Appendix E.)

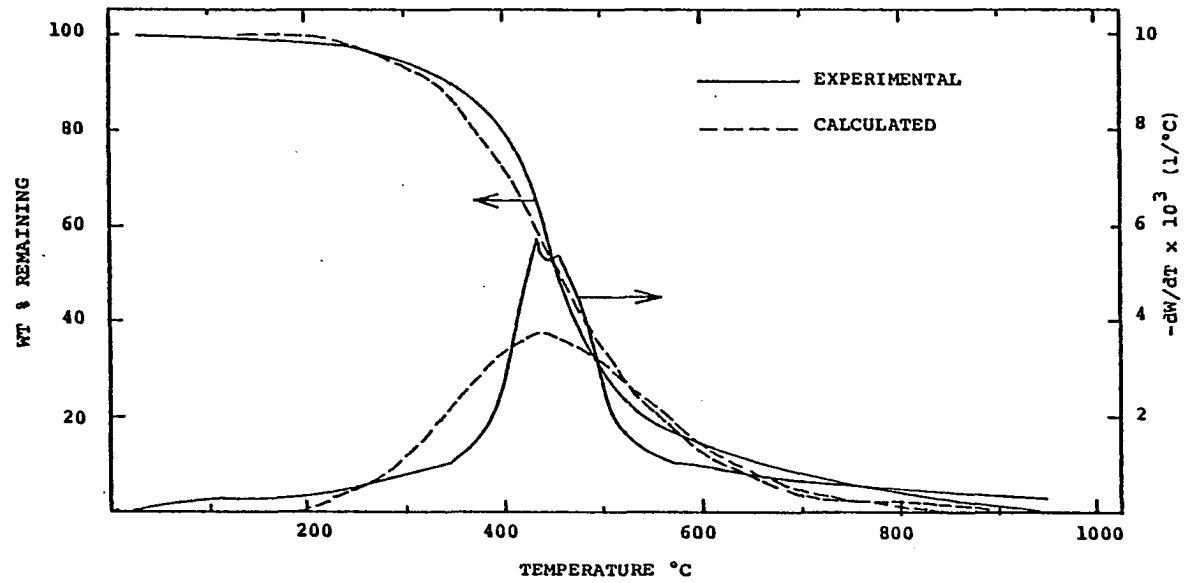


Figure IV-24. Comparison Between Experimental and Calculated (by the Kinetic Parameters Listed in Table IV-1 for 10°C/min Heating Rate) TGA Thermograms for Coal Sample E at 10°C/min. (Experimental Data as Shown in Figure E-5 of Appendix E.)

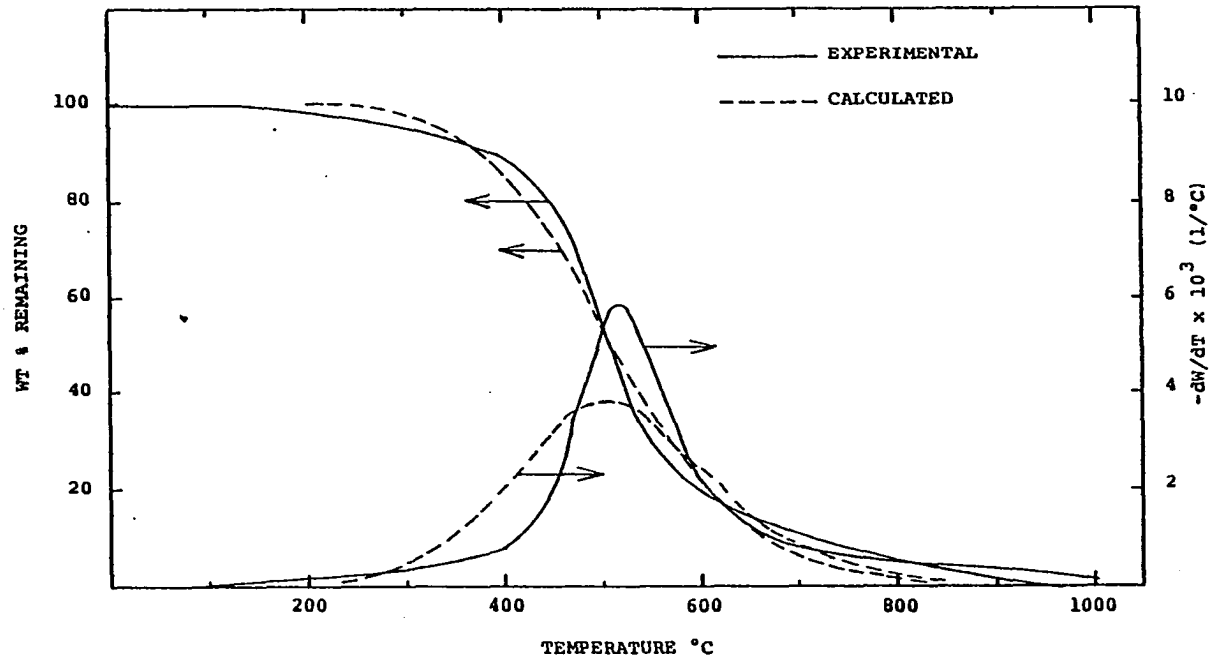


Figure IV-25. Comparison Between Experimental and Calculated (by the Kinetic Parameters Listed in Table IV-1 for 160°C/min Heating Rate) TGA Thermograms for Coal Sample H at 160°C/min. (Experimental Data as also Shown in Figure H-1 of Appendix H.)

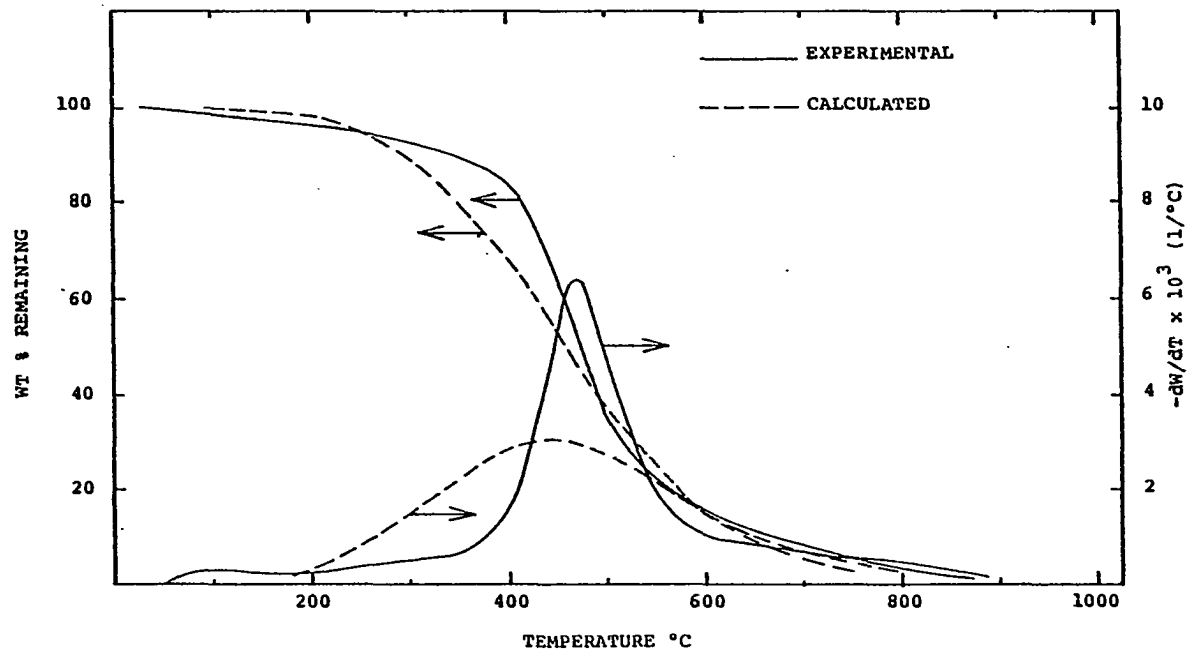


Figure IV-26. Comparison Between Experimental and Calculated (by the Kinetic Parameters Listed in Table IV-1 for 60°C/min Heating Rate) TGA Thermograms for Coal Sample H at 40°C/min. (Experimental Data as Shown in Figure H-3 of Appendix H.)

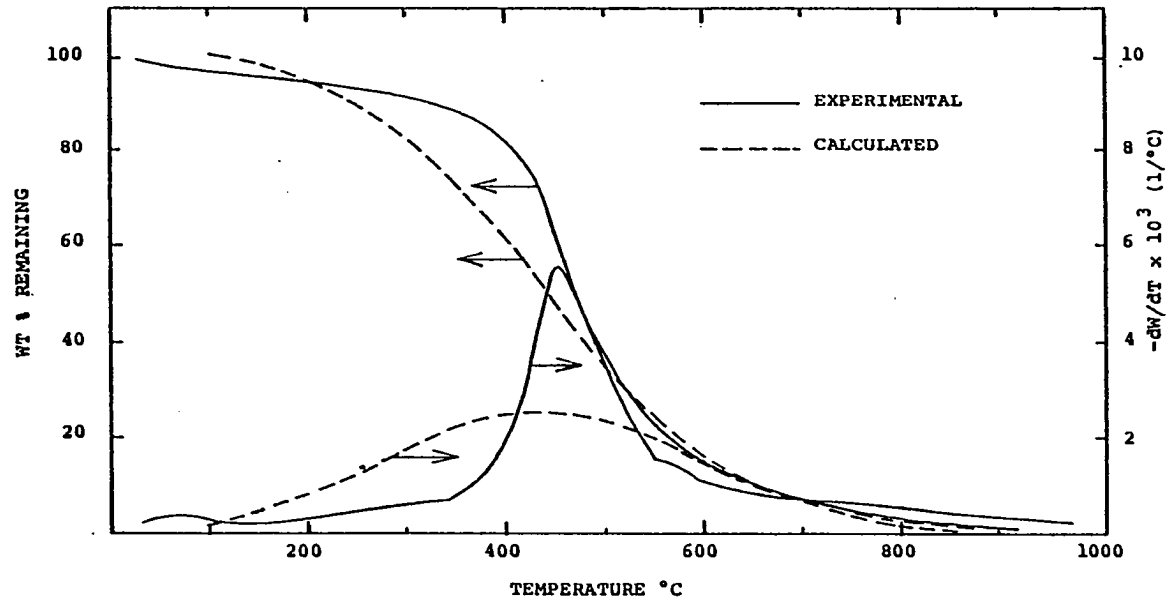


Figure IV-27. Comparison Between Experimental and Calculated (by the Kinetic Parameters Listed in Table IV-1 for 10°C/min Heating Rate) TGA Thermograms for Coal Sample H at 10°C/min. (Experimental Data as Shown in Figure H-5 of Appendix H.)

One approach to improve the comparison between the experimental and calculated curves is to obtain a set of kinetic parameters using the experimental data for the temperature range where most of the coal devolatilization occurs. In other words, initial and final parts of the weight loss curves must be neglected from consideration. These initial and final ends of the curve show low rates of weight loss and are, therefore, less accurate. The initial weight loss also includes weight loss due to moisture removal from the sample. Thus, using the experimental data of the high rate of weight loss sections (which usually occurred in the temperature range 400-700°C) of the TGA curves, revised sets of kinetic parameters were computed for coal Samples A, E, and H for three heating rates (160, 40, and 10°C/min). These sets of kinetic parameters are listed in Table IV-2. As discussed, this approach for comparison required that the weight loss data from the ends (initial and final sections) be neglected for computation. The percentage weight loss data that were not considered for the computation of kinetic parameters are also reported in Table IV-2. For example, the kinetic parameters for coal Sample E were obtained from the middle 68 percent weight loss data; the initial 16 percent and final 16 percent of the experimental weight loss data were not considered for computation. The calculated TGA curves were calculated from the kinetic parameters listed in Table IV-2 and are shown on Figures IV-28 to IV-36 for three coal samples and three heating rates. It is observed from these figures that calculated and experimental data, in the temperature range where high rates of weight loss are observed, compare better than shown in Figures IV-19 to IV-27.

Table IV-2

REVISED KINETIC PARAMETERS FOR COAL SAMPLES-A, E AND H

COAL SAMPLE	HEATING RATE °C/min	WEIGHT PERCENT NEGLECTED		KINETIC PARAMETER		
		From Front	From the End	Log A	E	n
A	160	8.0	8.0	7.81	25659.1	3.07
	40	8.0	8.0	13.93	44542.7	6.12
	10	16.0	16.0	9.93	34217.0	4.89
E	160	16.0	16.0	10.18	34519.8	1.67
	40	16.0	16.0	10.22	34102.5	2.90
	10	16.0	16.0	12.99	43185.7	4.47
H	160	20.0	20.0	14.15	47134.7	3.32
	40	20.0	20.0	15.94	51786.6	4.69
	10	20.0	20.0	18.25	60340.2	6.13

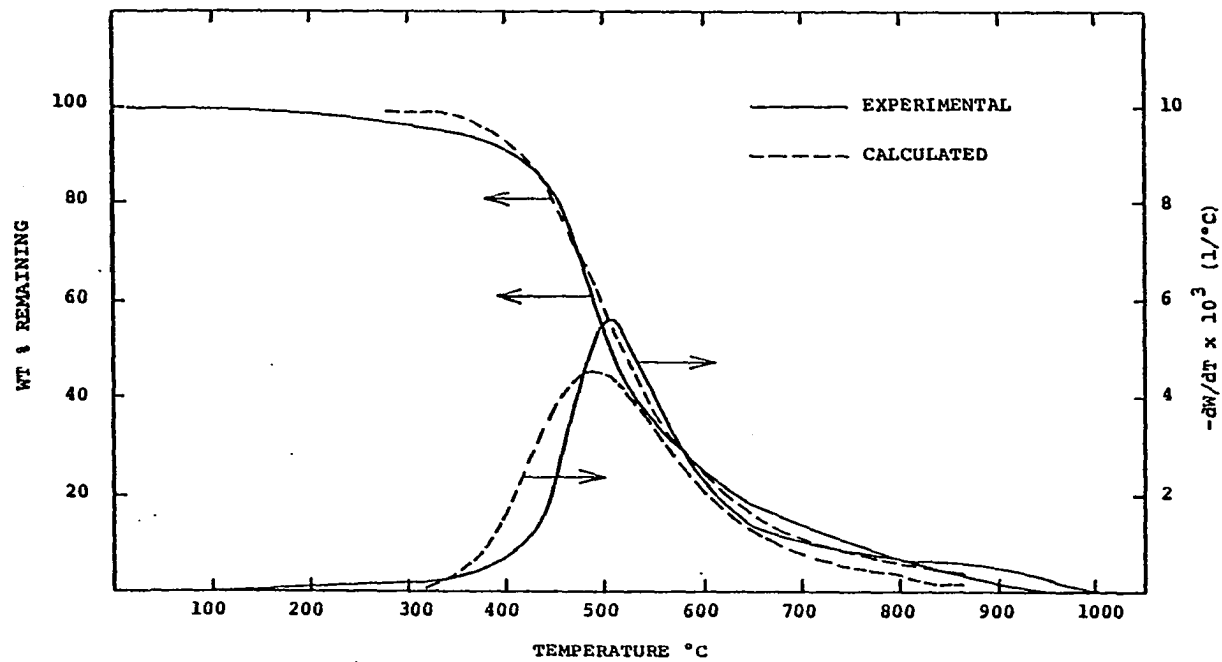


Figure IV-28. Comparison Between Experimental and Calculated (by the Kinetic Parameters Listed in Table IV-2 for 160°C/min Heating Rate) TGA Thermograms for Coal Sample A at 160°C/min. (Experimental Data as Shown in Figure A-1 of Appendix A.)

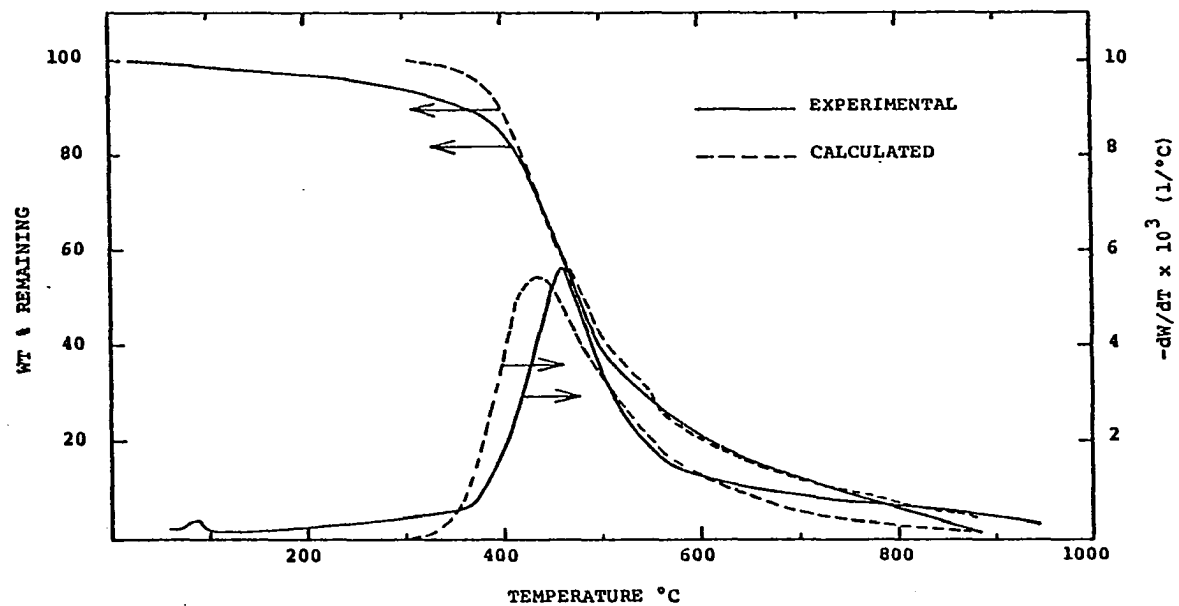


Figure IV-29. Comparison Between Experimental and Calculated (by the Kinetic Parameters Listed in Table IV-2 for 40°C/min Heating Rate) TGA Thermograms for Coal Sample A at 40°C/min. (Experimental Data from Figure A-3 of Appendix A.)

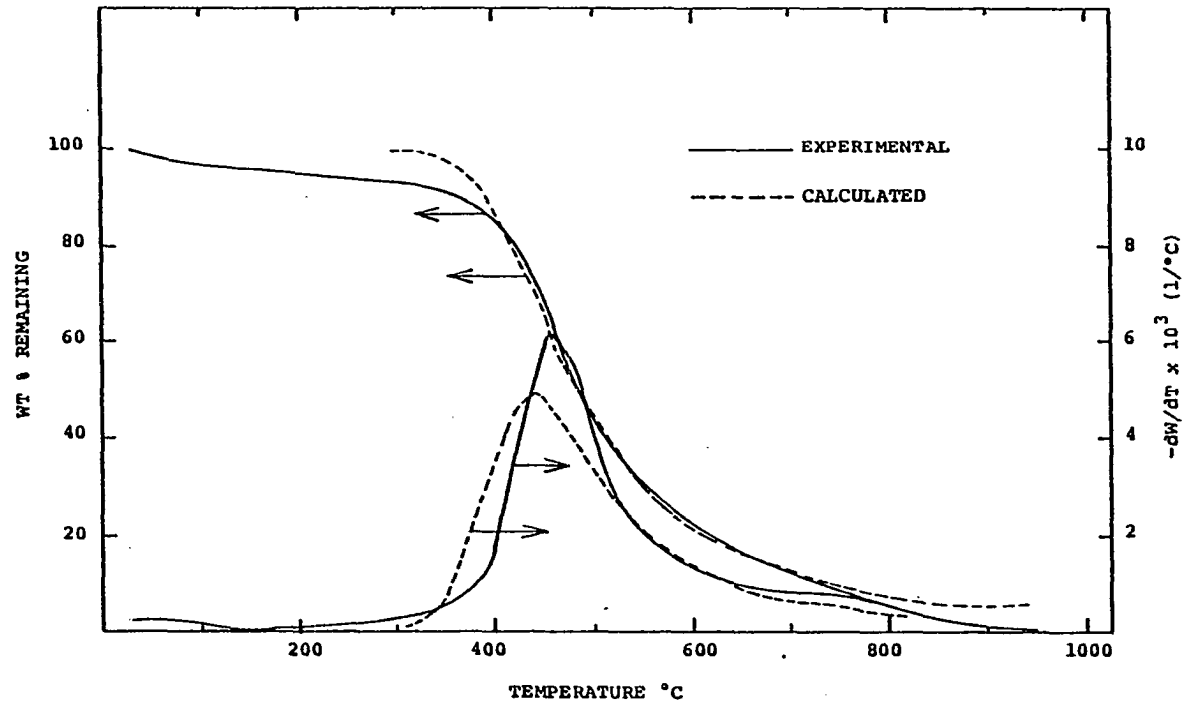


Figure IV-30. Comparison Between Experimental and Calculated (by the Kinetic Parameters Listed in Table IV-2 for 10°C/min Heating Rate) TGA Thermograms for Coal Sample A at 10°C/min. (Experimental Data as Shown in Figure A-5 of Appendix A.)

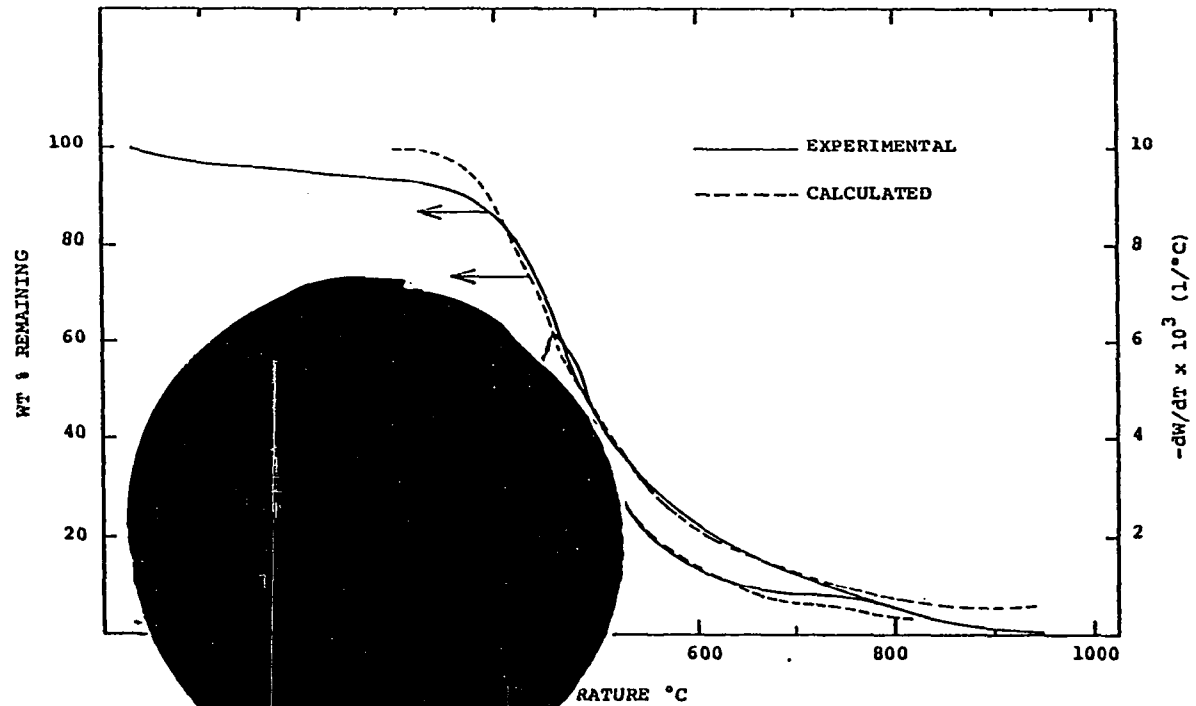


FIG. 4. Comparison of Experimental and Calculated (by the Kinetic Model Described in Table IV-2 for 10°C/min Heating Rate) TGA Curves for Coal Sample A at 10°C/min. (Experimental Data as Shown in Figure A-5 of Appendix A.)

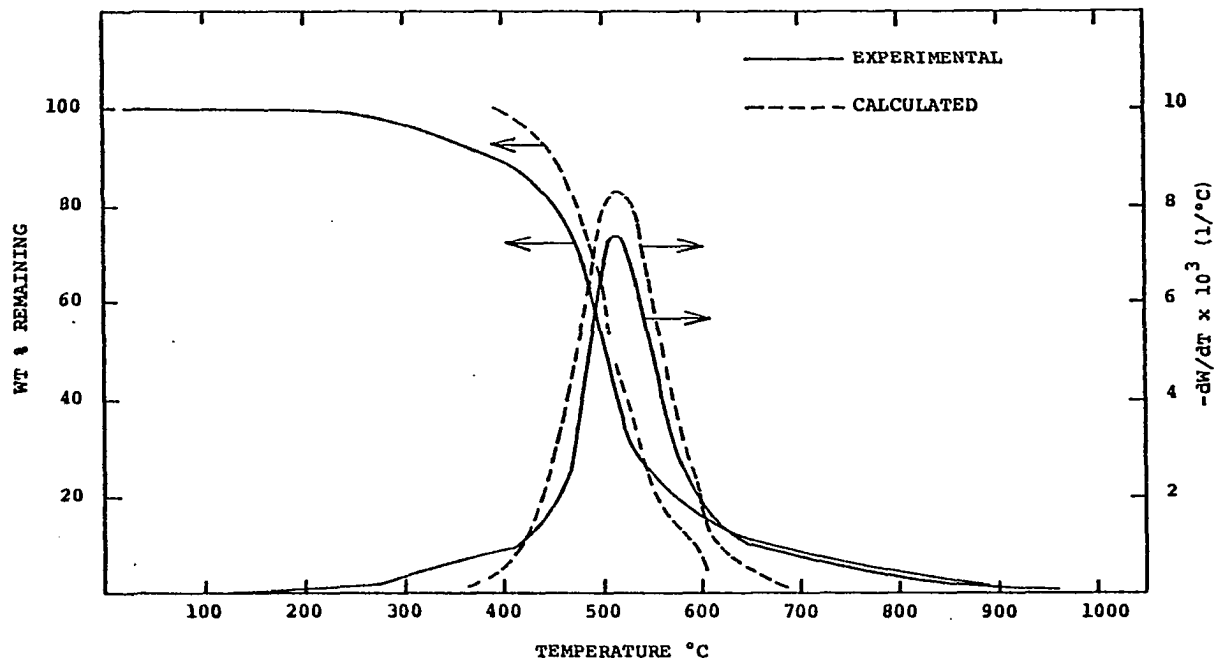


Figure IV-31. Comparison Between Experimental and Calculated (by the Kinetic Parameters Listed in Table IV-2 for 160°C/min Heating Rate) TGA Thermograms for Coal Sample E at 160°C/min. (Experimental Data as Shown in Figure E-1 of Appendix E.)

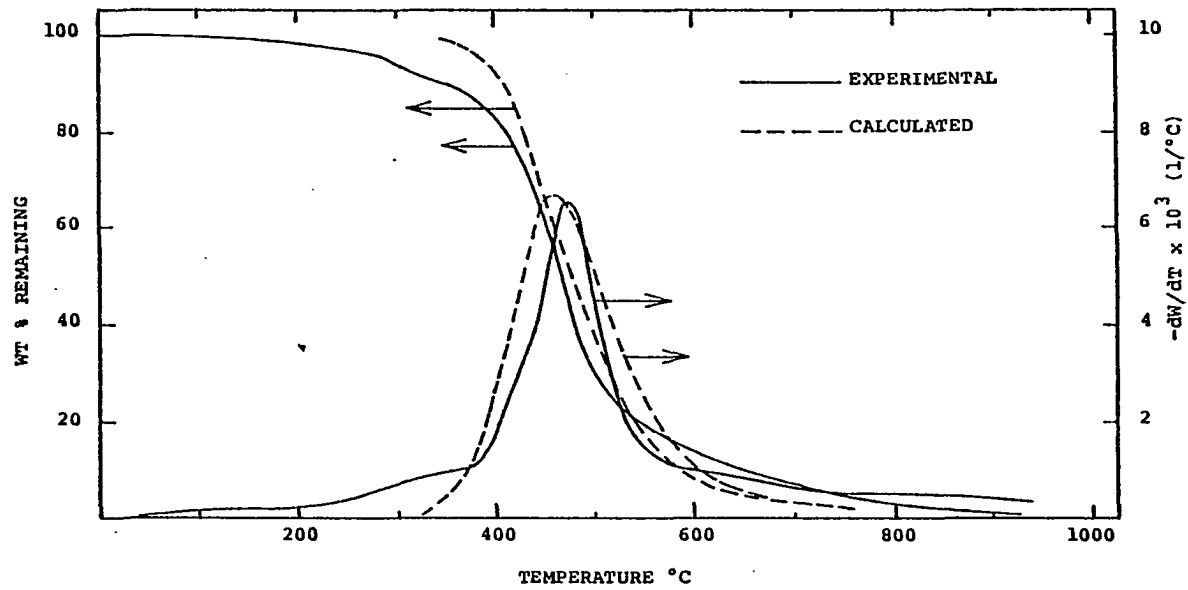


Figure IV-32. Comparison Between Experimental and Calculated (by the Kinetic Parameters Listed in Table IV-2 for 40°C/min Heating Rate) TGA Thermograms for Coal Sample E at 40°C/min. (Experimental Data as Shown in Figure E-3 of Appendix E.)

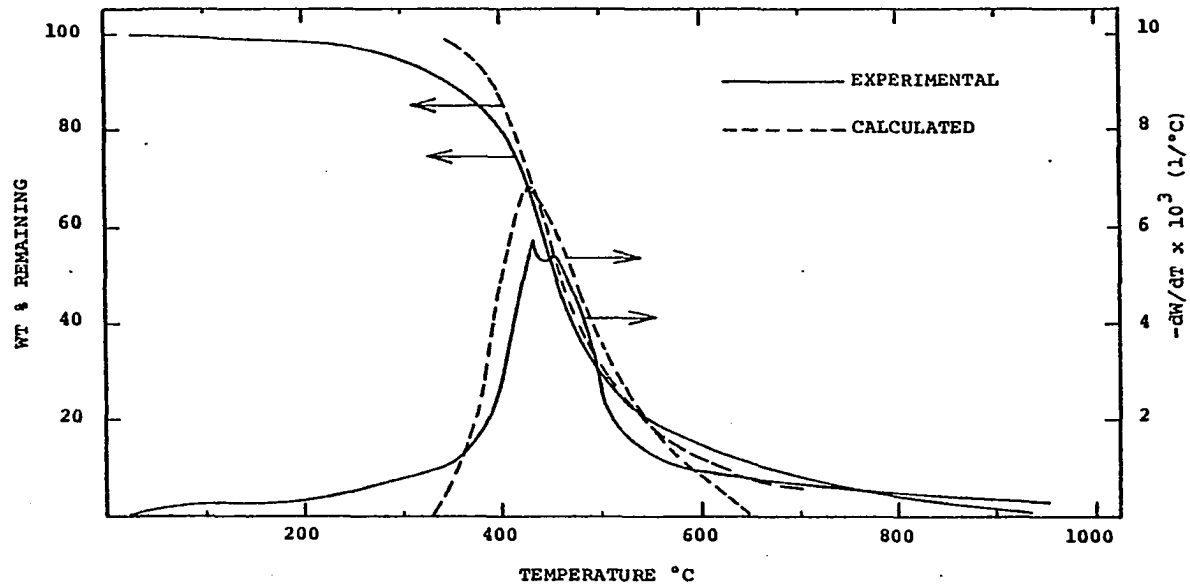


Figure IV-33. Comparison Between Experimental and Calculated (by the Kinetic Parameters Listed in Table IV-2 for 10°C/min Heating Rate) TGA Thermograms for Coal Sample E at 10°C/min. (Experimental Data as Reported in Figure E-5 of Appendix E.)

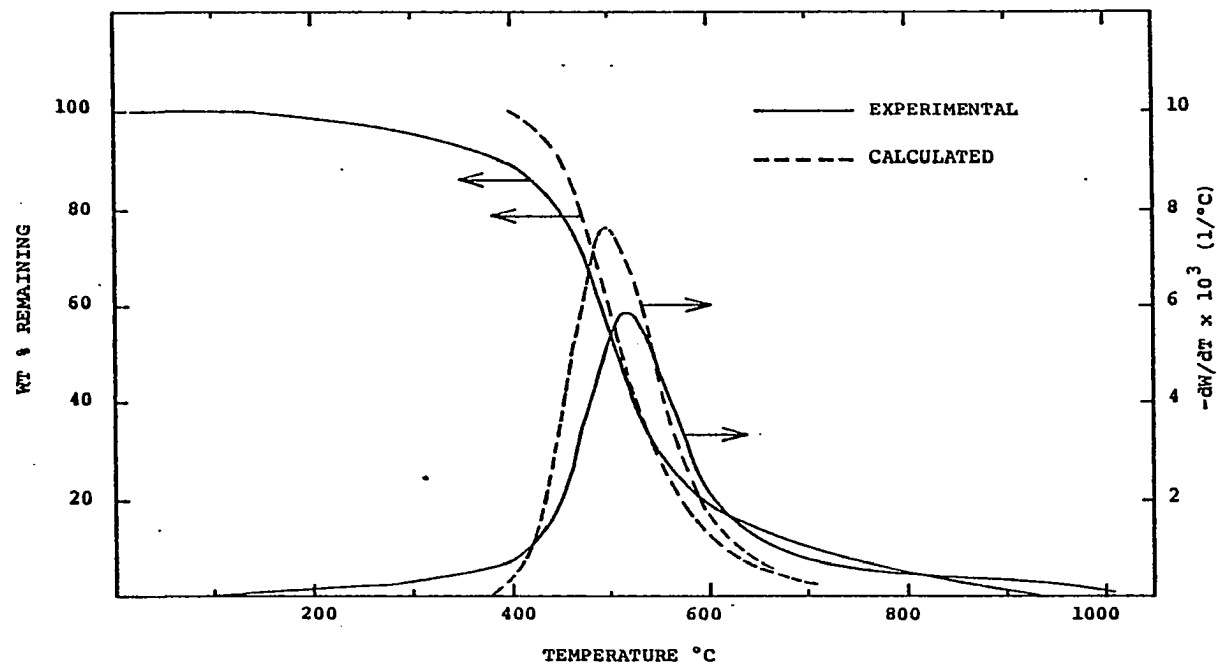


Figure IV-34. Comparison Between Experimental and Calculated (by the Kinetic Parameters Listed in Table IV-2 for 160°C/min Heating Rate) TGA Thermograms for Coal Sample H at 160°C/min. (Experimental Data as Reported in Figure H-1 of Appendix H.)

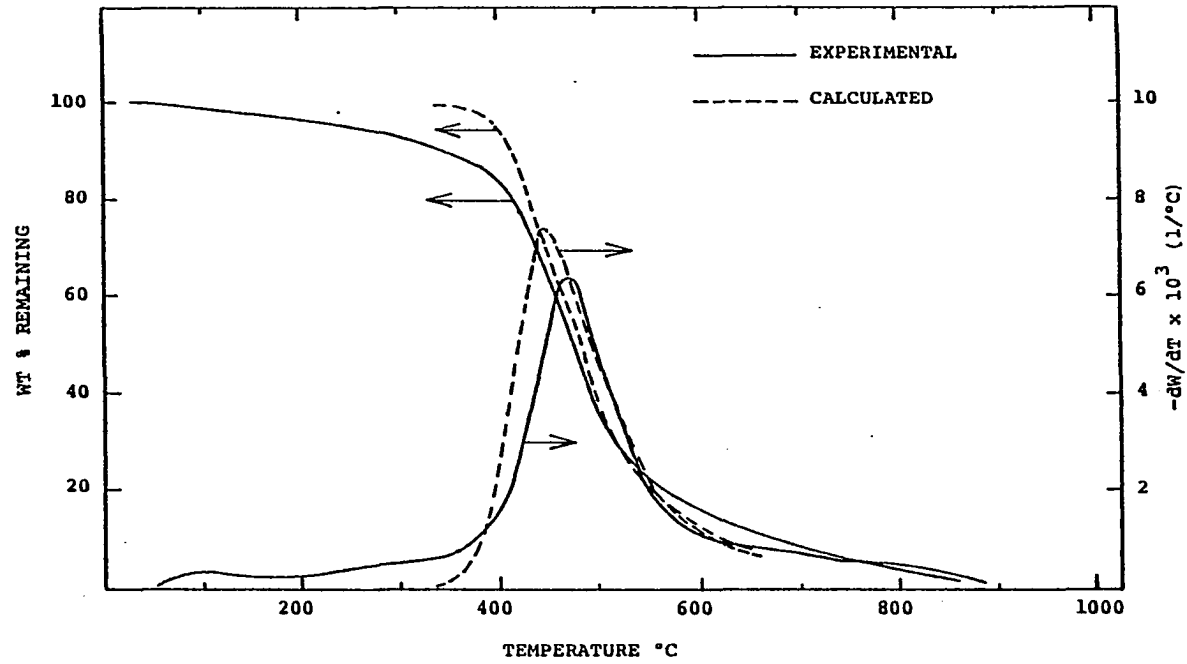


Figure IV-35. Comparison Between Experimental and Calculated (by the Kinetic Parameters Listed in Table IV-2 for 40°C/min Heating Rate) TGA Thermograms for Coal Sample H at 40°C/min. (Experimental Data as Reported in Figure H-3 of Appendix H.)

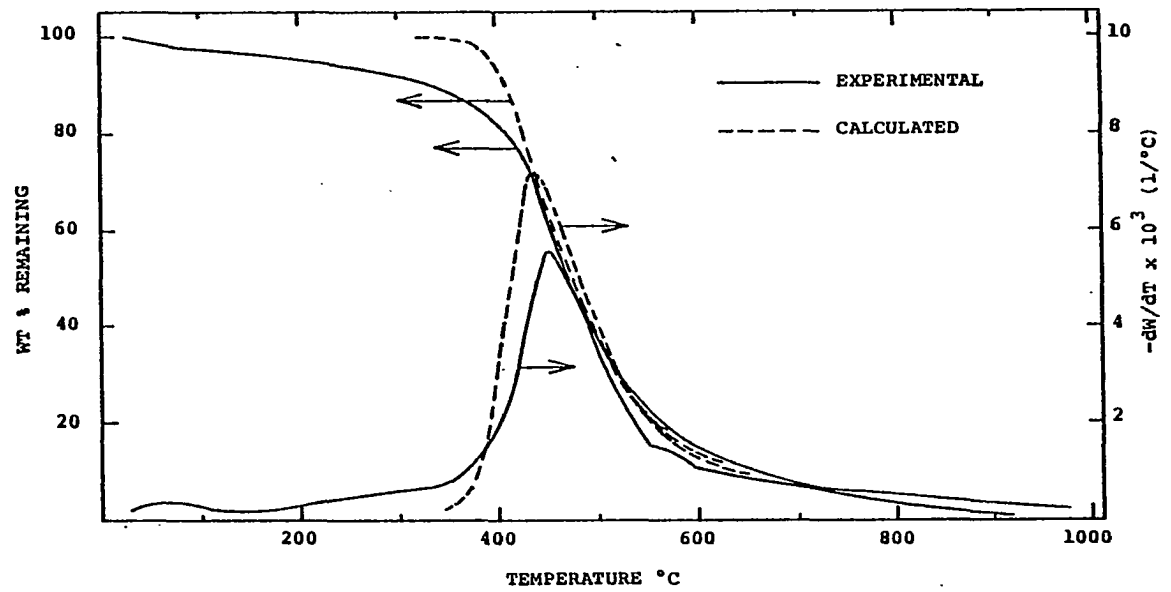


Figure IV-36. Comparison Between Experimental and Calculated (by the Kinetic Parameters Listed in Table IV-2 for 10°C/min Heating Rate) TGA Thermograms for Coal Sample H at 10°C/min. (Experimental Data as Shown in Figure H-5 of Appendix H.)

This improvement in the comparisons between theory and experiment for the three coals and three heating rates suggests that it is possible that three sets of kinetic parameters may be required to describe the entire experimental TGA curves for each sample and for each heating rate. In other words, a separate set of kinetic parameters for each of the initial, mid, and final sections of the TG and DTG curves is indicated.

Differential Scanning Calorimetry of Coal

After the DSC experimentation on coal Sample H was completed (as described earlier), DSC runs were made on the other eight coal samples at heating rates of 320, 160, and 40°C/min. In order to compare runs made with different coating conditions, one run with a partially (only inside of the sample holder cover) "Oildag" coated cover and one run with a fully coated cover for each sample were made at a heating rate of 160°C/min. Two runs with fully coated covers were made for each sample at 320 and 40°C/min heating rates. Data related to all DSC runs are tabulated in Table J-2 of Appendix J.

Figures IV-37 and IV-38 show DSC runs as obtained on the recorder chart paper. In Figure IV-37, a run for coal Sample H is shown as obtained on the DSC-2 at a heating rate of 160°C/min. It is representative of runs which showed an acceptable level, according to the DSC-2 instruction manual, of baseline shift (defined as the difference between the final energy levels of the sample scan and baseline scan at 727°C). Other runs which showed an acceptable baseline shift (+5 chart divisions) were run 82 (coal Sample C at 160°C/min) and run 141 (Sample H at 320°C/min). These sample scans showed, as seen in Figure IV-37, a swing to the exothermic direction during the temperature scan.

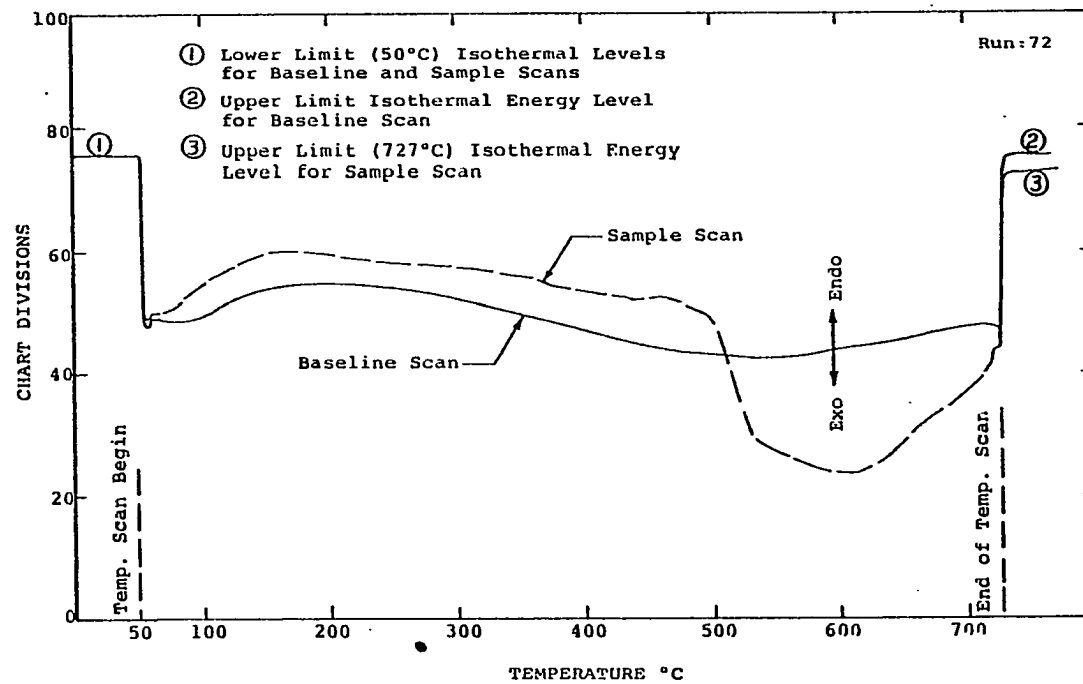


Figure IV-37. An Uncorrected DSC Run as Obtained on the Chart Paper at a 160°C/min Heating Rate for Coal Sample H.

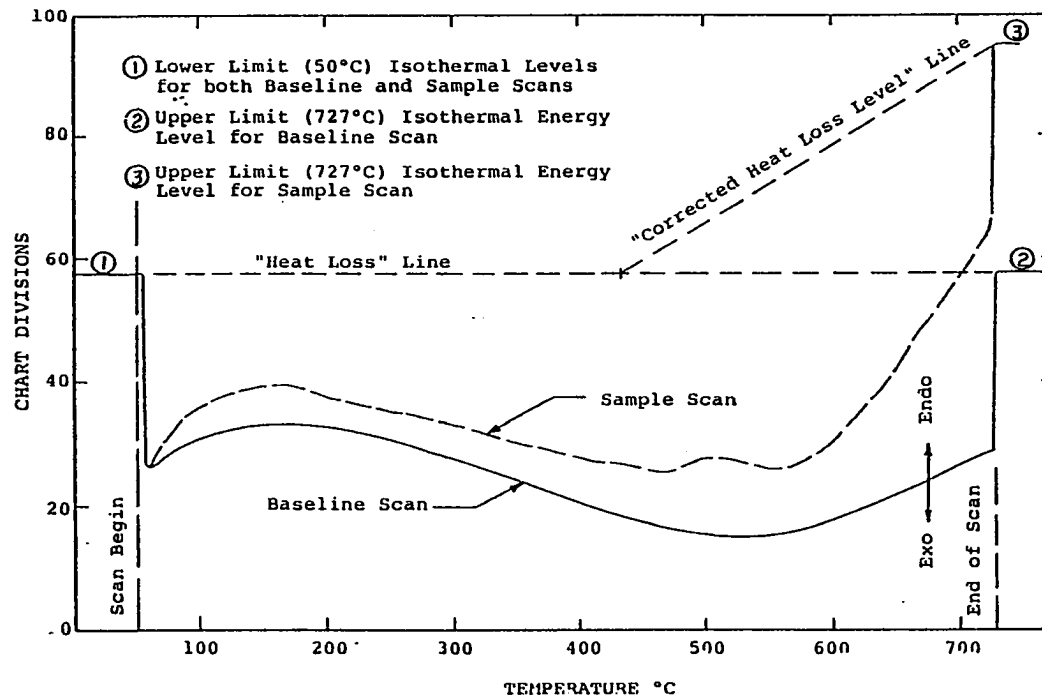


Figure IV-38. An Uncorrected DSC Run as Obtained on the Chart Paper at a 160°C/min Heating Rate for Coal Sample A.

It was observed for most DSC runs that the final energy level, at 727°C, was considerably higher than the final energy level established at the end of the baseline scan. Figure IV-38 is representative of the majority of DSC runs that showed a large baseline shift. A run for coal Sample A, as obtained on the chart, is shown in Figure IV-38 in which the difference between the sample energy level and baseline energy level at 727°C was 37 divisions in the endothermic direction. Also, the sample scan stayed above the baseline scan (endothermic direction) during the temperature scan at 160°C/min. Condensation of devolatilization products on the sample holder cover is the most obvious reason that the final energy level attained at the end (727°C) of the baseline scan (as shown by point 2 in Figure IV-38) shifts gradually during the sample scan and eventually ends up at a considerably different level (as shown by point 3 in Figure IV-38). This shift in baseline occurs because of changes in the radiation heat transfer characteristics resulting from the condensation of pyrolysis products. These products evolve from the coal sample at a rapid rate during the 400-700°C temperature range and condense on the sample holder cover. The importance of the repeatability of these heat loss characteristics during the sample scan on the results from DSC has been discussed by Havens (1969), Brown (1972), and Duvvuri (1974). Havens (1969) states that a 10 percent difference in radiation heat transfer characteristics at 400°C increases the differential energy requirement by a factor of 23 compared to the energy requirement for a typical transition, thereby completely masking this effect. (Rogers and Morris, 1966, have emphasized the effect of emissivity change on the DSC measurements.) Thus, it is essential that the radiation characteristics remain the same

for both the baseline and sample scans. Any changes in the radiation characteristics are indicated at the end of the scan; for example, the difference in the ordinate at 3 and 2 in Figure IV-38 represents the magnitude of the shift. The operating manual suggests that if this shift is small (baseline shift of about 5 divisions, as in Figure IV-37, was considered small), a "correction" can be made with confidence. Nevertheless, even though the baseline shift for most of the DSC runs exceeded 5 divisions, the following correction procedure was employed as the only alternative for interpreting the data:

1. A "heat-loss level" line (horizontal) drawn by connecting the initial energy level (at 50°C) and final energy level for the baseline scan. In Figure IV-38 this line establishes the heat transfer characteristics for the baseline scan.
2. A temperature, T_c , from which the sample scan is to be corrected is located on the "heat-loss level" line. The temperatures for correcting all DSC runs are listed in Table J-2. For most DSC runs, the temperature, T_c , was arbitrarily selected in the range of 434-475°C, where most of the volatilization takes place. For some runs analyzed in the early part of this project, these runs were corrected from the temperature at which the difference between the baseline scan and the sample scan began to increase. This increase in difference, however, always occurred within the temperature range 400-500°C. For the run shown in Figure IV-38, T_c was chosen as 434°C.
3. A "corrected heat-loss level" line is drawn by connecting the temperature point T_c on the heat-loss level line with the final energy level for the sample scan. (See line joining T_c and 3 in Figure IV-39).

4. The sample scan was shifted within this temperature range (434 to 727°C) range, towards the baseline at all temperatures by the amount of difference (in number of chart divisions) between the "heat-loss level line" and "corrected heat-loss level line" at each temperature.

All runs for coal samples were corrected in this manner. Two runs (one run for each of 320°C/min and 160°C/min heating rates for coal Sample H) showed final energy level of the sample scan lower (3 or 5 divisions) than the final energy level for baseline scan. In these cases the baselines were shifted upward in the endothermic direction.

It is important to know here that the correction applied to the DSC curves of this work is not the same as the correction for weight changes applied to DTA and DSC cell thermograms by other investigators. For the reasons already described, the thermograms obtained by conventional DTA methods ('Standard DTA' or 'Boersma Type') have to be corrected for weight change where material undergoes pyrolysis. It is not necessary to correct the thermograms obtained by a Perkin-Elmer DSC-2 for mass changes because (1) the output curves are directly in terms of differential energy calculated (per unit original weight of coal) by measuring the deflection of the sample scan from the level of the baseline scan and (2) principle of operation of DSC-2 is not dependent on the measurement of differential temperature.

The corrected DSC thermograms are shown for nine coal samples in Figures 6, 7, and 8 of Appendices A through I. For example, DSC thermograms for coal Sample A obtained at 320°C/min, 160°C/min and 40°C/min are shown in Figures A-6, A-7, and A-8 of Appendix A, respectively. Since the change in heat losses was assumed linear over the

temperature range (T_c to 727°C) for correcting the DSC curves, it is desirable that all runs made at one heating rate be tested for reproducibility; therefore, all corrected DSC thermograms are presented in the following discussion.

Each of Figures IV-39 through IV-65 show two corrected DSC runs obtained for each sample at the same heating rate. Figures IV-39 through IV-47 show thermograms obtained for coal samples at $320^\circ\text{C}/\text{min}$. The corrected DSC runs made at $160^\circ\text{C}/\text{min}$ are shown in Figures IV-48 through IV-56 and $40^\circ\text{C}/\text{min}$ thermograms are shown in Figures IV-57 through IV-65. Most of these figures present comparison between two identically obtained DSC runs. Since one run with fully coated covers and one run with partially coated covers were made at $160^\circ\text{C}/\text{min}$ for Samples B through I, the Figures IV-48 through IV-56 show comparisons between two runs obtained with different coating conditions but at the same heating rate. For most of the runs, the value of T_c was selected at 434°C , the temperature at which the correction for baseline shift was initiated. However, in some cases where the onset of decomposition was delayed, a higher value of T_c was selected. In these cases (Figure IV-52, -56, -57, -58, -59) the values of T_c for the two runs being compared were different and are so indicated on the figures. For some runs, for example, run 125 (Sample A, $320^\circ\text{C}/\text{min}$), run 173 (Sample E, $40^\circ\text{C}/\text{min}$), run 81 (Sample I, $160^\circ\text{C}/\text{min}$), etc., deflections large enough to exceed the DSC-2 millivolt output range were observed during the sample scan or at the end of the sample scan due to baseline shift. In cases where the final energy level for the sample scan could not be located because the output exceeded the range of instrument, the range limit was considered as the final

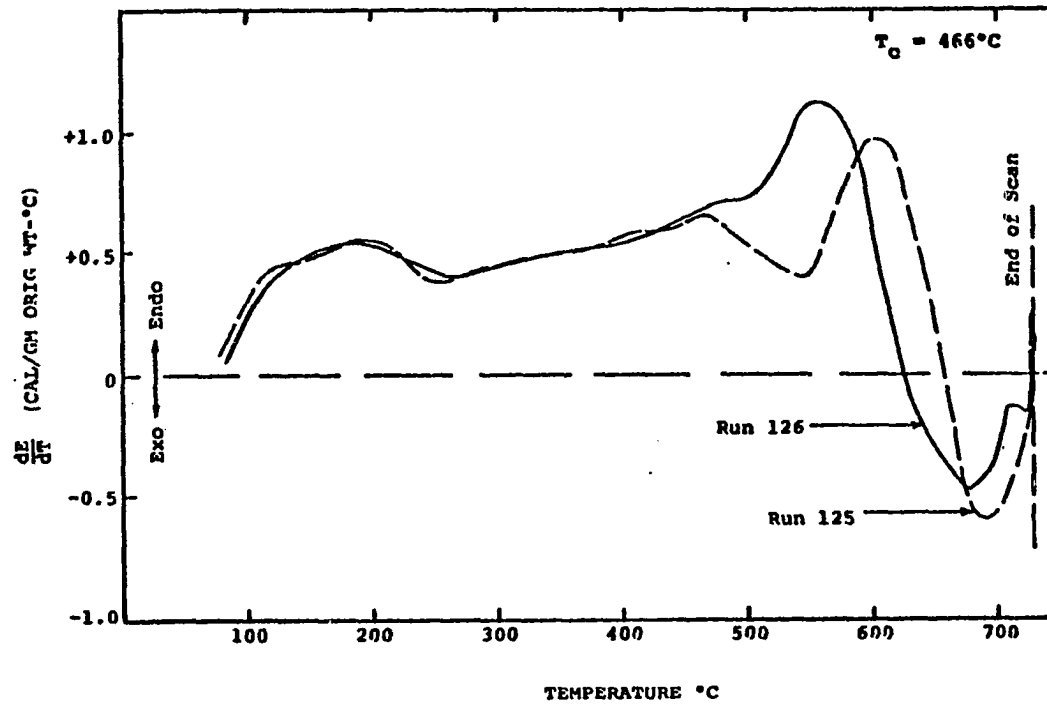


Figure IV-39. Comparison of Runs Obtained on DSC at a Heating Rate of 320°C/min for Coal Sample A. [Note: 'E' of dE/dT mentioned in DSC discussion and figures is not the same as kinetic parameter E mentioned during the TGA discussion. For unit original sample weight, the value of dE/dT at a temperature is equal to the specific heat of coal sample, which is the product of ordinate displacement constant (K_d , as discussed on page 51) and chart displacement for the coal sample from the baseline level, at that temperature.]

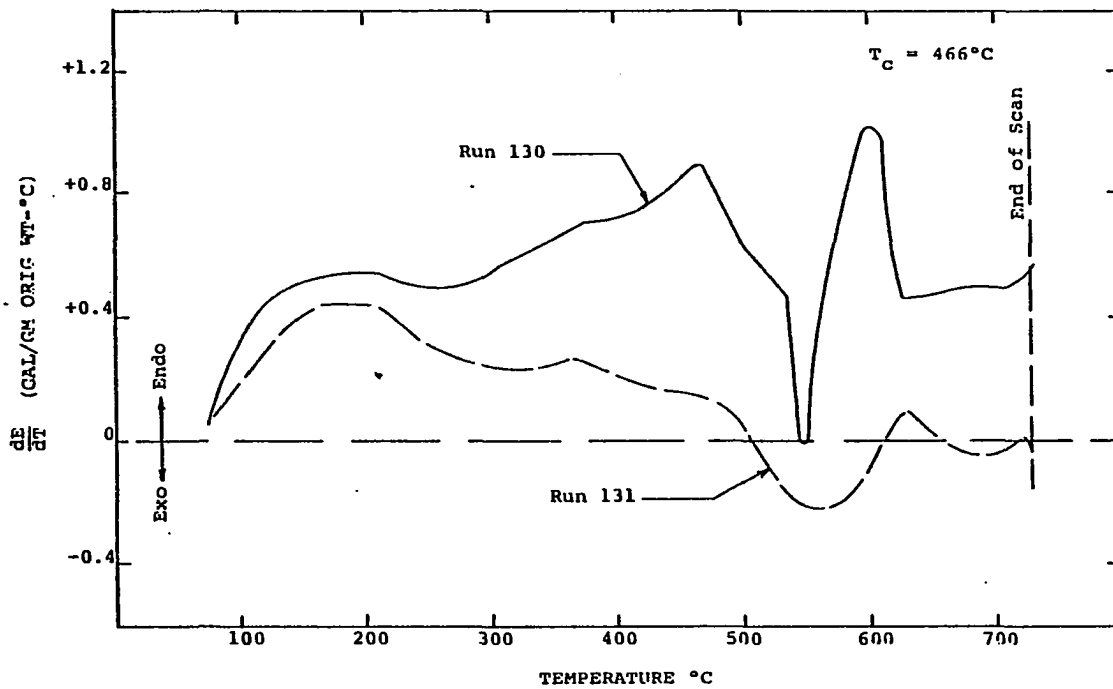


Figure IV-40. Comparison of Runs Obtained on DSC at a Heating Rate of 320°C/min for Coal Sample B.

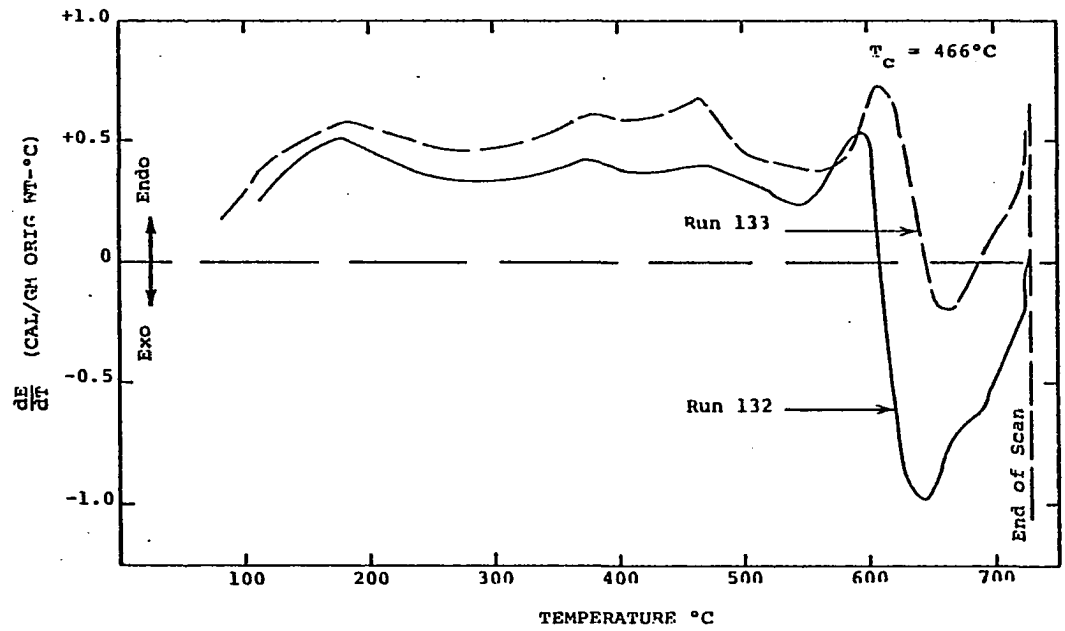


Figure IV-41. Comparison of Runs Obtained on DSC at a Heating Rate of 320°C/min for Coal Sample C.

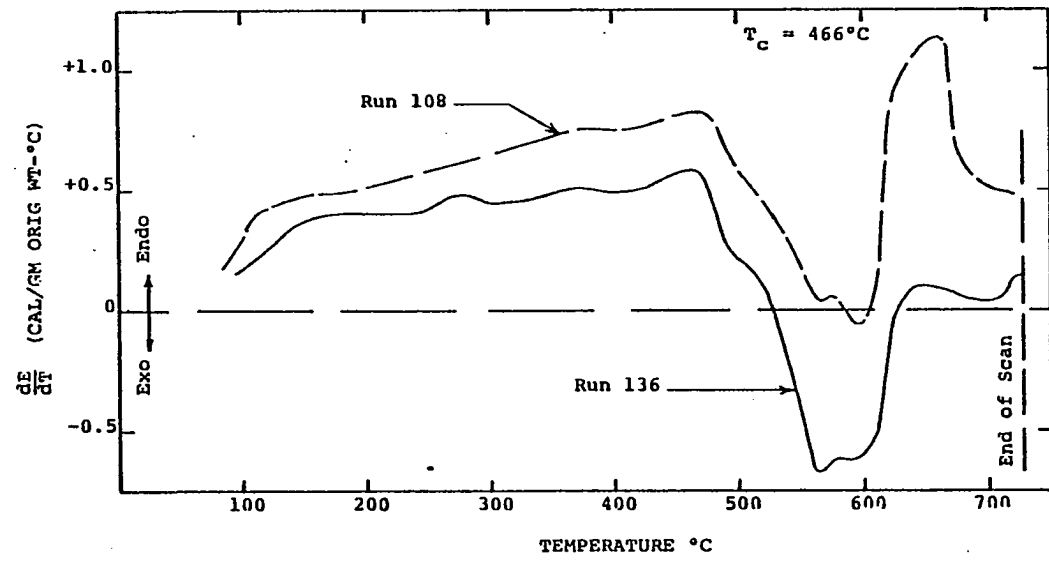


Figure IV-42. Comparison of Runs Obtained on DSC at a Heating Rate of 320°C/min for Coal Sample D.

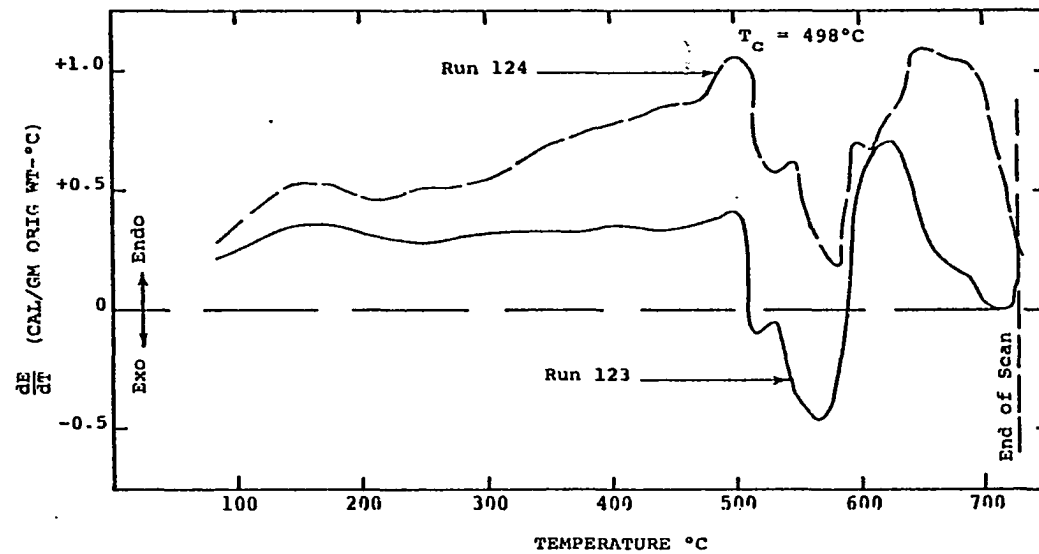


Figure IV-43. Comparison of Runs Obtained on DSC at a Heating Rate of 320°C/min for Coal Sample E.

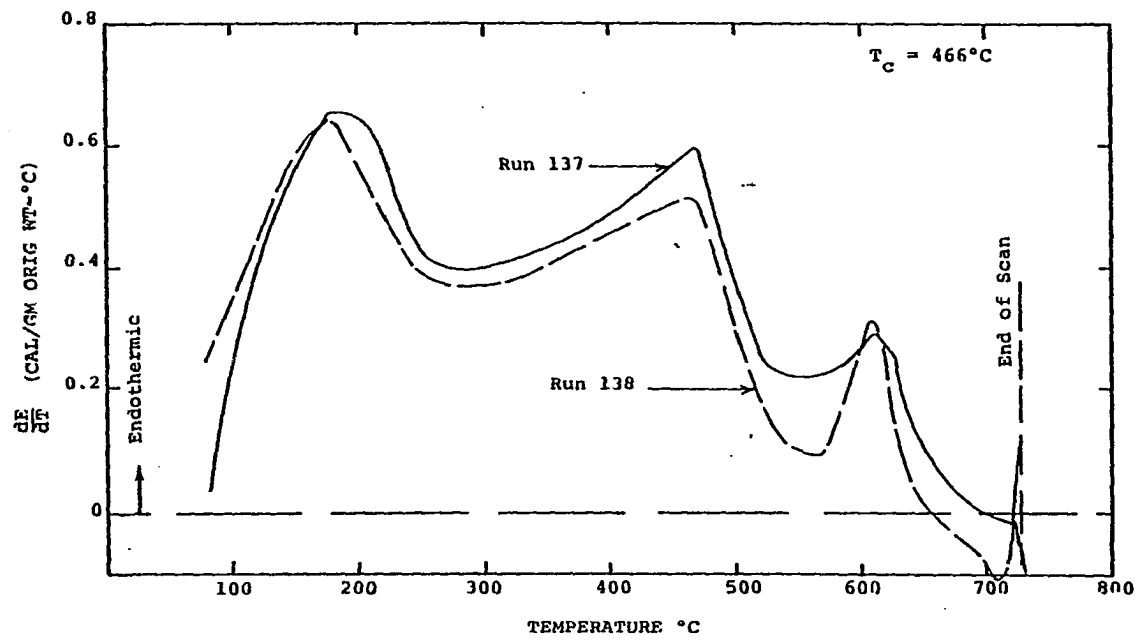


Figure IV-44. Comparison of Runs Obtained on DSC at a Heating Rate of 320°C/min for Coal Sample F.

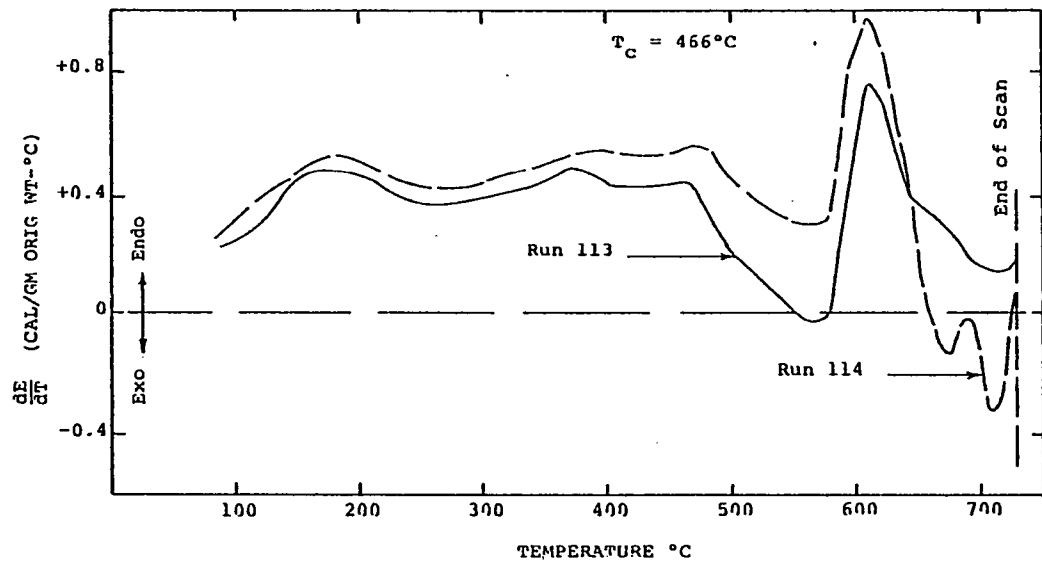


Figure IV-45. Comparison of Runs Obtained on DSC at a Heating Rate of 320°C/min for Coal Sample G.

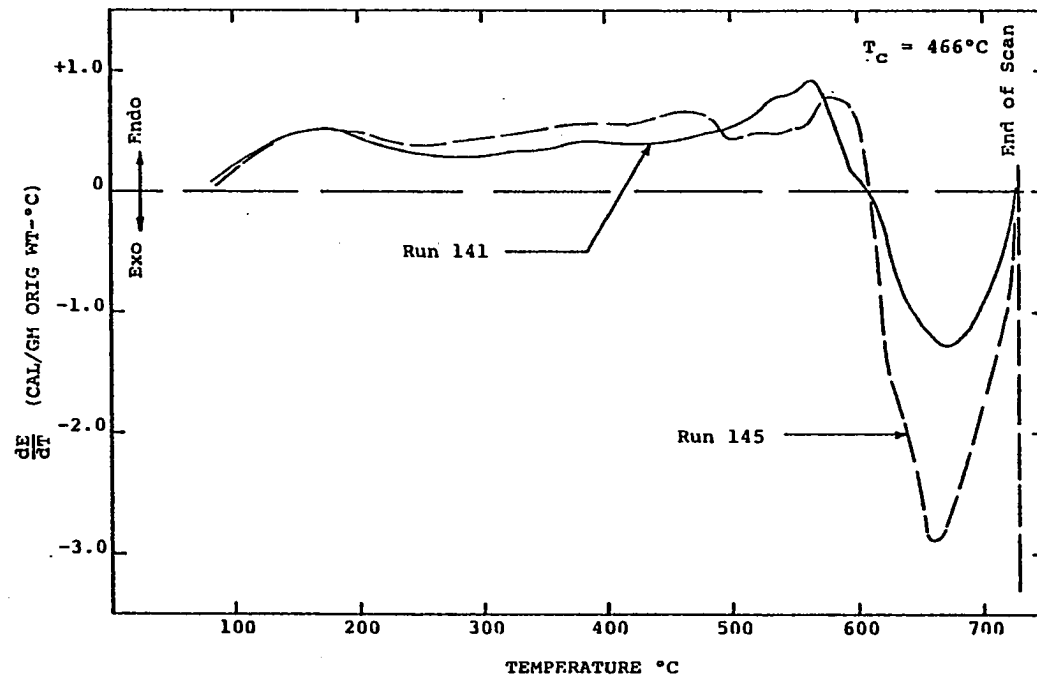


Figure IV-46. Comparison of Runs Obtained on DSC at a Heating Rate of 320°C/min for Coal Sample H.

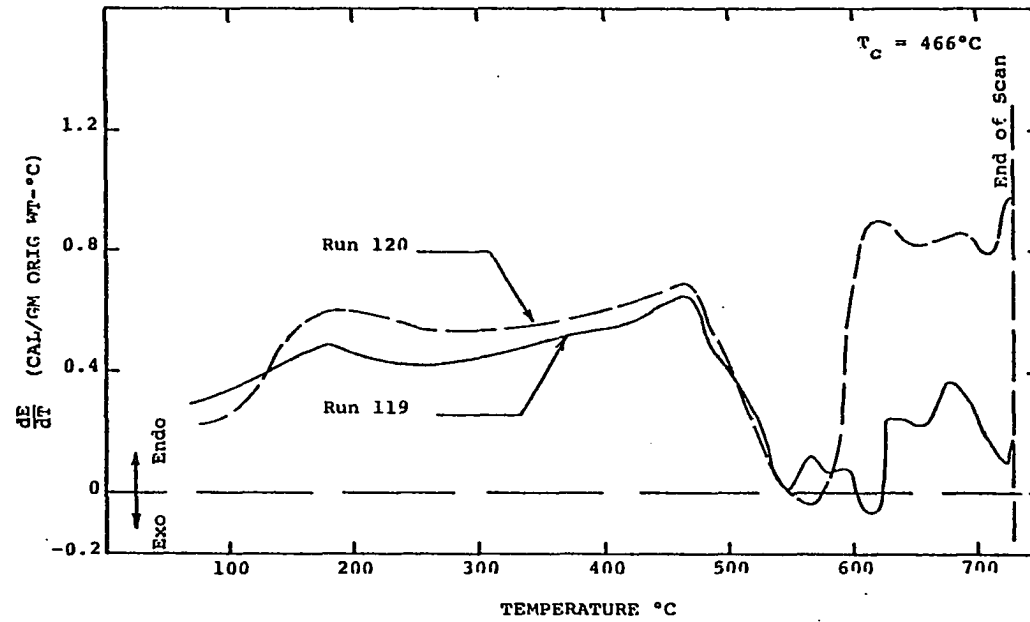


Figure IV-47. Comparison of Runs Obtained on DSC at a Heating Rate of 320°C/min for Coal Sample I.

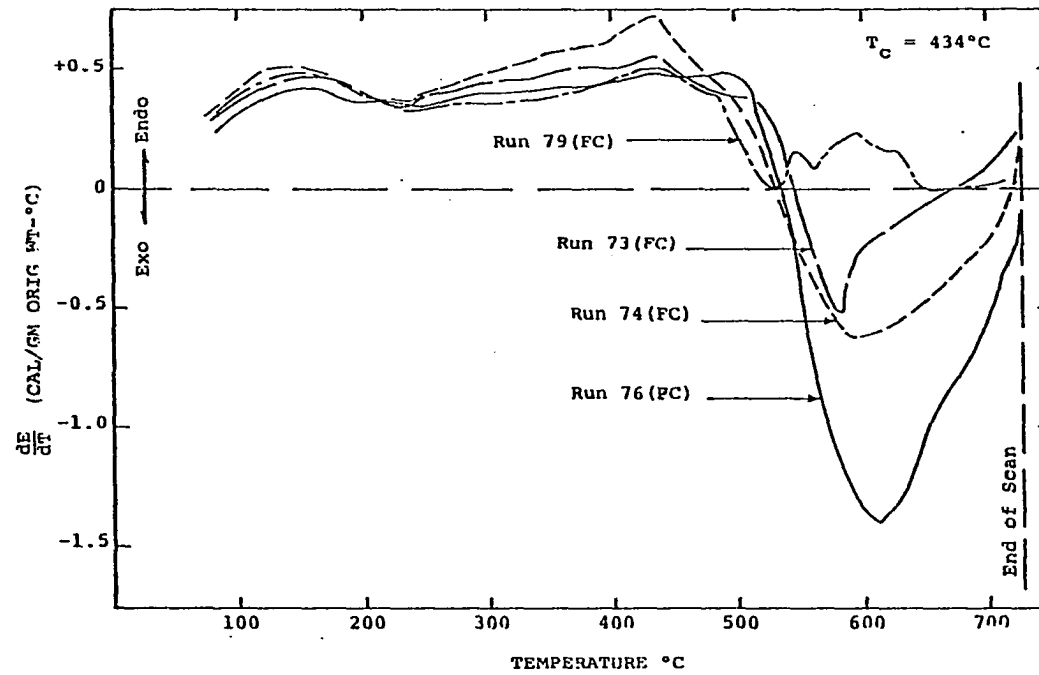


Figure IV-48. Comparison of Runs Obtained on DSC at a Heating Rate of 160°C/min for Coal Sample A. 'FC' or 'PC' in Figures IV-48 through IV-57 indicate coating condition (fully or partially coated) of covers for the run.

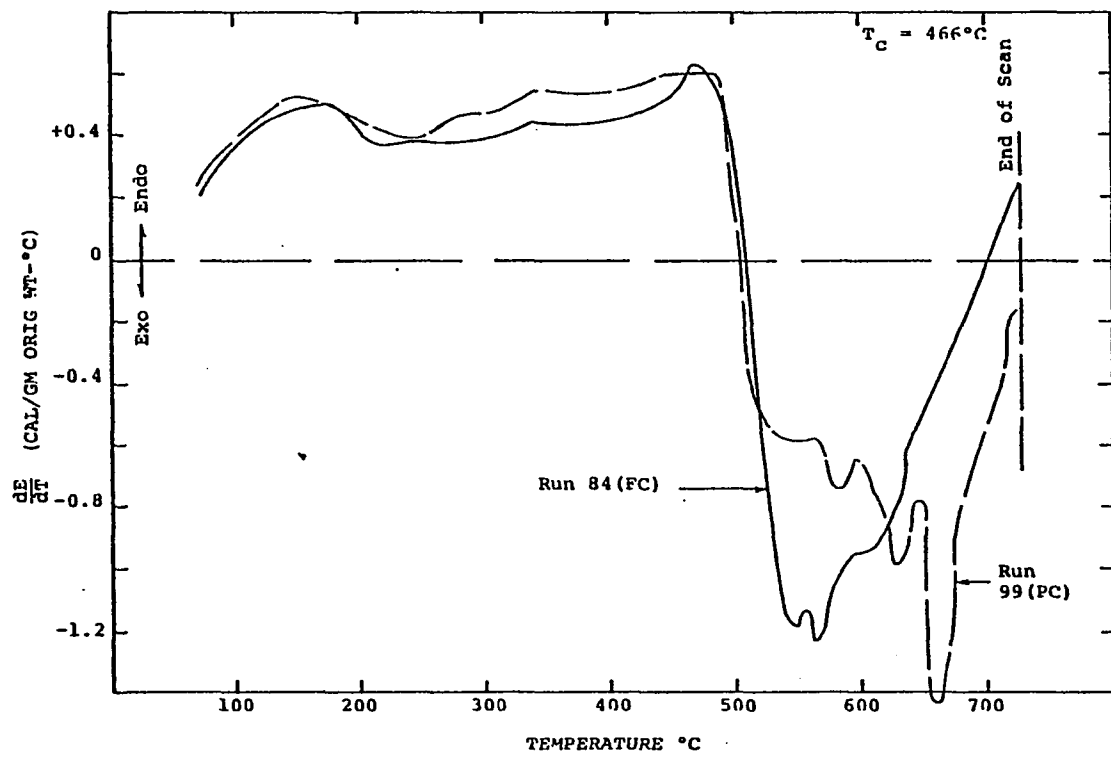


Figure IV-49. Comparison of Runs Obtained on DSC at a Heating Rate of 160°C/min for Coal Sample B.

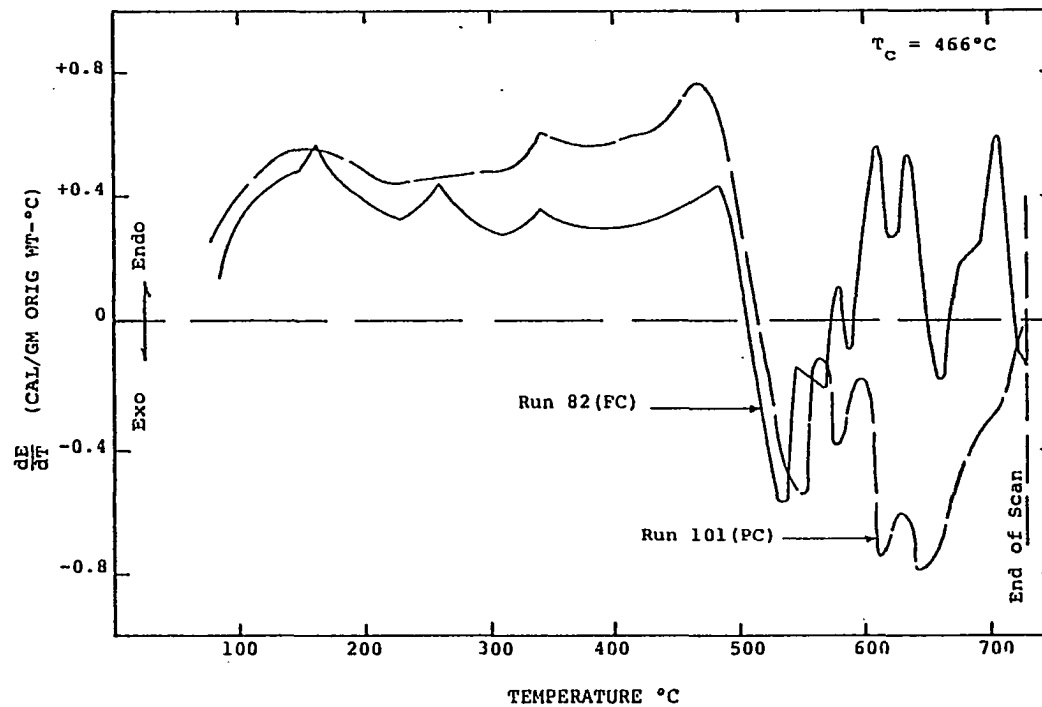


Figure IV-50. Comparison of Runs Obtained on DSC at a Heating Rate of 160°C/min for Coal Sample C.

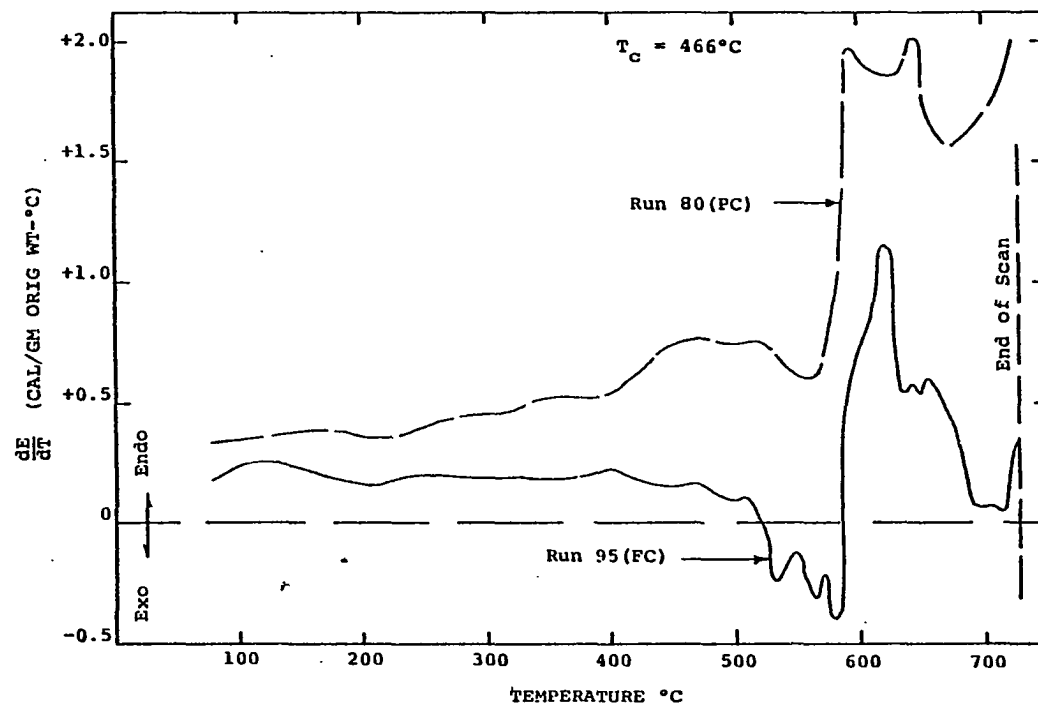


Figure IV-51. Comparison of Runs Obtained on DSC at a Heating Rate of 160°C/min for Coal Sample D.

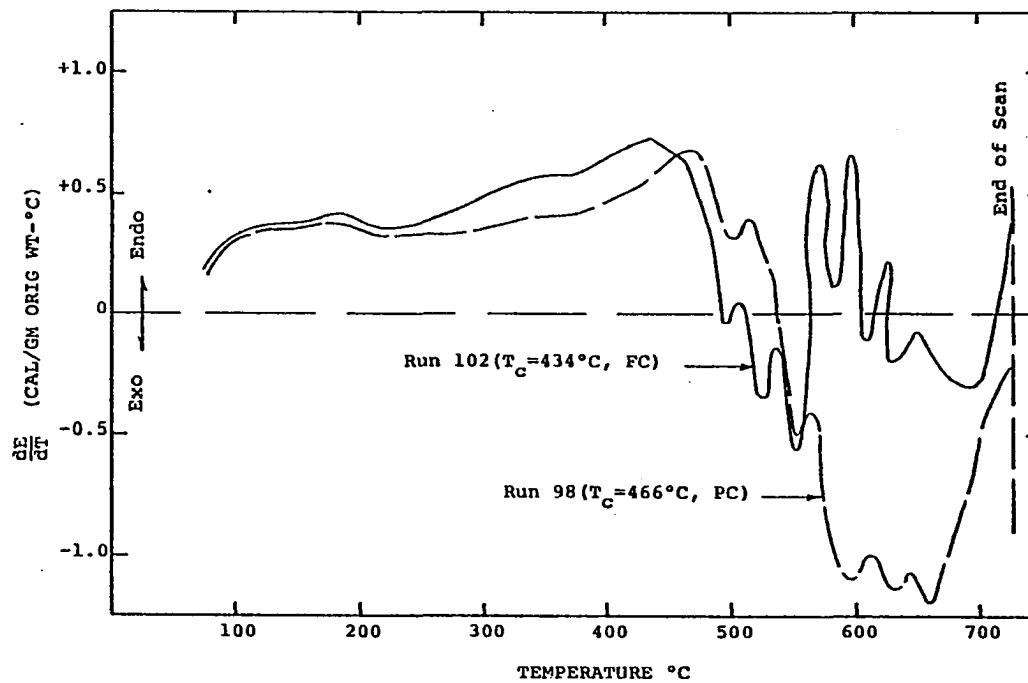


Figure IV-52. Comparison of Runs Obtained on DSC at a Heating Rate of 160°C/min for Coal Sample E.

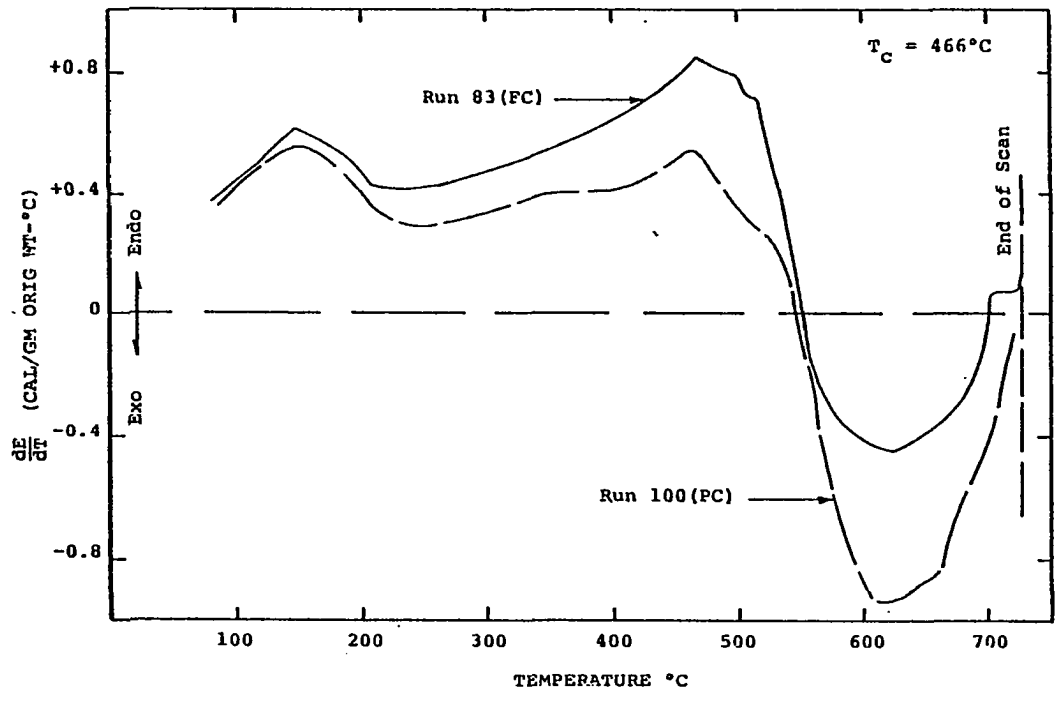


Figure IV-53. Comparison of Runs Obtained on DSC at a Heating Rate of 160°C/min for Coal Sample F.

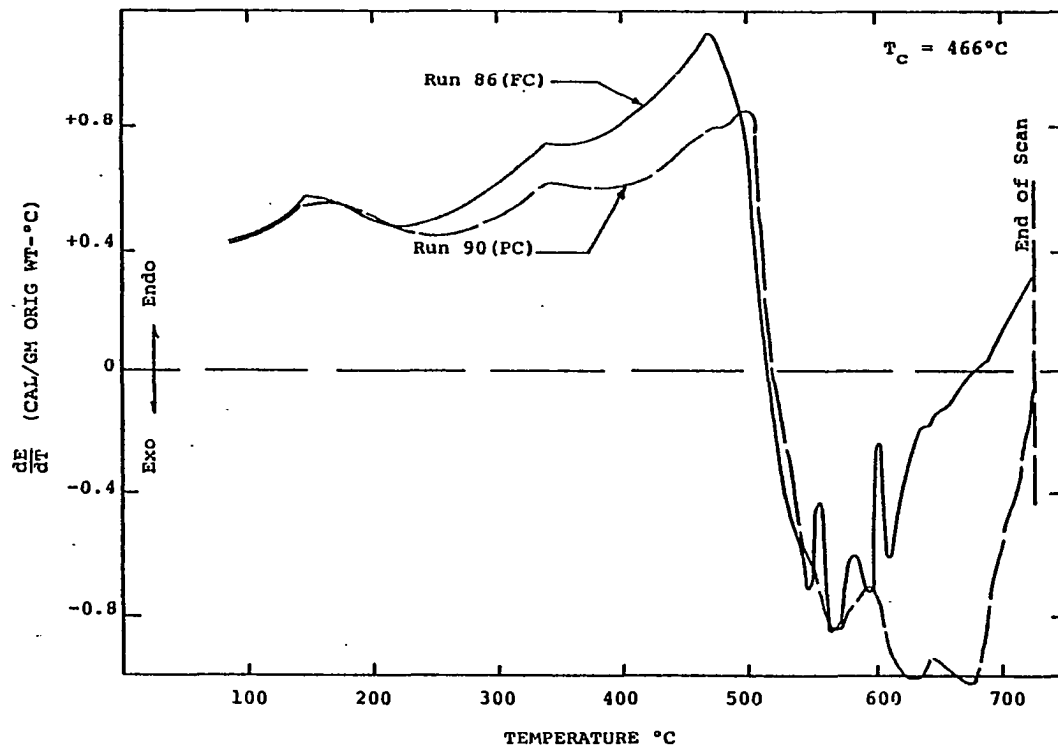


Figure IV-54. Comparison of Runs Obtained on DSC at a Heating Rate of 160°C/min for Coal Sample G.

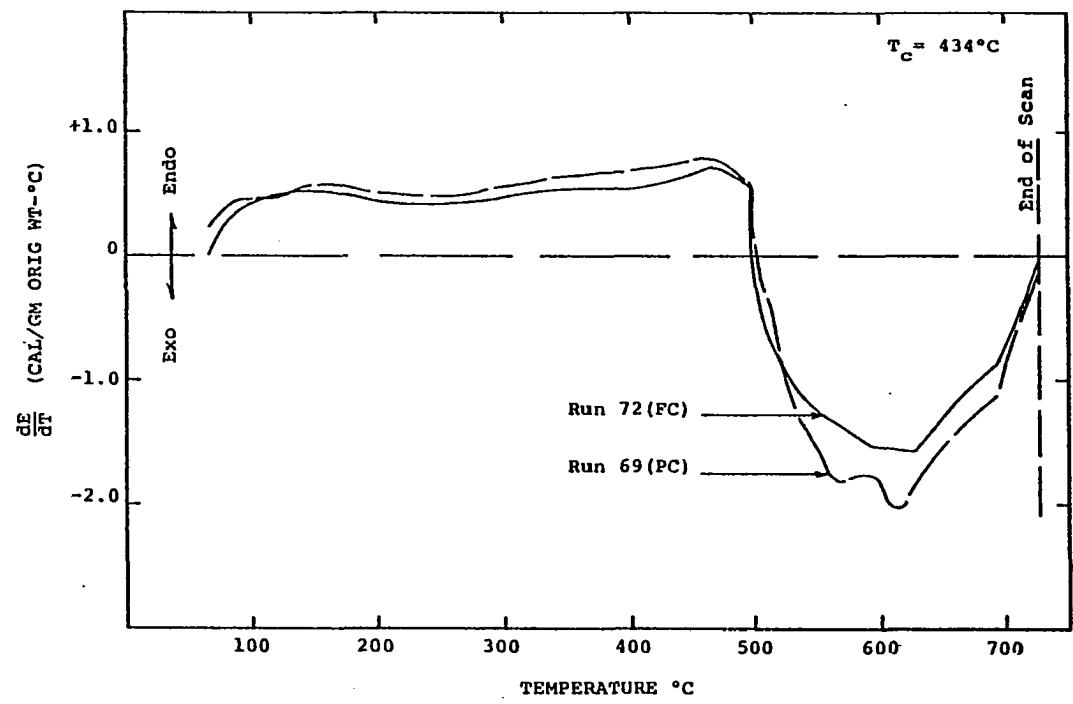


Figure IV-55. Comparison of Runs Obtained on DSC at a Heating Rate of 160°C/min for Coal Sample H.

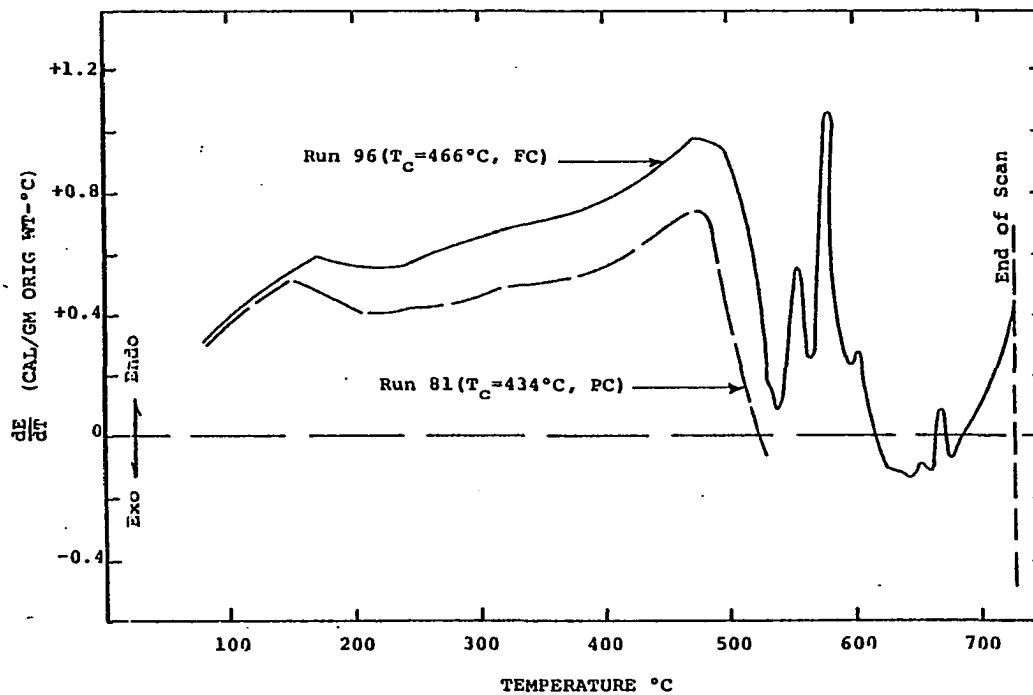


Figure IV-56. Comparison of Runs Obtained on DSC at a Heating Rate of 160°C/min for Coal Sample I.

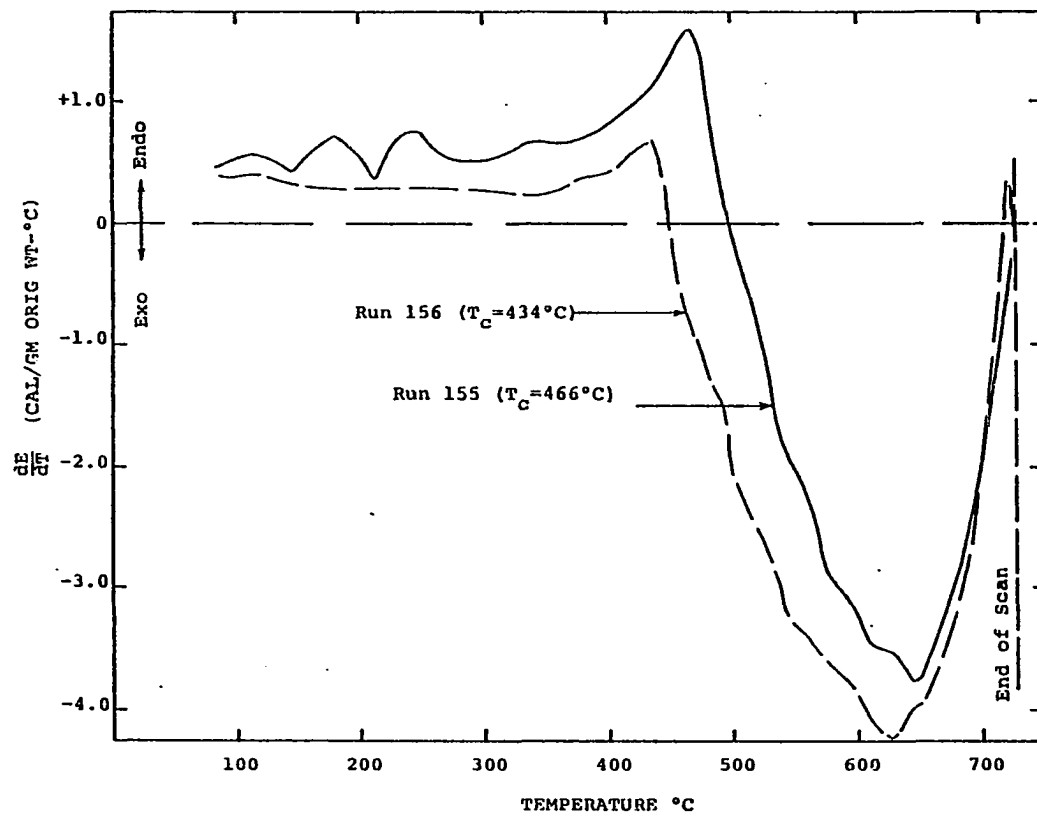


Figure IV-57. Comparison of Runs Obtained on DSC at a Heating Rate of 40°C/min for Coal Sample A.

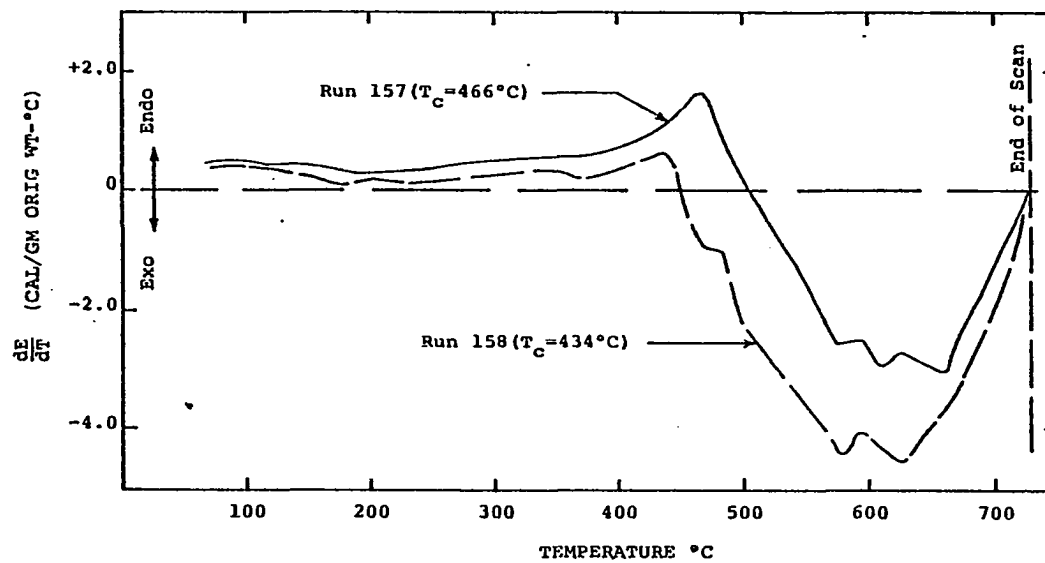


Figure IV-58. Comparison of Runs Obtained on DSC at a Heating Rate of 40°C/min for Coal Sample B.

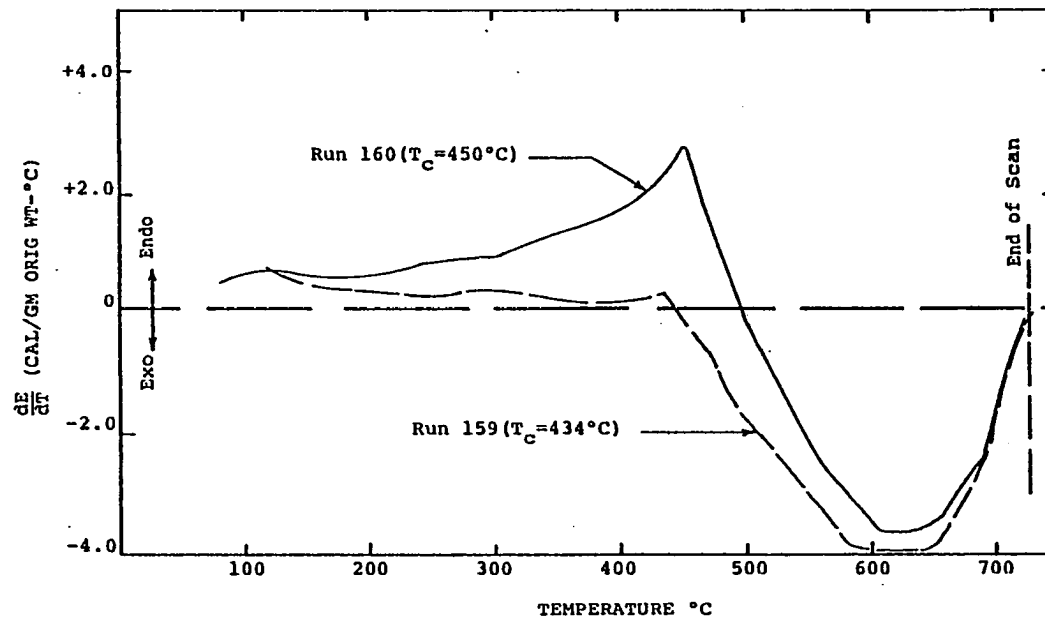


Figure IV-59. Comparison of Runs Obtained on DSC at a Heating Rate of 40°C/min for Coal Sample C.

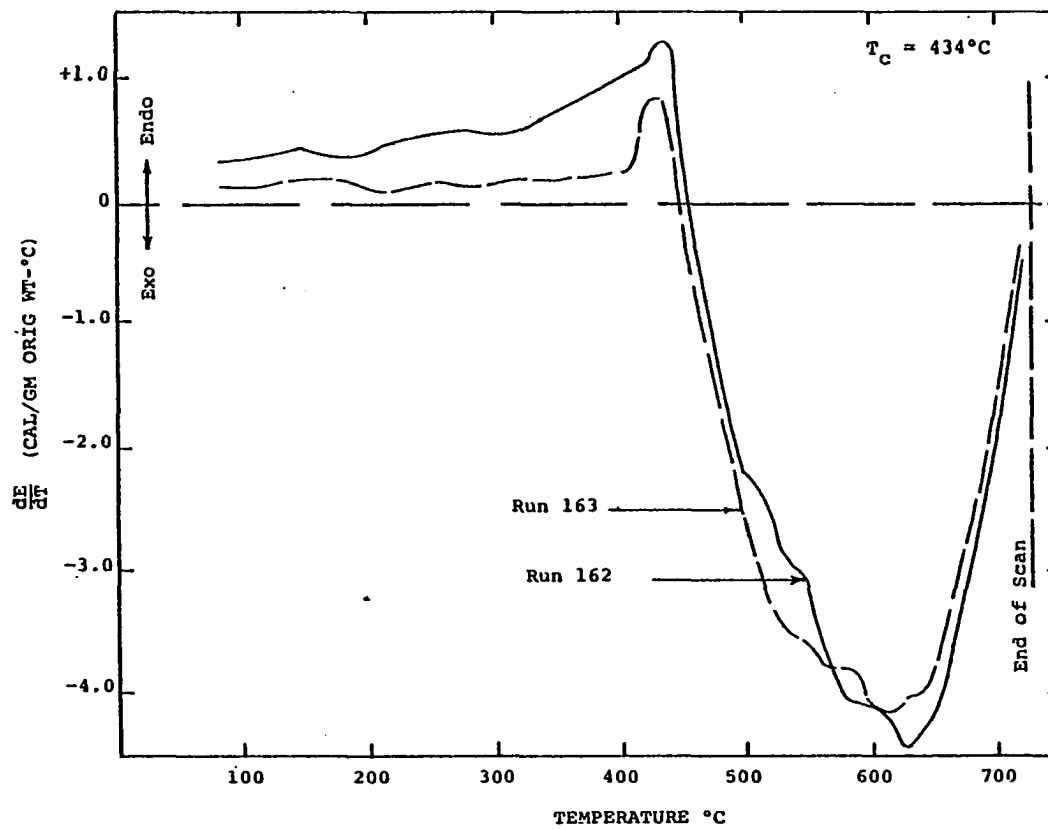


Figure IV-60. Comparison of Runs Obtained on DSC at a Heating Rate of 40°C/min for Coal Sample D.

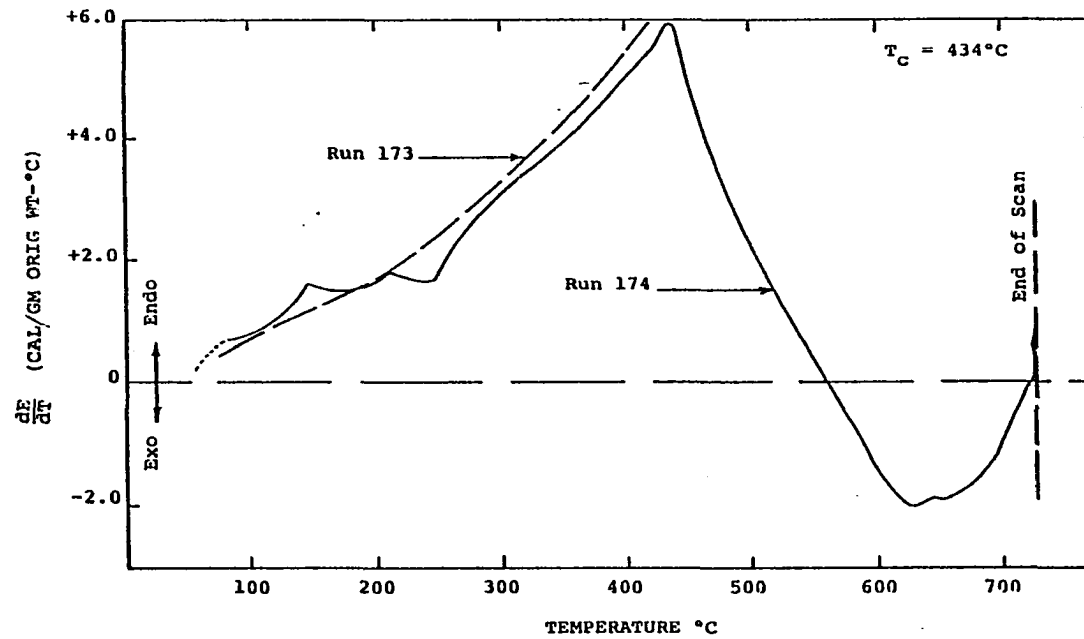


Figure IV-61. Comparison of Runs Obtained on DSC at a Heating Rate of 40°C/min for Coal Sample E.

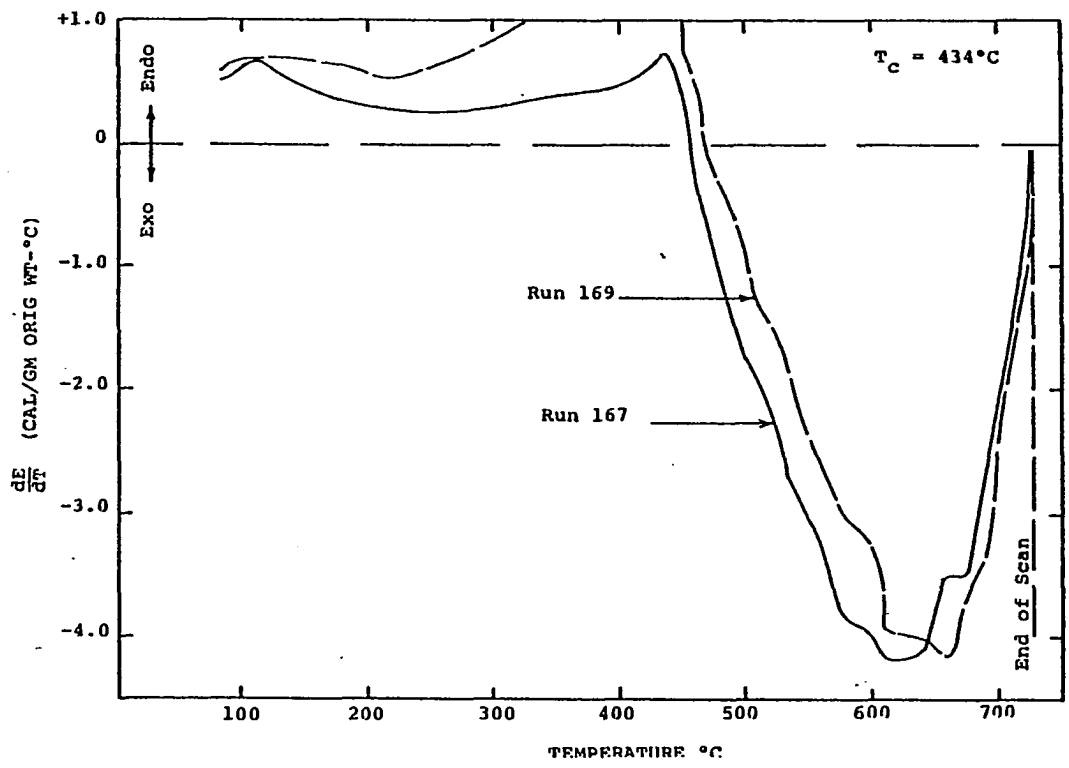


Figure IV-62. Comparison of Runs Obtained on DSC at a Heating Rate of 40°C/min for Coal Sample F.

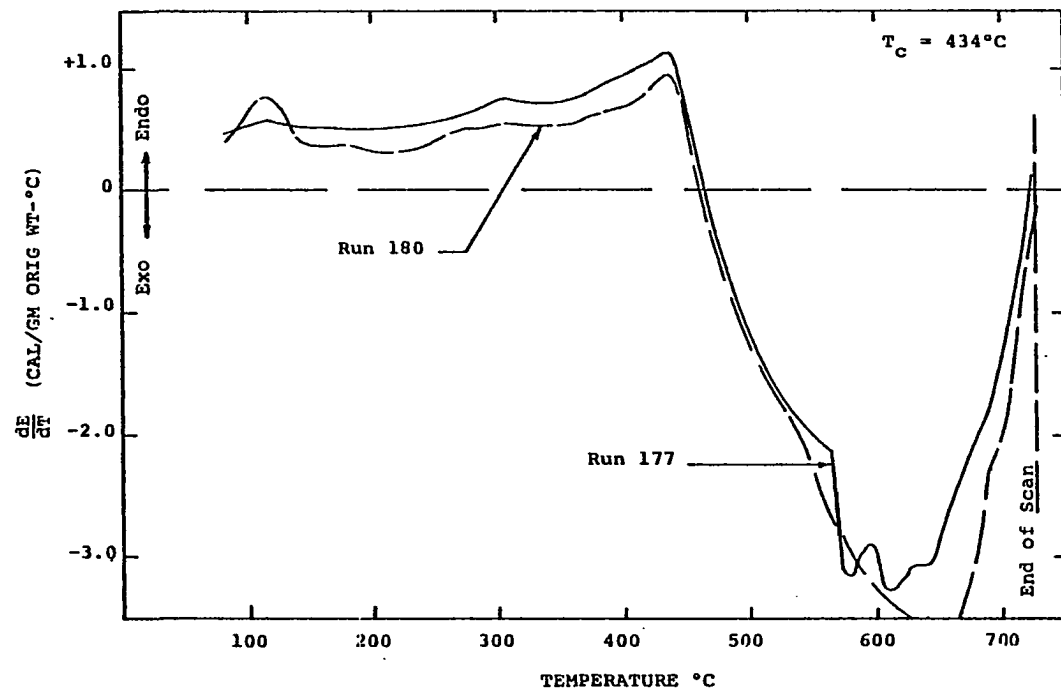


Figure IV-63. Comparison of Runs Obtained on DSC at a Heating Rate of 40°C/min for Coal Sample G.

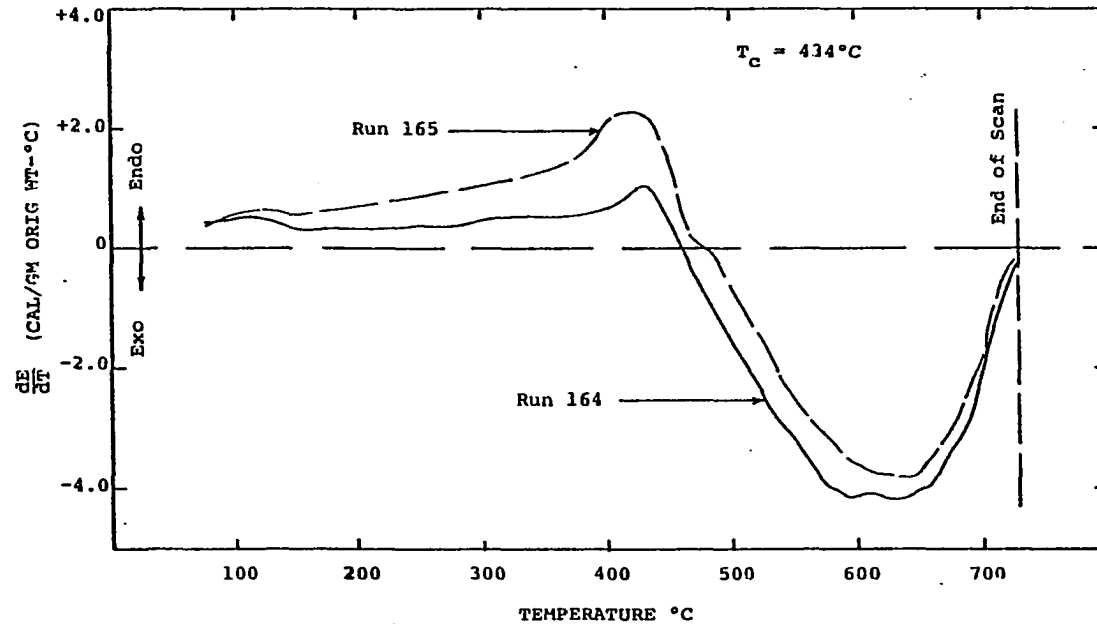


Figure IV-64. Comparison of Runs Obtained on DSC at a Heating Rate of 40°C/min for Coal Sample H.

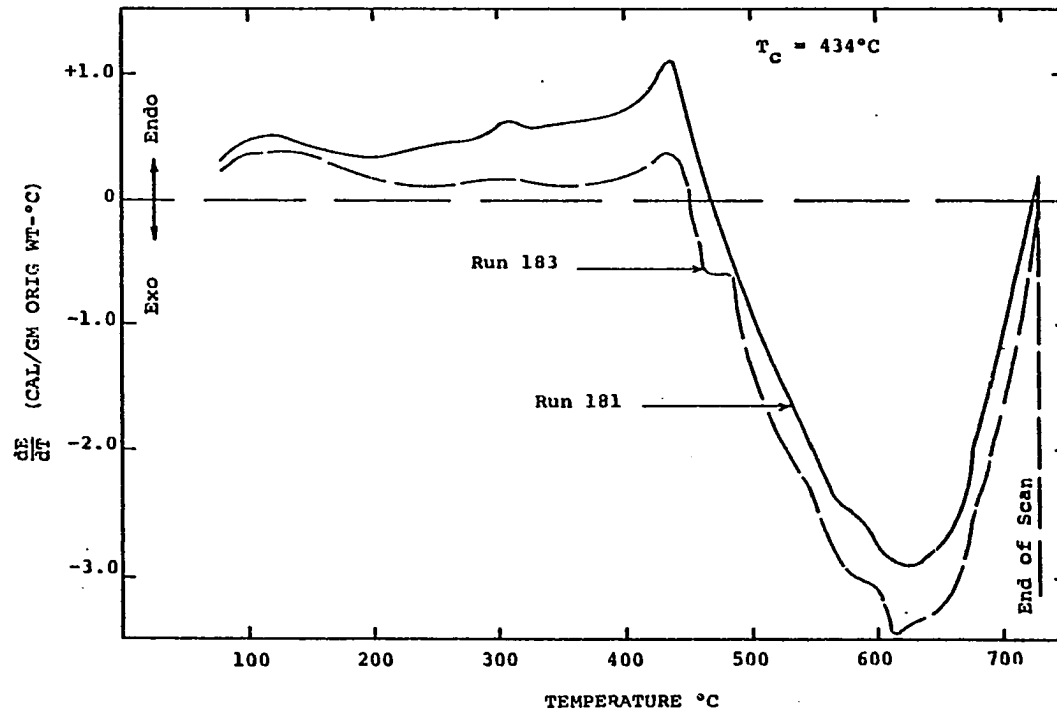


Figure IV-65. Comparison of Runs Obtained on DSC at a Heating Rate of 40°C/min for Coal Sample I.

sample energy level. These scans, therefore, were corrected for 5 to 7 fewer divisions. For two runs, run 81 (Sample I, 160°C/min) and run 173 (Sample E, 40°C/min) the deflection exceeded the output range during the sample scan, and, therefore, the complete curves could not be shown on Figures IV-56 and IV-61.

The following observations were made from Figures IV-39 through IV-65:

1. The shape of the curve was the same for scans obtained at one heating rate. A scan for coal Sample B was not observed to follow this observation for reasons that could not be explained. DSC thermograms obtained at 160°C/min showed a large number of small peaks and valleys for coal Samples C, D, and G on one run but these peaks were absent on the other scan. This lack of reproducibility of small peaks is probably due to inhomogeneities caused by small sample sizes that must be used in the DSC system.
2. In general, the comparison between repetitive runs indicates that the resulting DSC thermograms are similar quantitatively up to a temperature of 500 to 600°C but are displaced quantitatively to varying degrees from an insignificant amount to as much as a factor of 2. The reason for this variation among the coal samples is not known; possibly the energy level shift may be due to a change in coating conditions between the runs or due to inherent differences in applying new coatings (covers were recoated every three or four runs).
3. Figure IV-48 shows four runs for coal Sample A obtained at a heating rate of 160°C/min. The runs show that energetics of coal

pyrolysis are endothermic up to a temperature of 500°C. After 500°C, two runs showed exothermic energies but one run showed endothermic behavior within 500-727°C. The fourth run, obtained with one partially coated cover, showed the largest exothermic peak of all four sample scans.

4. The comparison of two runs obtained by 160°C/min for each sample (Figures IV-48 through IV-56) shows that the run with the partially "Oildag" coated cover shows an exotherm larger than the run made with two fully coated covers.
5. At low temperatures, (50-400°C), the two scans obtained at the 40°C/min heating rate differ considerably in values of dE/dT . This difference is larger than the differences observed for scans obtained at high heating rates (320 or 160°C/min) in the temperature range 50-400°C.
6. The two runs for coal Sample E made at 40°C/min showed large endothermic behavior (Figure IV-61) in the beginning of the temperature scan. This behavior was unique since it was not observed for any other coal samples.
7. When one scan is corrected over a wider temperature range than the other, the scan that is corrected over the wider temperature shifts to the exothermic direction at a lower temperature than the scan corrected over a narrow range.

The differential energy versus temperature thermograms for nine coal samples, Figures 6, 7, and 8 of Appendices A through I, and also shown in Figures IV-39 through IV-65, were integrated to find the energies of pyrolysis by measuring the area under the curves. The

results are reported in Tables IV-3, IV-4, and IV-5 in which the endothermic and exothermic temperature are defined for coal sample scans made at 320, 160, and 40°C/min heating rates. The total energy required to pyrolyze a coal sample is obtained by adding the energies of the endothermic and exothermic portions for each sample scan. Tables IV-3, IV-4, and IV-5 also list the result of this addition.

Effect of Heating Rate on the DSC Thermogram

The thermograms found in the Appendices for each sample are shown in Figures IV-66 through IV-74 to illustrate the effect of the heating rate on the DSC curves of coal samples.

The following observations were made from Figures IV-66 through IV-74:

1. The temperature range for the initial endothermic section increases with an increase in the heating rate for most of the coal samples. This observation is apparent from Figures IV-66, IV-68, IV-69, IV-71, IV-72, and IV-73.
2. The temperature at which the endotherm swings toward the exothermic direction is shifted to a higher temperature with an increase in the heating rate.
3. The coal Samples C, D, and G (Figures IV-68, IV-69, and IV-72) show small peaks and valleys for the scans obtained at 160°C/min. The absence of these peaks in scans made at 320 and 40°C/min may be due to limited response of the DSC-2 instrument combined with a small sample size for the experiments. Low sensitivity was necessary since operation of the DSC-2 instrument over a wide temperature range, 50-727°C, was required to record energy changes occurring during coal pyrolysis.

Table IV-3

HEATS OF PYROLYSIS FOR COAL SAMPLES FOR A
HEATING RATE OF 320°C/MIN AS OBTAINED BY DSC

SAMPLE	RUN	ENDOTHERMIC		EXOTHERMIC		TOTAL
		RANGE OF TEMP	CAL/GM*	RANGE OF TEMP	CAL/GM*	
A	126	100 - 625°C	+309.2	625 - 727°C	- 27.6	+281.6
B	130	100 - 540°C	+266.0			+367.6
		550 - 727°C	+101.6			
C	132	100 - 610°C	+188.4	610 - 727°C	- 75.6	+112.8
D	136A	100 - 485°C	+167.2	485 - 727°C	-175.6	- 8.4
E	123	100 - 508°C	+132.8	508 - 580°C	- 19.2	+160.4
		580 - 705°C	+ 46.8			
F	137	100 - 700°C	+232.8			+232.8
G	113	100 - 555°C	+182.0			+239.4
		575 - 727°C	+ 57.4			
H	141	100 - 605°C	+215.6	605 - 727°C	- 99.6	+116.0
I	119	100 - 605°C	+216.8			+247.6
		615 - 727°C	+ 30.8			

* Endothermic is positive and exothermic is negative. Weights are based on as received sample and energy is based on the original weight of the sample.

Table IV-4

HEATS OF PYROLYSIS FOR COAL SAMPLES FOR A
HEATING RATE OF 160°C/MIN AS OBTAINED BY DSC

SAMPLE	RUN	ENDOTHERMIC		EXOTHERMIC		TOTAL
		RANGE OF TEMP	CAL/GM*	RANGE OF TEMP	CAL/GM*	
A	74	100 - 525°C	+210.0	525 - 727°C	- 72.0	+138.0
B	84	100 - 510°C	+180.4	508 - 703°C	-140.4	+ 44.4
		703 - 727°C	+ 4.4			
C	82	100 - 505°C	+148.0	505 - 575°C	- 19.2	+159.2
		585 - 650°C	+ 21.6	650 - 670°C	- 4.8	
		670 - 720°C	+ 13.6			
D	95	100 - 520°C	+ 78.8	520 - 585°C	- 16.4	+133.6
		585 - 726.9°C	+ 71.2			
E	102	100 - 500°C	+202.0	505 - 555°C	- 14.8	+198.0
		555 - 605°C	+ 17.6	605 - 620°C	- 0.8	
		620 - 637°C	+ 2.0	637 - 710°C	- 10.8	
		710 - 727°C	+ 2.8			
F	83	100 - 552°C	+256.8	552 - 727°C	- 49.6	+207.2
G	86	100 - 515°C	+278.0	515 - 670°C	- 65.6	+220.4
		680 - 727°C	+ 8.0			
H	72	100 - 500°C	+208.0	500 - 727°C	- 249.0	- 41.0
I	96	100 - 615°C	+326.4	615 - 685°C	- 5.2	+329.6
		685 - 727°C	+ 8.4			

* Endothermic is positive and exothermic is negative. Weights are based on as received sample and energy is based on the original weight of the sample.

Table IV-5

HEATS OF PYROLYSIS FOR COAL SAMPLES FOR A
HEATING RATE OF 40°C/MIN AS OBTAINED BY DSC

SAMPLE	RUN	ENDOTHERMIC		EXOTHERMIC		TOTAL
		RANGE OF TEMP	CAL/GM*	RANGE OF TEMP	CAL/GM*	
A	155	100 - 497°C	+281	497 - 727°C	-518	-237
B	157	100 - 505°C	+251	505 - 727°C	-422	-171
C	160	100 - 505°C	+452	505 - 727°C	-538	- 86
D	162	100 - 455°C	+226	455 - 727°C	-783	-557
E	174	100 - 555°C	+1276	555 - 727°C	-216	+1060
F	167	100 - 455°C	+149	455 - 727°C	-746	-597
G	177	100 - 465°C	+253	465 - 727°C	-521	-268
H	164	100 - 460°C	+180	460 - 727°C	-740	-560
I	181	100 - 470°C	+206	470 - 727°C	-471	-265

* Endothermic is positive and exothermic is negative. Weights are based on as received sample and energy is based on the original weight of the sample.

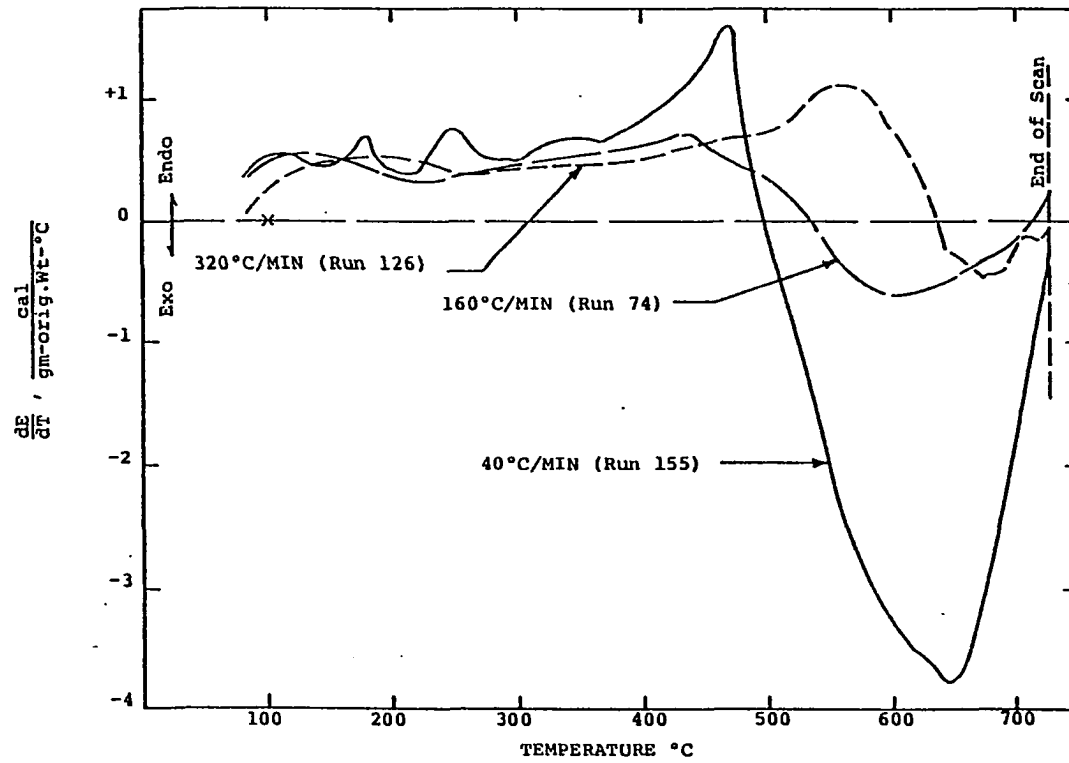


Figure IV-66. Effect of Heating Rate on DSC Thermograms for Coal Sample A. (Thermograms also shown in Figures 6, 7, and 8 of Appendix A.)

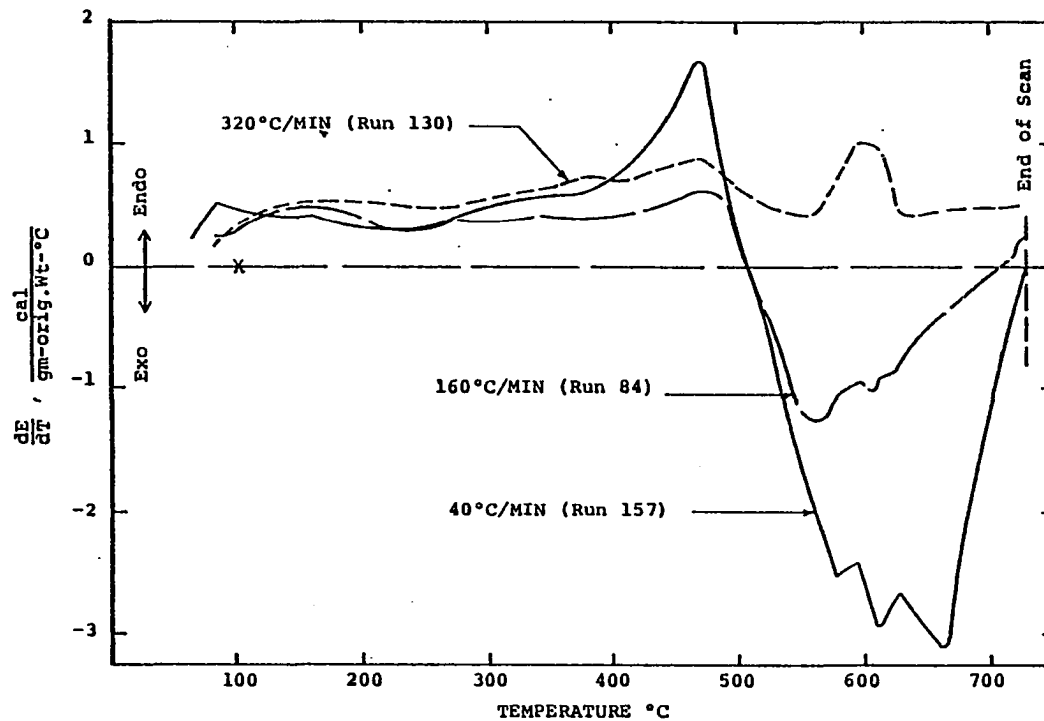


Figure IV-67. Effect of Heating Rate on DSC Thermograms for Coal Sample B (Thermograms also Shown in Figures 6, 7, and 8 of Appendix B).

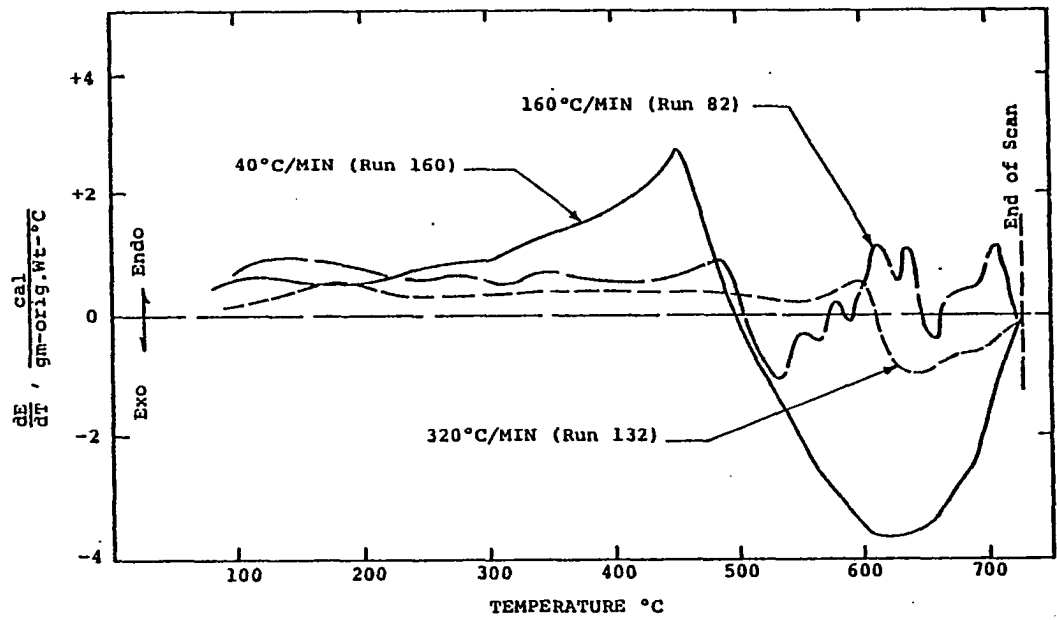


Figure IV-68. Effect of Heating Rate on DSC Thermograms for Coal Sample C (Thermograms also Shown in Figures 6, 7, and 8 of Appendix C).

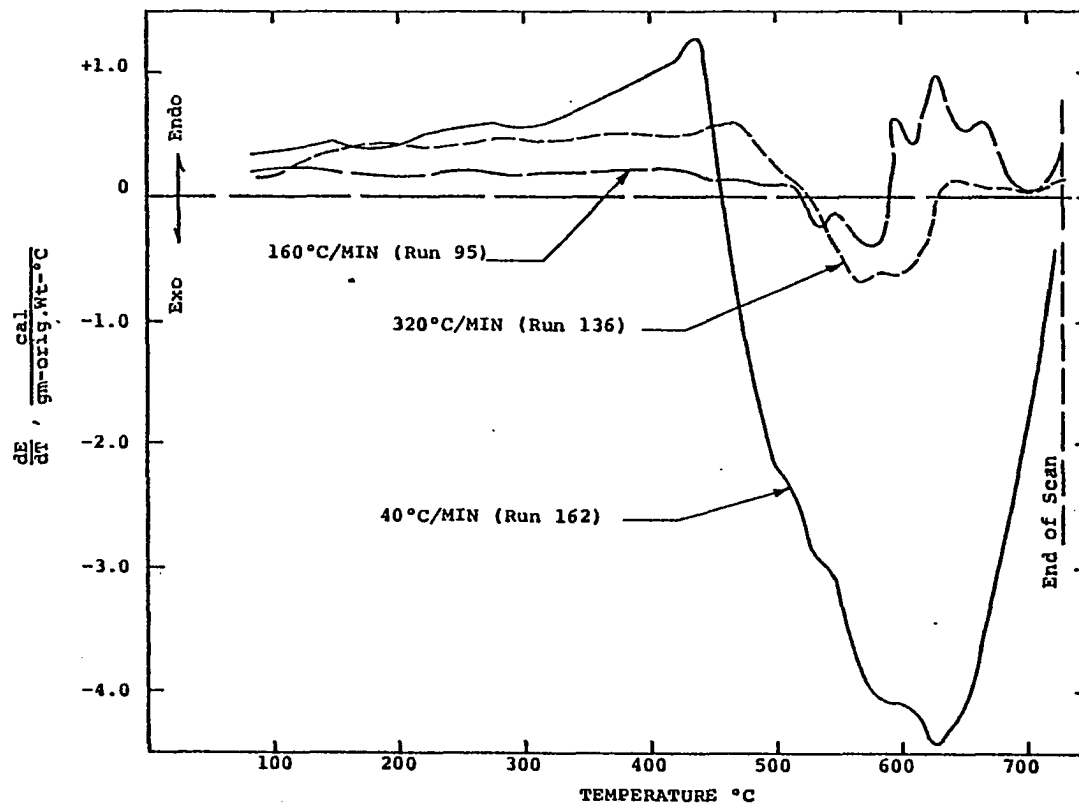


Figure IV-69. Effect of Heating Rate on DSC Thermograms for Coal Sample D (Thermograms also Shown in Figures 6, 7, and 8 of Appendix D).

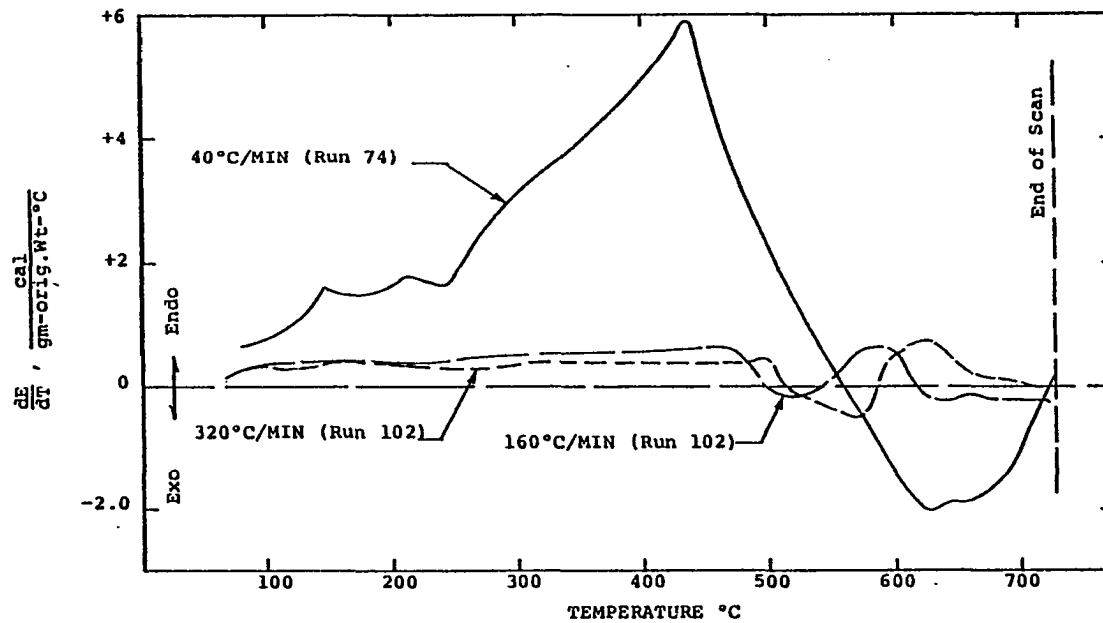


Figure IV-70. Effect of Heating Rate on DSC Thermograms for Coal Sample E (Thermograms also Shown in Figures 6, 7, and 8 of Appendix E).

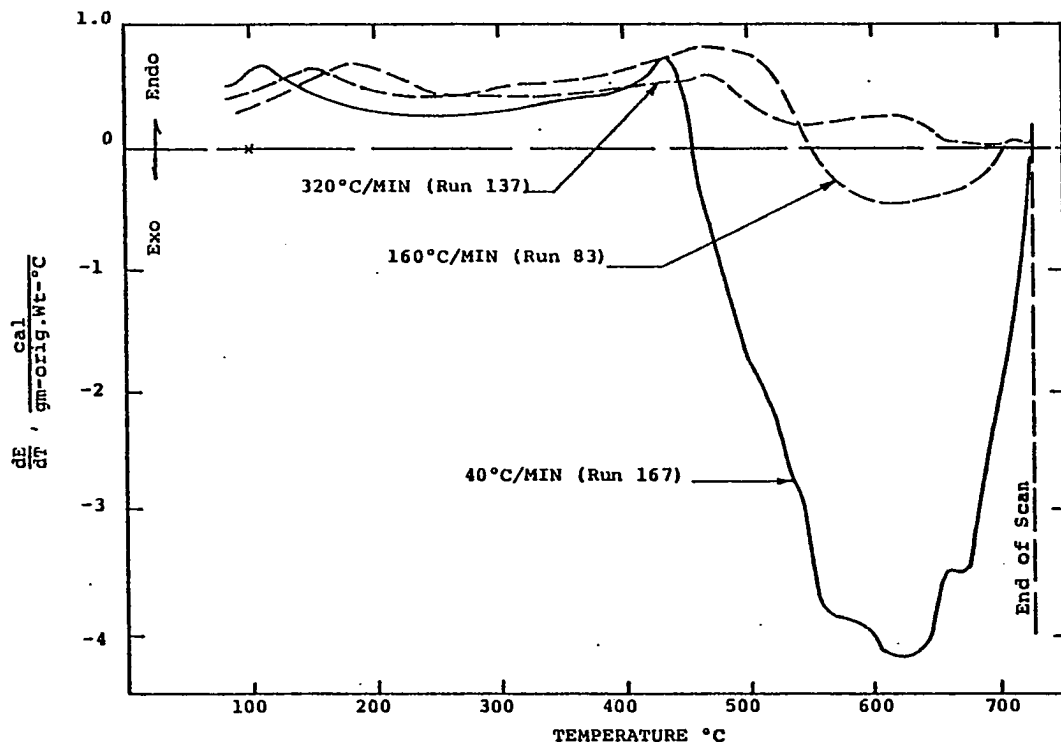


Figure IV-71. Effect of Heating Rate on DSC Thermograms for Coal Sample F (Thermograms also Shown in Figures 6, 7, and 8 of Appendix F).

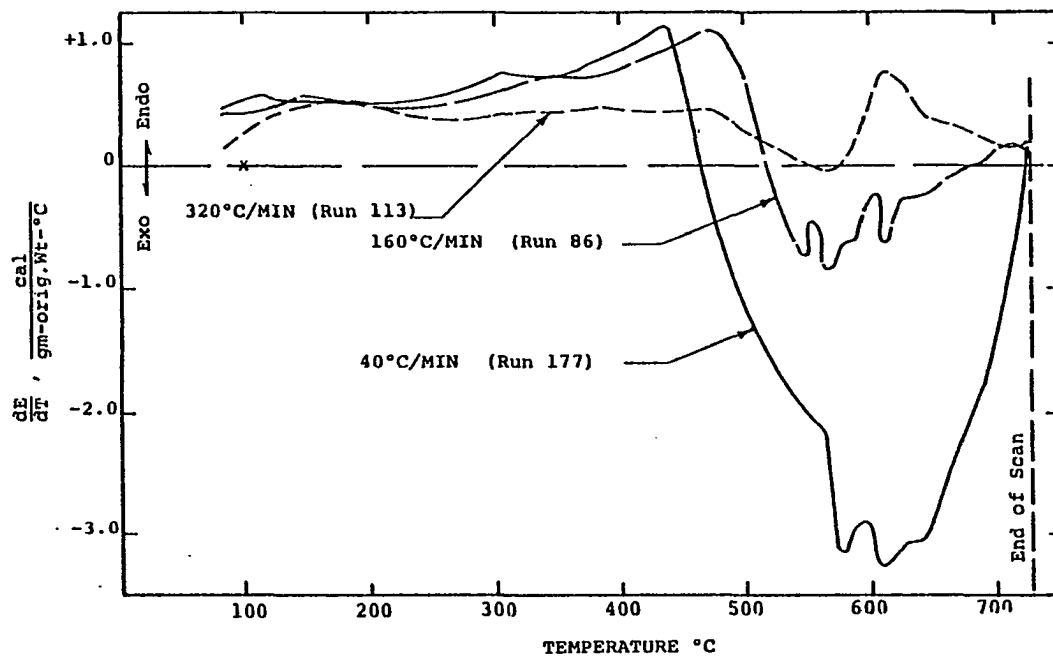


Figure IV-72. Effect of Heating Rate on DSC Thermograms for Coal Sample G (Thermograms also Shown in Figures 6, 7, and 8 of Appendix G).

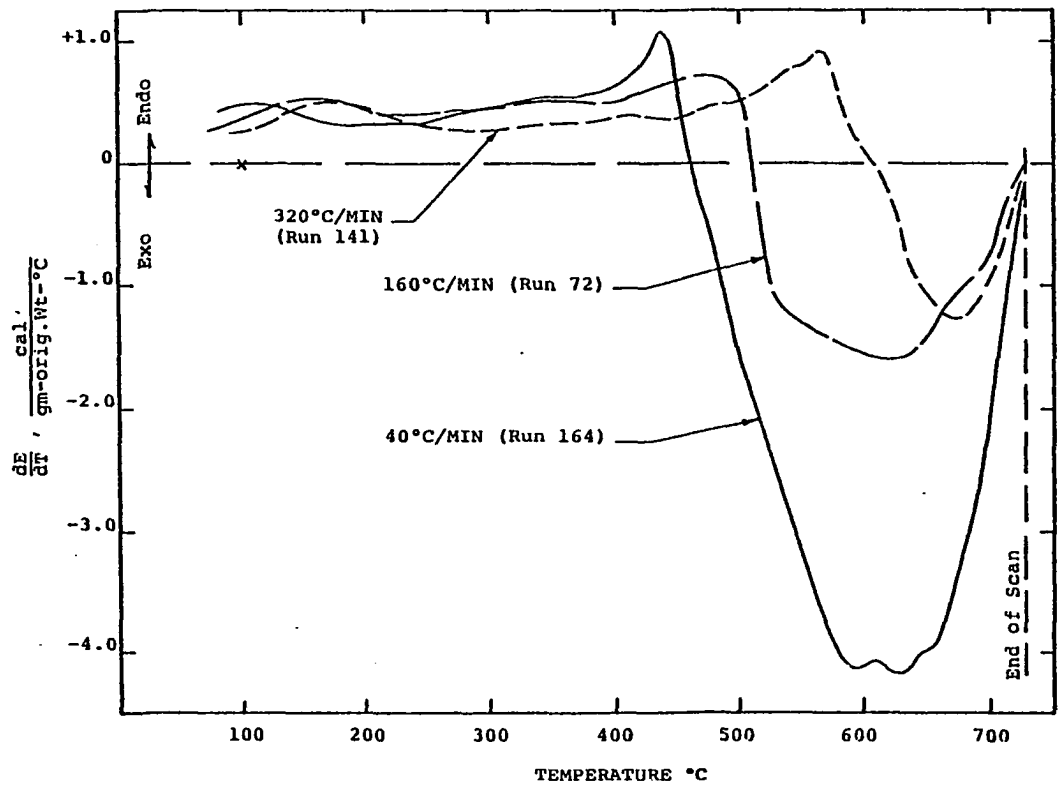


Figure IV-73. Effect of Heating Rate on DSC Thermograms for Coal Sample H (Thermograms also Shown in Figures 6, 7, and 8 of Appendix H).

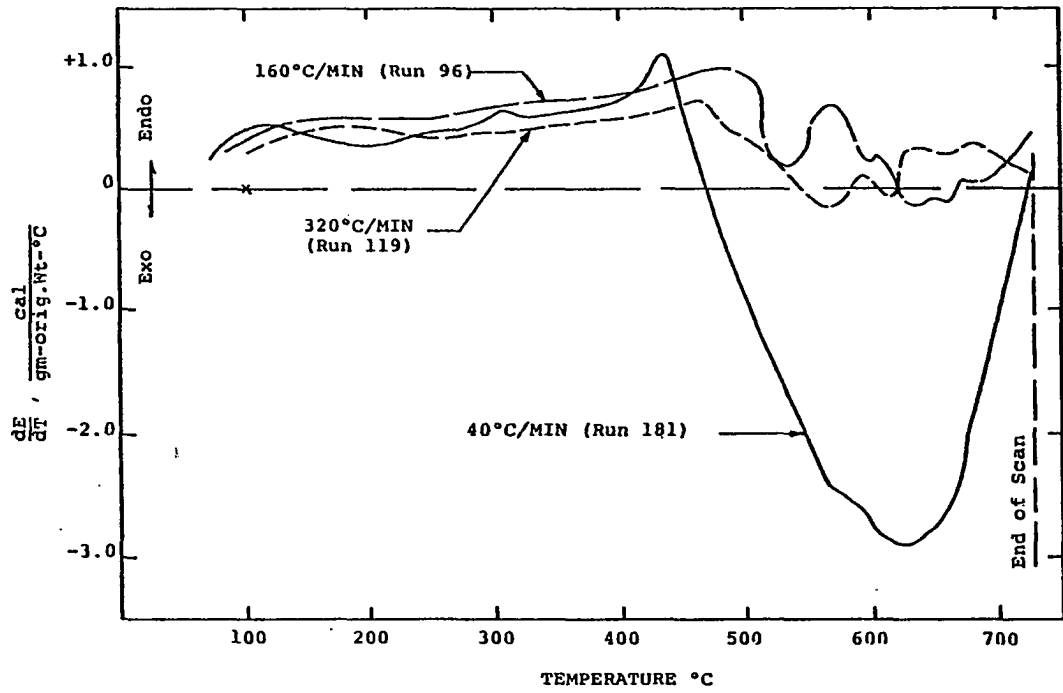


Figure IV-74. Effect of Heating Rate on DSC Thermograms for Coal Sample I (Thermograms also Shown in Figures 6, 7, and 8 of Appendix I).

4. It was also observed that for most samples (except Sample E) the exothermic sections are larger for a coal thermogram obtained at a 40°C/min heating rate than the exothermic sections observed on scans made at the other heating rates (320 and 160°C/min). This effect is probably due to the additional pyrolysis of the coal sample because of the slow rate of heating and, therefore, a longer residence time for the coal and coal pyrolysis products in the sample holder.

It was observed from the discussion on the DSC results on coal that the coal decomposition reactions are endothermic up to a temperature of approximately 500°C and are exothermic above 500°C for most coals.

The results also indicate that additional reactions, which do not take place when the coal is heated at 160 or 320°C/min, occur when coal is heated at a 40°C/min heating rate, as indicated by the higher exothermic levels at the lower heating rate. In contrast, the DSC results of wood pyrolysis by Duvvuri (1974) and Muhlenkamp (1975) showed that the DSC energy level (Value for dE/dT) at a particular temperature remained nearly the same for scans made at different heating rates. (The total energy of pyrolysis of wood has also been observed to change slightly with a decrease in the heating rate). The conclusion that additional coal decomposition reactions occur at lower heating rates is further supported when the initial sample weight and final sample weight data for DSC runs made at different heating rates are compared. These data are reported in Table J-2. For example, weight loss data for coal Sample A indicate that more weight loss was observed when the DSC scan was made at 40°C/min than the weight loss observed for scans made at

320°C/min. A similar observation may also be obtained from the results of thermogravimetric analysis of coals. However, additional DSC experimentation is required at low heating rates.

To our knowledge, this study is the first on a Perkin-Elmer DSC-2 over the entire temperature range of operation of the instrument (to 727°C) for any material undergoing simultaneous decomposition. Consequently, DSC results for any material that undergoes decomposition at temperatures higher than 500°C are not available to check the instrument performance. However, DSC data for several types of wood have been obtained at this laboratory to 500°C. Since DSC pyrolysis experimentation above 500°C is also unique to this laboratory, a performance test of the DSC-2 instrument over the entire temperature range was carried out with wood of known DSC behavior. The differential energy curve and total heat of pyrolysis data for milled oak wood have been reported by Havens (1969) and Brown (1972) to a maximum temperature of about 500°C for a 20°C/min heating rate. In these studies it was observed that pyrolysis reactions of most wood samples shift to higher temperatures with increasing heating rate. In order to extend pyrolysis, an oak wood sample was run on the DSC-2 instrument over the entire temperature range of operation at a heating rate of 320°C/min. The run made at this heating rate for oak wood looked similar to a scan for coal samples on the recorder chart at temperatures above 500°C. The final energy level (at 727°C) for oak wood scan was also higher than the baseline final energy level. The scan was corrected in the same manner as the coal scans. This corrected scan for oak wood obtained at 320°C/min is compared with the scan obtained by Havens (1969) at 20°C/min in Figure IV-75. It can be seen

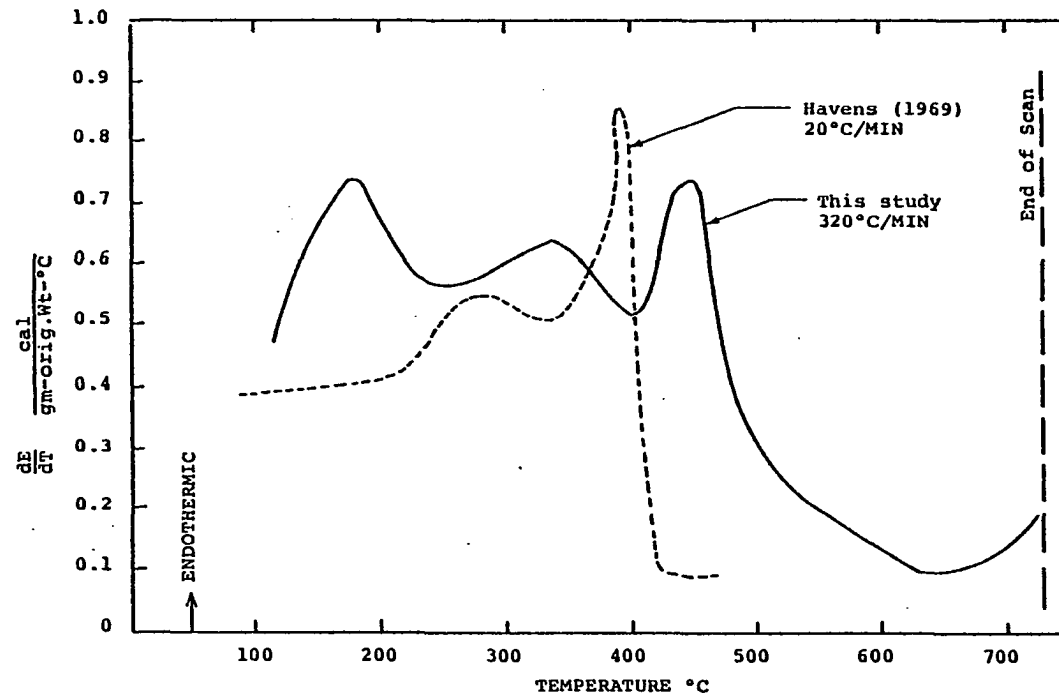


Figure IV-75. Comparison Between an Oak Wood DSC Run Made by Havens (1969) at 20°C/min and a DSC Run for Oak Wood Made at 320°C/min in This Work.

on Figure IV-75 that the peak of the dE/dT curve obtained in this study occurs at a higher temperature than the scan obtained by Havens (1969) at 20°C/min. This observation is in agreement with Brown (1972).

(Havens, 1969, also found that the temperature at which the maximum rate of weight loss occurred in the TGA of oak wood also corresponds to the temperature at which the maximum energy is absorbed by the oak wood sample). These observations explain the temperature difference in the peaks of the two oak wood curves shown in Figure IV-75. The two curves are nearly similar in shape except for the initial peak observed for the scan made at 320°C/min in this study, which is believed to be due to the release of moisture from the oak wood sample. Havens (1969) dried his samples before DSC scans were made. The similarity in the curves shown on Figure IV-75 indicate that the performance of the instrument and the method of correction of the DSC curves are reasonable at least for scans made at high heating rates.

In retrospect, it is also possible that longer residence time for the coal samples within the sample holder and the pyrolysis products that have condensed on the inside of the sample holder cover may have caused larger baseline shift, particularly at slow heating rates. Heat losses associated with this baseline shift were accounted for as part of the energies of the coal pyrolysis because of the manner in which the DSC-2 thermograms were analyzed. The exact contribution of heat losses, reflected as the baseline shift, to the total energies of coal decomposition reactions cannot be determined because the heat loss levels established during the baseline scan could not be exactly reproduced during the scan with the coal sample. In this respect, therefore,

the Perkin-Elmer DSC-2 did not yield reliable data about quantitative energetics of coal pyrolysis reactions over the entire temperature range (50 - 727°C) of the instrument. It must be stated that these heat losses are not even identifiable (but they do occur) in other types of differential thermal analyzers, discussed in Chapter II, because of difference in the basic principle of operation of DTA and true DSC instruments.

Comparison Between the Results of Conventional DTA

Studies on Coal and Results of this Study

Several differential thermal analysis (DTA) studies have been reported involving carbonization of static beds of coal. Breger and Whitehead (1951), Yagashita and Araki (1955), Glass (1954), Clegg (1955), and King and Kelley (1955) are only some of the contributors to the literature of DTA of coals. Almost all of the studies have sought qualitative results from DTA of coals and made studies at low heating rates. The results of these studies indicate coal carbonization is either predominantly endothermic (Breger-Whitehead, 1951), or partly endothermic and partly exothermic, or wholly exothermic (King-Kelley, 1955). As also explained in Chapter II, Clegg (1955) mentioned many variables that influence the curves of differential thermal analysis.

The results of this study indicate that pyrolysis of most coal samples is endothermic in the temperature region from ambient to 500°C and then remains exothermic until the end of the scan.

Kirov and Stephens (1967) have described a fluidized bed calorimeter originally suggested by Basden (1960). The specific heats of coals and semi-cokes were measured at several temperatures. A method was

also described on how to obtain specific heats at all temperatures. A value of mean specific heat was used to estimate total heat of coking. Since actual DTA runs were not made, no qualitative information was available. This problem led to the assumption that the coal carbonization was "thermally neutral." That is, the net heat of pyrolysis is zero. Over the temperature range 20-700°C, the estimated total heat of coking ranged from 250-300 cal/gm depending on the proximate analysis of coal.

Quantitative results of this work are reported in Table IV-2, IV-3, and IV-4. Although actual heat of pyrolysis is thermally defined (endothermic or exothermic) in the results obtained in this study, the values reported for 160°C/min of some coals are comparable with the estimated total heat of coking, reported by Kirov and Stephens (1967).

Comparison of Results of Coal Pyrolysis Obtained

on DuPont 'DSC Cell' and Perkin-Elmer DSC-2

Recently, a coal pyrolysis study was reported by Mahajan, Tomita and Walker (1976) which involved use of the duPont 'DSC Cell' to perform differential thermal analysis of coals. The pyrolysis was performed in a closed system and under helium pressure. Coals were pyrolyzed over the temperature range 100-580°C at a heating rate of 10°C/min. The 'DSC Cell' thermograms were corrected for mass changes occurring during the scan. After correction, high rank coals (anthracite to hv-c) showed endothermic behavior over the entire temperature (100-580°C) range whereas exothermic behavior was observed for low rank coals (such as sub-bituminous coal and lignites). One sub-bituminous coal (Sbb-B) showed both endothermic and exothermic behavior over the

temperature range studied. (Results of the present studies on the Perkin-Elmer DSC-2 clearly indicated that the coal decomposition reactions are endothermic up to a temperature of about 500°C; at higher temperatures - to 727°C - both endothermic and exothermic -- predominately the latter -- reactions were noted).

Mahajan, et al. (1976) observed smaller deflections, as indicated by the sensitivity of 0.2 mcal/sec on the duPont DSC Cell, for coal pyrolysis in helium than were obtained for coal pyrolysis in nitrogen on the Perkin-Elmer DSC-2 in the present study. This difference is also evident in the values of heat of reaction reported by Mahajan, et. al. (1976), for two - endothermic and exothermic - sections of the curves. A high sensitivity, 20 mcal/sec, had to be used in the present study because the experimentation was over a wide temperature range. For an adequate comparison, it would be desirable to make a run in a helium environment on the Perkin-Elmer DSC-2. Unfortunately, helium cannot be used in the Perkin-Elmer DSC-2 above 427°C because the instrument becomes power limited due to the high thermal conductivity of helium.

Although an objective evaluation of Mahajan's results is not possible without a more thorough familiarity of the exact experimental procedure, the following comments are offered:

1. Mahajan obtained the baseline only after the sample run. Since the pyrolysis of coal always yields volatile products, the thermal behavior of the holder is different before and after the run.
2. It is not clear from Mahajan's paper whether the decomposition products were continuously removed from the cell which was

maintained under helium pressure. In the present study, it was found that the method of product removal exerted a significant effect on the results.

3. Although the calibration coefficient was averaged by Mahajan over small temperature sections of 50°C, the overall effect of temperature on the calibration coefficient may be significant, particularly in view of the low sensitivity of 0.2 mcal/sec.
4. The thermograms were corrected for weight loss by observing the deflections (Δy) at the beginning of the scan and at the end of pyrolysis. This procedure assumes that the weight loss is linear with an increase in temperature, contrary to their TGA results.

Summary

Although every reasonable effort was made to extract as much quantitative information from the TGS and DSC experimental runs, the end results were far from satisfying. In other words the absolute magnitudes of the kinetic parameters, based on the TGS experiments, as reported in Table IV-1, page 83, are open to question. For this reason, the last column in the table which lists the overall results is intended to provide only relative comparisons of the kinetic parameters for the various coals, even though the overall concept appears to have little, if any, physical significance. Similar reservations are advanced for the DSC results reported in Tables IV-3, IV-4, and IV-5 on pages 142 and 143, which are further clouded by the aforementioned deficiencies in the experimental apparatus and technique.

CHAPTER V

CONCLUSIONS AND RECOMMENDATIONS

The results of thermogravimetric analysis of nine coal samples, performed over a temperature range of 25-1000°C at 160, 80, 40, 20, and 10°C/min heating rates on a Perkin-Elmer TGS-1 thermobalance, showed that:

1. Most of the coal sample weight loss occurs in the 400-700°C temperature range. At other temperatures, the rate of weight loss is low.
2. The temperature at which the maximum rate of weight loss is observed is shifted to a higher temperature with increasing heating rate.

This behavior suggests that the extent of pyrolysis is greater at lower heating rates for a pyrolysis covering a specified temperature range.

3. As would be expected, a medium volatile coal (coal Sample D) showed that a higher temperature was required to achieve a maximum rate of devolatilization than the other eight high volatile coal samples.

The kinetic model suggested by Goldfarb (1968) is also proposed to describe TGA thermograms of coal samples. However, it was observed that a separate set of kinetic parameters (Log A, E, and n) was required to describe adequately the high rate of weight loss sections of the TGA curves.

The qualitative and quantitative results of differential thermal analysis of coal pyrolysis were obtained on a Perkin-Elmer DSC-2 instrument over a temperature range of 50-727°C for all coal samples. The results show that the coal pyrolysis reactions are endothermic up to a temperature of about 500°C and are predominantly exothermic over the range 500-727°C. Since additional pyrolysis of coal occurs at lower heating rates, the results of DSC thermograms obtained at 40°C/min show larger exotherms over the approximate temperature range 500-727°C than exotherms shown on scans made at 320 and 160°C/min heating rates. No attempt was made to relate the DSC results with rank of the coal since variation in analyses of coal samples was insufficient.

The results of the DSC scans were obtained after appropriate corrections were applied to the DSC runs for change in baseline levels. This shift in baseline level was attributed to the coal pyrolysis products condensing on the cover and changing the radiative heat loss characteristics of the sample holder. Therefore, future coal related experimentation on the Perkin-Elmer DSC-2 must focus on alleviating problems related to the baseline shift. The solution to this problem may possibly be realized with the following experimental changes:

1. The baseline shift is less likely to occur if the products are removed as soon as they are evolved. Perkin-Elmer has recently introduced (Hall and Cassel, 1976) a change in the manner these volatile products are removed from the holders. This change presumably allows the products (and nitrogen) to vent directly above the holders.
2. It was also suggested (Hall and Cassel, 1976) that pyrolysis experiments be conducted in argon rather than in nitrogen.

Presumably, because argon has a lower thermal conductivity and a higher molecular weight, and is more inert, than nitrogen, establishing a baseline should be facilitated.

It is evident from this study that the Perkin-Elmer DSC-2 falls short of giving reproducible, and therefore reliable, quantitative measurements of the energetics for coal decompositions. Qualitatively, it is probably superior to other differential thermal analyzers.

BIBLIOGRAPHY

1. Anthony, D. B., et al. (1976). Fuel, 55, 121.
2. Anthony, D. B. and Howard, J. R. (1976). AIChE Journal, Vol. 22, No. 4, 625.
3. Audibert, E. (1926). Rev. ind. minerale, 115-36; Chem. Abs., 20, 2239 (1926); (As reported by Howard 1963).
4. Badzioch, S. (1961). British Coal Utilization Research Association Monthly Bulletin, 25, No. 8, 285 (1961), (As quoted by Anthony and Howard, 1976).
5. Basden, K. S. (1960). Fuel, 39, 270-272; 359-360.
6. Berkowitz, N. (1957). Fuel, 36, 355.
7. Boersma, S. L. (1955). Journal of Ame. Ceramic Society, 38, No. 1, pp. 281-284.
8. Boyer, A. F. (1953). Assoc. Tech. Ind. Gaz. France, Congres. (As quoted by Kirov and Stephens, 1967).
9. Breger, I. A. and Whitehead, W. L. (1951). Fuel, 30, pp. 247-53.
10. Brown, H. R. (1957). J. Inst. Fuel, 30 pp. 137-59. (As referred by Howard, 1963).
11. Brown, L. E. (1972). "An Experimental and Analytical Study of Wood Pyrolysis." Ph.D. Dissertation, University of Oklahoma, Norman, Oklahoma
12. Chermin, H. A. G. and Van Krevelen, D. W. (1957). Fuel, 36, 85.
13. Clegg, K. E. (1955). Illinois State Geological Survey, Report of Investigations No. 190, 30 p.
14. Dubois, P. (1935). Ph.D. thesis, Paris No. 24228; (As reported by Kirov and Stephens, 1967).
15. Duvvuri, M. S. (1974). "The Pyrolysis Energy of Wildland Fuels." Ph.D. Dissertation, University of Oklahoma, Norman, Oklahoma.

16. Ginnings, D. C. and Furukawa, T. (1953). J. Am. Chem. Soc., 75, 522.
17. Glass, H. D. (1955). Fuel, 34, 253.
18. Goldfarb, I. J., McGuchan, R. and Meeks, A. C. (1968). Kinetic Analysis of Thermogravimetry, Part II. Programmed Temperatures." Air Force Materials Laboratory, Wright-Patterson Air Force Base, Ohio. ARML-TR-68-181. Part 2.
19. Guichard, M. (1925). Bull. Soc. Chem. 37, 62, 251, 381 (As quoted by Kirov and Stephens, 1967).
20. Hall, J. and Cassel, B. (1976). Communication During a Perkin-Elmer Seminar Meeting, Dallas, Texas, December 16.
21. Havens, J. A. (1969). "Thermal Decomposition of Wood," Ph.D. Dissertation, University of Oklahoma, Norman, Oklahoma.
22. Hollings, H. and Cobb, J. W. (1914). J. Gas-Ltg, 126, 917 (As quoted by Lawson, 1970).
23. Hollings, H. and Cobb, J. W. (1915). J. Chem. Soc., 107, 1106, (As reported by Lawson, 1970).
24. Hollings, H. and Cobb, J. W. (1923). Fuel, 2, 322, (As reported by Lawson, 1970).
25. Howard, H. C. (1963). "Chemistry of Coal Utilization," (H. H. Lowry, Ed.). Wiley, New York. Supplementary Volume, p. 340.
26. Johnson, A. J. and Auth, G. H. (1951). Fuels and Combustion Handbook, First Ed. New York, McGraw Hill.
27. Jones, W. I. (1964). J. Inst. Fuel, 37, 3 (As reported by Anthony and Howard, 1976).
28. Jouin, Y. (1947). Chemie et Industrie, Vol. 58, 24 (As quoted by Kirov and Stephens, 1967).
29. Jountgen, H. and van Heek, K. H. (1968). Fuel, 47, 103.
30. Kessler, M. F. and Romavackova, H. (1961). Fuel, 40, 161.
31. King, L. H. and Kelley, D. G. (1955). Econ. Geol., 50, 832.
32. King, L. H. and Whitehead, W. L. (1955). Econ. Geol., 50, 22.
33. Kirov, N. Y. and Stephens, J. N. (1967). "Physical Aspects of Coal Carbonizations." A Research Monograph, Dept. of Fuel Technology, University of New South Wales, Sydney Australia.
34. Kroger, C. and Pohl, A. (1957). Brennstoff Chemie, 38, 179 (As reported by Lawson, 1970).

35. Lawson, G. J. (1970). "Differential Thermal Analysis, Vol. 1 Fundamental Aspects," (R. C. MacKenzie, Ed.). Academic Press, New York, p. 705.
36. Longehambon, H. (1936). Bull. Soc. France Mineral, V. 59, 145 (As reported by Kirov and Stephens, 1967).
37. Luther, H., Eisenhut, W. and Abel, O. (1966). Brennstoff-Chemie, 47, 258. (As quoted by Lawson, 1970).
38. Mahajan, O. P., Tomita, A., and Walker, P. L., Jr. (1976). "Differential Scanning Calorimetry Studies of Coal. I. Pyrolysis in Inert Atmosphere," Fuel, 55, 63.
39. Mentser, M., O'Donnell, H. J. and Ergun, S. (1970). Am Chem. Soc., Div. of Fuel Chem. Preprints, 14, 5, 94 (As quoted by Anthony and Howard, 1976).
40. Muhlenkamp, S. P. (1975). "Pyrolysis of Living Wildland Fuels." Ph.D. Dissertation, University of Oklahoma, Norman, Oklahoma.
41. O'Neil, M. J. (1964). Anal. Chem., 36, 7, 1233.
42. Peters, W. and Bertling, H. (1965). Fuel, 44, 317 (As reported by Anthony and Howard, 1976).
43. Pieper, L. (1956). Brennstoff-Chemie, Vol. 37, 161, 211, 239. (As reported by Kirov and Stephens, 1967).
44. Puskoor, S. R. (1975). "Thermogravimetric Analysis of Plant Constitutents." M.S. Thesis. University of Oklahoma, Norman, Oklahoma.
45. Reidelbach, H. and Summerfield, M. (1975). Am. Chem. Soc. Div. of Fuel Chem. Preprints, 20, 1, 161 (As reported by Anthony and Howard, 1976).
46. Rigollet, C. (1934). Diploma of Higher Studies, Paris, no. 552 (as quoted by Kirov and Stephens, 1967).
47. Rogers, R. N. and Morris, E. D., Jr., (1966). Anal. Chem., 38, 3, 410.
48. Sardesai, U. V. (1973). "Thermogravimetric Analysis of Cellulose." M.S. Thesis, University of Oklahoma, Norman, Oklahoma.
49. Sanyal, A. (1960). Ph.D. Thesis, Sheffield University, Dept. of Fuel Tech. and Chem. Engr. (As reported by Kirov and Stephens, 1967).
50. Schweite, H. E. and Ziegler, G. (1958). Ber. Deut. Keram Ges. 35, 193 (As reported by Havens, 1969).

51. Shapatina, E. A., Kalyuzhnyi, V. V., and Chukhanov, Z. F. (1950). Doklady Akad. Nauk S.S.S.R. 72, 869; Chem. Abs., 44, 10294 (As reported by Howard, 1963).
52. Smothers, W. J., and Chiang, Yao (1966). Handbook of Differential Thermal Analysis, New York, Chemical Publ. Co.
53. Smutkina, Z. S., and Kasatochkin, V. V. (1957). Journ. Chem. Tech. Fuels and Oils No. 5, 27 (As reported by Kirov and Stephens, 1967).
54. Speil, S., Kerkelhammer, L. H., Pask, J. A., and Davis B. (1945). U. S. Bureau of Mines Technical Papers, 664, (As reported by Havens, 1969).
55. Stephens, J. N. (1963). Fuel, 42, 179.
56. Stone, H. N., Batchelor, J. D., and Johnstone, H. F. (1954). Ind. Eng. Chem., 46, 274.
57. Terres, E. (1928). Proc. Second Int'l Conf. Bit. Coal, Carnegie Inst. of Tech., Pittsburgh, Pa. Vol. 2, 657. (As reported by Kirov and Stephens, 1967).
58. Vallet, P. (1932). Compt. rend. V. 195, 1074 (As quoted by Kirov and Stephens, 1967).
59. Van Krevelen, D. W., Van Heerden, C., and Huntjens, F. J. (1951). Fuel, 30, 253.
60. Van Krevelen, D. W., Huntjens, F. J. and Dormans, H. N. M. (1956). Fuel, 35, 462.
61. Waters, P. L. (1956). Nature, 178, 324.
62. Whitehead, W. L. and King, L. H. (1951). Econ. Geol., 46, 808.
63. Woodard, W. M. (1974). "Thermal Decomposition of Synthetic Polymers," Ph.D. Dissertation, University of Oklahoma, Norman, Oklahoma.
64. Yagishita, H., and Araki, H. (1951). Mis. Rep. Res. Inst. Nat. Resource Tokyo. No. 23, p. 28 (As reported by Lawson, 1970).
65. Yoshimura, F., and Mitsui, S. (1966). J. Fuel Soc. Japan, 45, 191 (As quoted by Lawson, 1970).

APPENDICES

APPENDIX A

TGA AND DSC THERMOGRAMS FOR COAL SAMPLE A

Coal Sample : A
Source Identification: Illinois #6
Rank of Coal : Not Available
Mine Designation : Orient Mine
Seam Designation : Illinois #6
Location in U. S. A. : Illinois

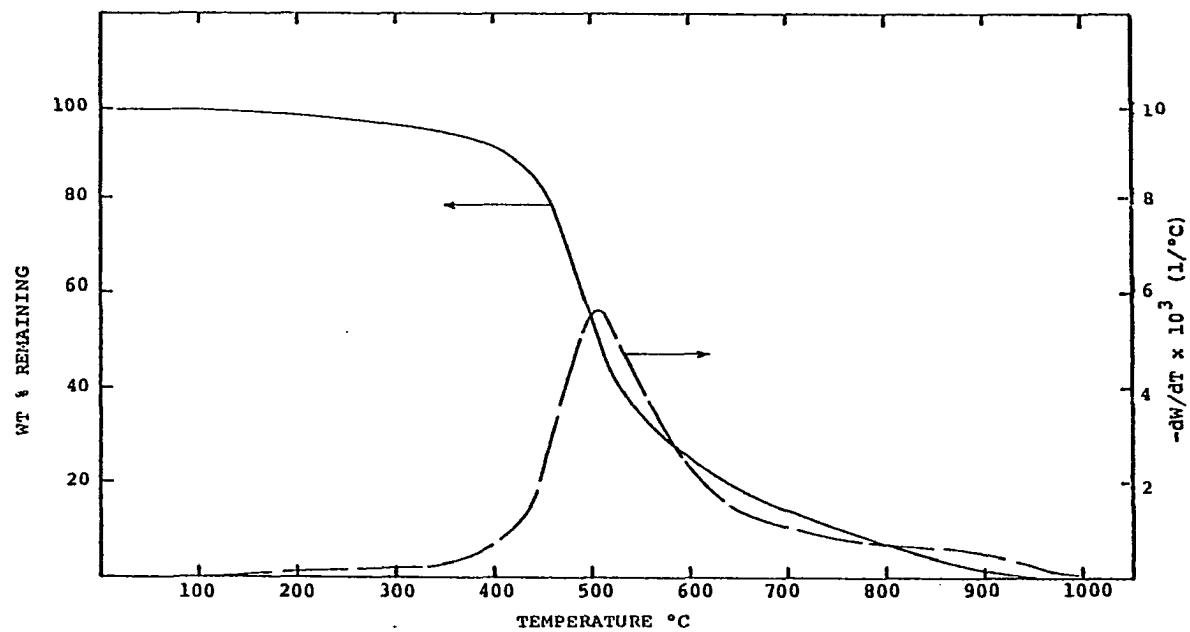


Figure A-1. TGA Thermograms (Weight Loss and Rate of Weight Loss) for Coal Sample A at 160°C/min.

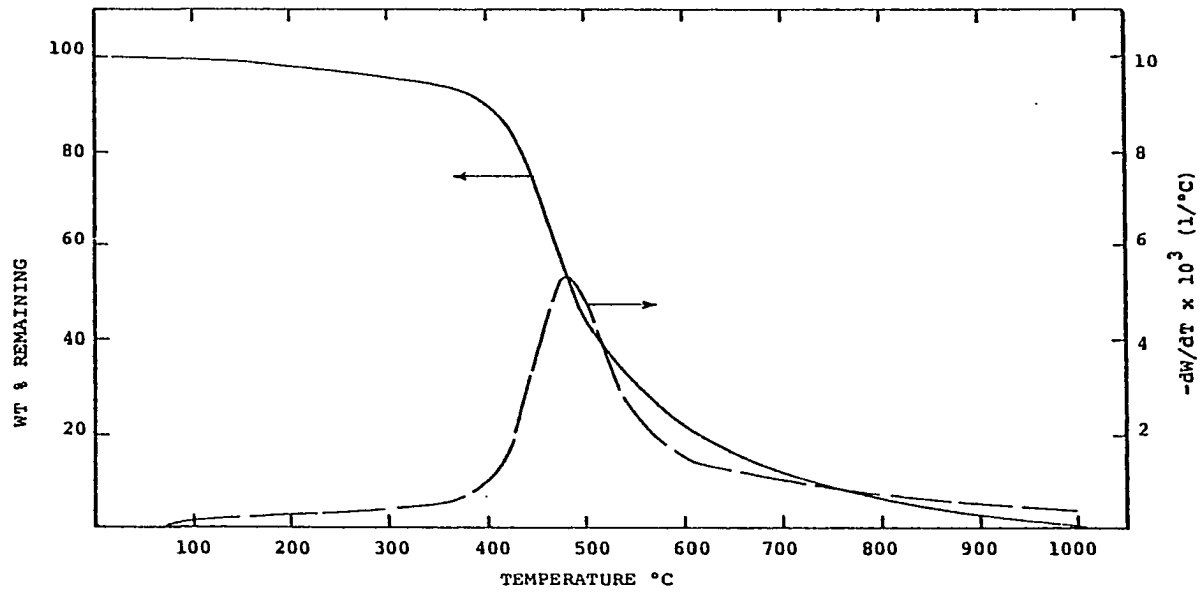


Figure A-2. TGA Thermograms (Weight Loss and Rate of Weight Loss) for Coal Sample A at 80°C/min.

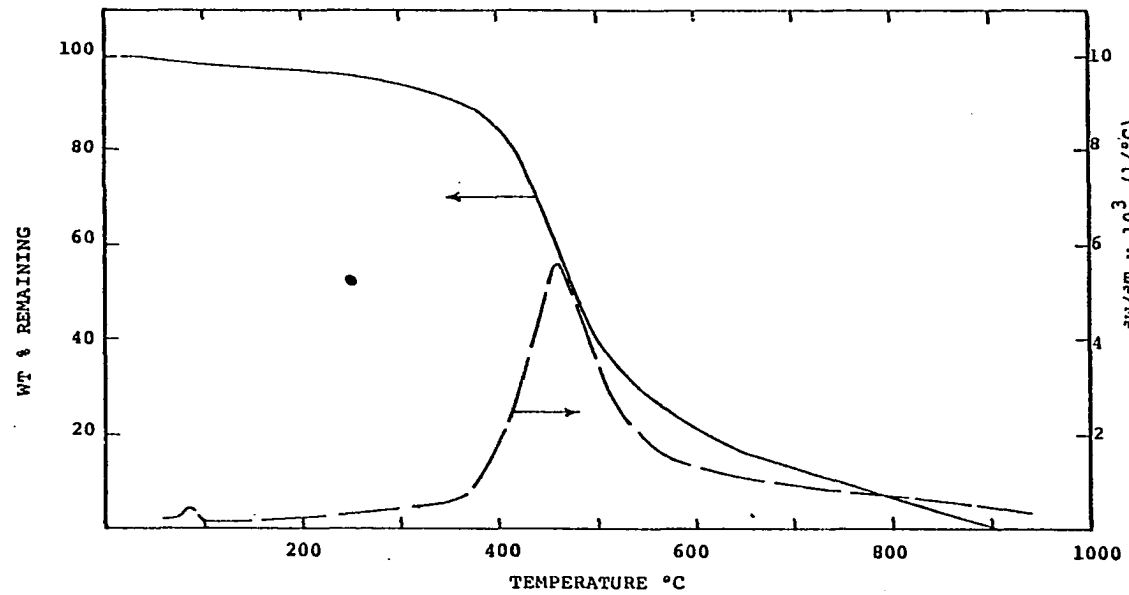


Figure A-3. TGA Thermograms (Weight Loss and Rate of Weight Loss) for Coal Sample A at 40°C/min.

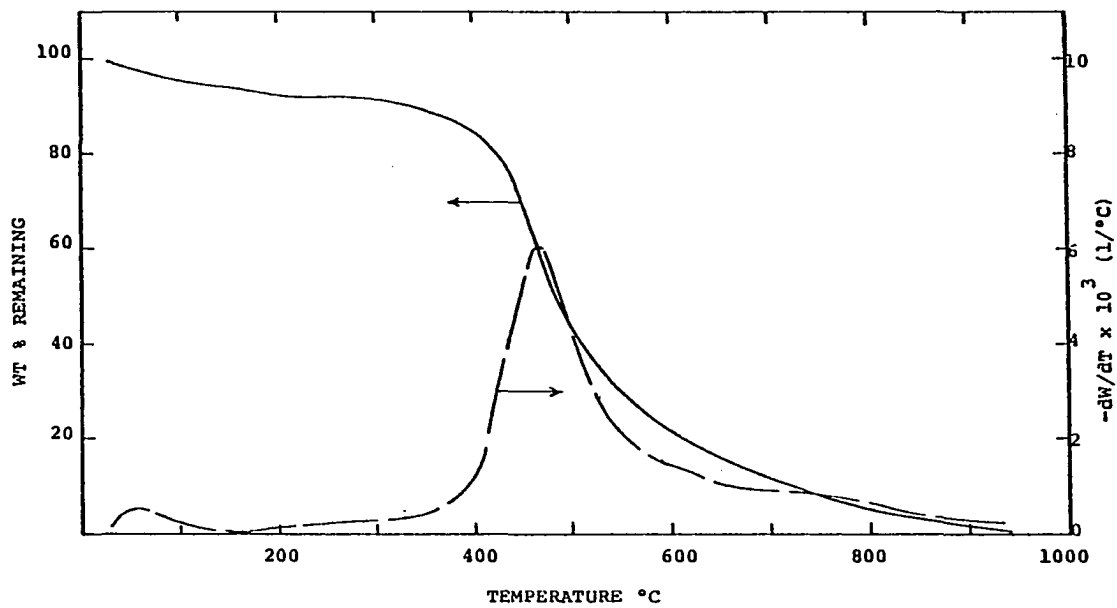


Figure A-4. TGA Thermograms (Weight Loss and Rate of Weight Loss) for Coal Sample A at 20°C/min.

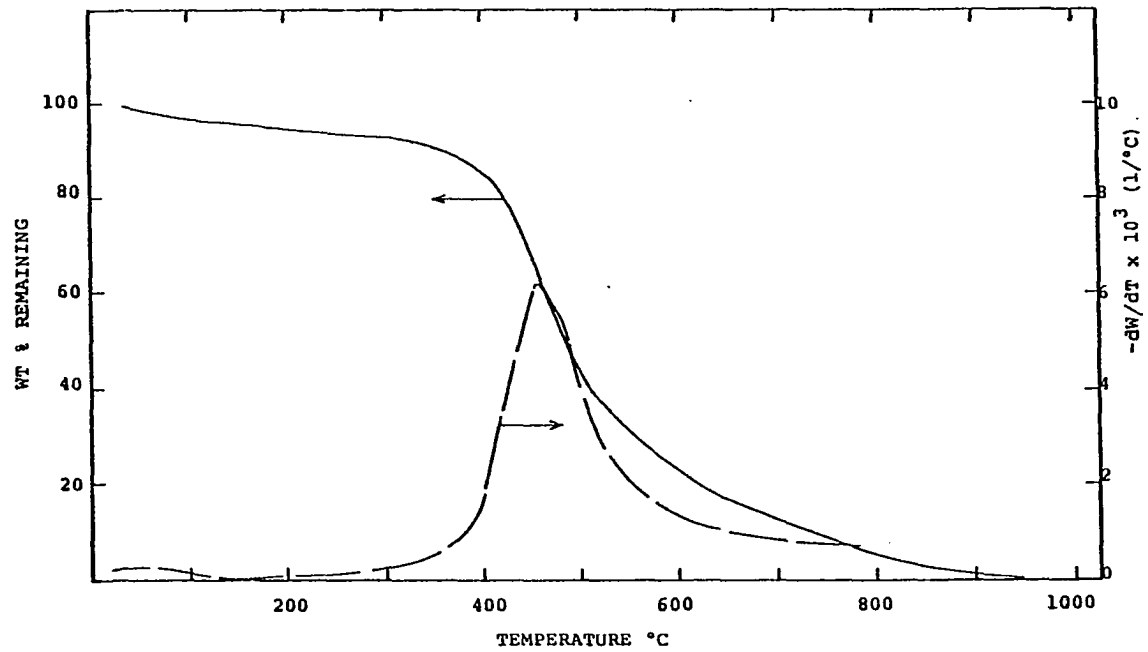


Figure A-5. TGA Thermograms (Weight Loss and Rate of Weight Loss) for Coal Sample A at 10°C/min.

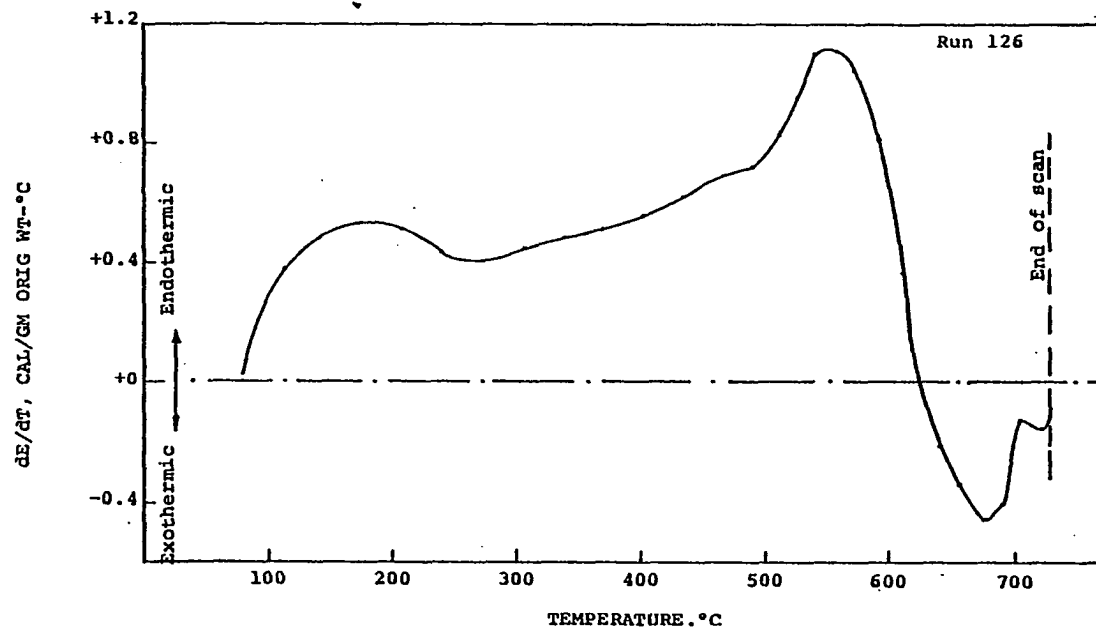


Figure A-6. Corrected DSC Scan for the Coal Sample A at a Heating Rate of 320°C/min.

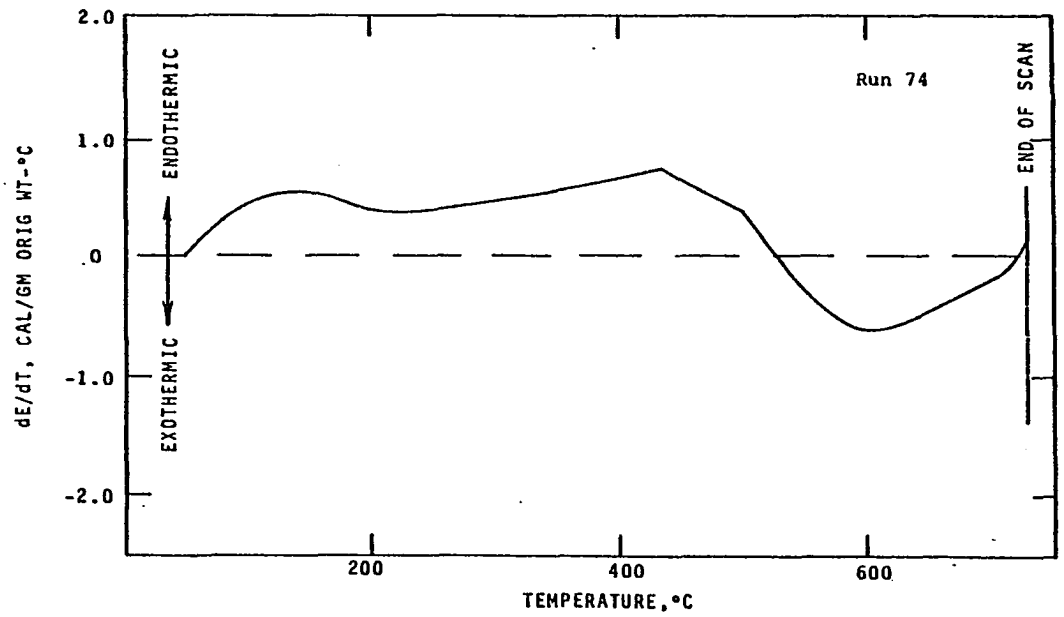


Figure A-7. Corrected DSC Scan for the Coal Sample A at a Heating Rate of 160°C/min.

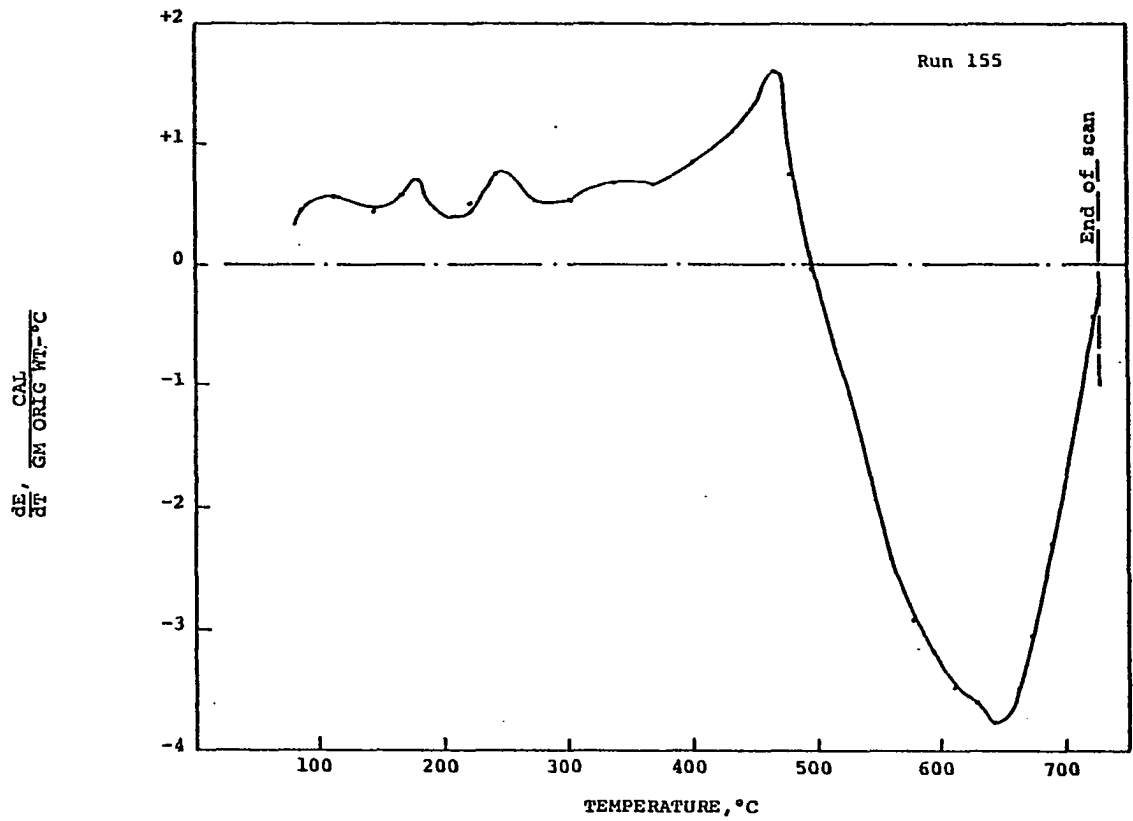


Figure A-8. Corrected DSC Scan for the Coal Sample A at a Heating Rate of 40°C/min.

APPENDIX B

TGA AND DSC THERMOGRAMS FOR COAL SAMPLE B

Coal Sample : B
Source Identification: Indiana #6
Rank of Coal : hvbb
Mine Designation : Chrisney #1, Spencer County
Seam Designation : Indiana #6
Location in U. S. A. : Indiana

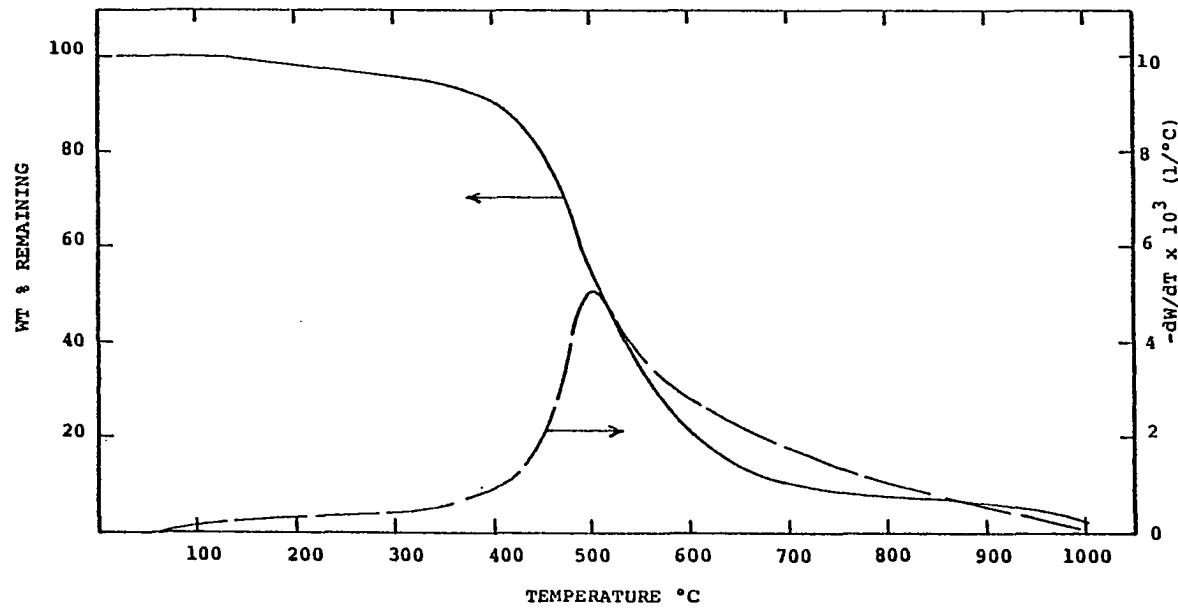


Figure B-1. TGA Thermograms (Weight Loss and Rate of Weight Loss) for Coal Sample B at 160°C/min.

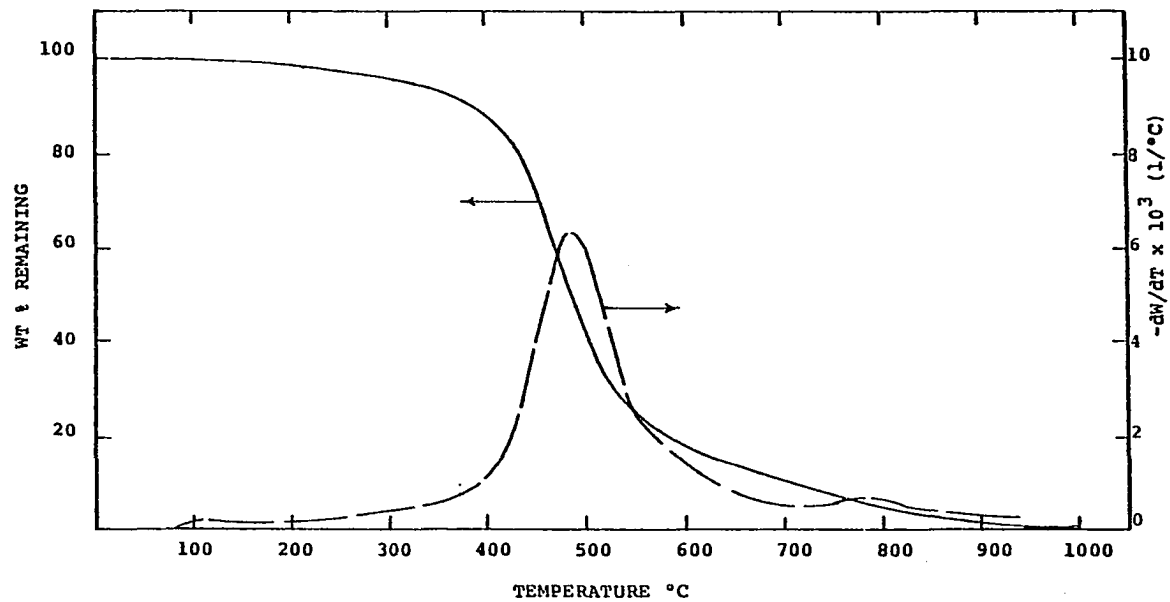


Figure B-2. TGA Thermograms (Weight Loss and Rate of Weight Loss) for Coal Sample B at 80°C/min.

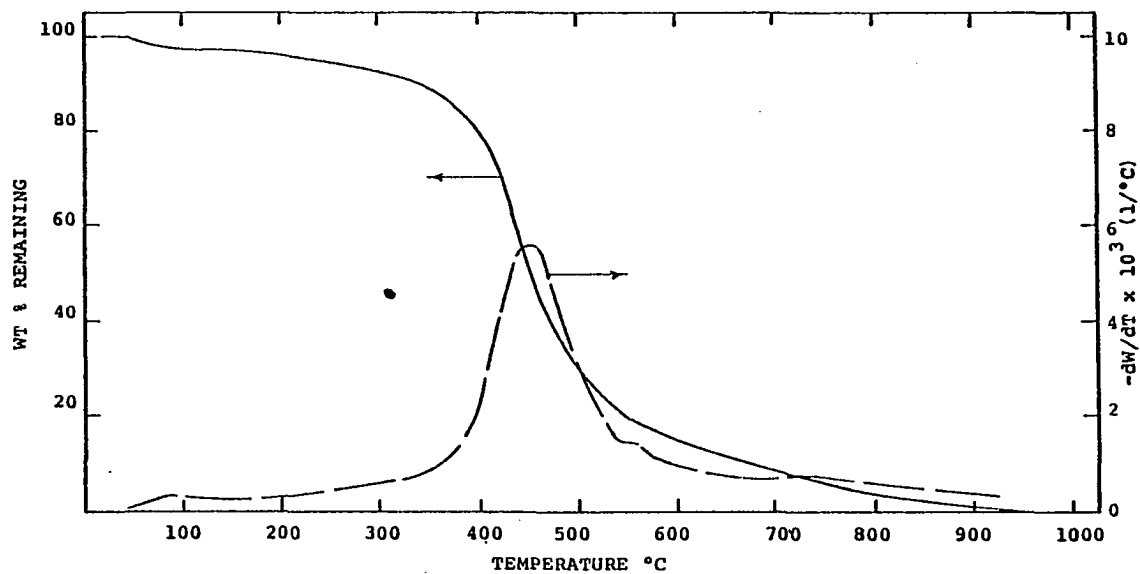


Figure B-3. TGA Thermograms (Weight Loss and Rate of Weight Loss) for Coal Sample B at 40°C/min.

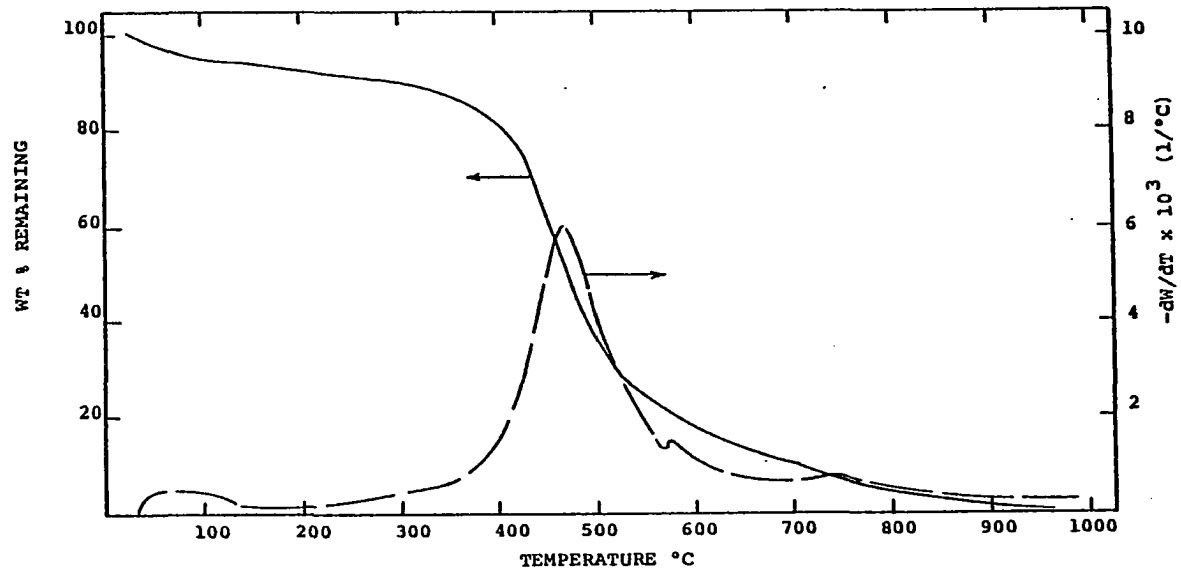


Figure B-4. TGA Thermograms (Weight Loss and Rate of Weight Loss) for Coal Sample B at 20°C/min.

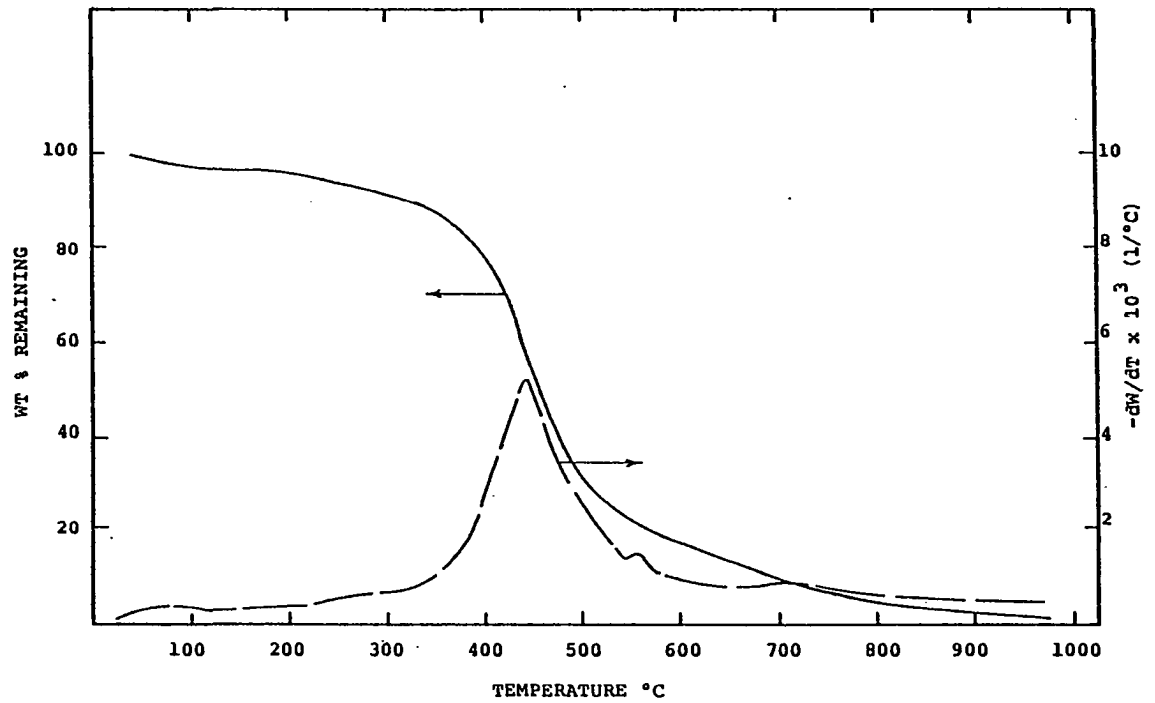


Figure B-5. TGA Thermograms (Weight Loss and Rate of Weight Loss) for Coal Sample B at 10°C/min.

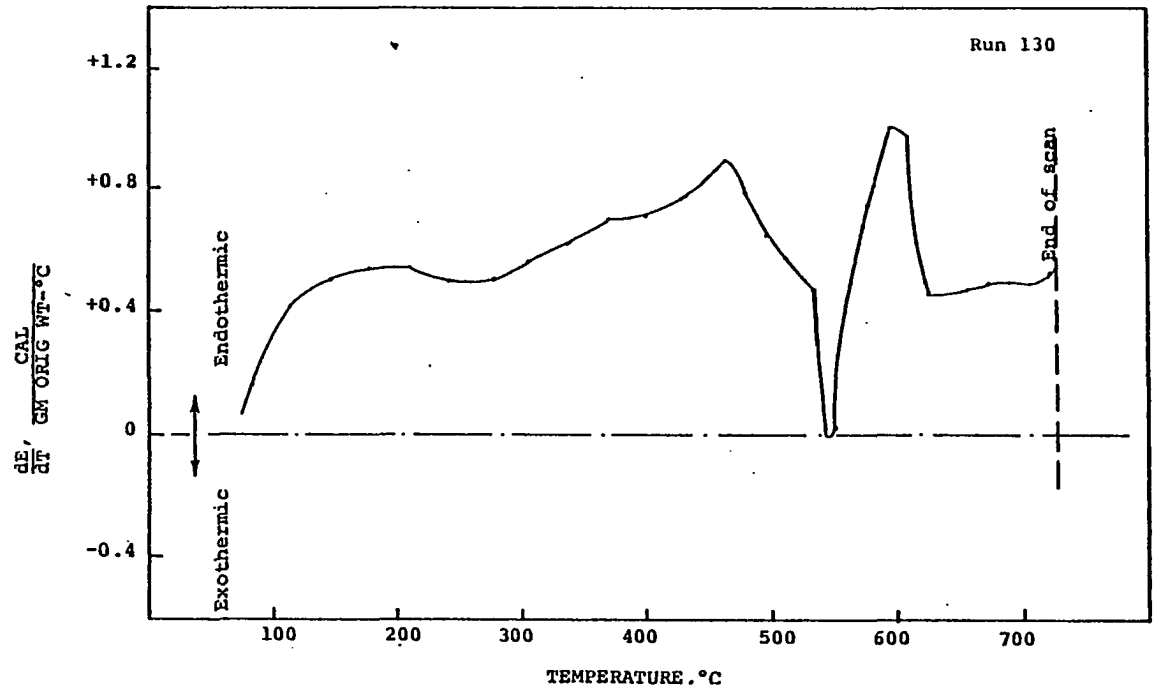


Figure B-6. Corrected DSC Scan for the Coal Sample B at a Heating Rate of 320°C/min.

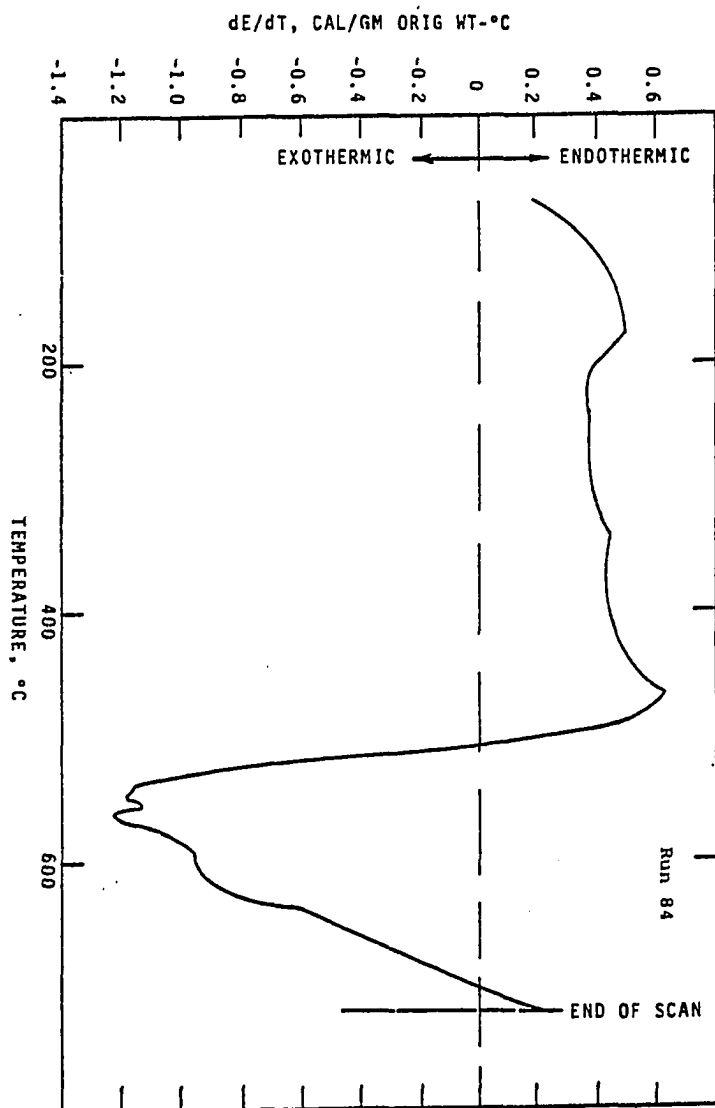


Figure B-7. Corrected DSC Scan for the Coal Sample B at a Heating Rate of 160 $^\circ\text{C}/\text{min}$.

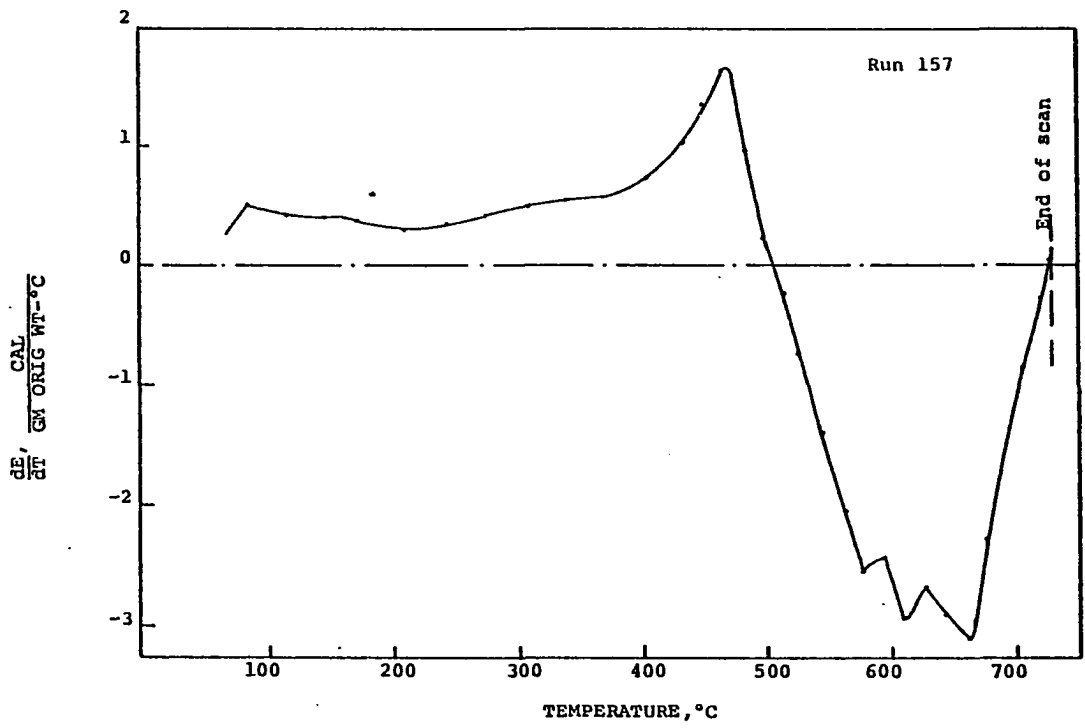


Figure B-8. Corrected DSC Scan for the Coal Sample B at a Heating Rate of 40°C/min.

APPENDIX C

TGA AND DSC THERMOGRAMS FOR COAL SAMPLE C

Coal Sample : C
Source Identification: Kentucky Blend
Rank of Coal : hvab
Mine Designation : Ohio County, West Kentucky
Seam Designation : Blend of Seams #9, #11, and #12
Location in U. S. A. : Kentucky

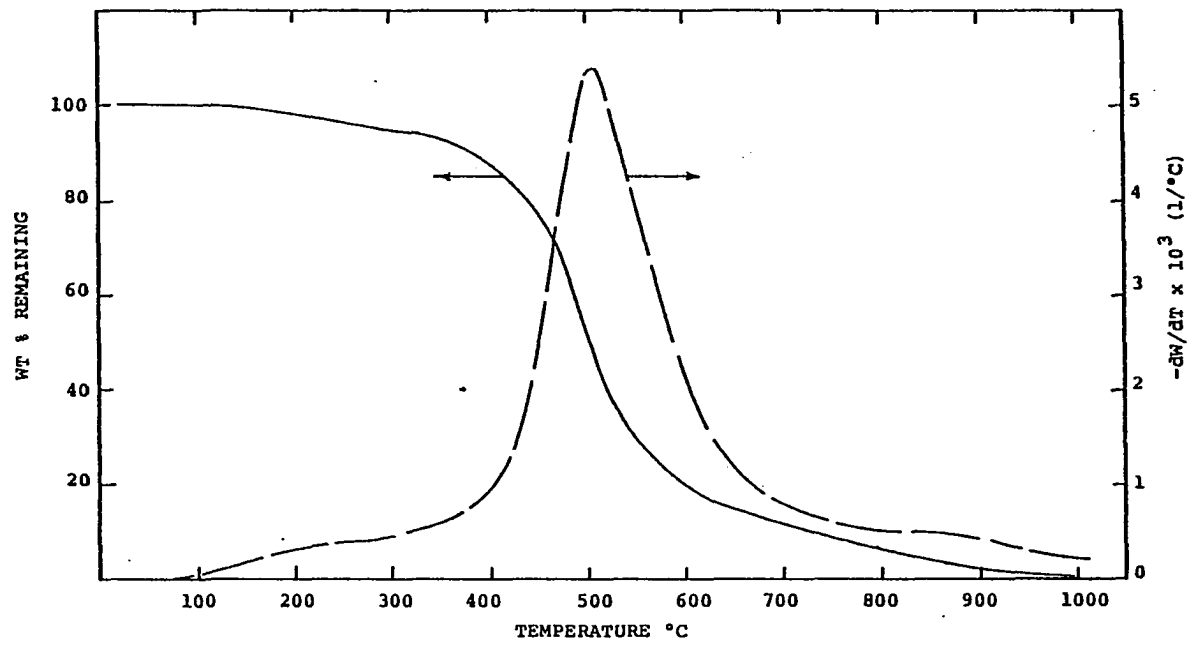


Figure C-1. TGA Thermograms (Weight Loss and Rate of Weight Loss) for Coal Sample C at 160°C/min.

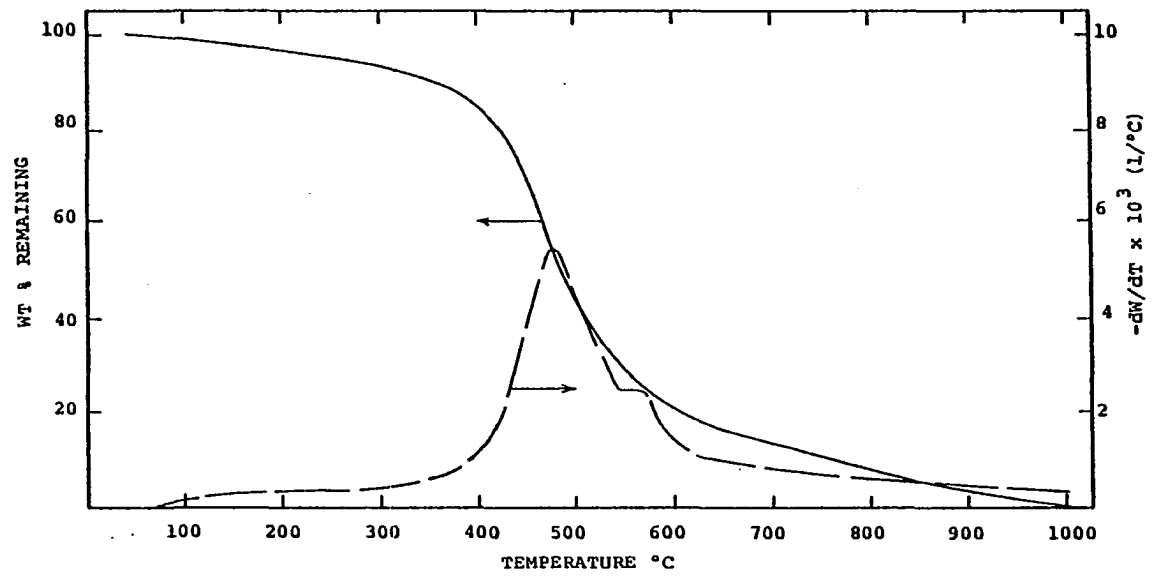


Figure C-2. TGA Thermograms (Weight Loss and Rate of Weight Loss) for Coal Sample C at 80°C/min.

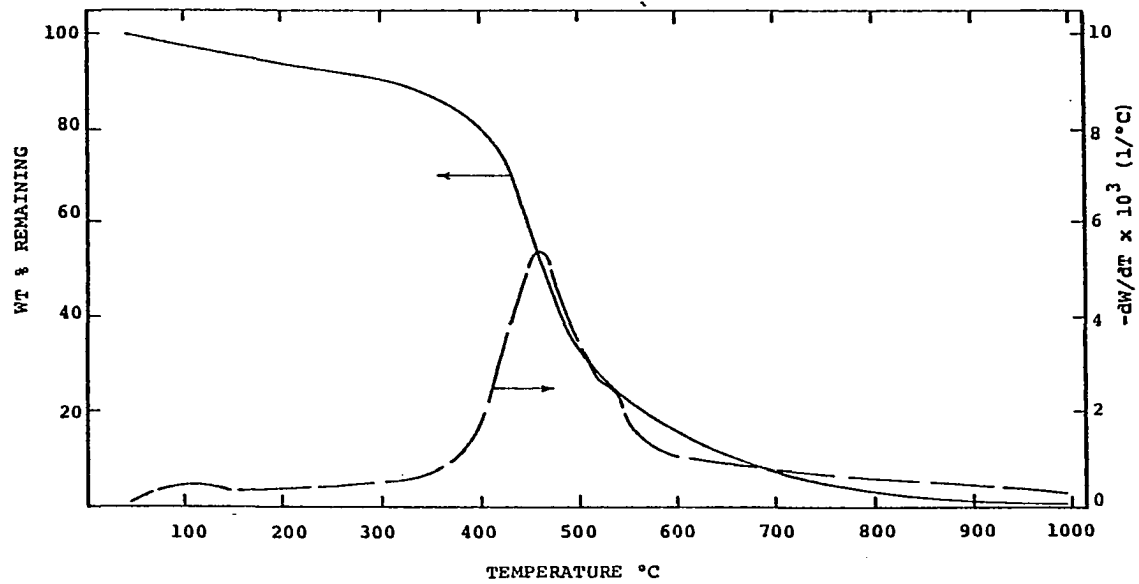


Figure C-3. TGA Thermograms (Weight Loss and Rate of Weight Loss) for Coal Sample C at 40°C/min.

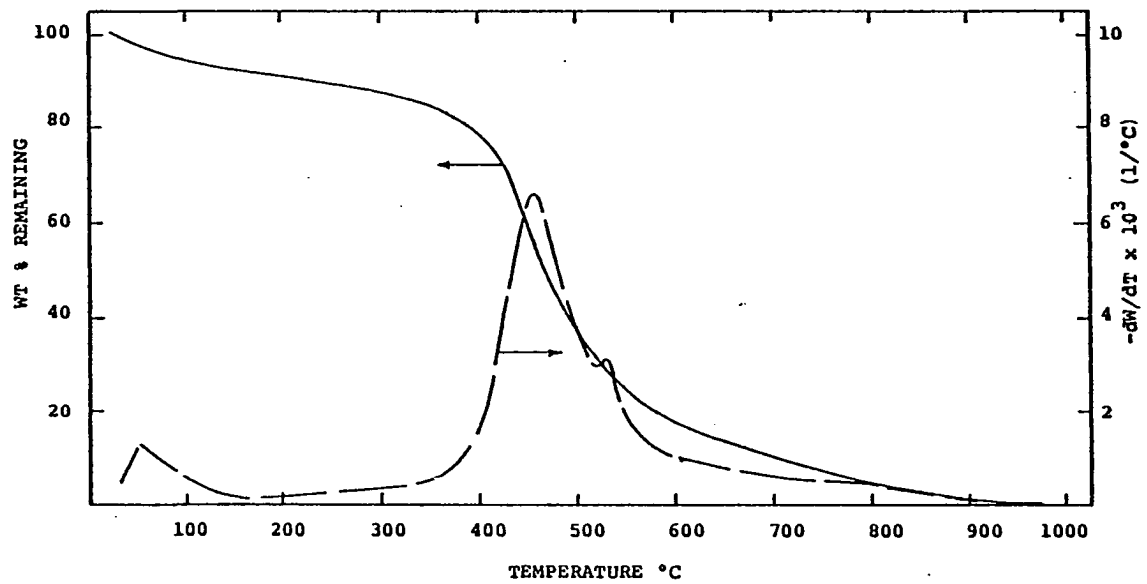


Figure C-4. TGA Thermograms (Weight Loss and Rate of Weight Loss) for Coal Sample C at 20°/min.

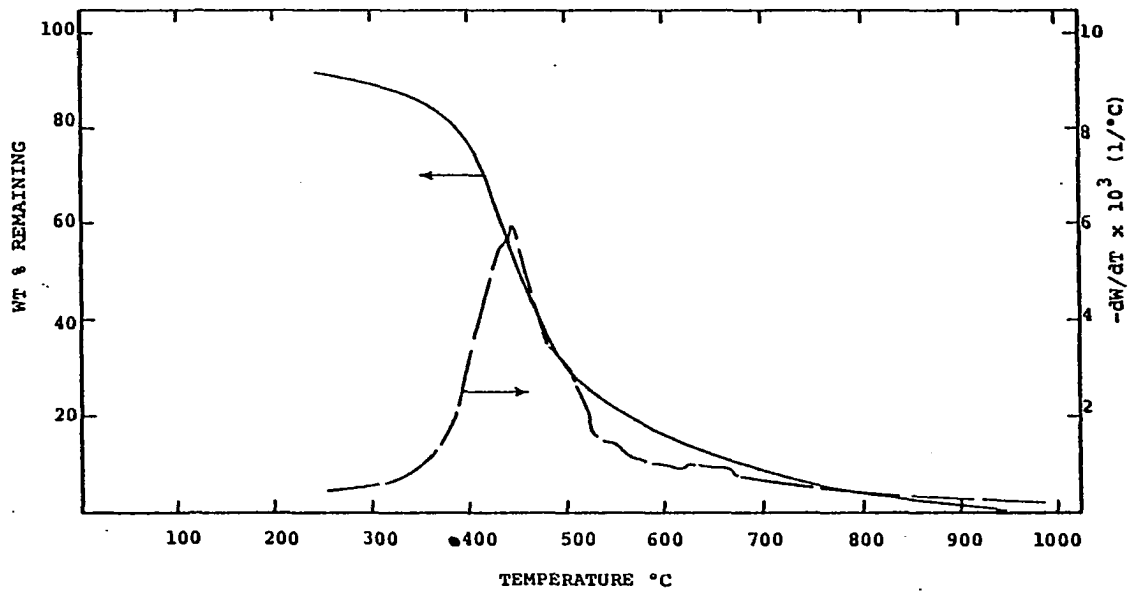


Figure C-5. TGA Thermograms (Weight Loss and Rate of Weight Loss) for Coal Sample C at 10°C/min.

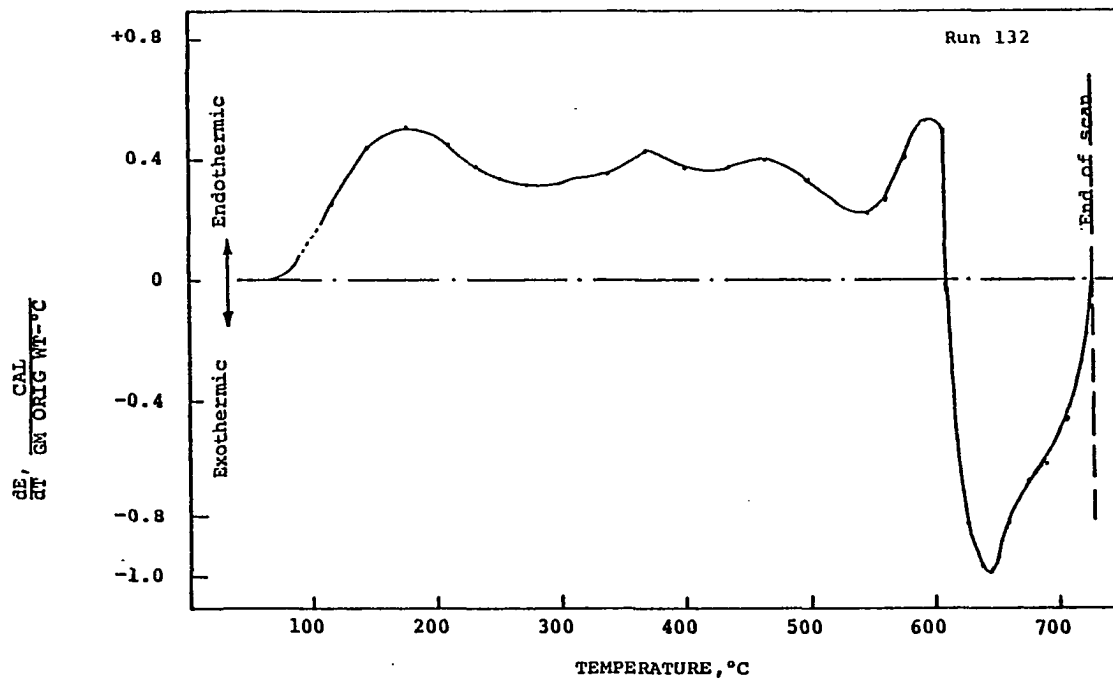


Figure C-6. Corrected DSC Scan for the Coal Sample C at a Heating Rate of 320°C/min.

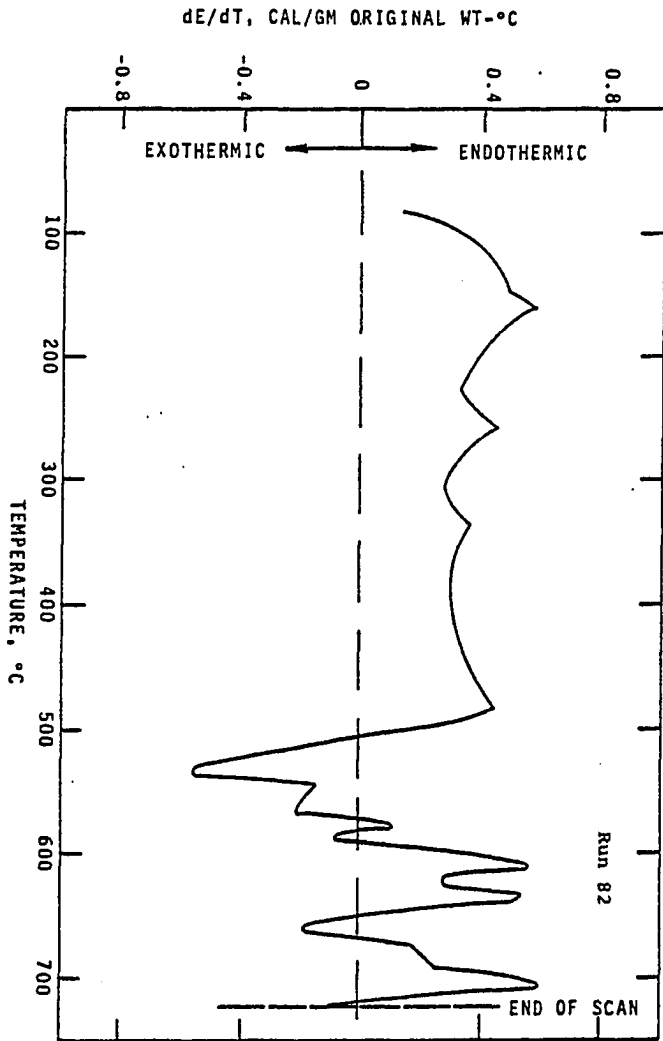


Figure C-7. Corrected DSC Scan for the Coal Sample C at a Heating Rate of $160^\circ\text{C}/\text{min}$.

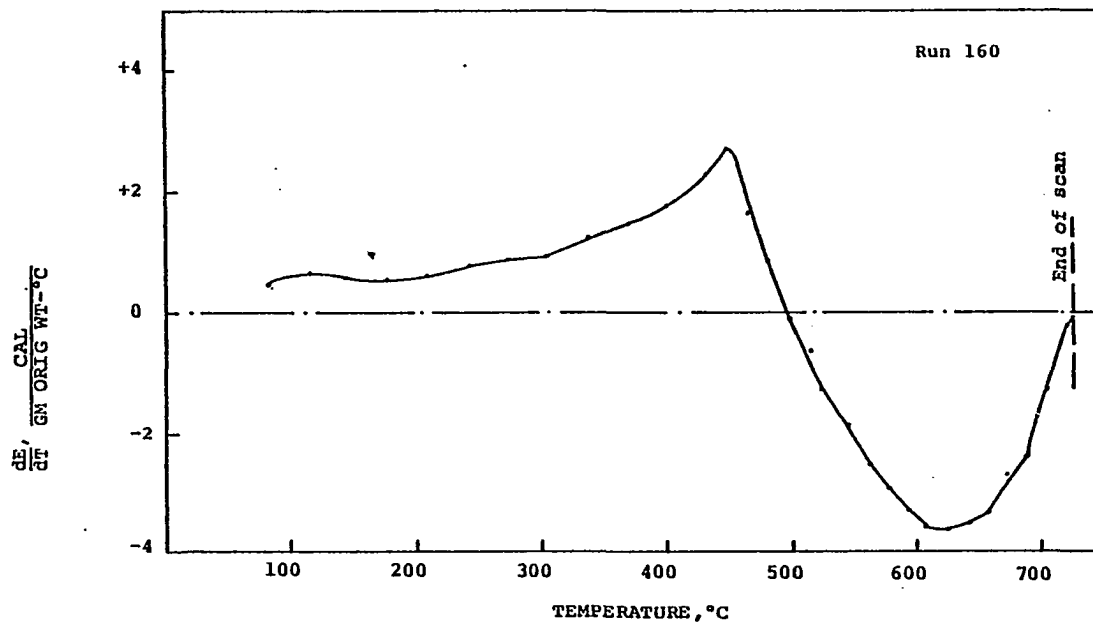


Figure C-8. Corrected DSC Scan for the Coal Sample C at a Heating Rate of 40°C/min.

APPENDIX D

TGA AND DSC THERMOGRAMS FOR COAL SAMPLE D

Coal Sample : D
Source Identification: Pennsylvania Coal
Rank of Coal : mvb
Mine Designation : Manor #44 Mine
Seam Designation : Clearfield Lower Kittanning Bed
Location in U. S. A. : Pennsylvania

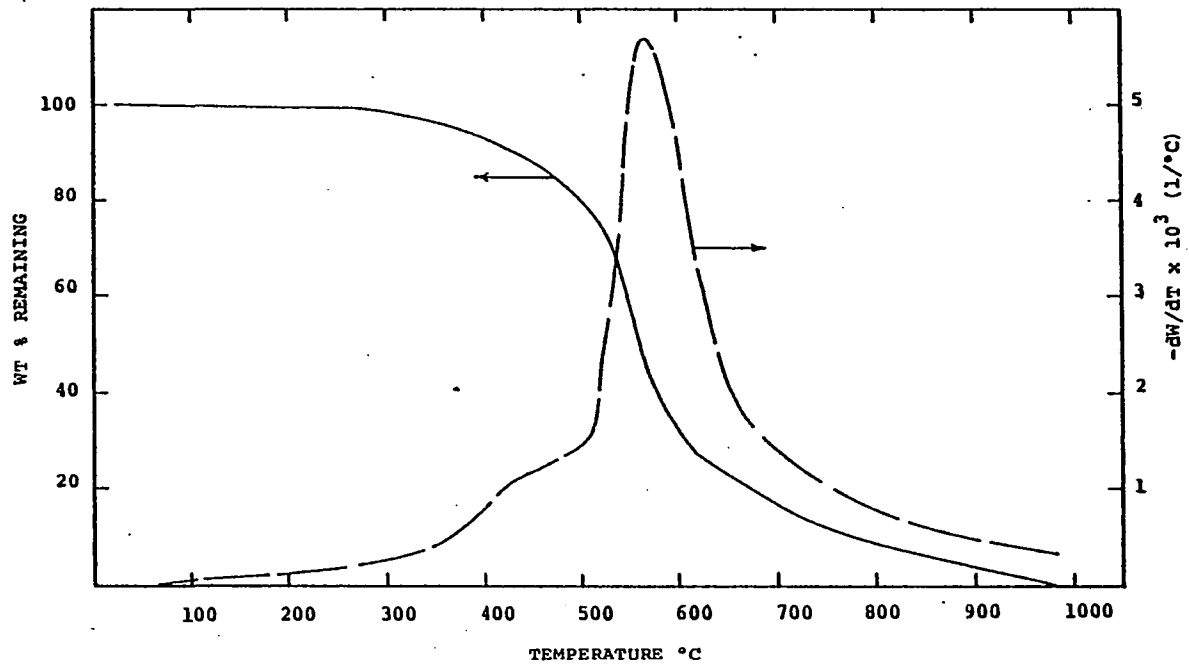


Figure D-1. TGA Thermograms (Weight Loss and Rate of Weight Loss) for Coal Sample D at 160°C/min.

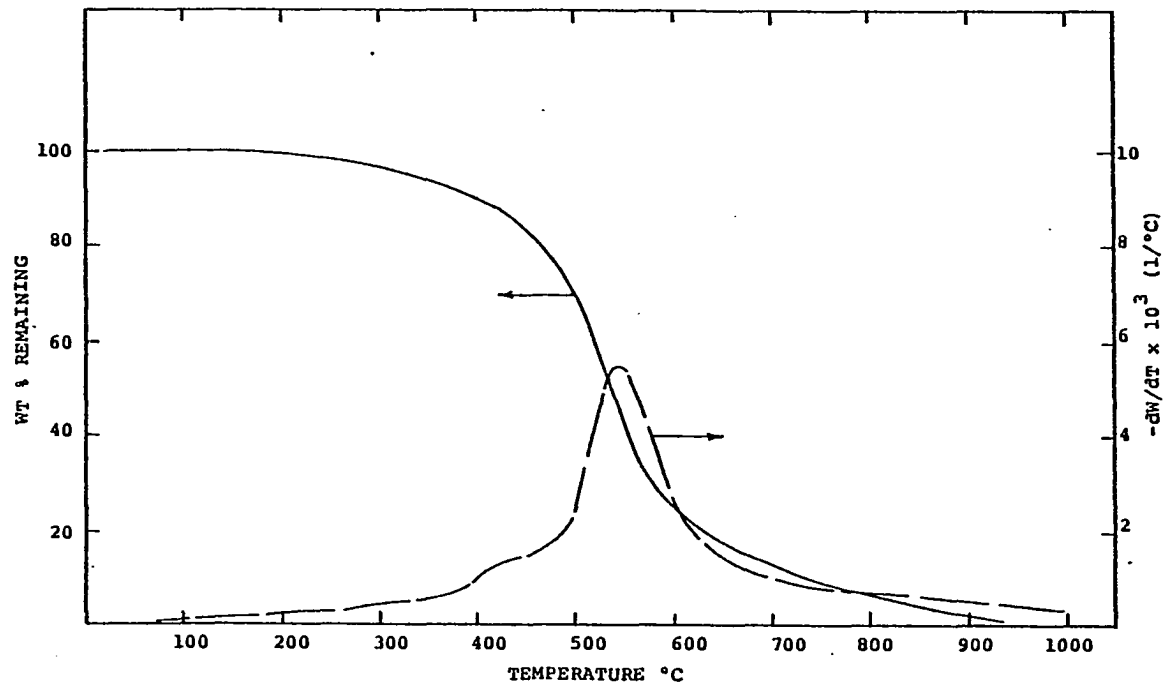


Figure D-2. TGA Thermograms (Weight Loss and Rate of Weight Loss) for Coal Sample D at 80°C/min.

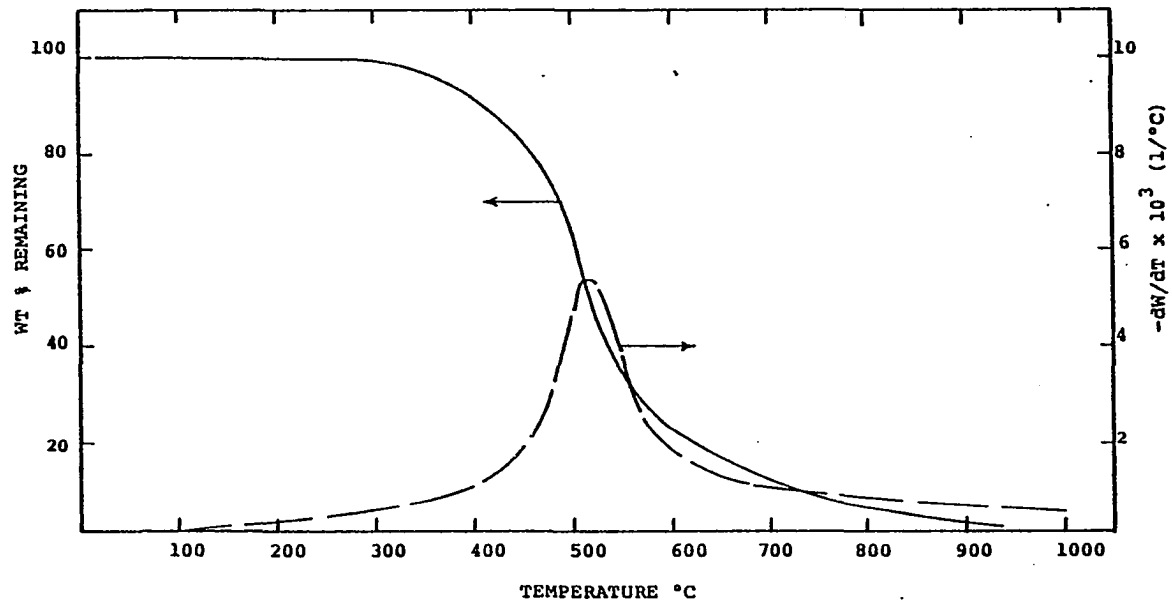


Figure D-3. TGA Thermograms (Weight Loss and Rate of Weight Loss) for Coal Sample D at 40°C/min.

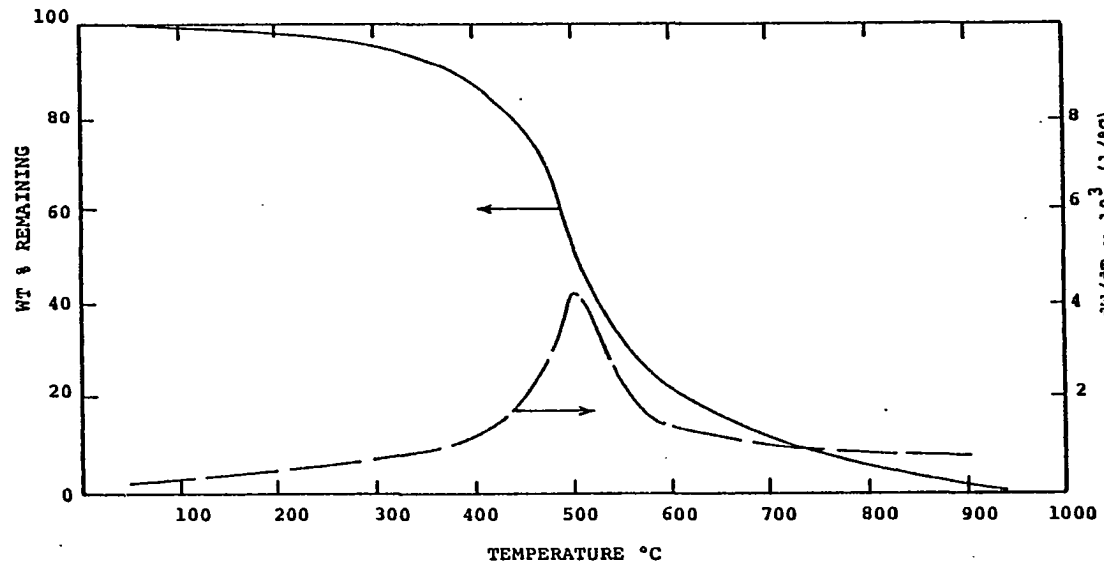


Figure D-4. TGA Thermograms (Weight Loss and Rate of Weight Loss) for Coal Sample D at 20°C/min.

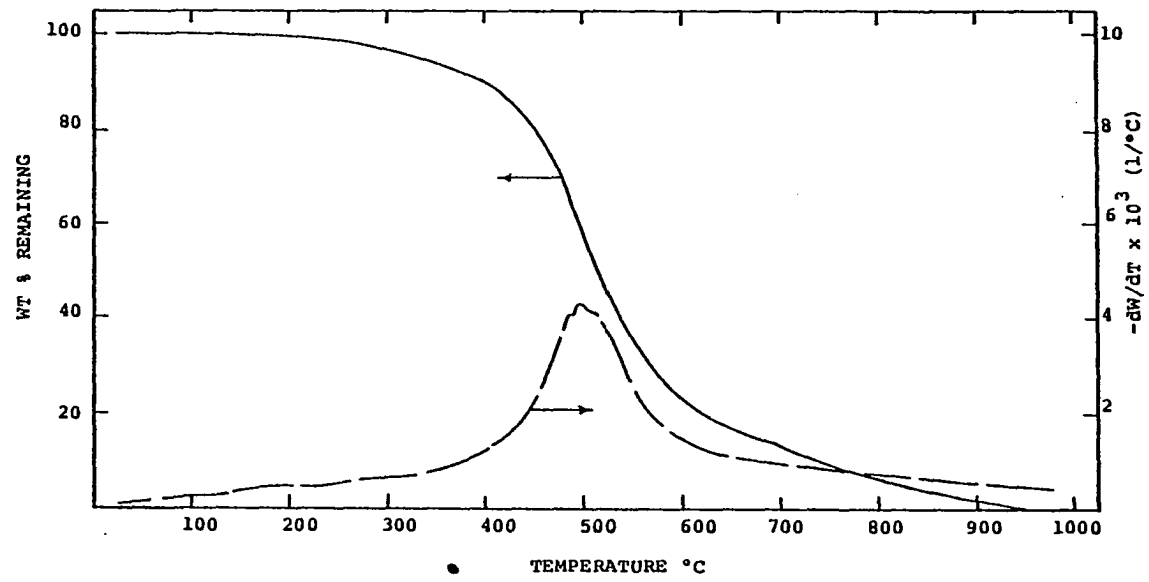


Figure D-5. TGA Thermograms (Weight Loss and Rate of Weight Loss) for Coal Sample D at 10°C/min.

$\frac{dH}{dT}, \frac{CAL}{GM \cdot ^\circ C}$

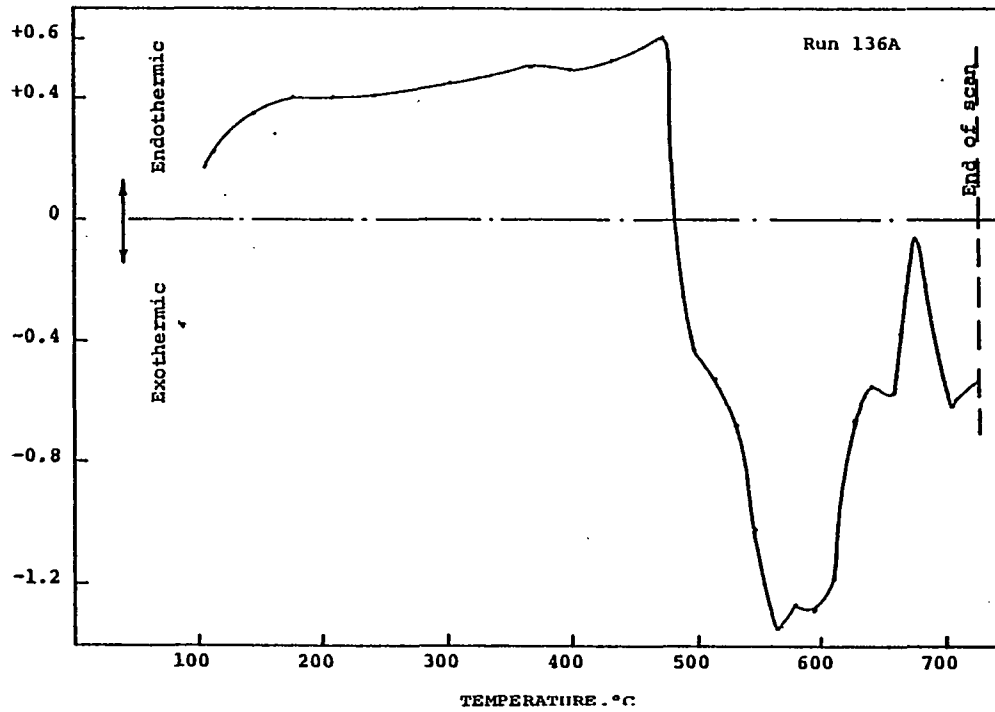


Figure D-6. Corrected DSC Scan for the Coal Sample D at a Heating Rate of 320 $^\circ C$ /min.

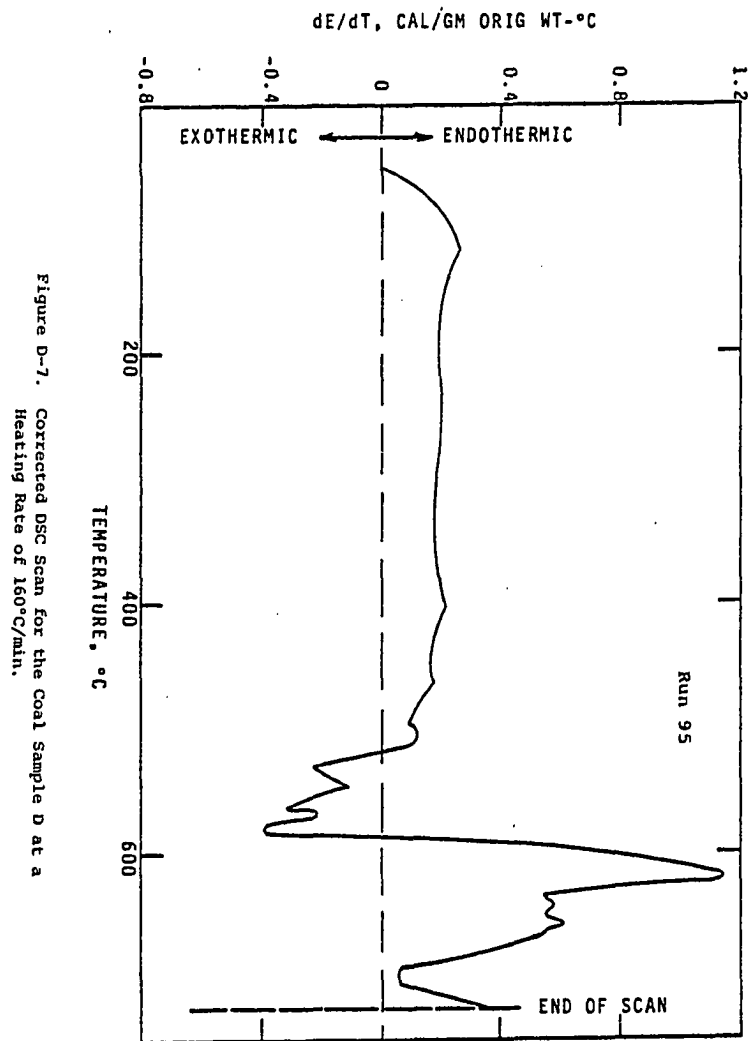


Figure D-7. Corrected DSC Scan for the Coal Sample D at a Heating Rate of $160^\circ\text{C}/\text{min}$.

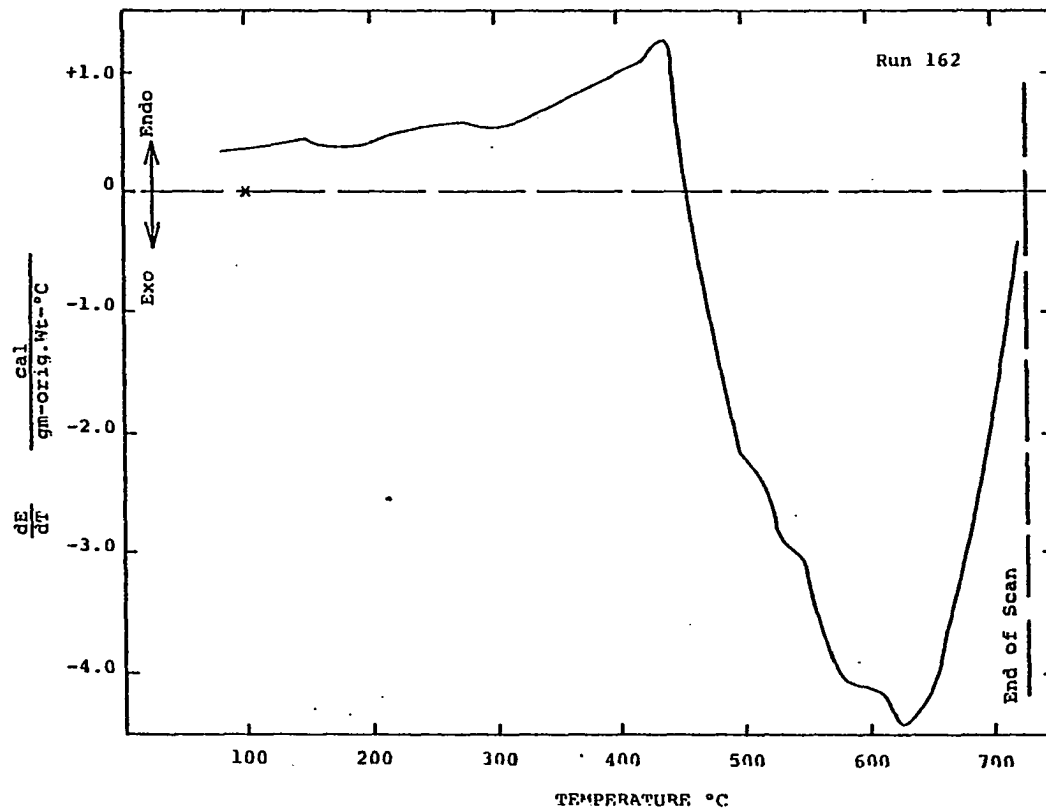


Figure D-8. Corrected DSC Scan for the Coal Sample D at a Heating Rate of 40°C/min.

APPENDIX E

TGA AND DSC THERMOGRAMS FOR COAL SAMPLE E

Coal Sample : E
Source Identification: West Virginia
Rank of Coal : hvab
Mine Designation : Ireland Mine, West Virginia
Seam Designation : Pittsburgh Seam
Location in U. S. A. : West Virginia

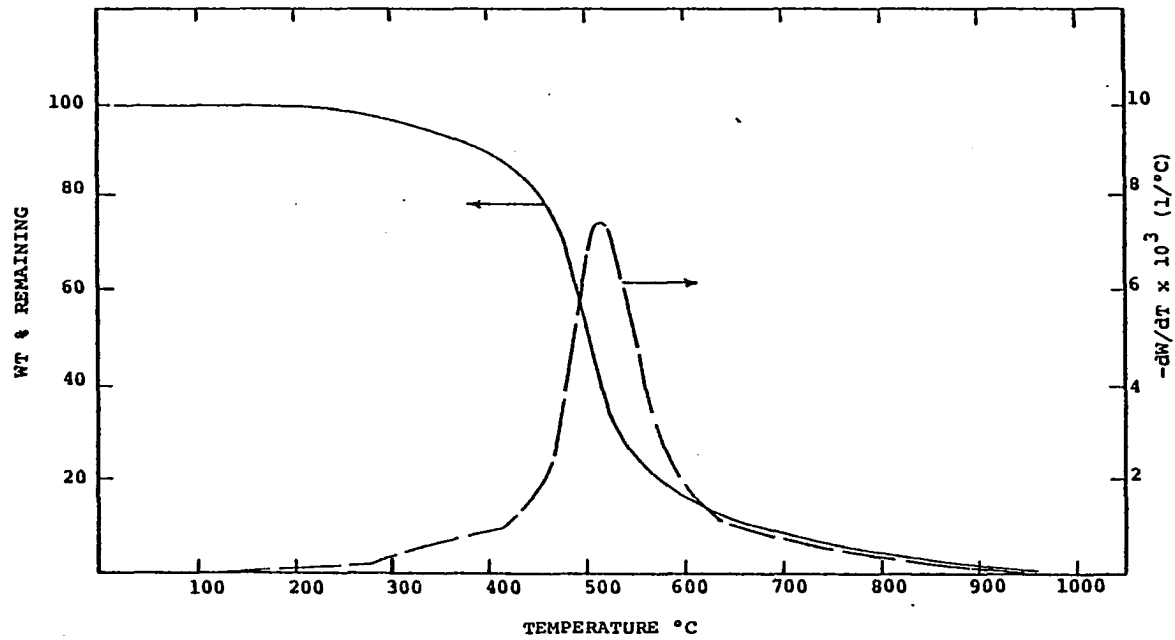


Figure E-1. TGA Thermograms (Weight Loss and Rate of Weight Loss) for Coal Sample E at 160°C/min.

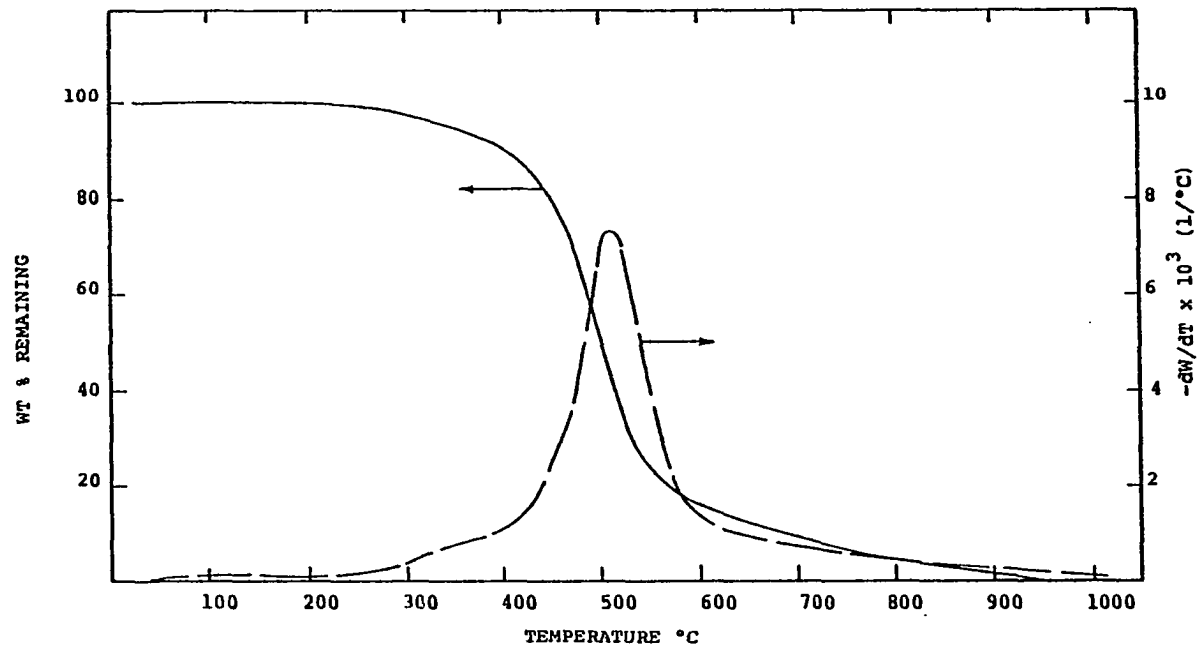


Figure E-2. TGA Thermograms (Weight Loss and Rate of Weight Loss) for Coal Sample E at 80°C/min.

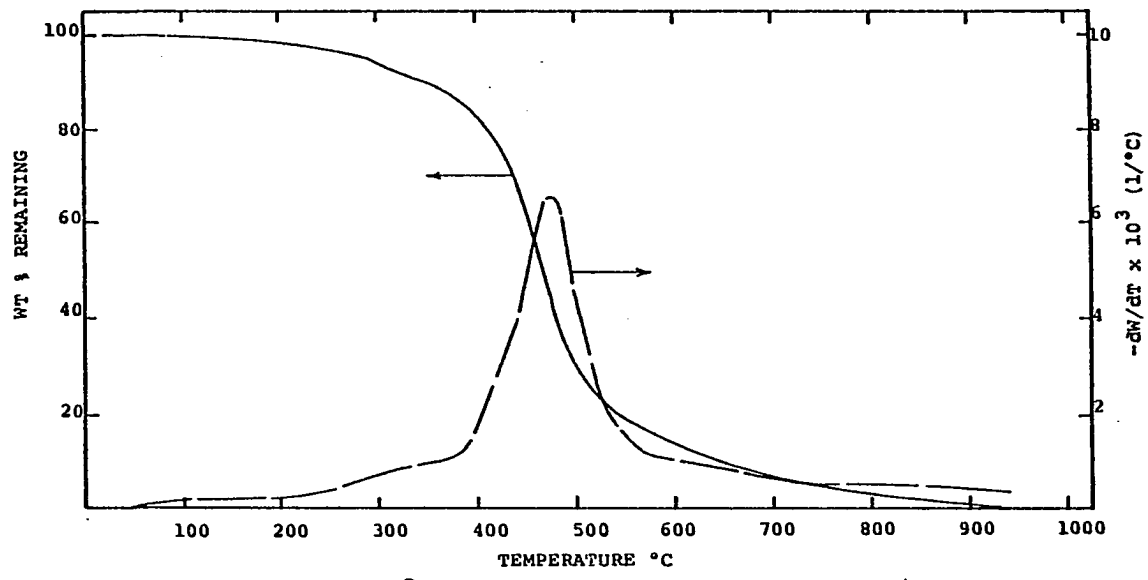


Figure E-3. TGA Thermograms (Weight Loss and Rate of Weight Loss) for Coal Sample E at 40°C/min.

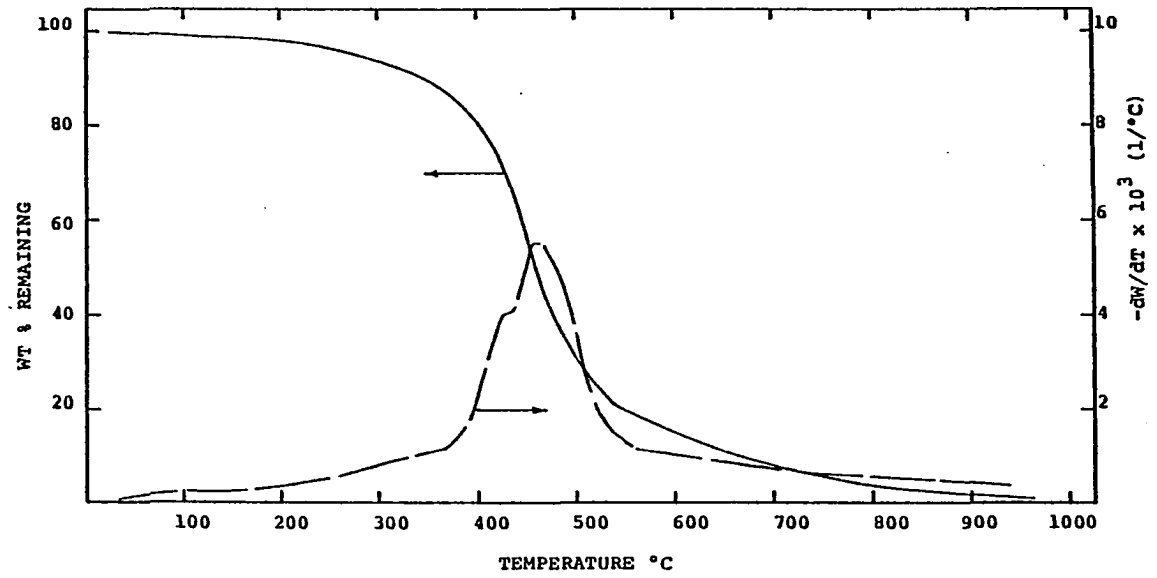


Figure.E-4. TGA Thermograms (Weight Loss and Rate of Weight Loss) for Coal Sample E at 20°C/min.

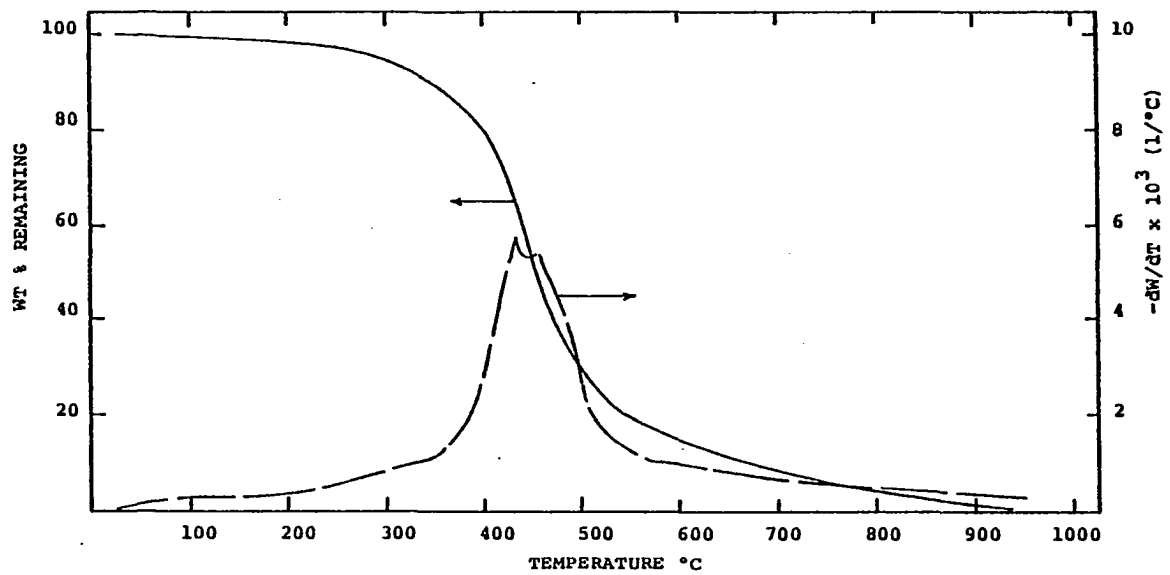


Figure E-5. TGA Thermograms (Weight Loss and Rate of Weight Loss) for Coal Sample E at 10°C/min.

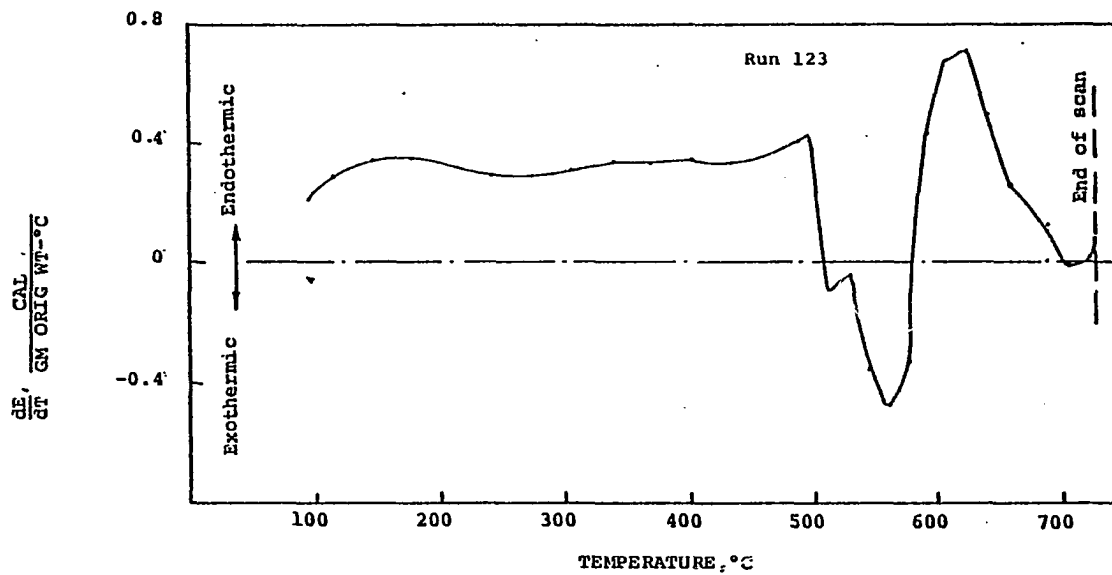


Figure E-6. Corrected DSC Scan for the Coal Sample E at a Heating Rate of 320°C/min.

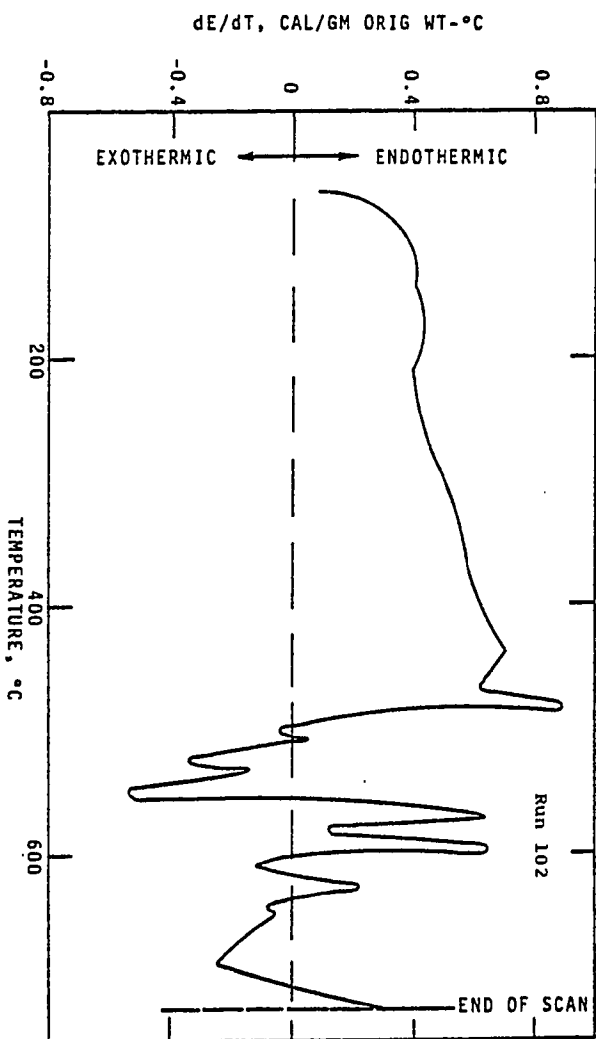


Figure E-7. Corrected DSC Scan for the Coal Sample E at a Heating Rate of 160°C/min.

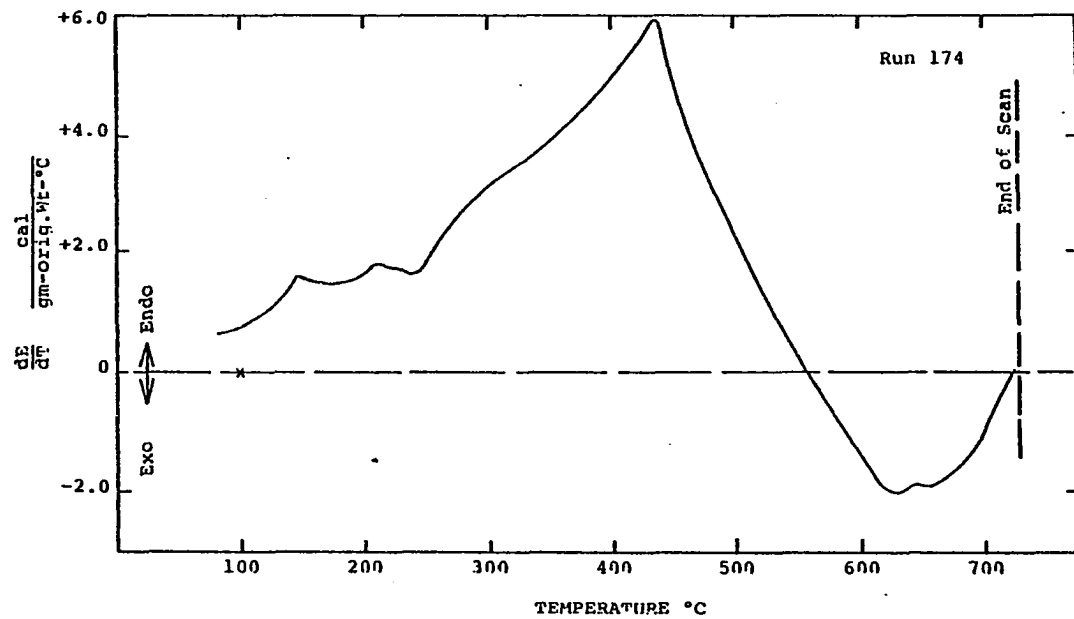


Figure E-8. Corrected DSC Scan for the Coal Sample E at a Heating Rate of 40°C/min.

APPENDIX F

TGA AND DSC THERMOGRAMS FOR COAL SAMPLE F

Coal Sample : F
Source Identification: Wyoming (1)
Rank of Coal : hvb
Mine Designation : . . .
Seam Designation : Rock Springs, Wyoming
Location in U. S. A. : Wyoming

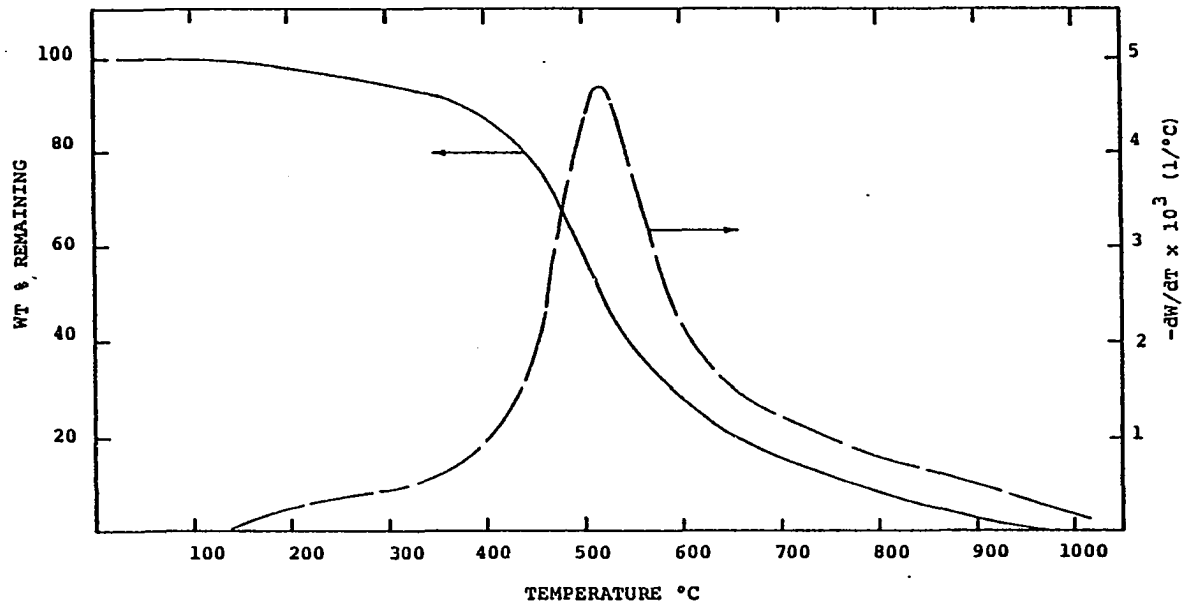


Figure F-1. TGA Thermograms (Weight Loss and Rate of Weight Loss) for Coal Sample F at 160°C/min.

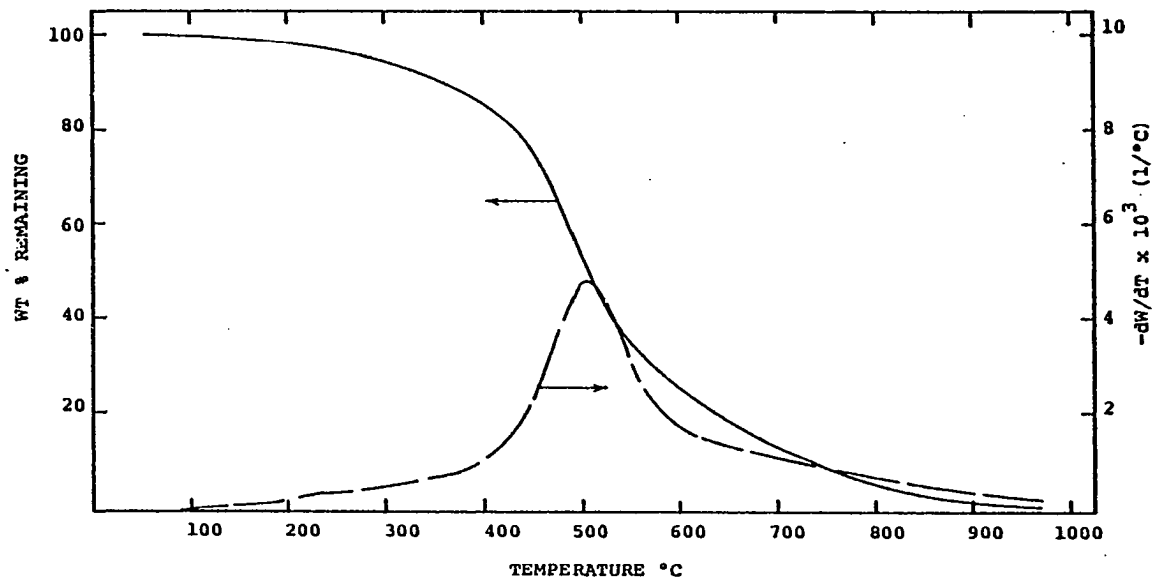


Figure F-2. TGA Thermograms (Weight Loss and Rate of Weight Loss) for Coal Sample F at 80°C/min.

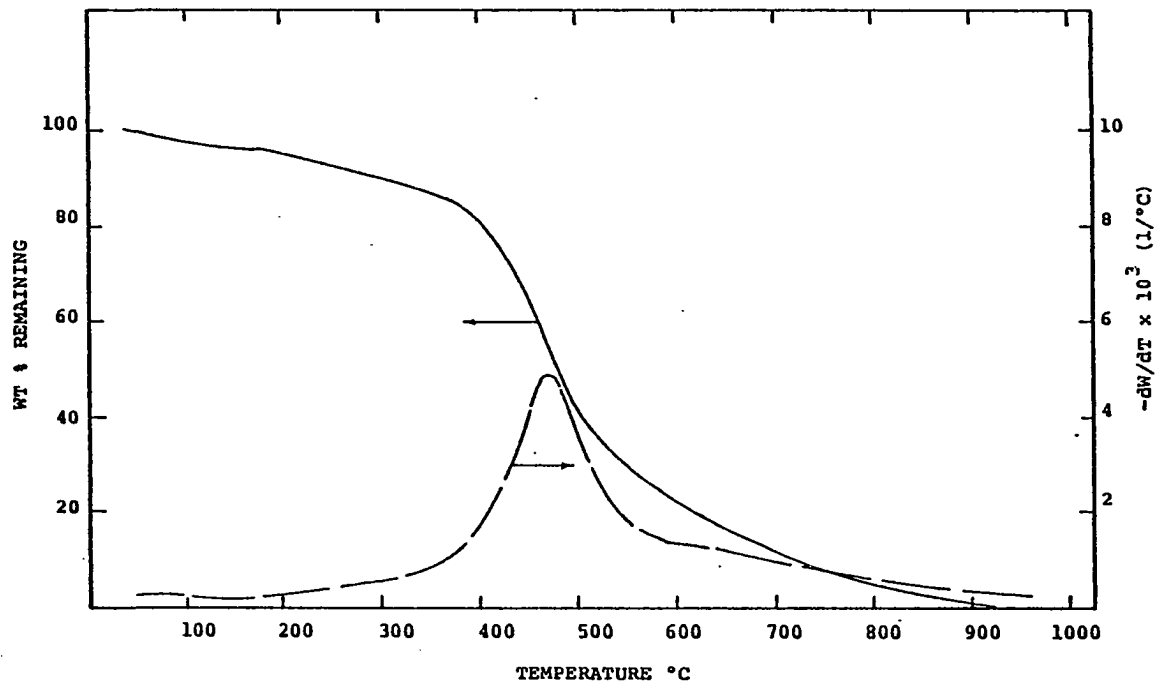


Figure F-3. TGA Thermograms (Weight Loss and Rate of Weight Loss) for Coal Sample F at 40°C/min.

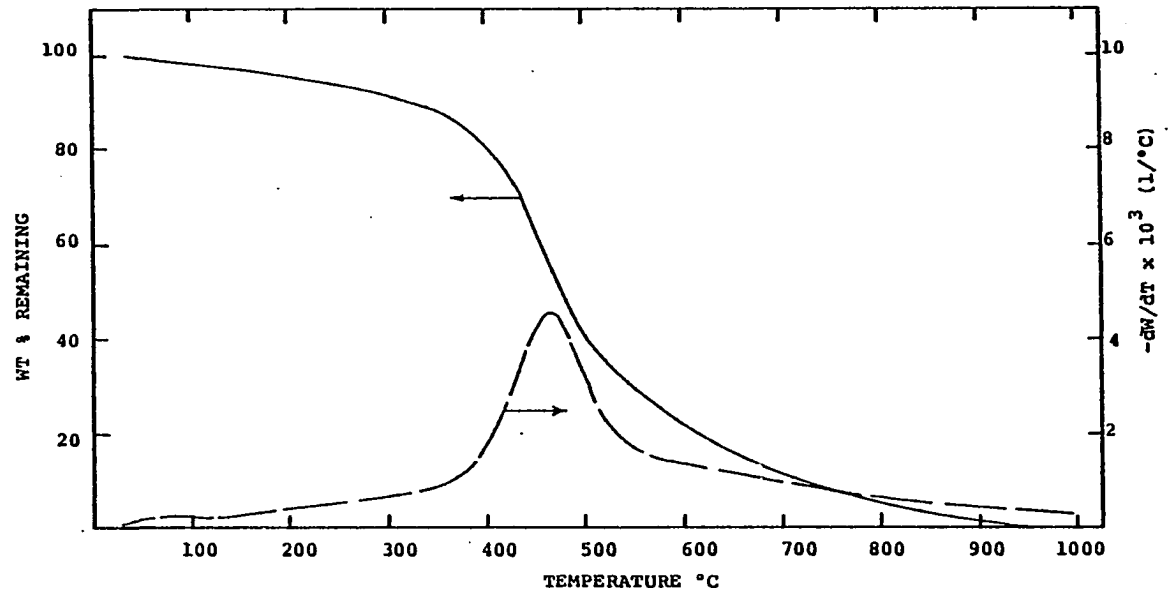


Figure F-4. TGA Thermograms (Weight Loss and Rate of Weight Loss) for Coal Sample F at 20°C/min.

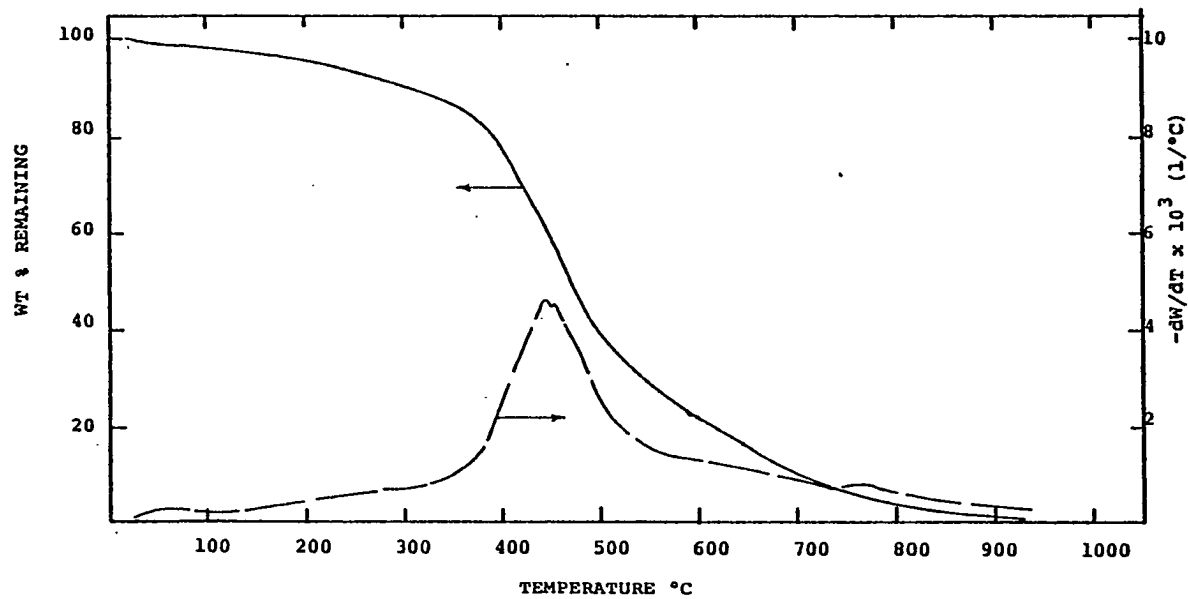


Figure F-5. TGA Thermograms (Weight Loss and Rate of Weight Loss) for Coal Sample F at 10°C/min.

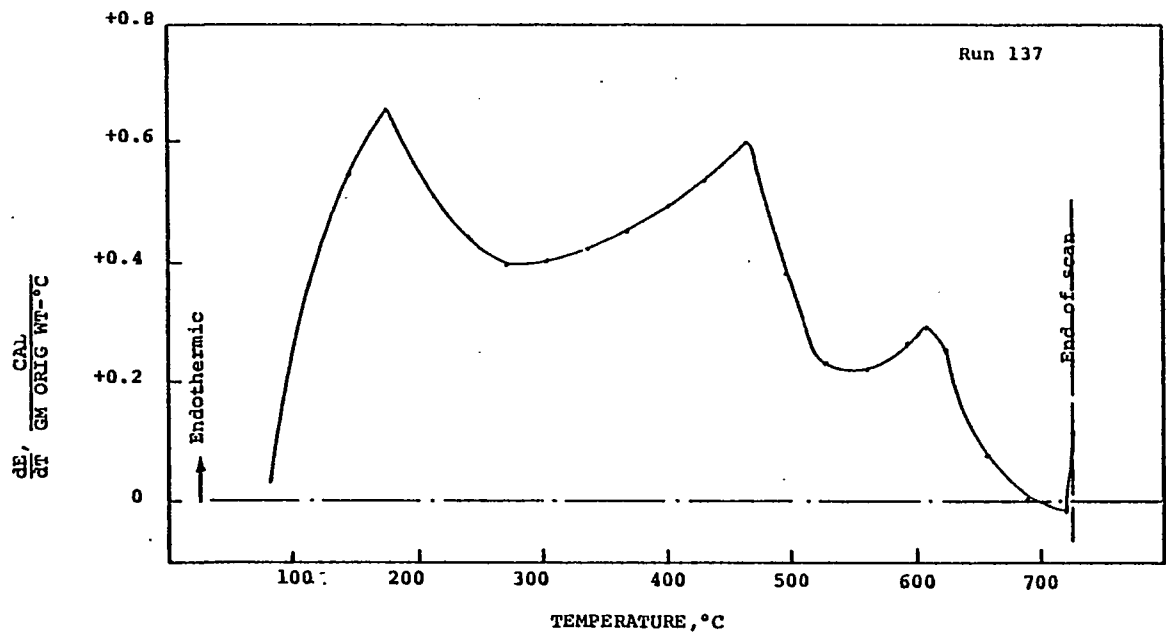


Figure F-6. Corrected DSC Scan for the Coal Sample F at a Heating Rate of 320°C/min.

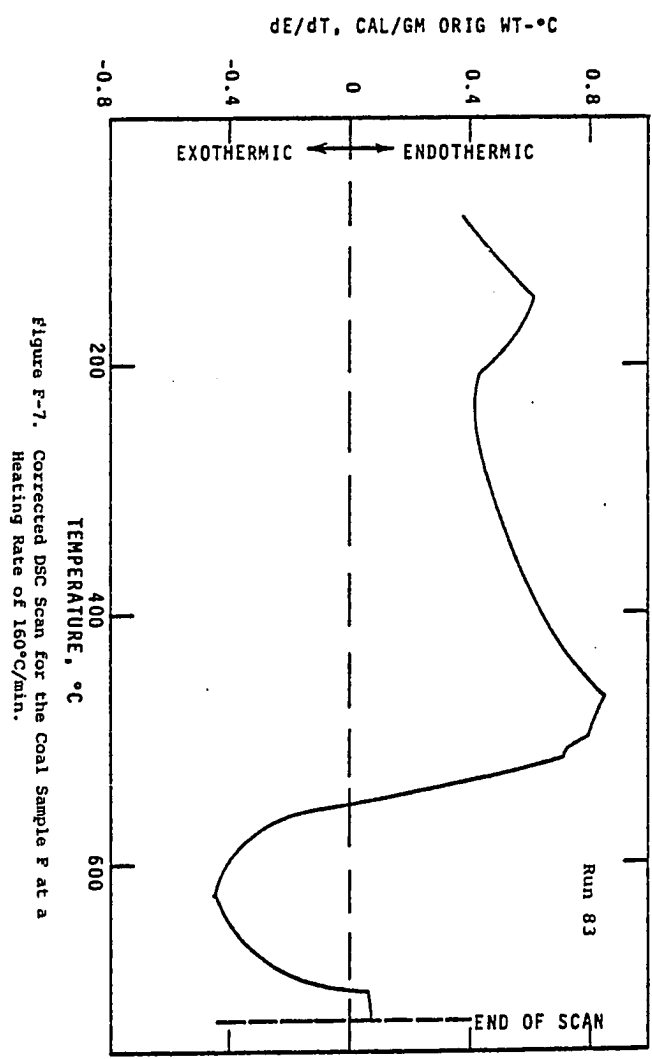


Figure F-7. Corrected DSC Scan for the Coal Sample F at a Heating Rate of 160 $^\circ\text{C}/\text{min}$.

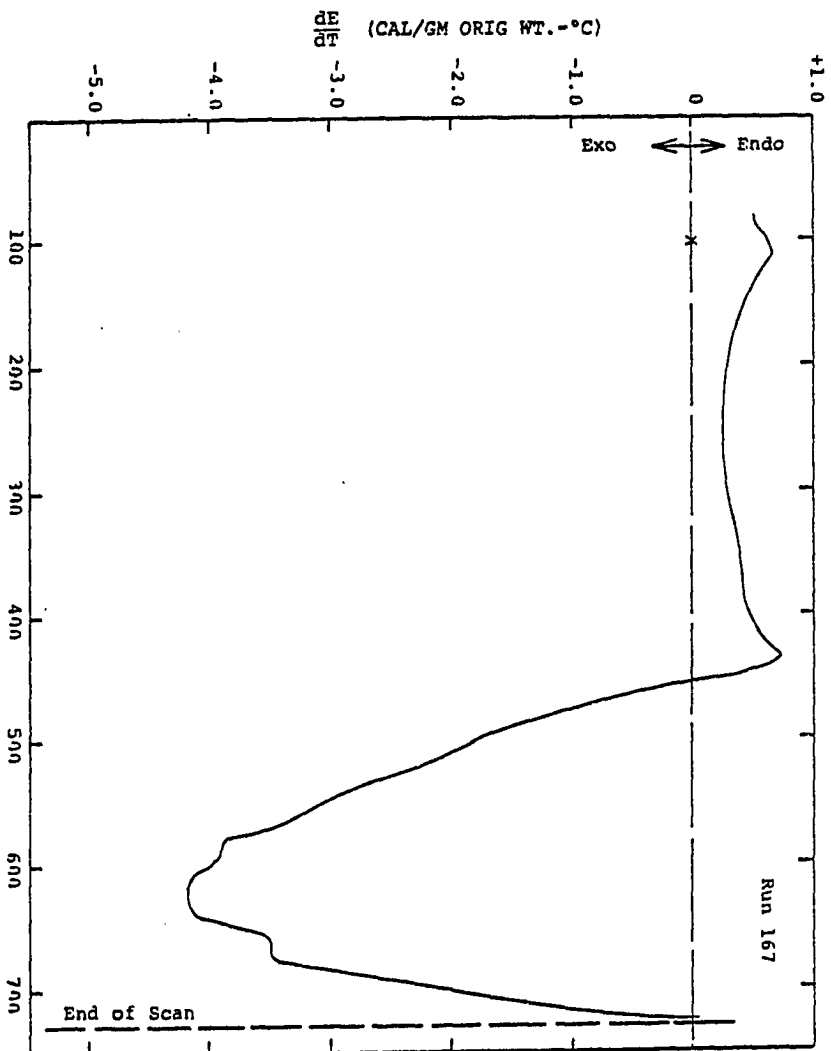


Figure F-8. Corrected DSC Scan for the Coal Sample F at a Heating Rate of 40°C/min.

APPENDIX G

TGA AND DSC THERMOGRAMS FOR COAL SAMPLE G

Coal Sample : G
Source Identification: FSOC-026
Rank of Coal : hvc
Mine Designation : Not Available
Seam Designation : Sahara #6
Location in U. S. A. : Illinois

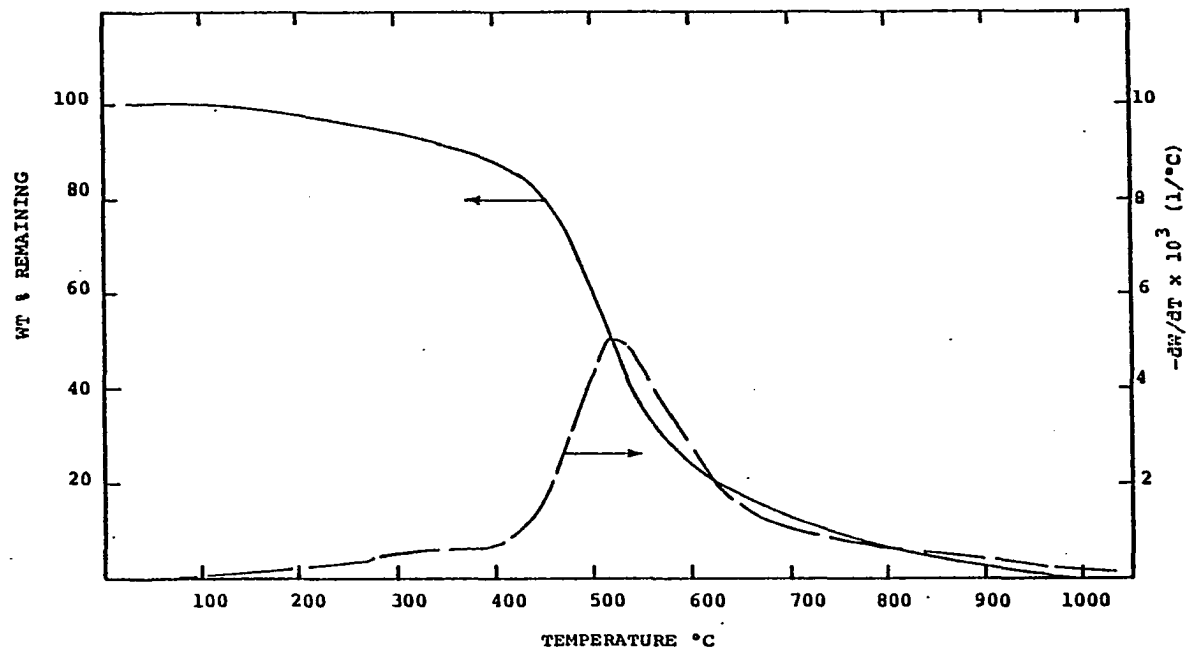


Figure G-1. TGA Thermograms (Weight Loss and Rate of Weight Loss) for Coal Sample G at 160°C/min.

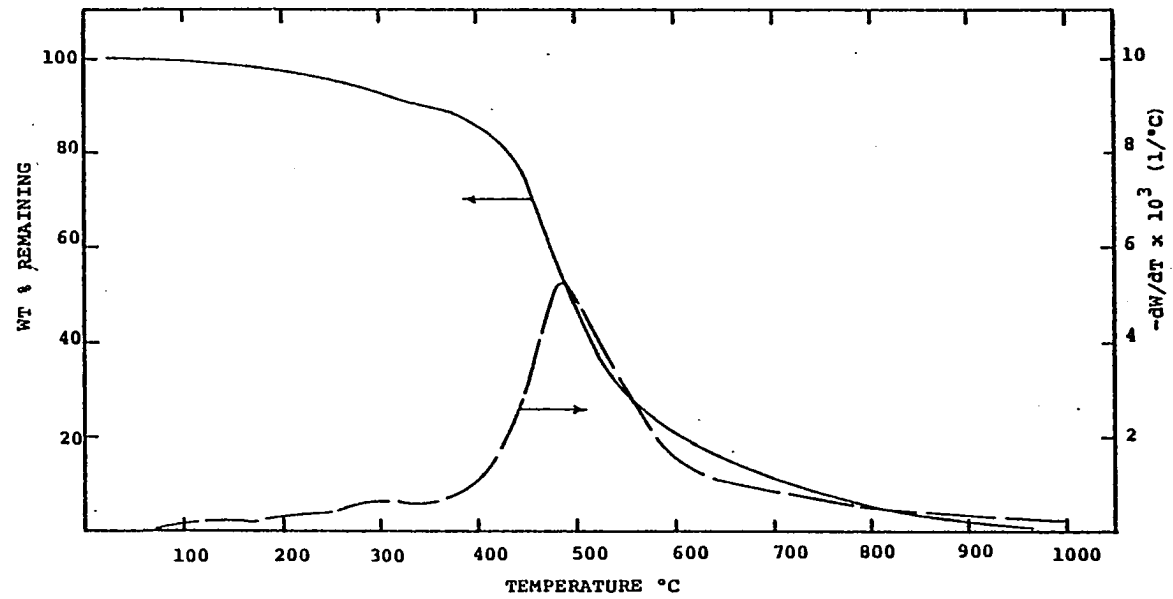


Figure G-2. TGA Thermograms (Weight Loss and Rate of Weight Loss) for Coal Sample G at 80°C/min.

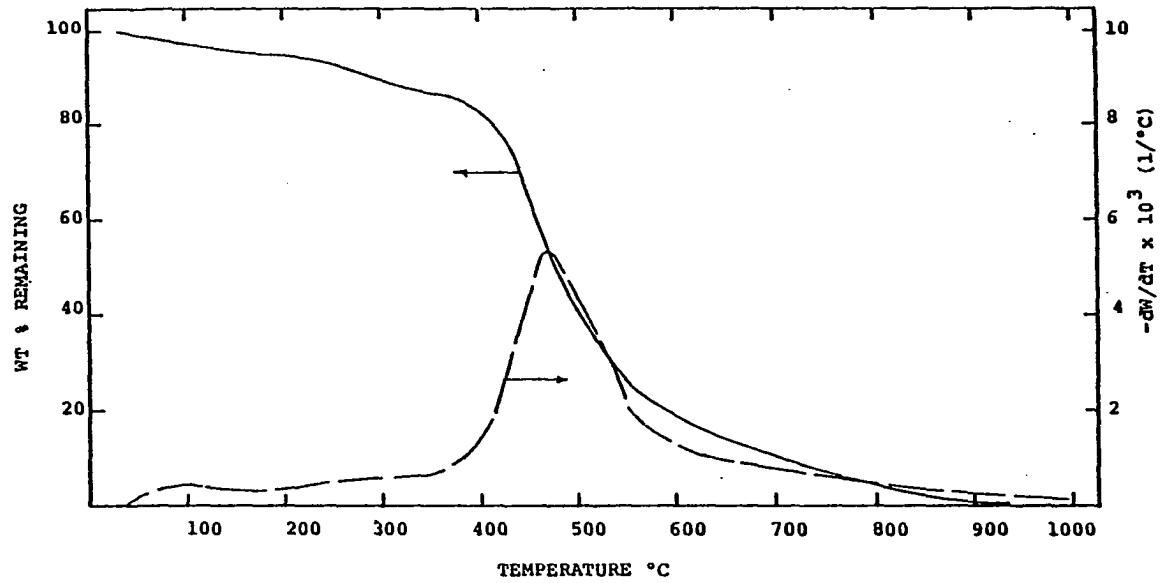


Figure G-3. TGA Thermograms (Weight Loss and Rate of Weight Loss) for Coal Sample G at 40°C/min.

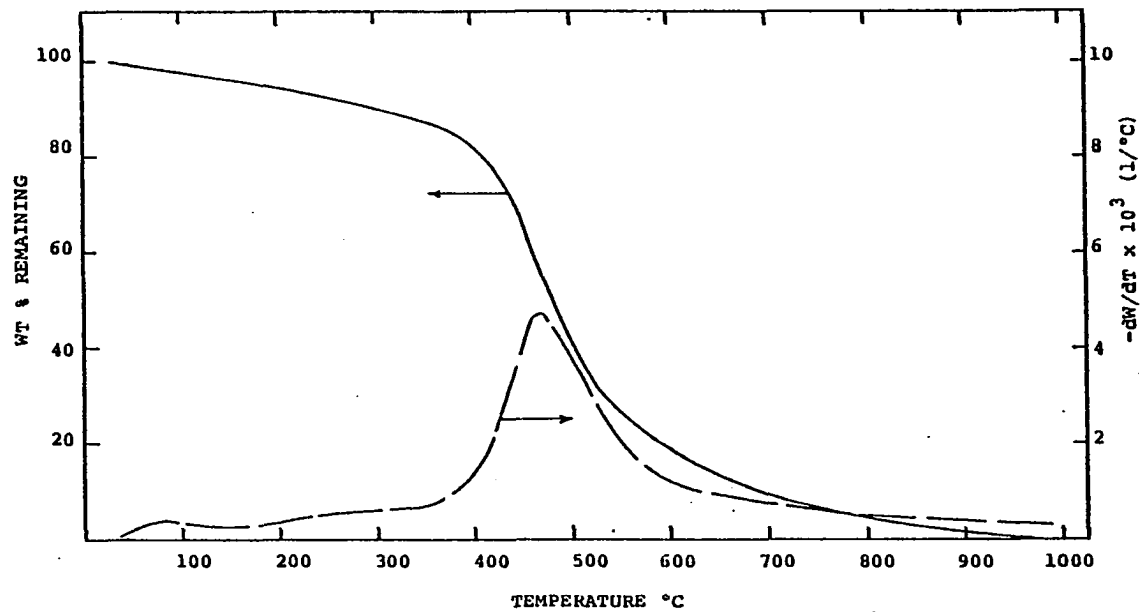


Figure G-4. TGA Thermograms (Weight Loss and Rate of Weight Loss) for Coal Sample G at 20°C/min.

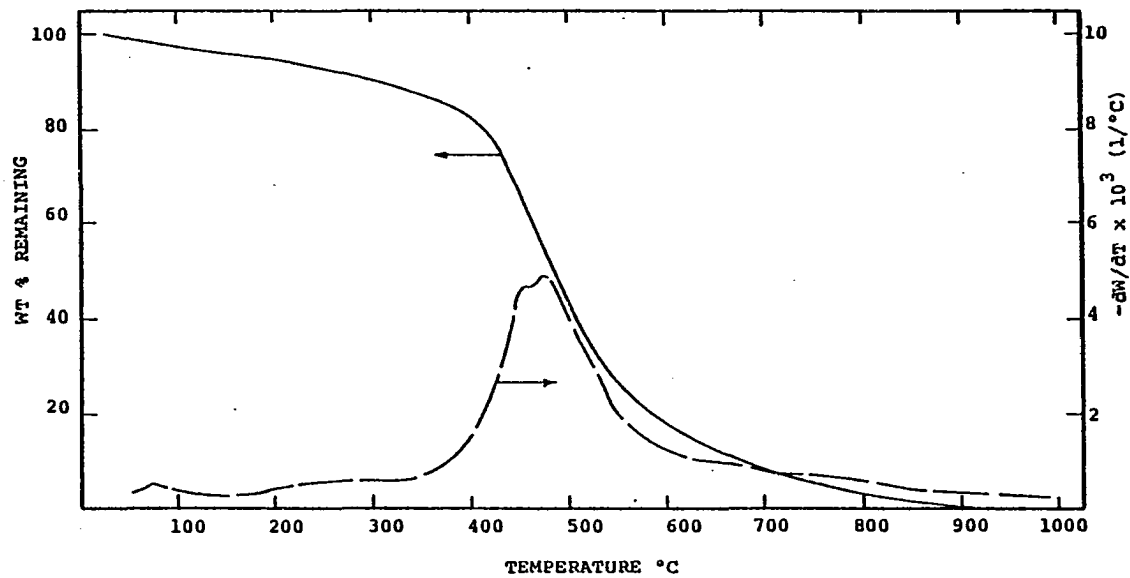


Figure G-5. TGA Thermograms (Weight Loss and Rate of Weight Loss) for Coal Sample G at 10°C/min.

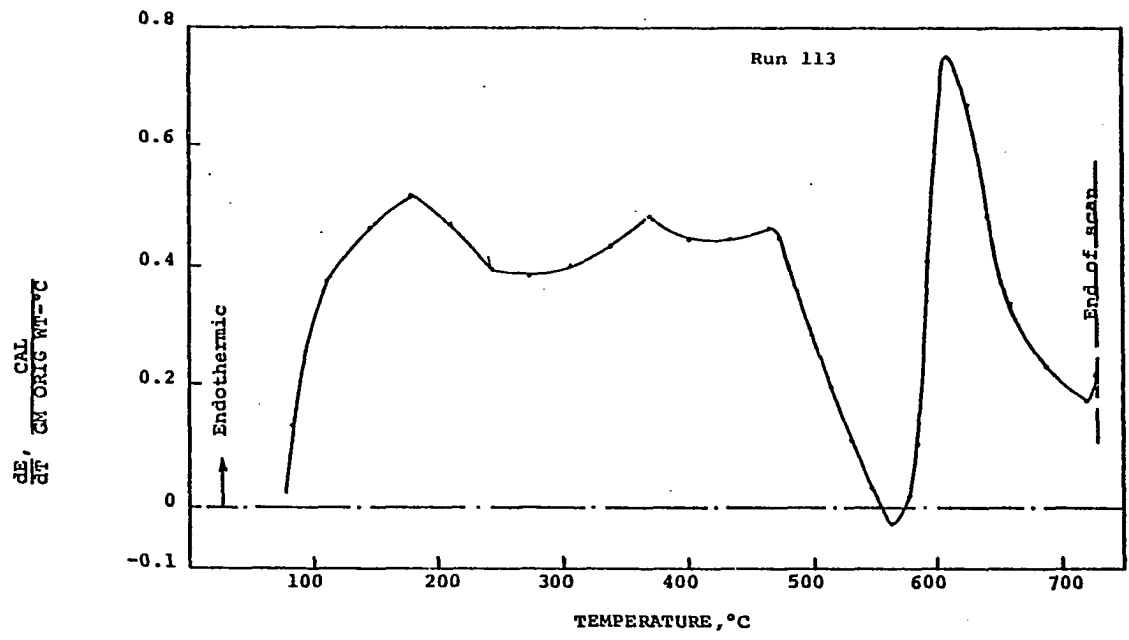


Figure G-6. Corrected DSC Scan for the Coal Sample G at a Heating Rate of 320°C/min.

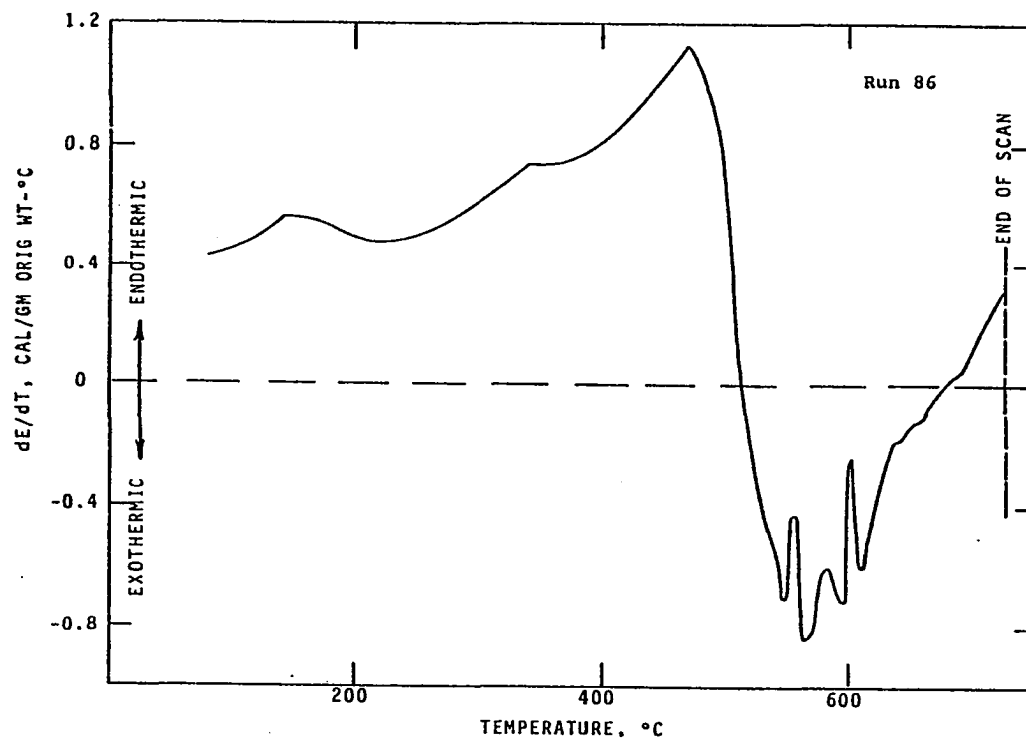


Figure G-7. Corrected DSC Scan for the Coal Sample G at a Heating Rate of 160°C/min.

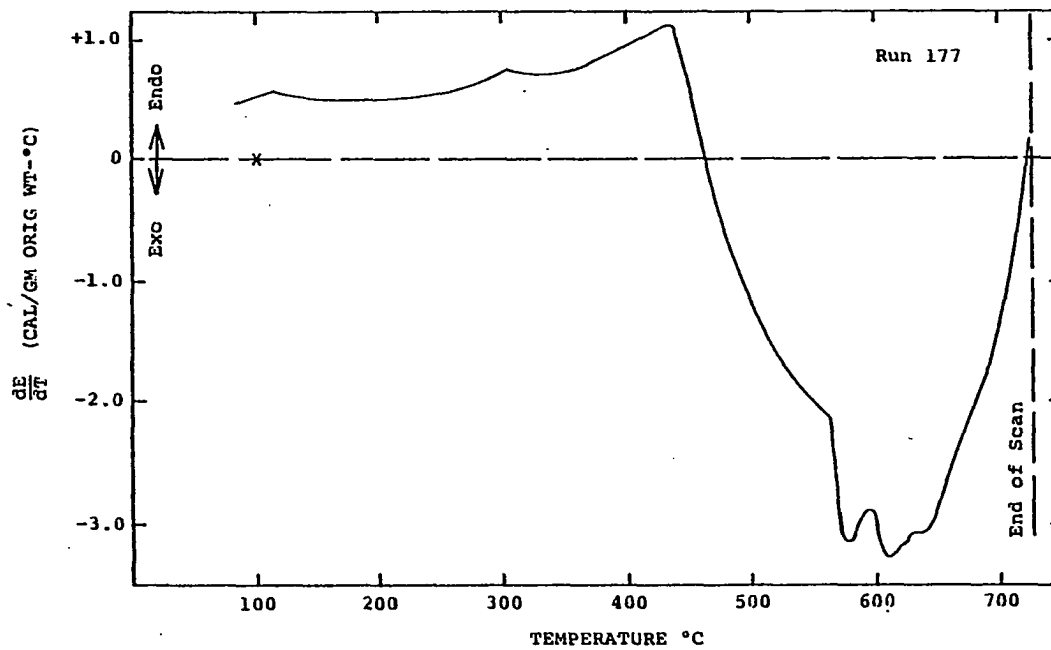


Figure G-8. Corrected DSC Scan for the Coal Sample G at a Heating Rate of 40°C/min.

APPENDIX H

TGA AND DSC THERMOGRAMS FOR COAL SAMPLE H

Coal Sample : H
Source Identification: PSOC-216
Rank of Coal : hvb
Mine Designation : Colonial
Seam Designation : Kentucky #14
Location in U. S. A. : Kentucky

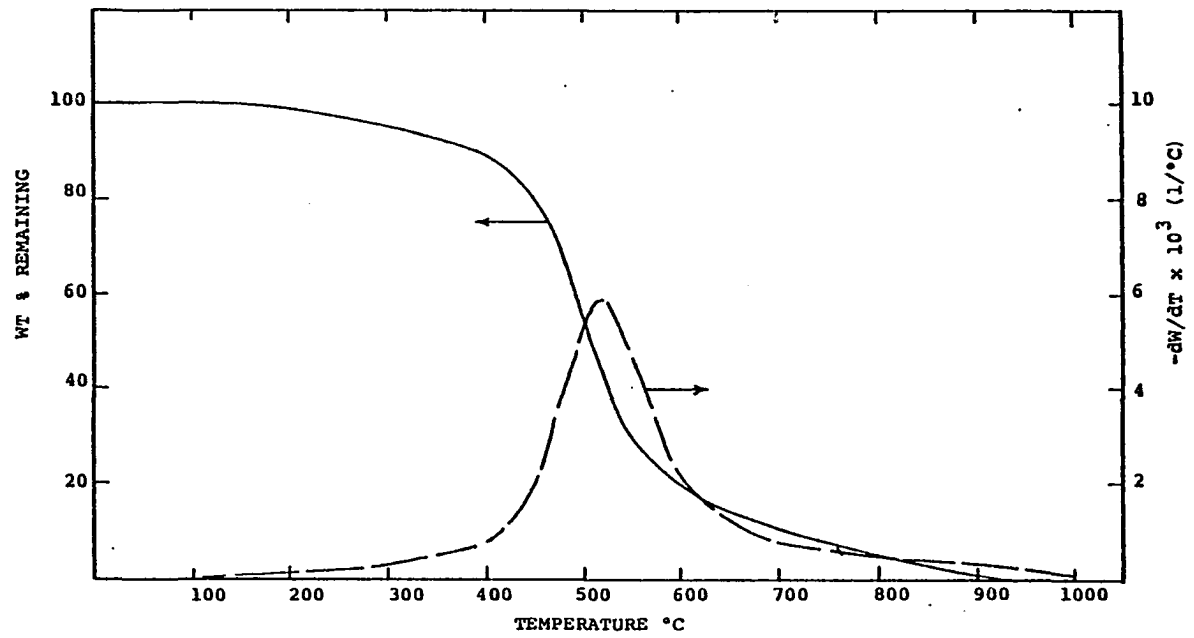


Figure H-1. TGA Thermograms (Weight Loss and Rate of Weight Loss) for Coal Sample H at 160°C/min.

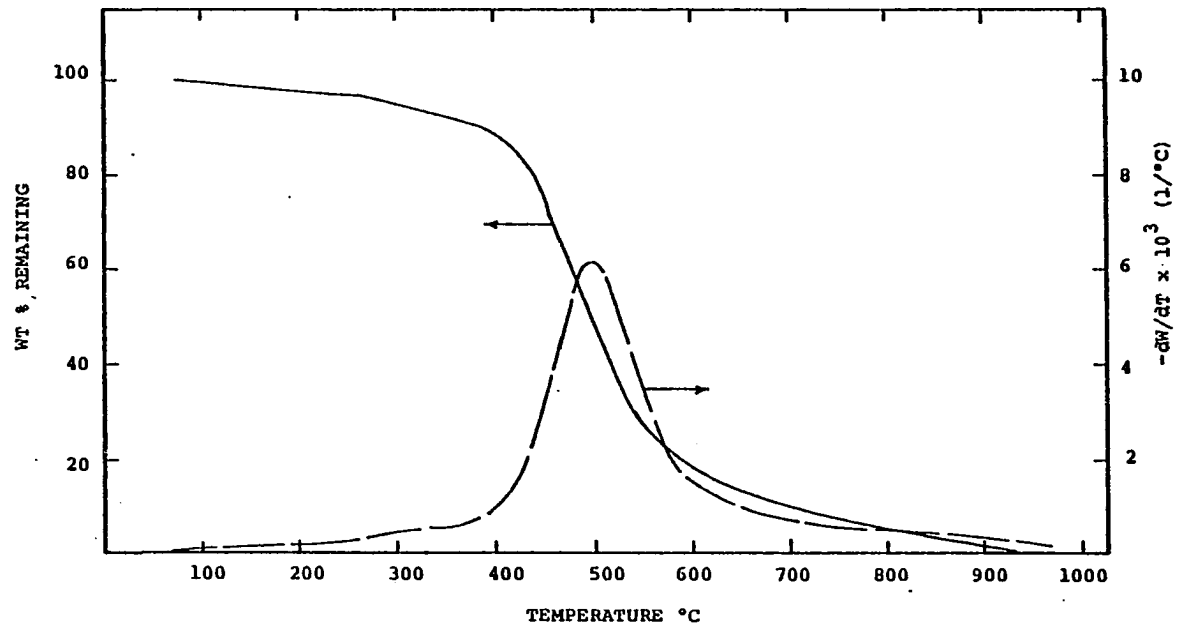


Figure H-2. TGA Thermograms (Weight Loss and Rate of Weight Loss) for Coal Sample H at 80°C/min.

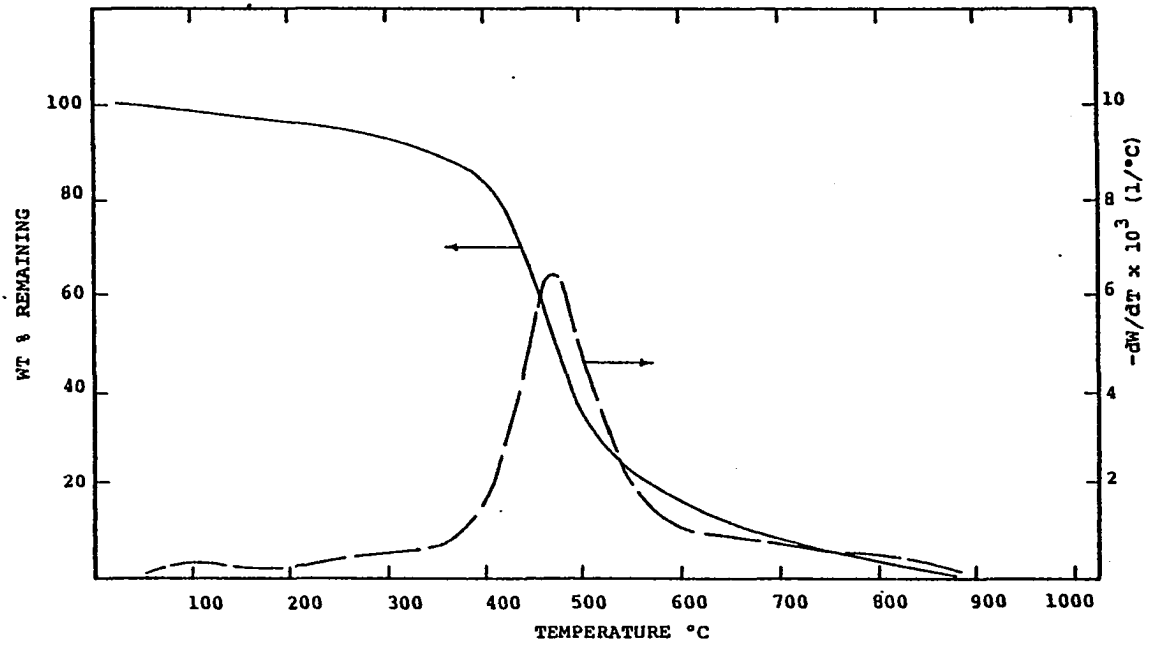


Figure H-3. TGA Thermograms (Weight Loss and Rate of Weight Loss) for Coal Sample H at 40°C/min.

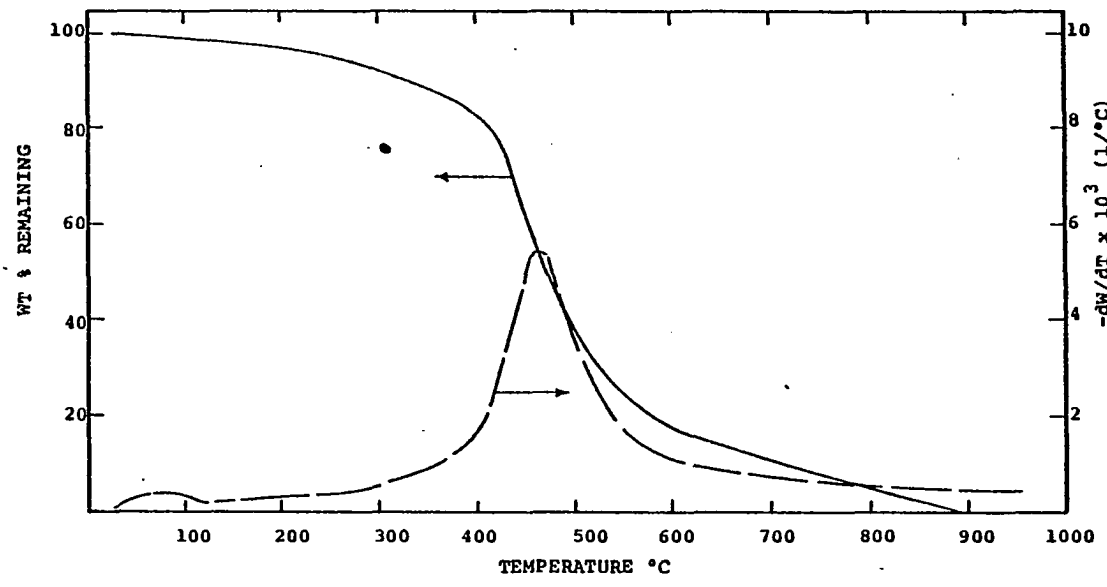


Figure H-4. TGA Thermograms (Weight Loss and Rate of Weight Loss) for Coal Sample H at 20°C/min.

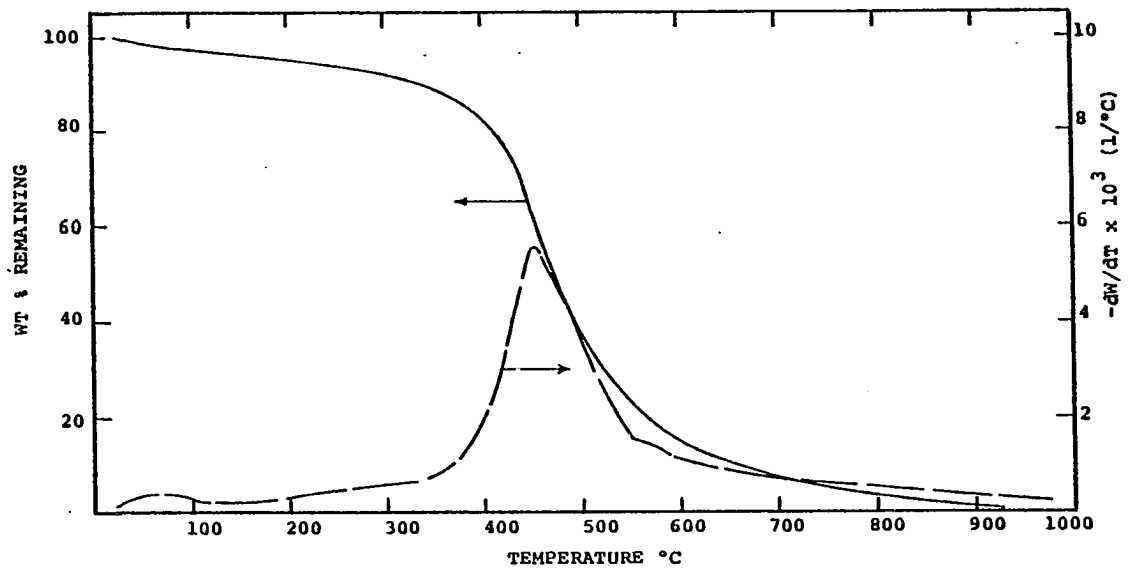


Figure H-5. TGA Thermograms (Weight Loss and Rate of Weight Loss) for Coal Sample H at 10°C/min.

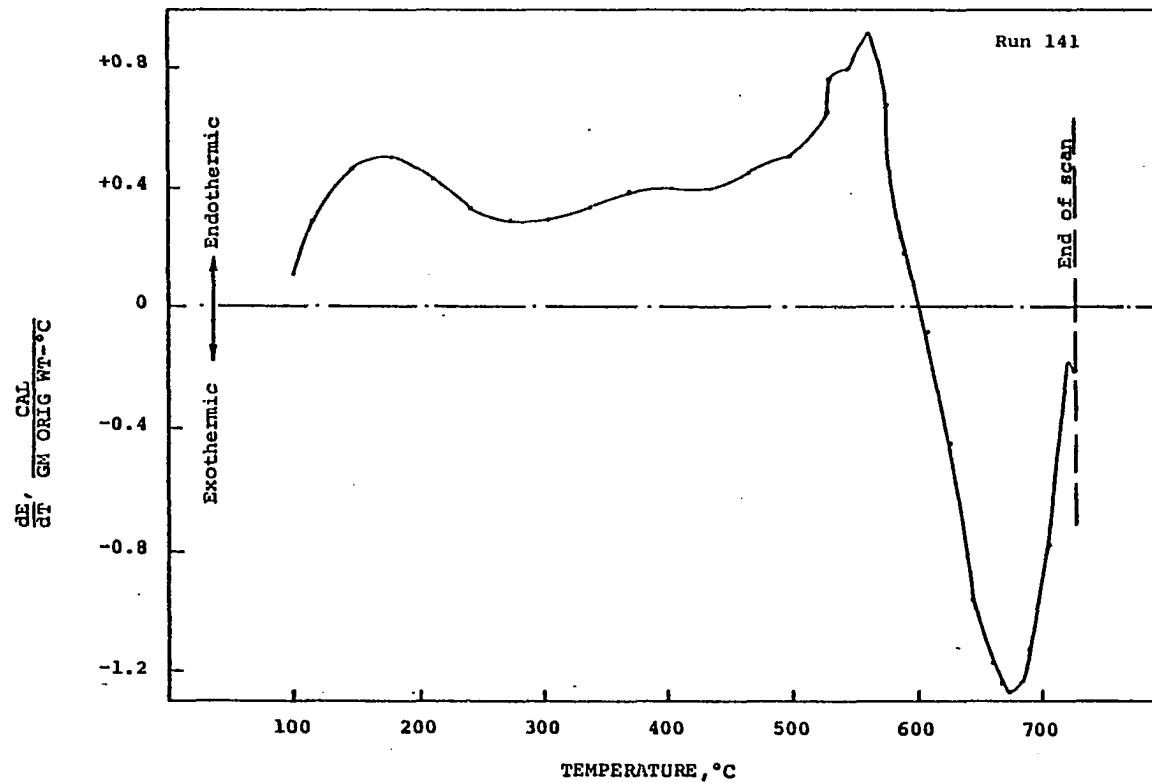


Figure H-6. Corrected DSC Scan for the Coal Sample H at a Heating Rate of 320°C/min.

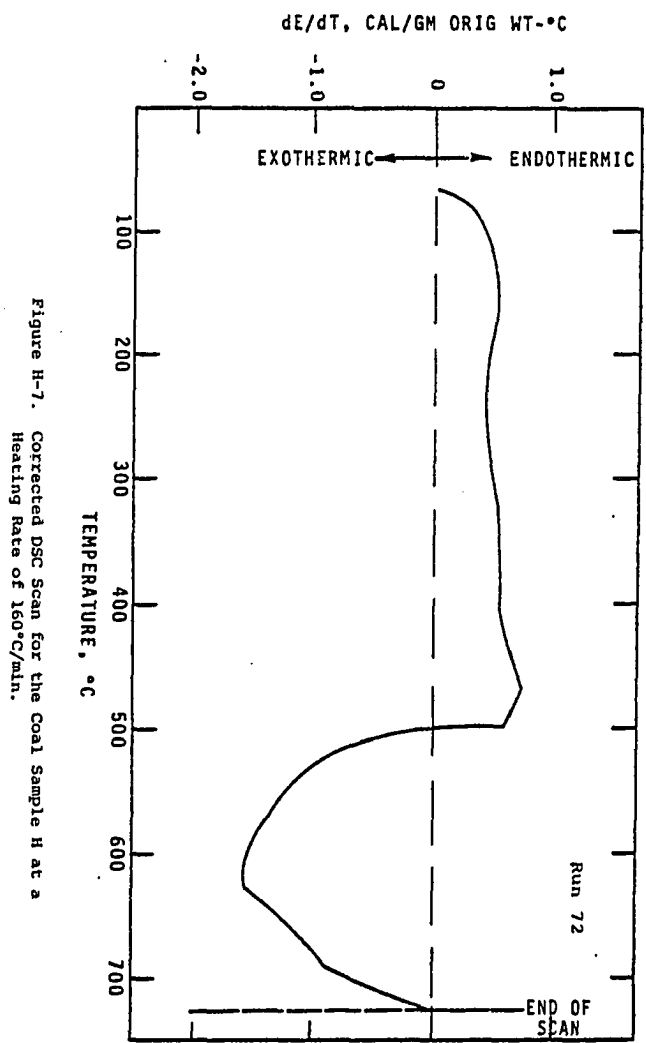


Figure H-7. Corrected DSC Scan for the Coal Sample H at a Heating Rate of 160°C/min.

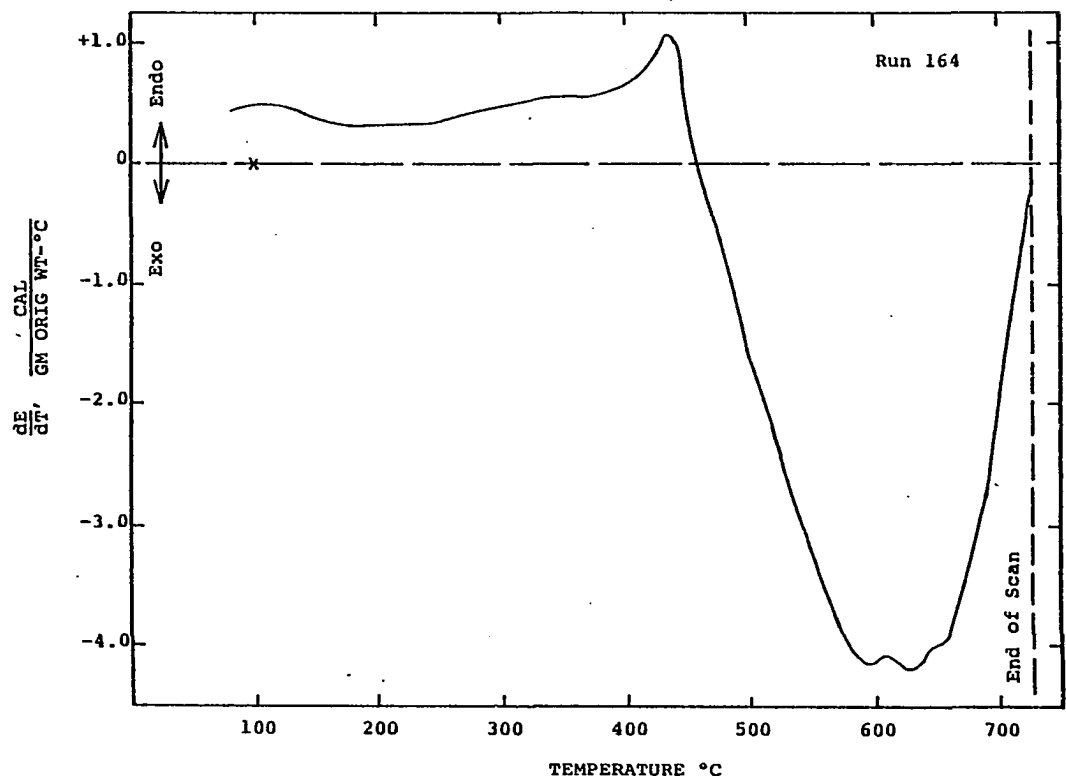


Figure H-8. Corrected DSC Scan for the Coal Sample H at a Heating Rate of 40°C/min.

APPENDIX I

TGA AND DSC THERMOGRAMS FOR COAL SAMPLE I

Coal Sample : I
Source Identification: PSOC-272
Rank of Coal : hvb
Mine Designation : Sinclair Strip Mine
Seam Designation : Kentucky #9 Seam
Location in U. S. A. : Kentucky

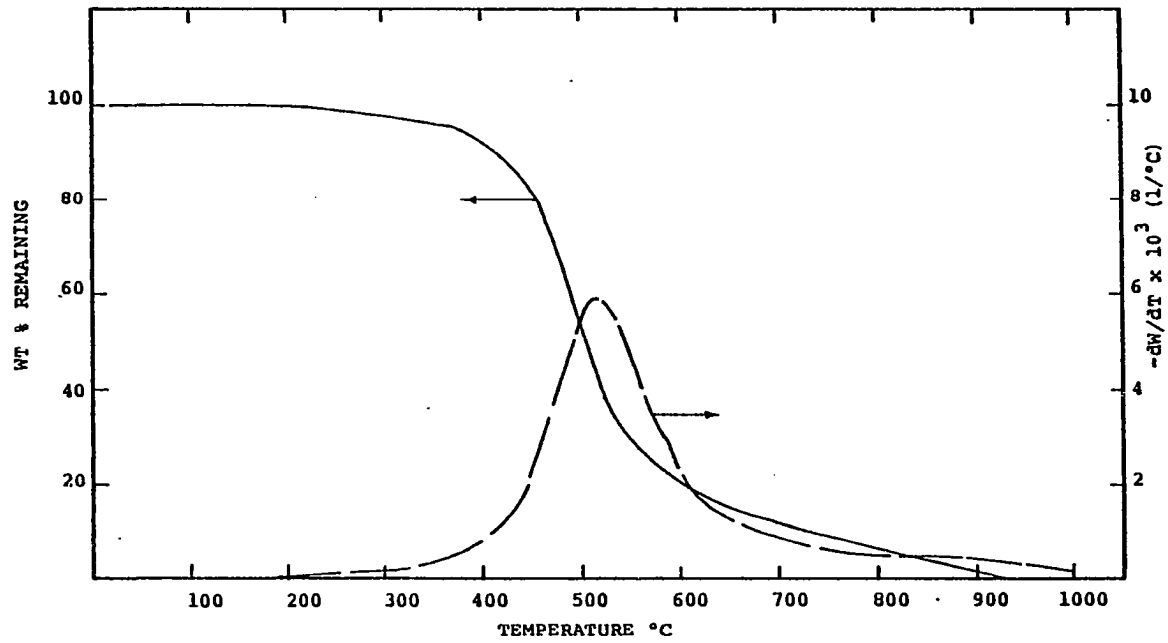


Figure I-1. TGA Thermograms (Weight Loss and Rate of Weight Loss) for Coal Sample I at 160°C/min.

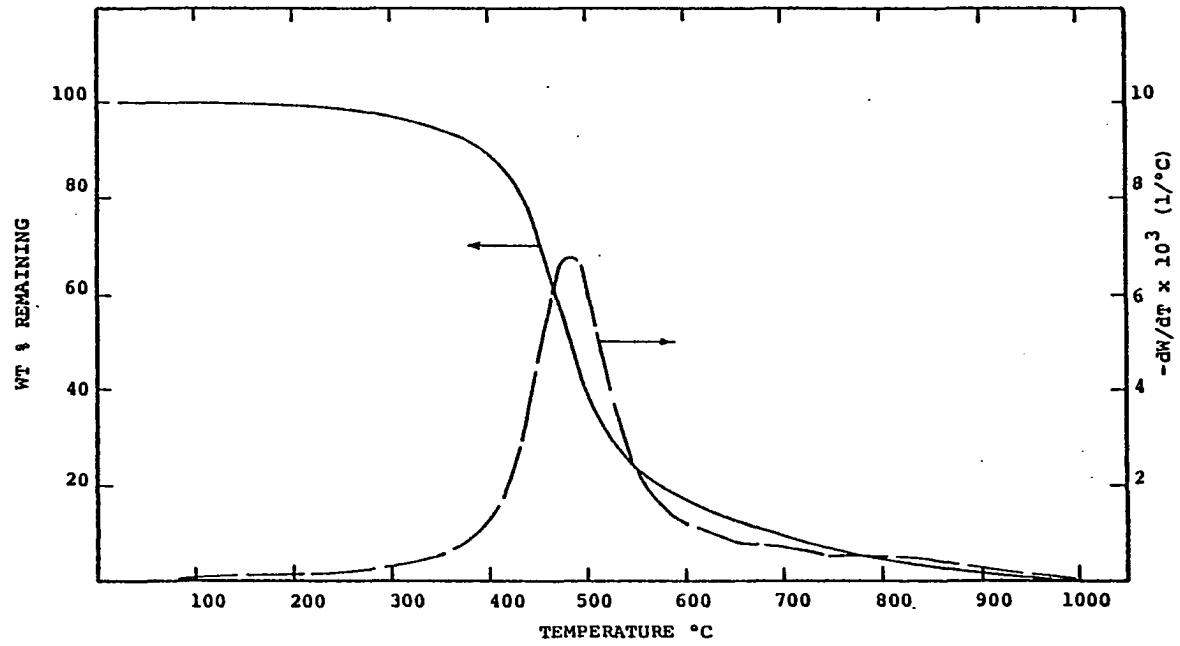


Figure I-2. TGA Thermograms (Weight Loss and Rate of Weight Loss) for Coal Sample I at 80°C/min.

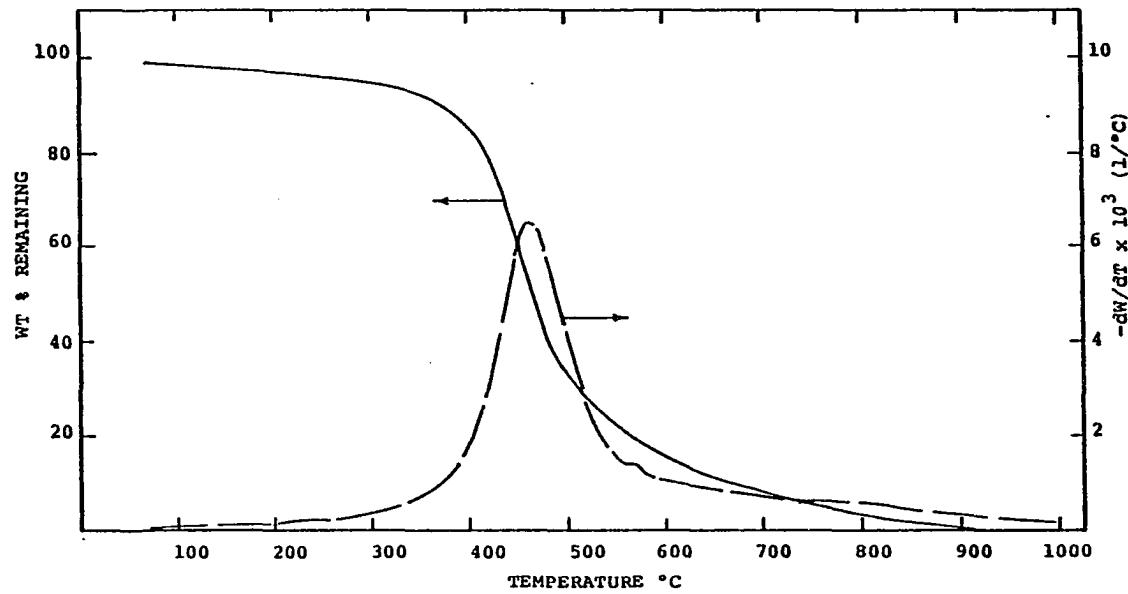


Figure I-3. TGA Thermograms (Weight Loss and Rate of Weight Loss) for Coal Sample I at 40°C/min.

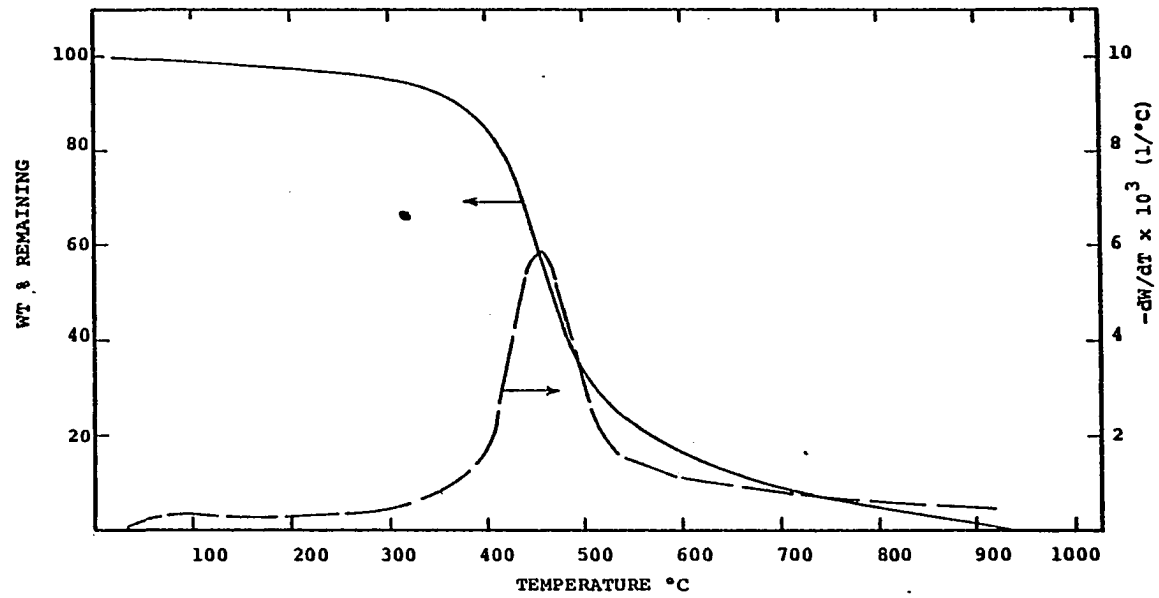


Figure I-4. TGA Thermograms (Weight Loss and Rate of Weight Loss) for Coal Sample I at 20°C/min.

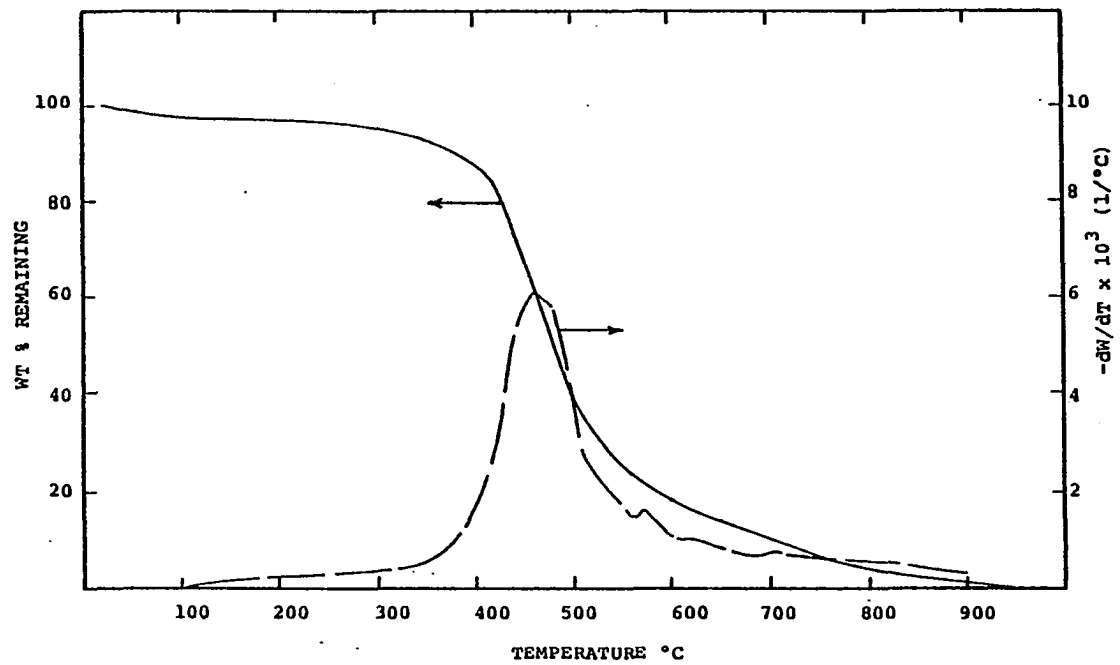


Figure I-5. TGA Thermograms (Weight Loss and Rate of Weight Loss) for Coal Sample I at 10°C/min.

$\frac{dE}{dT}, \frac{CAL}{GM \text{ ORIG. WT.}} \text{--}^{\circ}\text{C}$

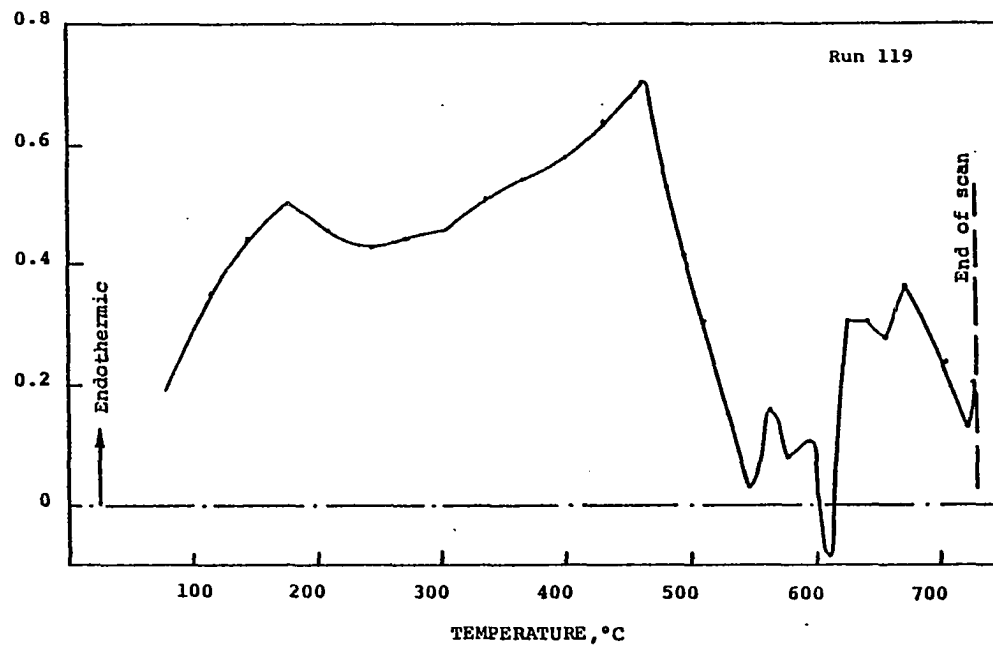


Figure I-6. Corrected DSC Scan for the Coal Sample I at a Heating Rate of 320°C/min.

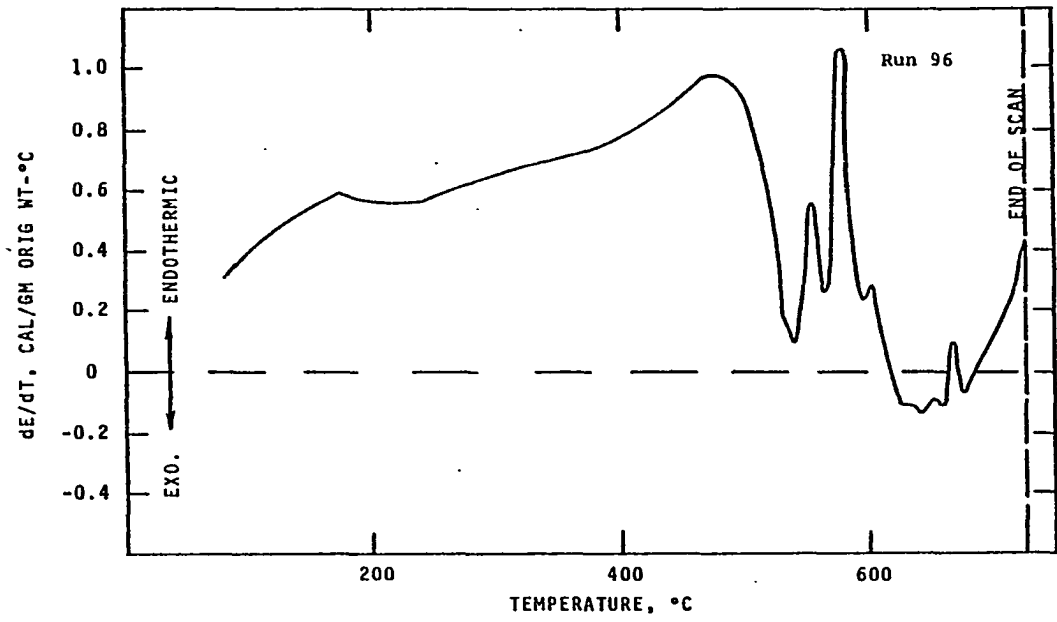


Figure I-7. Corrected DSC Scan for the Coal Sample I at a Heating Rate of 160°C/min.

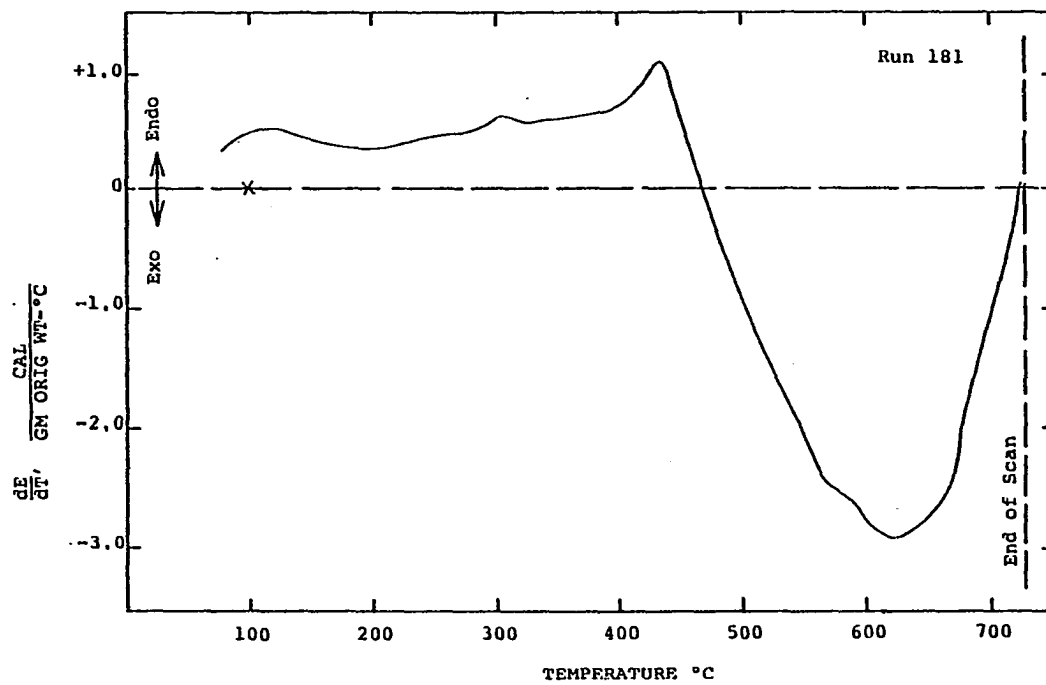


Figure I-8. Corrected DSC Scan for the Coal Sample I at a Heating Rate of 40°C/min.

APPENDIX J

TABULATED DATA FROM TGA AND DSC RUNS

Table J-1
 TABULATED DATA FROM TGA OF COAL SAMPLES

SAMPLE	RUN NO.	HEATING RATE °C/min	INITIAL WEIGHT mg.	FINAL WEIGHT mg.	MAXIMUM RATE OF WEIGHT LOSS PER MIN.	MAXIMUM RATE OF WEIGHT LOSS PER °C	TEMPERATURE AT MAXIMUM RATE OF WEIGHT LOSS °C	
A	2	160	1.74	1.14	0.8232	0.00515	518	
	5	160	2.26	1.54	0.8979	0.00562	509	
	4	80	2.34	1.60	0.3888	0.00486	488	
	7R*	80	0.95	0.60	0.4242	0.00530	480	
	1R	40	2.42	1.60	0.2959	0.00740	462	
	3R	40	2.16	1.46	0.2249	0.00560	463	
	1	20	2.64	1.78	0.1202	0.00601	468	
	2	20	2.66	1.80	0.1154	0.00577	468	
	1R	10	3.51	2.44	0.0615	0.00615	459	
	B	1	160	2.24	1.30	0.8073	0.00505	509
		3	160	2.40	1.40	0.9332	0.00583	509
		5	80	1.59	0.95	0.5012	0.00627	489
6		80	1.66	0.94	0.5054	0.00632	488	
2		40	2.11	1.21	0.2424	0.00608	455	
3		40	2.09	1.20	0.2225	0.00556	452	
1		20	2.05	1.14	0.1201	0.00601	458	
2		20	2.70	1.52	0.1350	0.00675	458	
1R		10	2.64	1.51	0.0520	0.00520	445	

Table J-1 (continued)

SAMPLE	RUN NO.	HEATING RATE °C/min	INITIAL WEIGHT mg.	FINAL WEIGHT mg.	MAXIMUM RATE OF WEIGHT LOSS PER MIN	MAXIMUM RATE OF WEIGHT LOSS PER °C	TEMPERATURE AT MAXIMUM RATE OF WEIGHT LOSS °C
C	1	160	2.20	1.28	0.9375	0.00586	518
	3	160	2.20	1.35	0.8578	0.00536	508
	1	80	1.12	0.60	0.4286	0.00536	481
	2	80	1.34	0.80	0.4538	0.00567	480
	2	40	2.20	1.28		0.00560	454
	3	40	1.99	1.15	0.2135	0.00536	463
	1	20	2.26	1.28	0.1323	0.00662	458
	2	20	2.47	1.42	0.1307	0.00654	458
	1	10	2.52	1.48	0.0595	0.00595	444
	D	2	160	1.70	1.28	0.9096	0.00568
5		160	1.28	0.96	0.8468	0.00530	576
2		80	1.07	0.74	0.4318	0.00544	546
3		80	1.22	0.93	0.4471	0.00559	546
1		40	0.96	0.70	0.2097	0.00525	523
2		40	1.20	0.90	0.2064	0.00516	523
1		20	1.51	1.11	0.1018	0.00509	509
2		20	1.64	1.20	0.0838	0.00419	505
1		10	2.14	1.60	0.0426	0.00437	496

Table J-1 (continued)

SAMPLE	RUN NO.	HEATING RATE °C/min	INITIAL WEIGHT mg.	FINAL WEIGHT mg.	MAXIMUM RATE OF WEIGHT LOSS PER MIN.	MAXIMUM RATE OF WEIGHT LOSS PER °C	TEMPERATURE AT MAXIMUM RATE OF WEIGHT LOSS °C
E	2	160	1.54	0.90	1.1489	0.00718	518
	4	160	1.60	0.94	1.1875	0.00742	518
	1	80	1.40	0.84	0.5980	0.00726	513
	4	80	2.72	1.62	0.6083	0.00760	513
	5	40	1.60	0.86	0.2693	0.00673	463
	6	40	1.72	0.98	0.2600	0.00650	476
	2	20	2.32	1.40	0.1100	0.00550	468
	3	20	2.08	1.24	0.1164	0.00582	452
	1	10	2.38	1.38	0.0575	0.00575	435
	F	4	160	2.16	1.28	0.7480	0.00467
5		160	2.24	1.32	0.7543	0.00471	518
1		80	1.32	0.80	0.3849	0.00481	504
2		80	1.70	1.02	0.3972	0.00496	496
1		40	1.68	0.96	0.2218	0.00554	470
2R*		40	1.54	0.94	0.1947	0.00487	469
1		20	1.90	1.15	0.0820	0.00410	468
2		20	1.90	1.15	0.0820	0.00410	463
1		10	2.66	1.54	0.0464	0.00464	444

Table J-1 (continued)

SAMPLE	RUN NO.	HEATING RATE °C/min	INITIAL WEIGHT mg.	FINAL WEIGHT mg.	MAXIMUM RATE OF WEIGHT LOSS PER MIN.	MAXIMUM RATE OF WEIGHT LOSS PER °C	TEMPERATURE AT MAXIMUM RATE OF WEIGHT LOSS °C
G	2	160	2.10	1.36	0.8105	0.00507	518
	3	160	2.44	1.58	0.8067	0.00504	526
	1	80	1.52	0.96	0.4185	0.00523	488
	2	80	1.34	0.82	0.3924	0.00491	488
	1	40	2.22	1.37	0.2145	0.00536	477
	2	40	2.14	1.34	0.2040	0.00510	469
	1	20	2.28	1.38	0.0942	0.00471	468
	2	20	2.16	1.35	0.0955	0.00477	468
	1	10	3.39	2.04	0.0556	0.00556	454
	H	3	160	2.30	1.32	0.9414	0.00588
4		160	1.36	0.90	0.9171	0.00573	518
1		80	1.80	1.06	0.4936	0.00617	497
2		80	1.64	0.96	0.4948	0.00619	497
1		40	2.06	1.19	0.2749	0.00687	468
2		40	1.98	1.11	0.2553	0.00638	472
1		20	1.86	1.06	0.1189	0.00594	468
2		20	1.75	0.96	0.1153	0.00570	465
1R*		10	3.50	2.04	0.0556	0.00556	454

Table J-1 (continued)

SAMPLE	RUN NO.	HEATING RATE °C/min	INITIAL WEIGHT mg.	FINAL WEIGHT mg.	MAXIMUM RATE OF WEIGHT LOSS PER MIN.	MAXIMUM RATE OF WEIGHT LOSS PER °C	TEMPERATURE AT MAXIMUM RATE OF WEIGHT LOSS °C
I	2	160	2.02	1.18	0.9507	0.00594	518
	3	160	2.04	1.20	0.9417	0.00588	518
	2	80	1.46	0.84	0.5396	0.00674	480
	3	80	1.74	0.98	0.5506	0.00680	480
	1	40	1.62	0.96	0.2973	0.00743	460
	2	40	1.76	0.98	0.2547	0.00649	459
	1	20	1.92	1.14	0.1283	0.00641	458
	2	20	1.69	1.02	0.1183	0.00591	457
	1	10	2.66	1.55	0.0612	0.00612	460

* 'R' in this column indicates that a run was repeated because of some experimental problem in the previous run of the same number.

Table J-2
 TABULATED DATA FROM THE BEST DSC RUNS

SAMPLE	RUN NO.	HEATING RATE °C/min	SAMPLE WEIGHT mg.	FINAL WEIGHT mg.	BASE-LINE SHIFT*	TEMPERATURE AT WHICH THE CURVE WAS CORRECTED FROM T _c , °C	FIGURE NO.** IN THIS REPORT
A	126	320	1.81	1.36	11	466	A-6
	125	320	1.80	1.34	46†	466	-
	74	160	1.80	1.26	37	434	A-7
	76	160	1.80	1.28	15	434	-
	155	40	1.80	1.30	53	466	A-8
	156	40	1.77	1.28	53	434	-
B	130	320	1.30	0.88	53	466	B-6
	131	320	1.30	.86	35	466	-
	84	160	1.78	1.14	16	466	B-7
	99	160	1.80	1.10	29	466	-
	157	40	1.80	1.10	52	466	B-8
	158	40	1.80	1.10	48	434	-
C	132	320	1.79	1.16	37	466	C-6
	133	320	1.80	1.16	57	466	-
	82	160	1.80	1.16	3	466	C-7
	101	160	1.80	1.14	35	466	-
	160	40	1.80	1.16	63	450	C-8
	159	40	1.78	1.14	38	434	-
D	136	320	1.18	0.96	56	466	D-6
	108	320	1.80	1.46	53	466	-
	95	160	1.82	1.47	23	466	D-7
	80	160	1.80	1.42	37†	466	-
	162	40	1.79	1.41	51	434	D-8
	163	40	1.74	1.38	51	434	-
E	123	320	0.56	0.38	37	498	E-6
	124	320	0.58	0.38	40†	498	-
	102	160	1.80	1.14	20	434	E-7
	98	160	1.80	1.14	32	466	-
	174	40	1.74	1.10	76	434	E-8
	173	40	1.77	1.11	--†	-	-
F	137	320	1.81	1.14	55	466	F-6
	138	320	1.80	1.14	54	466	-
	83	160	1.80	1.16	24	466	F-7
	100	160	1.80	1.10	29	466	-
	167	40	1.78	1.10	39	434	F-8
	169	40	1.76	1.08	45	434	-

Table J-2 (continued)

SAMPLE	RUN NO.	HEATING RATE °C/min	SAMPLE WEIGHT mg.	FINAL WEIGHT mg.	BASE-LINE SHIFT*	TEMPERATURE AT WHICH THE CURVE WAS CORRECTED FROM T _c , °C	FIGURE NO.** IN THIS REPORT
G	113	320	1.80	1.22	49	466	G-6
	114	320	1.80	1.22	53	466	-
	86	160	1.80	1.20	39	466	G-7
	90	160	1.78	1.18	15	466	-
	177	40	1.80	1.20	45	434	G-8
	180	40	1.80	1.18	46	434	-
H	141	320	1.80	1.18	-5	466	H-6
	145	320	1.30	0.82	42	466	-
	72	160	1.80	1.10	-3	434	H-7
	69	160	1.80	1.10	16	434	-
	164	40	1.78	1.10	50	434	H-8
	165	40	1.82	1.14	61	434	-
I	119	320	1.00	0.66	48	466	I-6
	120	320	1.00	0.66	43†	466	-
	96	160	1.80	1.16	25	466	I-7
	81	160	1.78	1.16	41†	434	-
	181	40	1.80	1.14	38	434	I-8
	183	40	1.78	1.15	38	434	-

* Baseline shift (in no. of chart divisions) is the difference between the final energy levels of the baseline scan and the sample scan. A Leeds and Northrup Chart No. 990173 (100 divisions in 25 cm chart span) was used for all DSC runs. Sensitivity setting on the instrument was 20 mcal/sec and recorder full scale, was 20 mv.

** All the DSC runs listed in this table are also shown in the text.

† Baseline shift exceeded the equipment millivolt output range.